

# **AIS 2021**

16th International Symposium on  
Applied Informatics and Related Areas

## **PROCEEDINGS**

Óbuda University

November 11, 2021

Székesfehérvár, Hungary

ISBN 978-963-449-263-4

## Contents

<b>Oral Session I. ....</b>	<b>1</b>
Levente Dimén and Borşan Tudor: The e-Learning – Between the Path to Modernity and Emergency Stairs .....	2
Rozália Lakner: Structural Startability of Reaction Pathways with Petri Net Analysis.....	6
Gergely Vakulya: Evaluation of a Genetic Algorithm Based Image Approximation Method .....	12
Gábor Nagy: Using Sector Based Linear Regression in Epidemic Data .....	16
<b>Oral Session II. ....</b>	<b>19</b>
Jozsef Halasz, Erika Peukert, Edina Lukacs and Aniko Mahler: Forced Facial Expression – the Effect of Different Emotions and Temporal Patterns .....	20
Anikó Szarvák and Valéria Póser: Review of Knowledge Base according to Information Technology Safety Awareness .....	25
Márk Rátosi, Gergely Vakulya and Gyula Simon: Methods for High Precision Shutter Speed Measurements.....	30
Tamas Jancso: Error Detection Methods in Photogrammetry .....	35
<b>Poster Session I. – Applied Informatics.....</b>	<b>39</b>
Dávid Fischer, Mátyás Marx and Monika Pogátsnik: Smart Pedestrian Crossing for the Blind and Visually Impaired .....	40
Daniyar Kaliyev, Olga Shvets and György Györök: UAV Based Navigation System for Forest Fires Monitoring .....	47
János Sári and Károly Széll: The Applicability of ROS in the Use of Unmanned Combat Aerial Vehicles.....	51
Éva Hajnal, Gergely Vakulya, Péter Udvardy and Levente Kovács: Acceleration Measurement Experiments in Dairy Cattle .....	55
Bertalan Beszédes and György Györök: Photovoltaic Panel Failure Prediction Using a Thermal Imaging Camera.....	59
Judit Módné Takács, Nikoletta Tolner and Monika Pogátsnik: Diverse Approach of Cybersecurity Culture in Education .....	64
Gábor Nagy: Analysis of a Prime-Representing Constant .....	69

<b>Poster Session II. - Robotics and Industrial Applications .....</b>	<b>71</b>
Dávid Bárándi and Károly Széll: Hand Gesture Controlled Robot.....	72
István Elek Kiss and Károly Széll: Dynamic Arc Stabilization Options for Gas Metal Arc MIG / MAG Robot Welding.....	76
Albin Nátrán and Károly Széll: Mobile Robot Environment for SLAM .....	80
Márk Liszi and Károly Széll: Automation of EDM Machines .....	84
Olga Shvets, Bauyrzhan Smakanov and Zhanerke Bakatbayeva: Monitoring Of The State Of A Person At Hazardous Work .....	88
<b>Poster Session III. – Geodesy and Geoinformatics .....</b>	<b>92</b>
Eszter Duleba, Gergely László and Zoltán Tóth: Establishment of GNSS Calibration Network .....	93
János Katona and Andrea Pődör: Increasing Urban Development Efficiency through Land Value Capture Mechanisms .....	97
Gergely László, Gabriella Bor, Grégory Lucas and Csaba Lénárt: Application Development Supporting Orthophoto Documentation.....	102

**ORAL SESSION I.**  
**Applied Informatics I.**

# The e-Learning – Between the Path to Modernity and Emergency Stairs

Levente Dimén

Center for Distance Education  
1 Decembrie 1918 University of Alba  
Iulia  
Alba Iulia, Romania,  
ldimen@uab.ro

Borşan Tudor

Dep. of Cadastre and Civil  
Engineering  
1 Decembrie 1918 University of Alba  
Iulia  
Alba Iulia, Romania,  
tborsan@uab.ro

**Abstract** - In recent decades, our existence has been marked by amazing developments in science, especially in areas such as economy, technology, information and more. People all over the world are experiencing changes on an accelerated time, entailing radical changes. Thus, inevitably, daily activities must be brought into line with time requirements.

Education is also an area that should be adjusted in order to deal with rapid modernization of the society in which we live. Over time, it was found that the delivery mode and the content of traditional education, too is no longer suitable to meet current requirements. Thus, education providers (staff or institutions) had to switch to new more efficient ways of teaching the courses. In the society we are living, a society of information and knowledge, the courses have become today increasingly digital.

The present crisis that accompanies the COVID-19 pandemic has severely influenced our personal and professional experiences. Educational institutions and their actors have felt the impact of this crisis, through significant disorders at all levels of operation. For university education, the transfer from courses and seminars in the virtual environment proved to be more than a temporary challenge, it deeply affected the efficiency of activities, but this reality did not act as factor which weaken the motivation to preserve the quality of the educational act. Its demanding and unpredictable nature has been and continues to be a good opportunity to test and validate our resilient skills in conjunction with our ability to successfully adapt to new contexts. On the other hand, it is a test through which we can verify the usefulness of teaching experience and expertise.

**Keywords**—*e-learning, technology based education, instructional paradigm*

## I. WHY E-LEARNING ?

Occurred after 1993, an e-Learning system is a type of distance education, a teaching-learning activity organized by an institution that provides materials in a logical order, sequential, to be treated by the receptors.

Nowadays, can be easily observed that the world is moving increasingly toward a paperless world. The society in which we are living is an information society. Thus, any economic, social and policy field is redefined under the impact of information and its technologies.

We see today how humanity is transformed into a computer society; IT and technical progress become the essential elements and without it no field can not arise, can not exist and develop.

Communications networks with high speed and wide area which facilitates links initially impossible to imagine,

causes significant changes in all areas of society; thus, whether is an economic, social, political, cultural or any other aspect, is re-sized by new technology. The best example is the Internet, with the help of it are removed barriers related to geographical distance, culture, mind. Any information from anywhere in the world can be accessed with a simple click.

This dynamic of science, technology and socio-economic development, laid the foundations of modern society, an information society. The changes mentioned influence the education field, too. It is difficult to be constantly ready to respond all the changes that we face it. One solution might be continuous training to acquire new and new knowledge. We already know that those young children who benefit from modern methods of instruction are much more evolved, most profound in what they think and what they do than those educated by traditional methods.

Education is required to prepare a human type, for a modern society, an informatics one. We ask ourselves if this is really possible through traditional means. Opinions are divided; on the one hand it is difficult to use primitive traditional means and methods, while the younger generation is keeping the step with the technology of our times - so the entire education system must be restyle according to specificity of each young people. But still this modern process of society educating has to accomplish the same objectives, which emphasizes the role of education in the life of any individual. Basically, the same traditional goals are now achieved by modern means.

An E-Learning System means all educational situations where are significantly used modern means of information technology. E-Learning System is considered to be a virtual institution. Generally, such an institution is involved in educational activities which promote their products (programs, curricula, courses) through communication technologies. A virtual institution can be found in every field, be it public or private, but at different levels of education: elementary, secondary, university, etc. A virtual institution is designed to facilitate teaching and learning without the direct involvement as a provider of educational programs

## II. THE CHARACTERISTICS OF THE E-LEARNING PROCESS

Although internationally, the system develops rapidly, in our country the E-Learning and its development is very uncertain. There are many barriers or obstacles of this phenomenon development in our country; among the most important are:

- reluctance of the teachers for the new system implementation;
- maintaining and using traditional methods of teaching and learning;
- conventional thinking of many users, of this system, which in terms of traditional culture in which they have developed, are reluctant.

In Romania, this new form of education is proposed at the national level than in the higher cycles of faculty and master. No matter how much the prestigious institutions of our country exert to develop at national level the program, launching attractive offers in online education, can not speak about a rising of this segment in education market.

The important aspect of E-Learning system is that in addition to eliminating obstacles of spatial order, provide study opportunities for broad social categories without interrupting their work. This is the main argument for the system is especially viable for higher learning cycles. It is not yet possible to speak of implementing such a system at primary and secondary cycles. This would lead to the decline of the Romanian educational system. Can not be implemented an educational system at primary school because here is established the foundations of education and learning system. At most, can speak of a bimodal system consisting of traditional (classical) and modern methods.

E-Learning system gathers all the other features of traditional education rolled into one concept. This E-Learning System includes everything in one system and traditional teaching: content, planning, specific, methodology, interaction, support and evaluation. Practical, E-Learning system is a new way of looking at learning process, a way in which the basic elements remain the same, the traditional ones, but it change the means of acquiring knowledge.

The main feature of e-Learning system is interactivity, an important feature of modern online programs offered by the increasing importance of student involvement. With the evolution of these online systems, many individuals have appeared who claim that the lack of interaction leads to lower their effectiveness. However, online programs, especially those relating to on-line masters, gain more and more ground due to the benefits provided to their students, in the context of modern society, a society where everything is computerized.

In the concept of some authors, an E-learning process represent, providing education, training or education by electronic means. E-learning system is simply a new clothing of education process. Practical, the elements, the objectives remain the same but the means of acquiring knowledge changes. The Internet is the launch pad for E-learning. Lifelong learning acquires new dimensions, achievable with E-learning software platform. Analyzing even the term "E-Learning" we highlight four key features present in the prefix of "exploration, experience, commitment, ease of use.

E-learning means:

- learning through the Internet;
- learn quickly at low cost;;
- free access to education for all participants;

- use information technology to form and manage learning

Through E-Learning, each student is able to form the learning mode in its own style. Thus, it can store the materials, courses hearing being able to be performed continuously or gradually, depending on the time available, the student having total control over its information.

The E-Learning system gathers all the other features of traditional education rolled into one concept. Thus the E-Learning system gathers all that a traditional teaching system contains: content, planning, specific, methodology, interaction, support and evaluation.

Practical, the E-Learning system is a new way of looking at the learning process, a way in which the basic elements remains the same, the traditional ones, but the means of acquiring knowledge is changing.

### III. ADVANTAGES AND LIMITATIONS OF E-LEARNING.

With reference to the traditional model we can highlight some major advantages of online education. First using the Internet all resources can be accessed as quickly as possible, anywhere.

With E-Learning systems audience is increased and students who are not present in the mainstream may also participate at the course. Although distances between educational institutions and users of these E-learning systems are high, with modern technologies such courses are interactive, a real-time student can intervene can support formative and objective assessments.

Through e-learning each student can improve his learning a style in his own way. Thus the student can store materials, examination courses and could be taken continuously or gradually student having its control over his information

Through E-Learning system it is allocated a much lower time to follow their studies, thus, providing students the opportunity to continue their activities, so they offer greater flexibility, flexibility that is not offered by mainstream where the presence is necessary at well defined moments in time during the conduct of business.

The cost of an online system is another advantage. Although it is not much different than a traditional system, an online system is more beneficial for the client, for racing, because while endorsing knowledge he is able to continue working and he is not obliged to give up some financial services. At the same time less and indirect costs incurred by the presence in the university campus are decreasing. For the concept of cost to be indeed a benefit of these systems requires that when determining the price of such a system to take into account the price of the substitute products, more exactly the price of traditional education services

E-Learning System is now becoming more than a new type of education, it is a business solution, a successful option for institutions offering such courses. In this context it becomes more important the operation to establish the price of services offered by this system. Thus it should be well thought-out the strategy to be adopted to attract students.

Being new product the educational institutions may adopt "high price strategy". This strategy is used when launching a new product on the market. But given the fact that a new product is associated mostly with a degree of consumer confidence, as the market develops such a strategy fails if it doesn't have a reasonable quality- price rapport.

Another pricing strategy that can be adopted in these systems is the "price down strategy" which consists in setting low prices in order to gain a dominant market position. For E-Learning such a price strategy will be successful in a market, taking into account only the purchasing power of potential consumers. In a market such product has a high complexity and its quality is difficult to assess objectively.

In E-Learning, the price of such a system is not designed expressly for the company's immediate financial resources, but it is an instrument on which and the other its own market is based. Thus the product complexity and the high level of commitment that it requires from the consumer require to be given more attention to price for establishing strategies for the institutions that use these systems.

Regarding the evaluation system, E-Learning presents and on this issues a number of advantages. Thus the owner of the course is much advantaged in terms of assessment, he does not have to prepare materials for the large number of students, such holder being prepared to support anyone who can access anytime.

Like any new product on the market, E-Learning has some limits

First biggest difficulty relates to the high costs of developing the system. Everyone knows how hard it is to support such a large computer system, they include all technology expenses, charges for transmission network information, maintenance of equipment, materials and production expenses needed to develop the network

Another disadvantage would be the difficulty of implementing this system; increased efforts are required of students, teachers but also brokers, those who provide technical support and the administrative staff. In addition to these continued efforts of staff directly involved in implementing this system, it also contains those related to community belief of that system efficiency. This will not be easy because it's hard to fight against traditional mentality.

Early school drop-out includes him among the limits of e-Learning. Although not present in the same proportion as in traditional education, school drop-out phenomenon exists also for distance education, so students must be highly motivated to participate in this form of education.

Another disadvantage of this system would be that all these focuses on the system and not on the student, so every student should know the field of computers.

For all these limits to be exceeded, we need a clear strategy devised to overcome these things.

These strategies should take into account the overall needs assessment of hardware, software required to implement this system, visits to institutions using such systems must be enhanced - so said to be an assessment of national infrastructure. This is the main reason why online programs are distributed only to paid places.

The most important element to transform the limits of E-learning into objectives should be consulting experienced instructors who work with such online education systems, especially related to consulting learners and

employers views in order to co-opt a graduate course on-line. In Romania these concepts still exist. For now it is quite difficult for an employer to accept a graduate of the education system without any bias.

In case of e-learning system, there is no question about its survival but rather its long-term development of the business. Being a new market product, this must answer at logical objectives like high market share, consumer involvement of competitive products and other objectives like these.

#### IV. ONLINE EDUCATION - A RECONCEPTUALIZATION OF TEACHING STRATEGY

Prolongation of the COVID-19 crisis forces us to reconsider how we approach the teaching and the assessment of students. In order not to compromise the quality of the educational act, in this period, we need an a reconceptualization of the teaching-learning-evaluation activities. In this new context is expected the development and implementation of new teaching strategy. It will capitalize the strengths and good practices extracted from classical teaching, which will be adapted to the constraints of online education.

The increasing use of information technology forces us to specify the effective delivery of teaching sequences, which can be synchronous and asynchronous, respectively, so that online education is based on instructional plans that encompass four key components and require a well-established order of stages of elaboration. Here are the ones:

- Identifying objectives;
- Construction of evaluation tasks;
- Planning learning tasks and staging contents;
- Determining the delivery method: synchronous / asynchronous.

**Asynchronous teaching activities** - are teaching activities that support and strengthen the main advantage of online education, namely its flexible nature. The activities do not take place in real time, and the students do not access the transmitted / posted materials at the same time. Instead, they can browse the contents and solve work tasks in a truly flexible way, when their own schedule allows. More and more importantly, the asynchronous activities allow students to go through the content of the course at their own pace, while benefiting from an authentic guidance and feedback provided by the teacher.

**Teaching activities carried out synchronously** - are teaching sequences in which the interaction with and between students occurs in real time. It is one of the most common options when a teacher decides to make the transition to online courses. The teacher and students interact in real time, the teacher can send messages both verbally and nonverbally, can receive (at least in part) the nonverbal feedback of students and can adapt their teaching according to it, do it is possible to create a real learning community faster.

Interactivity is the key concept that defines the social-constructivist paradigm in education and, implicitly, it represents the guarantee of the correct implementation of a student-centered teaching-learning process. Active learning

theories emphasize the role that interaction with content and social interactions play in the construction of knowledge. Below we formulate some recommendations regarding the favoring of the two types of interactions.

In technology-mediated teaching, the teacher can use a series of strategies to organize the contents so as to facilitate the priority allocation by students of their cognitive resources in the direction of content processing and employment.

Recommendations for enhancing content interactions

In technology-mediated teaching, the teacher can use a series of interactive strategies to (re) organize the contents. The objective of this approach is to increase the clarity and intuitive nature of the supporting materials so that the resulting new organization facilitates in-depth learning, but also easy transfer to professional skills. The organization of the content is much easier if we organize in advance the workspace that the platform offers us.

Is important to organize the content into logical units or modules that have a certain degree of autonomy. Each module should be structured around a major theme that contains the relevant instructional objectives you are targeting, as well as the learning materials and activities associated with this content. The modules can be sorted chronologically or by content.

It is recommended that each module include:

- Module identification information: module number / week to be completed / start-end date / topic name.
- Module presentation: brief presentation of the module content and its connection with the other modules / presentation of the module objectives.
- Learning and assessment activities: work tasks assigned to students including their deadlines.
- 

## V. CONCLUSIONS

Online education involves a deliberate effort on the part of the teacher to stimulate three types of interactions. They take the form of the students' interaction with the support materials, the interaction you have with the students, respectively the interactions between the students. Their share during the delivery of disciplinary content is variable. In the context of classical teaching, face to face, these

interactions often occur spontaneously, instead, for online teaching, they require intentionality and planning. Interaction with others is a key component of the human being's ability to learn new things. Therefore, building communities and supporting collaboration are essential for promoting learning.

The efficiency of the online educational is primarily determined by the quality of the instructional paradigm used in the educational process. Regardless of the way in which we decide to deliver the informational contents, if we want an efficient technology based learning we will have to assume, first of all, a certain psycho-pedagogical conceptualization of the teaching-learning process. According to the latest reviews on the literature, the teaching-learning process (regardless of the means / method of implementation) is best based on the social-constructivist paradigm. According to her, the student is the one who, assisted correctly and constantly by the teacher, builds his own baggage of knowledge and skills.

## References

- [1] Bruher M. – „Customer orientation. Successful business trend", Economic Publishing House, Bucharest, 2004
- [2] Brut Mihaela – „ E-learning Tools", Polirom, Bucharest, 2004
- [3] Kevin Hogan - „How to sell yourself. Psychological tactics in selling "Header Publisher, Bucharest, 2004
- [4] Ionescu Eduard, Dumitru Marin – „Prices and Competition", Publisher of Tomorrow Foundation Romania, Bucharest, 2002
- [5] Tudorici Roxana - Educational Management in European context ", Publisher Meronia, Bucharest, 2007
- [6] Ionescu Ionel Eduard - Virtual education and e-learning systems - The central topic of the 6th edition of the annual eLearning and Software for Education (eLSE) 2010 is: Advanced Distributed Learning in education and training transformation, Vol 1, Carol I National Defence University, Bucharest, ISSN:2066-026X;
- [7] Ionescu Ionel Eduard, Oprea Constantin Cristian - New technologies in education e-learning system - The central topic of the 6th edition of the annual eLearning and Software for Education (eLSE) conference 2011: Advanced Distributed Learning in education and training transformation, Vol 1, Carol I National Defence University, Bucharest, ISSN:2066-026X;



# Structural Startability of Reaction Pathways with Petri Net Analysis

Rozália Lakner

*Alba Regia Technical Faculty*

*Óbuda University*

Székesfehérvár, Hungary

lakner.rozalia@amk.uni-obuda.hu

**Abstract** – The systematic exploration of candidate reaction pathways has theoretical and practical significance to understand the mechanism of a complex chemical and biochemical reaction and potentially improve its yield. Therefore, many works deal with issues related to the synthesis of reaction pathways for a given mechanism. One of the most effective method for reaction pathway synthesis is the P-graph algorithm, which is applicable to generate the feasible solution structures for complex reactions, including the catalytic and enzyme-catalytic reactions. As this method produce the possible structures based on dynamic equilibrium state, it is very important to investigate whether these states can be reached from the initial state of the system, i.e., whether the reaction pathway is structurally startable. The present work suggests Petri net analysis methods for the structural startability examinations.

**Keywords** – reaction pathway, structural startability, Petri net analysis, P-graph (process-graph).

## I. INTRODUCTION

The reaction mechanism serves as an accurate model for prediction of the behavior of the reaction and its control. The determination of the proper reaction mechanism is, therefore, a key point both in chemistry and industrial applications.

Chemical reactions often composed of individual sub-steps, so called elementary reactions. The network demonstrating the connections of the elementary reactions of the overall reaction is conventionally described as reaction pathway that is the basis for the reaction mechanism. Different pathways of a reaction may have different properties in terms of energy requirements, yield, and geometrical structure of final products.

There are experimental tools to determine the reaction mechanism, such as recognition of the appearance of reaction intermediates, where a set of hypothetical elementary reactions can be determined from the available intermediates. Besides that, there are graph-theoretic methods serving as effective tools for determination of the structure of reaction pathways, based on the elementary reactions. These methods generate the set of stoichiometrically feasible reaction pathways, that contains all possible alternatives, at the same time included unworkable ones. For practical reason, before the selection of the proper solution or solutions, it is useful to prune the unrealizable ones. Since startability is crucial for accomplishing a reaction pathway, the violation of startability is an obvious reason for the elimination. This paper presents different methods for recognizing if a reaction pathway is structurally startable or not. To do so, Petri net theory is used, based on stoichiometrically feasible solution structures generated by P-graph framework.

P-graph has been first applied for reaction pathway synthesis by Fan and Friedler [1] in 1997 utilizing Process Network Synthesis (PNS) algorithms originally developed for

chemical engineering process synthesis on a rigorous axiomatic basis and P-graph representation [2]. In 2001 Fan et al. [3] highlighted the specialties of reaction pathway synthesis among process synthesis problems and established new axiomatic system tailored for reaction pathway synthesis problems of catalytic reactions, as well as the algorithms tailored for reaction pathway synthesis.

Petri net is a modeling language that has both graphical and mathematical formalism for the description of concurrent, asynchronous, distributed systems [4]. In the last half-century, different extensions for Petri nets, e.g., colored, timed, hierarchical were developed and several successful applications have been done on a wide range of domains. These methods support both the modeling and the analysis of systems in different fields of application including process engineering, manufacturing systems and computer sciences [5].

Recently Petri net served as a promising modeling and analysis tool of reaction mechanism, which have successfully been applied to systems biology of metabolic and signal transduction pathways in modeling both discrete and continuous processes. Angeli et al. [6] investigated the conditions for persistence of chemical species in reaction systems based on Petri net theory. This property plays an important role in the ecosystems, where preserving non-zero populations of all the species which are present at the initial time is crucial.

The similarities between P-graphs and Petri nets mainly based on the similar structures, namely both have strict formal mathematical definitions and graph-representation, also. The unique feature of the P-graph framework due to the strict mathematical basis can generate all combinatorially feasible solution structures of a given problem, moreover, determine the optimal structure for predefined objective function. In contrast, the usage of Petri nets is to determine the behavior and the properties of a system given by a predefined structure [7].

In the present work Petri net analysis methodologies was applied for the determination of structural startability, based on the stoichiometrically feasible reaction pathways generated by P-graph algorithms. The proposed methods have been demonstrated by the well-known hydrogenation of ethylene to ethane on biactive-site platinum catalysts [8].

## II. PETRI NET METHODOLOGIES FOR DETERMINING THE STRUCTURAL STARTABILITY

To determine structural startability of a stoichiometrically feasible reaction pathway it must be examined whether all the elementary reactions operate from the given initially available species. These properties can be investigated based on the simulation and analysis of the Petri net, corresponds to the stoichiometrically feasible reaction pathway.

### A. Formal definition of Petri nets

A Petri net [4, 5] formally can be described by a quadruple in the form  $PN = \langle P, T, E, w \rangle$ , where  $P$  is the finite set of the places, and  $T$  is the finite set of the transitions, with  $P \cup T \neq \emptyset$  and  $P \cap T = \emptyset$ . Petri net is also called place/transition net, where places act as passive elements, e.g., states, conditions, chemical species, and transitions represent the active elements, e.g., events, actions, chemical reaction steps.  $E \subseteq (P \cup T) \times (T \cup P)$  defines the edges from places to transitions and vice versa, and the weight function of the edges ( $w$ ) is a mapping from  $E$  to  $\mathbb{N}^+$ .

The preset of a transition  $t \in T$  is the set of its input places (i.e. the places connected directly to  $t$  with arcs) denoted by  $\bullet t = \{p \in P \mid w(p, t) > 0\}$ , while its postset is the set of its output places (i.e. the places connected directly from  $t$  with arcs):  $t \bullet = \{p \in P \mid w(t, p) > 0\}$ .

The interpretations of preset and postset of a place are analogous.

A marking  $M$  of a Petri net is a mapping from  $P$  to  $\mathbb{N}$ , where  $M(p)$  denotes the state of  $p \in P$  defining with the number of tokens in place  $p$ . So, the state of the Petri net can be represented by a  $|P|$ -dimensional marking vector  $M$ , and  $M_0$  denotes the initial marking representing the initial state of the system, respectively.

The transitions can consume tokens from, and can produce tokens to their input and output places according to  $w$ .

Petri nets can be described as bipartite graphs, where places are indicated by circles and transitions by rectangles. The places and transitions are connected by weighted directed arcs representing the weight functions.

For the illustration of the formal definition of Petri nets, the reaction of nitrous oxide ( $N_2O$ ) and carbon monoxide ( $CO$ ) in the presence of rhodium catalyst (the active site is denoted by  $\ell$ ) to form dinitrogen ( $N_2$ ) and carbon dioxide ( $CO_2$ ) is introduced. [8] The elementary reactions are summarized in Table I.

TABLE I. ELEMENTARY REACTIONS OF THE SIMPLE EXAMPLE

	Elementary reaction
$e_1$	$N_2O + \ell \rightarrow N_2Ol$
$e_2$	$CO + \ell \rightarrow COL$
$e_3$	$N_2Ol \rightarrow N_2 + Ol$
$e_4$	$COL + Ol \rightarrow CO_2 + 2\ell$

Note that only forward steps are included in the illustration, i.e., the elementary reactions are irreversible. In contrast, for reversible elementary reactions both forward and reverse steps must be included in the set of elementary reactions. The overall reaction is  $N_2O + CO \rightarrow N_2 + CO_2$ .

The formal definition of Petri nets represents the reaction of nitrous oxide and carbon monoxide in the presence of rhodium catalyst to form dinitrogen and carbon dioxide is as follows:

$$P = \{N_2O, CO, \ell, N_2Ol, COL, Ol, N_2, CO_2\}$$

$$T = \{e_1, e_2, e_3, e_4\}$$

$$E = \{(N_2O, e_1), (\ell, e_1), (e_1, N_2Ol), (CO, e_2), (\ell, e_2), (e_2, COL),$$

$$(N_2Ol, e_3), (e_3, N_2), (e_3, Ol), (COL, e_4), (Ol, e_4), (e_4, CO_2), (e_4, \ell)\}$$

$$w((e_4, \ell)) = 2, \text{ otherwise } w = 1$$

$$M_0 = [1, 1, 2, 0, 0, 0, 0, 0].$$

The graph representation of the example is illustrated in Fig. 1(a). The Petri net figures are depicted by Petri net modeling tool Snoopy [9].

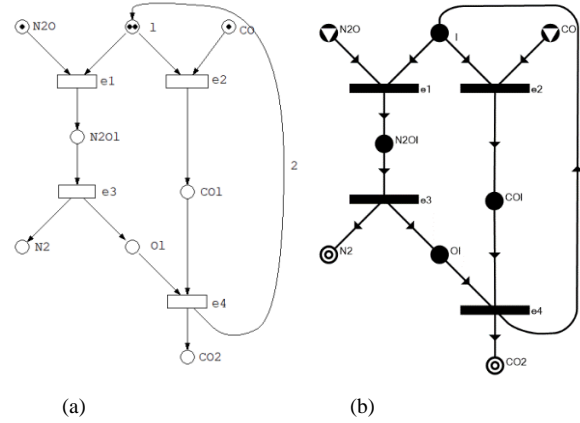


Fig. 1: Petri net representation with the initial marking (a) and P-graph representation (b) of the simple example.

The similarities between P-graphs and Petri nets are mainly comes from their structure, i.e., both are represented by bipartite directed graphs. The P-graph representation of the reaction pathway of the reaction nitrous oxide and carbon monoxide to form dinitrogen and carbon dioxide example is illustrated in Fig. 1(b), where the reaction pathway was determined by the help of P-graph Studio [10].

Both P-graphs and Petri nets are for complex systems. The major difference is that P-graphs are primarily for synthesis and Petri nets are primarily for simulation and analysis.

P-graph framework has effective algorithms to synthesize process systems to be constructed from potential building blocks, computes both the optimal structure and the optimal parameter values, but not used for examining the dynamics of the system. On contrary, Petri nets are tools for simulation and analysis of the dynamic behavior of complex systems. They are used for examining the operation of preliminarily defined model, but not support the synthesizing of the structure.

### B. Simulation and analysis of Petri nets

In state  $M$  of a Petri net the transition  $t$  is enabled, in other word fireable, if all of its input places contain at least the required numbers of tokens defined by the weight function, i.e.,  $\forall p \in \bullet t: M(p) \geq w(p, t)$ . When a transition  $t$  is firing, a defined number of tokens are consumed from its input places and produced to its output places, so the state of the net changes producing new marking  $M'$  according to:  $\forall p \in \bullet t: \forall p \in t \bullet: M'(p) = M(p) - w(p, t) + w(t, p)$ . The simulation of these two basic rules of enabling and firing transitions presents the dynamic behavior of a Petri net. Note that the execution of a Petri net is nondeterministic, i.e., when multiple transitions are enabled at the same time, any one of them may fire, and different transition sequences may lead to different states from the same initial state.

Petri nets serve for system analysis, too, where different system properties can be investigated, e.g., reachability, boundedness, reversibility, liveness, deadlock. Most of these properties can be examined with the help of reachability graph that contains all the possible states of the Petri net, constructed by all the sequences of the firing transitions from the initial state  $M_0$ .

The reachability graph of the simple example in Fig. 1(a) generated with Petri net analysis tool Charlie [11] can be seen in Fig. 2. The states of the Petri net are represented by graph nodes including the initial state as top node, and the graph edges are labeled with the identifier of the transitions.

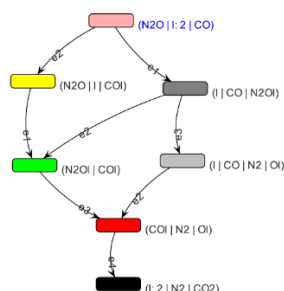


Fig. 2: The reachability graph of the simple example

The reachability graph serves information about system properties, such as

- **Reachability** - The state  $M$  is reachable, when there is a sequence of fireable transitions from the initial state to  $M$ . If  $M$  can be found as a node of the reachability graph, then  $M$  is reachable, otherwise not.
- $L_1$  **liveness** - The Petri net is  $L_1$  live when every transition fires at least once in some firing sequence from the initial state. If every transition can be found as arc label of the reachability graph, the Petri net is  $L_1$  live, otherwise it is dead.
- **Liveness** - The Petri net is live when every transition can fire from any reachable states.
- **Deadlock** - A reachable marking of the Petri net, where none of the transitions can fire. All deadlocks constitute leaves in the reachability graph, as node  $(\ell, N_2, CO_2)$  indicates in Fig. 2.

The properties of the Petri nets can be marking-dependent, or in other words behavioral, depending on both the structure and the initial state of the Petri net, and can be structural, independent of the initial marking. The behavioral properties, e.g., reachability, liveness, deadlock, can be investigated based on the reachability graph containing the state space of Petri net constructed from the initial state  $M_0$ . The main drawback of these investigations is their exhaustive characteristic, as the reachability graph can be very large, and both the time and the space requirement grow exponentially in the number of places. Therefore, this type of analysis is computationally hard.

Structural analysis enables the investigation of some properties without constructing the reachability graph. Most of the structural properties, e.g., place and transition invariant, siphon and trap analysis, can be easily determined by means of algebraic techniques.

As siphons and traps [12, 13] play essential role, and used extensively for the analysis of the reachability, liveness and

deadlock of Petri nets, their main characteristics and properties are summarized as follows.

A siphon is a non-empty set of places  $S \subseteq P$  whose presets are also postsets:  $\bullet S \subseteq S \bullet$ , i.e., every transition having an output place in  $S$  has an input place in  $S$ , too. An important property of the siphon  $S$  is, that if it once insufficiently marked, it will never be marked again, and consequently, all transitions having arcs from the places in  $S$  become dead. As a result, if a Petri net contains a blank siphon, liveness cannot be obtained. So, a Petri net without siphons is live, while if the system is in a deadlock, it must contain insufficiently marked siphon.

A trap is a non-empty set of places  $\tau \subseteq P$ , however its postsets are also presets:  $\tau \bullet \subseteq \bullet \tau$ , i.e., every transition having an input place in  $\tau$  has an output place in  $\tau$ . An essential property of the trap  $\tau$ , that if it catches tokens, then it keeps at least one of them, i.e., if once a trap has any token, it remains marked. Firing of the transitions can move tokens but cannot remove all the tokens from the trap. Consequently, from the definitions of siphon and trap, if a siphon contains a marked trap, it will never become blank.

The union of two siphons is a siphon, and a siphon is minimal if it does not contain any other siphon. The same goes for traps, too.

The Petri net in Fig. 1 (a) contains 4 minimal siphons and 3 minimal traps as summarized in Table II.

TABLE II. THE MINIMAL SIPHONS AND TRAPS OF PETRI NET

Minimal siphons	Minimal traps
$S_1 : \{ N_2O \}$	$\tau_1 : \{ N_2 \}$
$S_2 : \{ CO \}$	$\tau_2 : \{ CO_2 \}$
$S_3 : \{ N_2O\ell, O\ell, \ell \}$	$\tau_3 : \{ N_2O\ell, O\ell, CO\ell, \ell \}$
$S_4 : \{ CO\ell, \ell \}$	

In case of Petri net, that defines reaction pathway, siphons can represent both the starting reactants and the cyclic structures producing species by consuming themselves; moreover, traps can represent both the products and the cyclic structures consuming species produced by themselves.

### C. Determining the structural startability of reaction pathways with Petri nets

For the investigation of structural startability of stoichiometrically feasible reaction pathways, Petri net simulation and analysis was used for the predefined reaction pathway constructed with P-graph framework [14]. The elements of the reaction pathway represented by Petri net are as follows: the transitions correspond to the elementary reaction steps, and the places correspond to the species. So, the investigation of the structural startability of stoichiometrically feasible reaction pathway is as follows:

- an elementary reaction step  $e_i$  is structurally startable, if all the chemical or active species consumed by  $e_i$  are available, i.e., the transition corresponds to the elementary reaction step  $e_i$  is fireable
- a chemical or active species is available, if it is either an initially available species, or it produced by a structurally startable elementary reaction, i.e., the place correspond to the species is marked in the initial state or becomes marked after the firing of a fireable transition

- a reaction pathway is structurally startable, if all its elementary reaction steps are structurally startable, i.e., all transitions are fireable.

According to these basic statements, for determination of structural startability, it must be examined, whether every elementary reaction step operates from the given initially available species, i.e., all the transitions become fireable at least once from the given initial state. This examination corresponds to the determination of liveness, deadlock, and reachability analysis of the Petri net model of the reaction pathway.

### III. CASE STUDY

The proposed methods for determining the structural startability of stoichiometrically feasible reaction pathways are illustrated with the example of ethylene hydrogenation. The elementary reactions of the example [8] are summarized as Table III.

TABLE III. ELEMENTARY REACTIONS OF ETHYLENE HYDROGENATION [8]

Elementary reaction	
S <sub>11</sub>	$H_2 + 2 l_1 \leftrightarrow 2 Hl_1$
S <sub>12</sub>	$H_2 + 2 l_2 \leftrightarrow 2 Hl_2$
S <sub>13</sub>	$C_2H_4 + 2 l_1 \leftrightarrow l_1 C_2H_4 l_1$
S <sub>14</sub>	$l_1 C_2H_4 l_1 + Hl_1 \leftrightarrow C_2H_5 l_1 + 2 l_1$
S <sub>15</sub>	$l_1 C_2H_4 l_1 + Hl_2 \leftrightarrow C_2H_5 l_1 + l_1 + l_2$
S <sub>16</sub>	$C_2H_5 l_1 + Hl_1 \leftrightarrow C_2H_6 + 2 l_1$
S <sub>17</sub>	$C_2H_5 l_1 + Hl_2 \leftrightarrow C_2H_6 + l_1 + l_2$

The eight stoichiometrically feasible reaction pathways of the problem as far as it is given by Fan et al. [15] are demonstrated in Table IV. Note that all these solutions fulfill the axioms of the combinatorially feasible reaction pathways in P-graph framework [2] and the balances of the species in all elementary reactions of the reaction pathway and for the overall reaction of the problem  $C_2H_4 + H_2 = C_2H_6$ .

TABLE IV. STOICHIOMETRICALLY FEASIBLE REACTION PATHWAYS OF ETHYLENE HYDROGENATION

Reaction pathway	
RP <sub>1</sub> :	$S_{11} + S_{12} + 2S_{13} + 2S_{15} + 2S_{16}$
RP <sub>2</sub> :	$S_{11} + S_{12} + 2S_{13} + 2S_{14} + 2S_{17}$
RP <sub>3</sub> :	$S_{11} + S_{13} + S_{14} + S_{16}$
RP <sub>4</sub> :	$S_{11} + S_{13} + 2S_{14} + S_{15}(\text{reverse}) + S_{17}$
RP <sub>5</sub> :	$S_{11} + S_{13} + S_{15} + 2S_{16} + S_{17}(\text{reverse})$
RP <sub>6</sub> :	$S_{12} + S_{13} + S_{14}(\text{reverse}) + 2S_{15} + S_{16}$
RP <sub>7</sub> :	$S_{12} + S_{13} + S_{15} + S_{17}$
RP <sub>8</sub> :	$S_{12} + S_{13} + S_{14} + S_{16}(\text{reverse}) + 2S_{17}$

#### A. Structural startability determined by Petri net analysis

The structural startability of a stoichiometrically feasible reaction pathway can be investigated based on the simulation by Petri nets as follows. If all the transitions can fire at least once from the given initial state, the reaction pathway is structurally startable, otherwise not. The firing of every transition in a stoichiometrically feasible reaction pathway ensure, that the places correspond to the final products become available, i.e., states contain the final products reachable from the initial state. The hardness of this investigation lays on the situation, when two or more transitions are applicable at the same time, i.e., in case of concurrent system, when the next state depends on the selection from the fireable transitions.

For investigating all the possible states, the reachability graph of the Petri net from a predefined initial state is

generated. In this case the observation of the structural startability of reaction pathway is as follows: if all the transitions appear on the reachability graph as arc-label, the system is structurally startable, otherwise not.

The Petri net with the initial state and the resulted reachability graph of the investigated reaction pathway RP<sub>6</sub>:  $S_{12} + S_{13} + S_{14}(\text{reverse}) + 2S_{15} + S_{16}$  is shown in Fig. 3.

For defining the initial state, unbounded amounts of starting reactants are supposed, that is implemented by so called test arcs from place H<sub>2</sub> to transition S<sub>12</sub>, and from place C<sub>2</sub>H<sub>4</sub> to transition S<sub>13</sub>. The role of the test arcs is the initialization of their output transitions, while tokens in H<sub>2</sub> and C<sub>2</sub>H<sub>4</sub> remain unchanged. The initial tokens of places l<sub>1</sub> and l<sub>2</sub> representing the two catalysts in the system was set to 4 and 2, respectively, ensuring the firing of their output transitions S<sub>13</sub>, S<sub>14</sub> and S<sub>12</sub>.

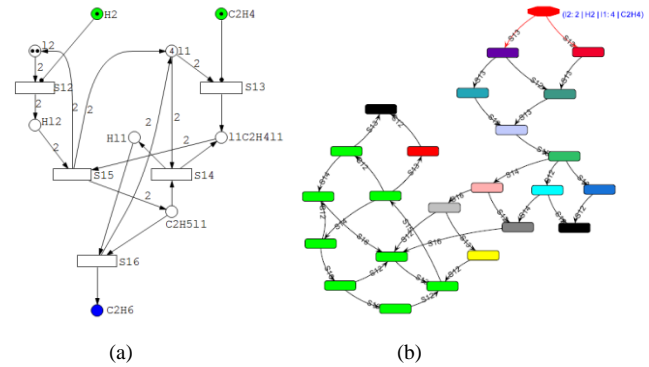


Fig. 3: The Petri net (a) and the reachability graph (b) of stoichiometrically feasible reaction pathway RP<sub>6</sub>.

The reachability graph in Fig. 3(b) shows that all the elementary reactions represented by transitions of the Petri net appear on the reachability graph as arc-label. This observation verify that the reaction pathway is structurally startable.

In case of stoichiometrically feasible reaction pathway RP<sub>5</sub>:  $S_{11} + S_{13} + S_{15} + 2S_{16} + S_{17}(\text{reverse})$  only two elementary reactions, S<sub>11</sub> and S<sub>13</sub> can be found on the reachability tree, as can be seen on Fig. 4(b). It means that there are elementary reactions that are not startable, and because of this, the reaction pathway is not structurally startable.

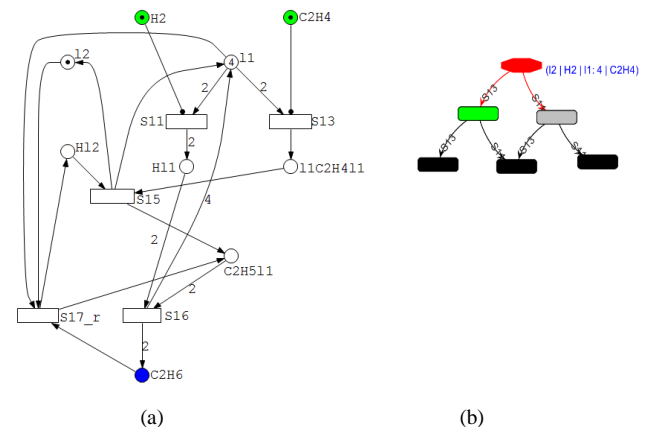


Fig. 4: The Petri net (a) and the reachability graph (b) of stoichiometrically feasible reaction pathway RP<sub>5</sub>.

Another method to determine the structural startability of reaction pathway is the siphon and trap analysis of Petri nets. The resulted minimal siphons of RP<sub>5</sub> and RP<sub>6</sub> reaction

pathways are shown in Fig. 5. and Fig. 7., respectively. The places of the siphons and the postset transitions of them are denoted by filled circles and rectangles, respectively.

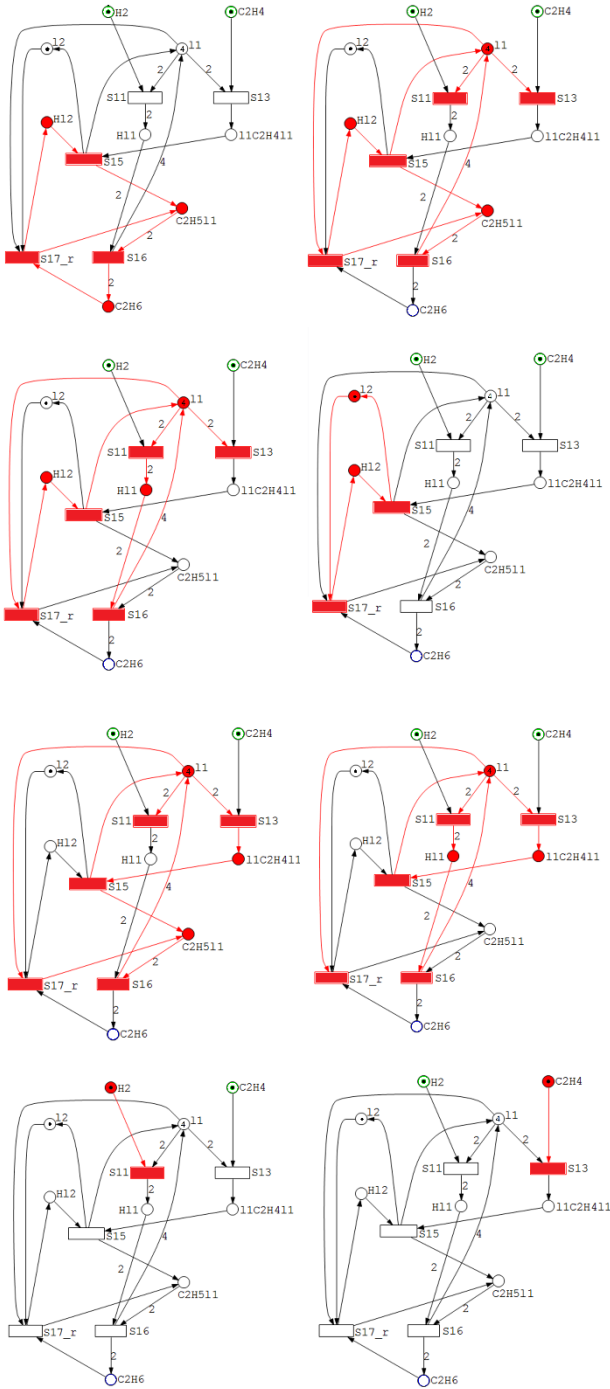


Fig. 5: Minimal siphons of stoichiometrically feasible independent pathway  $RP_5$ .

The necessary condition to avoid deadlock is, that every siphon must contain appropriate number of tokens, i.e., every siphon must have properly marked place(s) for firing almost one transition. In the initial state of reaction pathway  $RP_5$ :  $S_{11} + S_{13} + S_{15} + 2S_{16} + S_{17}(\text{reverse})$ , where the marked places are  $H_2$ ,  $C_2H_4$ ,  $l_1$  and  $l_2$ , as can be seen on Fig. 4(a), siphon  $S_1 = \{Hl_2, C_2H_5l_1, C_2H_6\}$  is empty. As a result of this, all transitions in postset of siphon  $S_1$ , namely  $S_{15}$ ,  $S_{16}$  and  $S_{17}(\text{reverse})$  are dead, therefore these elementary reaction steps are not

structurally startable, so the reaction pathway is not structurally startable.

For ensuring the necessary condition of deadlock-free in siphon  $S_1$ , at least one of the places of it, i.e.,  $Hl_2$  or  $C_2H_5l_1$  or  $C_2H_6$ , must be marked in the initial state. From a modified initial state, where  $H_2$ ,  $C_2H_4$ ,  $l_1$ ,  $l_2$  and  $C_2H_6$  are the initially available species, the resulted reachability graph of reaction pathway  $RP_5$  can be seen in Fig. 6. As all the elementary reactions can be found as arc label, the reaction pathway is structurally startable.

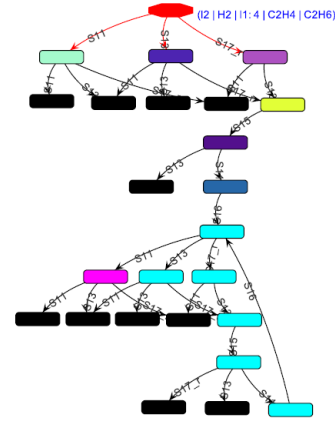


Fig. 6: The reachability graph of  $RP_5$  from initial state marked  $H_2$ ,  $C_2H_4$ ,  $l_1$ ,  $l_2$  and  $C_2H_6$ .

The stoichiometrically feasible independent pathway  $RP_5$ :  $S_{11} + S_{13} + S_{15} + 2S_{16} + S_{17}(\text{reverse})$  contains 8 minimal siphons and 4 minimal traps as summarized in Table V.

TABLE V. THE MINIMAL SIPHONS AND TRAPS OF  $RP_5$  REACTION PATHWAY

Minimal siphons	Minimal traps
$S_1 : \{ Hl_2, C_2H_5l_1, C_2H_6 \}$	$\tau_1 : \{ l_1, Hl_2, l_1C_2H_4l_1, Hl_1 \}$
$S_2 : \{ l_1, Hl_2, C_2H_5l_1 \}$	$\tau_2 : \{ l_2, Hl_2 \}$
$S_3 : \{ l_1, Hl_1, Hl_2 \}$	$\tau_3 : \{ l_1, l_1C_2H_4l_1, C_2H_5l_1, Hl_1 \}$
$S_4 : \{ l_1, Hl_2 \}$	$\tau_4 : \{ C_2H_5l_1, C_2H_6 \}$
$S_5 : \{ l_1, C_2H_5l_1, l_1C_2H_4l_1 \}$	
$S_6 : \{ l_1, Hl_1, l_1C_2H_4l_1 \}$	
$S_7 : \{ H_2 \}$	
$S_8 : \{ C_2H_4 \}$	

In case of reaction pathway  $RP_6$ :  $S_{12} + S_{13} + S_{14}(\text{reverse}) + 2S_{15} + S_{16}$ , when the marked places of the initial state are  $H_2$ ,  $C_2H_4$ ,  $l_1$  and  $l_2$ , as can be seen on Fig. 3(a), all the siphons are marked, so the necessary condition of the deadlock-free is fulfilled. The reaction pathway is structurally startable.

The stoichiometrically feasible independent pathway  $RP_6$ :  $S_{12} + S_{13} + S_{14}(\text{reverse}) + 2S_{15} + S_{16}$  contains 5 minimal siphons (see Fig. 7.) and 3 minimal traps as summarized in Table VI.

TABLE VI. THE MINIMAL SIPHONS AND TRAPS OF  $RP_6$  REACTION PATHWAY

Minimal siphons	Minimal traps
$S_1 : \{ l_2, Hl_2 \}$	$\tau_1 : \{ l_2, Hl_2 \}$
$S_2 : \{ l_1, l_1C_2H_4l_1, C_2H_5l_1 \}$	$\tau_2 : \{ l_1, l_1C_2H_4l_1 \}$
$S_3 : \{ l_1, l_1C_2H_4l_1, Hl_1 \}$	$\tau_3 : \{ C_2H_6 \}$
$S_4 : \{ H_2 \}$	
$S_5 : \{ C_2H_4 \}$	

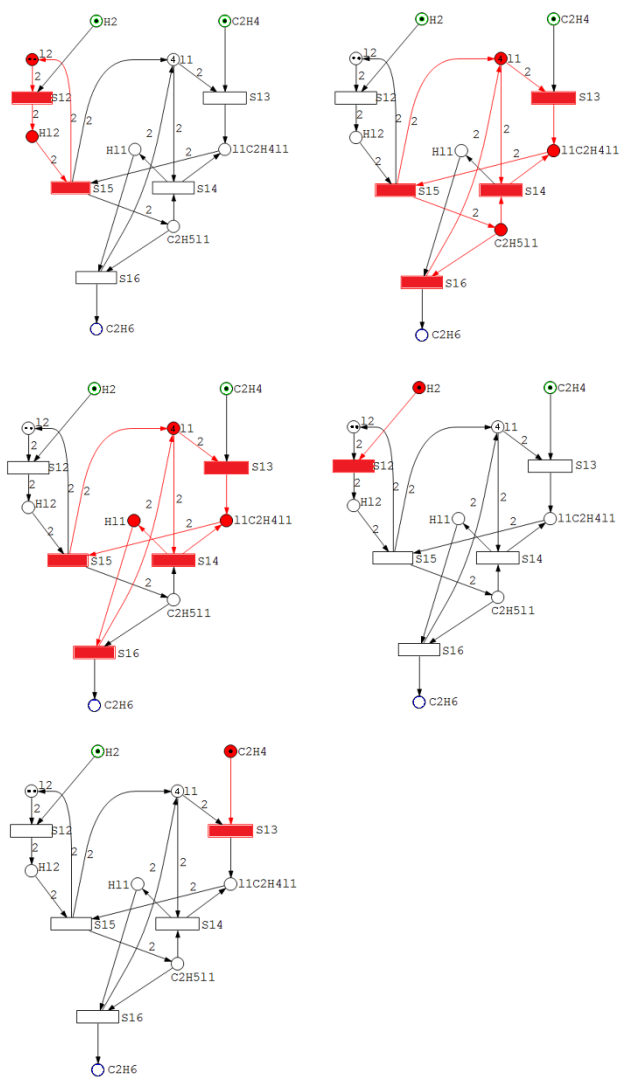


Fig. 7: Minimal siphons of stoichiometrically feasible independent pathway  $RP_6$ .

The places in siphon  $S_4$  and  $S_5$  represent the starting reactants. Therefore, these siphons remain marked until the starting reactants are available. Siphons  $S_1$ ,  $S_2$  and  $S_3$  contain minimal traps  $\tau_1$ ,  $\tau_2$  and  $\tau_2$ , respectively. As all these siphons are marked in the initial state, therefore according to the property of traps, they remain marked in any state. From the initial state where places  $H_2$ ,  $C_2H_4$ ,  $l_1$  and  $l_2$  are available, all the transitions can fire at least once (it means that every elementary reaction step operates), so the reaction pathway is structurally startable.

#### IV. CONCLUSIONS

P-graph framework can generate stoichiometrically feasible reaction pathways. The startability of these pathways can be tested by Petri net analysis. The reachability graph

analysis of Petri nets is theoretically capable of determining the startability of reaction pathway, but as this method is started with the generation of reachability graph, it is practically limited to small problems due to the computational effort growing exponentially according to the number of elementary reactions to be considered.

Contrarily structural startability examinations on siphon-trap analysis of Petri nets can effectively check the startability of reaction pathways. Moreover, the siphon-trap analysis helps identifying those initial states may potentially lead to a startable stoichiometrically feasible pathway.

All the major steps of the above proposed methods have been illustrated by case studies.

#### V. REFERENCES

- [1] Fan, L. T.; Friedler, F. Reaction Pathway Analysis by a Network Synthesis Technique. AIChE Annual Meeting 1997, Los Angeles, CA, U.S.A., November 16-21.
- [2] Friedler, F.; Tarjan, K.; Huang, Y.; Fan, L. Graph-theoretic approach to process synthesis: axioms and theorems. Chemical Engineering Science 1992, 47, 1973-1988.
- [3] Fan, L. T.; Bertok, B.; Friedler, F.; Shafie, S. Mechanisms of Ammonia-Synthesis Reaction Revisited with the Aid of a Novel Graph-Theoretic Method for Determining Candidate Mechanisms in Deriving the Rate Law of a Catalytic Reaction. Hungarian Journal of Industrial Chemistry 2001, 29, 71-80.
- [4] Petri, C. A. Kommunikation mit Automaten ; Rheinisch-Westfälisches Institut für Instrumentelle Mathematik an der Universität Bonn: Bonn, Germany, 1963.
- [5] Peterson, J. L. Petri Net Theory and the Modeling of Systems ; Prentice Hall: New Jersey, 1981.
- [6] Angeli, D.; De Leenheer, P.; Sontag, E. D. A Petri net approach to the study of persistence in chemical reaction networks. Mathematical Biosciences 2007, 201, 598-618.
- [7] Lakner R., Friedler F., Bertók B.: Synthesis and Analysis of Process Networks by Joint Application of P-graphs and Petri Nets. Lecture Notes in Artificial Intelligence, 10258 : Zaragoza 2017. 309-329.
- [8] Davis, M. E., Davis, R. J., Eds. Fundamentals of Chemical Reaction Engineering ; Mc-Graw - Hill: New York, 2003.
- [9] Heiner, M.; Herajy, M.; Liu, F.; Rohr, C.; Schwarick, M. Snoopy - a unifying Petri net tool. Proc. Petri nets 2012, LNCS 2012, 7347, 398-407.
- [10] Software P-graph Studio: <http://p-graph.org/downloads>
- [11] Heiner, M.; Schwarick, M.; Wegener, J. Charlie - an extensible Petri net analysis tool. Proc. Petri nets 2015, LNCS 2015, 9115, 200-211.
- [12] Murata, T. Petri Nets: properties, analysis and applications. Proc IEEE 1989, 77, 541-80.
- [13] Hideki, Y. On the Structure of Siphons of Petri Nets (Logics, Algebras and Languages in Computer Science). RIMS Kokyuroku 2014, 1915, 132-141.
- [14] Lakner R., Bertok B., Friedler F.: Synthesis of Startable Reaction Pathways. Chemical Engineering Transactions, 70, 2018, 1129-1134.
- [15] Fan, L. T.; Yu-Chuan, L.; Shafie, S.; Bertok, B.; Friedler, F. Exhaustive Identification of Feasible Pathways of the Reaction Catalyzed by a Catalyst with Multiactive Sites via a Highly Effective Graph-Theoretic Algorithm: Application to Ethylene Hydrogenation. Ind.Eng. Chem. Res. 2012, 51, 2548-2552.

# Evaluation of a genetic algorithm based image approximation method

Gergely Vakulya

Alba Regia Technical Faculty

Óbuda University

Székesfehérvár, Hungary

*vakulya.gergely@amk.uni-obuda.hu*

**Abstract**—In this paper a genetic algorithm (GA) based image approximation algorithm is presented for black and white images. The approximation uses a limited amount of triangles, where the GA is used to optimize their shape and position. The formal definitions, implementation details and test results are provided. The algorithm can produce recognizable approximations in less than 139 bytes.

**Keywords**—genetic algorithm, image approximation

## I. INTRODUCTION

Genetic algorithms (GA) [1] offer good approximations to various problems, where no fast algorithm is known to calculate the optimal solutions. It models the natural selection, where each member of a population (called specimen) represents one possible solution.

GA starts with an initial population, which is a set of possible solutions (e.g. empty or randomly generated). In each cycle GA produces new specimens by applying *mutation* and *crossover* operations on the existing ones. Then the population is evaluated by the *selection* operator based on the *fitness* function.

In this paper a GA-based lossy image compression method is presented. A number of triangles are used to approximate a monochromatic image; the position of the triangles are optimized with GA. The chromosome representation, the mutation and crossover operators and different selection strategies are evaluated. The algorithm is capable to give recognizable approximation of images in the 100 byte range, which means an extreme compression in exchange for the lower quality output.

## II. RELATED WORK

Genetic algorithms are suitable to problems, where there is no efficient solution available to calculate the optimal (or, in many cases, any) solution. An advantage of GA is the iterative operation, making it possible to stop the optimization process in any time and use the current best solution.

Scheduling is an everyday problem in industry [6] and transportation planning [3], where genetic algorithms can offer a good alternative to e.g. linear programming.

A similar area covers the Vehicle Routing Problems (VRP). A practical genetic algorithm based solution can be found in [4]. It is closely related to the traveling salesman problem, which can also be approximated with GA [5].

A good application of genetic algorithm is calculating the synaptic weights of neural networks. MarIO [2] is an AI player to the Super Mario game.

Genetic algorithms are also suitable to generate program code (genetic programming) to determine the behavior of e.g. autonomous robots. A good example is [7], where a specially tailored programming language (Robocode) is used to program virtual battle robots.

In economics portfolio optimization [8] and automatic trading [9] can be implemented with genetic algorithms.

In the area of image processing GA can be efficiently used in combination with neural networks for e.g. image segmentation [10] or image enhancement [12]. Image compression tends to use fast algorithms to give an identical (lossless compression) or an indistinguishable (lossy compression) representation of the input image, in significantly less space [11].

## III. THE GA-BASED IMAGE COMPRESSION

### A. Problem statement

An image *IMG* is given as square ( $n \times n$ ) matrix, where each pixel is either black or white:

$$IMG = (a_{ij}) \in \{0, 1\}^{n \times n} \quad (1)$$

An approximation is given as a set of  $n$  triangles. The vertices of the triangles are placed in the target image, in integer positions, and can have either black or white color. The  $k^{\text{th}}$  triangle  $t_k$  can be given as a quad:

$$t_k = (A, B, C, c), A, B, C \in 1 \dots n^2, c \in \{0, 1\} \quad (2)$$

Time  $I(t_k)$  image of triangle  $t_k$  is a set of points, which are geometrically between the vertices:

$$\begin{aligned} I(t_k) &= a_{ij}, \\ \exists \alpha, \beta &\in [0, 1] : \\ i &= \beta(\alpha A_1 + (1 - \alpha)B_1) + (1 - \beta)C_1 \\ j &= \beta(\alpha A_2 + (1 - \alpha)B_2) + (1 - \beta)C_2 \end{aligned} \quad (3)$$

### B. Chromosome representation

The chromosome representation of an approximation  $Q$  is a set of triangles, represented by a triplet  $(k, T, C)$ , where

- $k \in \mathbb{Z}$  is the number of triangles used in the approximation,
- $T \in \mathbb{Z}^{k \times 3 \times 2}$  is the set of triangles, given with 3 coordinate pairs,
- $C \in 0, 1^k$  is the set of triangle colors.

### C. Fitness function

The image form  $R$  of an approximation  $(k, T, C)$  is defined as follows:

$$R_{i,j}(k, T, C) = \begin{cases} C_v, & \exists v : (i, j) \in I(T_v), \\ \nexists w : w > v, (i, j) \in I(T_w), & \\ 1 \leq v, w \leq k & \\ 0, & \text{otherwise} \end{cases} \quad (4)$$

Instead of the fitness function, where the more suitable specimen have larger fitness, an  $E$  error function is used, representing the proportion of the mismatching area between the target image and the triangle based approximation, as a percentage.

$$E = \frac{\sum_{i,j} \left( \frac{|IMG_{i,j} - R_{i,j}|}{mn} \right)}{n^2} \cdot 100 \quad (5)$$

$1 \leq i, j \leq n$

### D. Genetic operators

The three genetic operators (mutation, crossover and selection) are implemented as follows. Three simple mutation types was built into the program.

- $M1$  removes a randomly selected triangle
- $M2$  adds a triangle with random coordinates
- $M3$  modifies the position of 1, 2 or 3 vertices of a triangle

The crossover operator takes triangles from two selected triangle-set and takes triangles from both, randomly.

During the selection the fitness function is calculated and a defined amount of the population is eliminated and overwritten by newly generated specimen (by crossover).

### E. Program flow

The flow of the program goes through the following steps.

- Step 1. Loading the reference image.
- Step 2. Generating the initial population, where each specimen consist of one randomly generated triangle.
- Step 3. Applying *mutation* operators for each specimen with predefined probabilities.
- Step 4. Calculating the *error* for each specimen.
- Step 5. Writing out statistical information.
- Step 6. Applying the *selection* operator, i.e. eliminating the specimen with the highest error.
- Step 7. Generating new specimen with *crossover* in place of the eliminated ones.
- Step 8. Repeating the procedure from Step 3 until achieving the desired number of generations.

### F. Software architecture

The image approximation algorithm is implemented in C, without using external libraries (besides glibc). This approach makes the code easily portable, but on the other hand it makes handling of different image formats more difficult. Thus, only loading and saving of BMP files with predefined resolution and color depth are supported.

The test program prints a short information line after each generation, which contains the generation number, the error of the best matching approximation and the current number of polygons. The best matching image is saved after each generation, to give more visual feedback.

With the actual settings each approximated image takes

- 8 bits to store the number of polygons,
  - $3 \times 2 \times 9 \times k$  bits to store the triangle coordinates,
  - and  $k$  bits to store the colors of the triangles,
- sum up to  $1 + \frac{55}{8}k$  bytes.

## IV. TEST RESULTS

To test the performance of the proposed image approximation method, two moderately complex test images was selected, as shown in Fig. 1. Both images have a resolution of  $512 \times 512$  pixels.

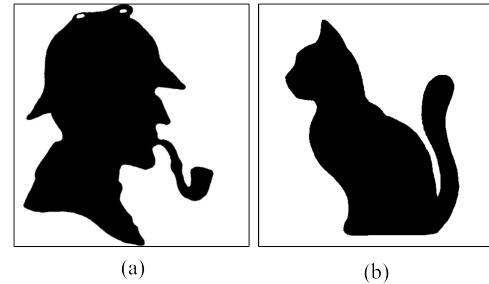


Fig. 1. The selected test images. (a) Silhouette of Sherlock Holmes, (b) Silhouette of a cat.

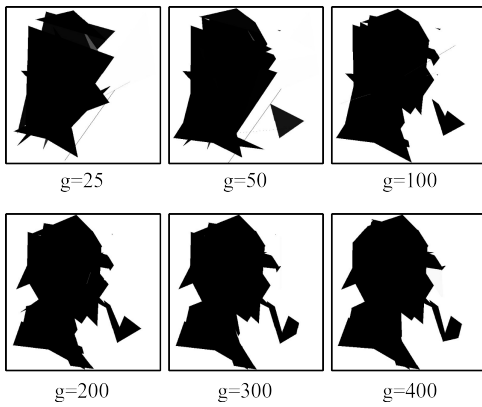
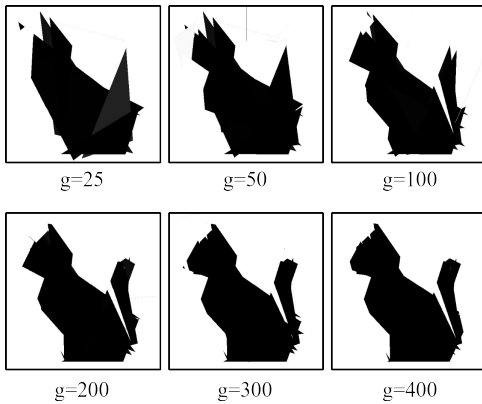
The approximation algorithm was tested with the selected images with the following settings. The size of the population is 2048. In each generation each specimen is mutated with the  $M1$ ,  $M2$  and  $M3$  operators with 10%, 50% and 80% probability, respectively. The 1800 worst specimen was overwritten with the crossover of randomly selected ones. Note that this is an elitist setup, which can lead to a fast convergence, at a risk of a less accurate final result.

The polygon limit was set to  $k_{max} = 5, 10, 15, 20, 30, 40, 50, 60, 70$  and  $80$ . Each different setup was run through 1000 generations.

Figures 2 and 3 show the image with the best fitness after 25, 50, 100, 200, 300 and 500 generations with  $k_{max} = 20$  polygons. As can be clearly seen, the accuracy of the approximation quickly increases first; both images are recognizable after 200 generations, but only slight improvements can be observed afterwards.

Figures 4 and 5 show the change of best observed fitness after each generation for the Sherlock and the cat images. Different colors mean different maximal triangle numbers. With



Fig. 2. The best matching Sherlock image after  $g$  generations.Fig. 3. The best matching cat image after  $g$  generations.

extremely low polygon count the approximation remains very rough. Adding more than approx. 30 triangles does not make any quantitative improvement, some extra detail was observed up to 60 triangles. A recognizable image approximated with 20 triangles takes 139 bytes of data.

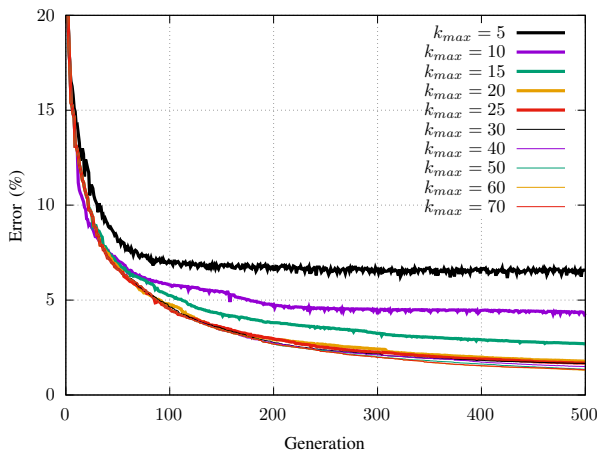


Fig. 4. Change of the fitness function during the approximation of the Sherlock image. The smallest error after each generation is shown for different polygon limits.

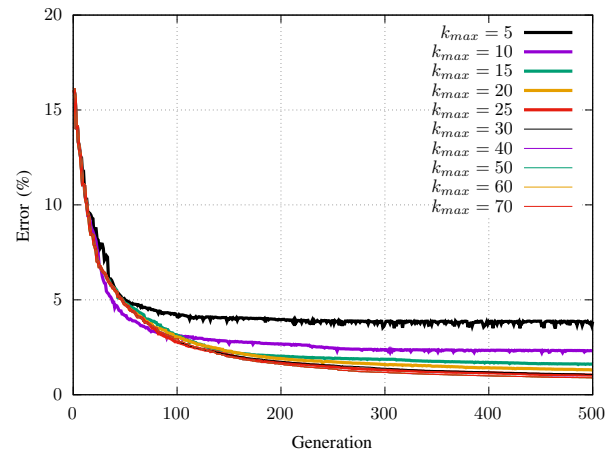


Fig. 5. Change of the fitness function during the approximation of the cat image. The smallest error after each generation is shown for different polygon limits.

TABLE I  
THE ERROR AFTER 1000 GENERATIONS WITH DIFFERENT  $k_{max}$  VALUES

Image name	$k_{max}$	Final error (%)	Size (bytes)
Sherlock	5	6.338	36
	10	4.218	70
	15	2.401	105
	20	1.439	139
	25	1.220	173
	30	1.301	207
	40	1.123	276
	50	1.006	345
	60	0.940	414
	70	0.898	483
Cat	5	3.775	36
	10	2.260	70
	15	1.320	105
	20	1.199	139
	25	0.837	173
	30	0.807	207
	40	0.532	276
	50	0.612	345
	60	0.569	414
	70	0.562	483

## V. COMPARISON TO COMPRESSION ALGORITHMS

Images can be compressed with (lossless and lossy) image compression algorithms and with general data compression software as well. To provide a comparison in term of size the test images were compressed with the two most well-known image compression methods (PNG and JPEG) and two general data compression solutions (rar and bzip2).

The compression level of PNG was set to the highest value and JPEG is tuned to worst quality (smallest file size) setting. Storing of extra data (i.e. EXIF, colorspace information) was turned off for both formats. Rar was used with `-m5 -md4096` settings, and the `-9` switch was used with bzip2. Both settings means the best possible compression. The proposed approximation algorithm was used with  $k_{max} = 20$  and  $k_{max} = 50$ . The results are summarized in Table II.

TABLE II  
THE RESULTING DATA AMOUNTS WITH IMAGE AND GENERAL DATA  
COMPRESSION ALGORITHMS AND WITH THE PROPOSED METHOD.

Compression method	Size (bytes)	
	Sherlock	cat
JPEG	2443	2521
PNG	2688	2247
rar	2059	1553
bzip2	1859	1690
GA ( $k_{max} = 20$ )	139	139
GA ( $k_{max} = 50$ )	345	345

## VI. SUMMARY

A genetic algorithm based image approximation method was proposed. The algorithm can approximate black and white images with a limited (definable) number of black and white triangles. The GA is implemented with 3 mutation and a crossover operator. Selection operator uses an elitist approach. Formal definition was given to the fitness function computation.

The proposed algorithm was implemented as a C language program and tested with different input images and with several maximal number of triangles.

The algorithm can generate a recognizable quality approximation of images with moderate complexity in less than 150 bytes with computation time under 10 minutes.

## REFERENCES

- [1] Sivanandam, S. N. and Deepa, S. N., "Introduction to Genetic Algorithms", Springer-Verlag Berlin Heidelberg, 2008, ISBN 978-3-540-73189-4
- [2] Baldominos A., Saez Y., Recio G., Calle J. "Learning Levels of Mario AI Using Genetic Algorithms", In: Advances in Artificial Intelligence. CAEPIA 2015. Lecture Notes in Computer Science, vol 9422. Springer, Cham. doi: 10.1007/978-3-319-24598-0\_24
- [3] C. Lin, J. Yu, J. Liu and C. Lee, "Genetic Algorithm for Shortest Driving Time in Intelligent Transportation Systems", 2008 International Conference on Multimedia and Ubiquitous Engineering, 2008, pp. 402-406, doi: 10.1109/MUE.2008.16.
- [4] Zhu, K. Q., "A new genetic algorithm for VRPTW", Proceedings of the international conference on artificial intelligence. 2000.
- [5] Ahmed, Z. H. "Genetic algorithm for the traveling salesman problem using sequential constructive crossover operator", International Journal of Biometrics & Bioinformatics (IJBB) 3.6 (2010): 96.
- [6] Lim, C., and Eoksu S., "Production planning in manufacturing/remanufacturing environment using genetic algorithm", Proceedings of the 7th annual conference on Genetic and evolutionary computation. 2005.
- [7] Shichel Y., Ziserman E., Sipper M., "Using Genetic Programming to Evolve Robocode Players" In: Genetic Programming. EuroGP 2005. Lecture Notes in Computer Science, vol 3447. Springer, Berlin, Heidelberg. [https://doi.org/10.1007/978-3-540-31989-4\\_13](https://doi.org/10.1007/978-3-540-31989-4_13)
- [8] S. Slimane and M. Benbouziane, "Portfolio Selection Using Genetic Algorithm" In: Journal of Applied Finance & Banking , Vol. 2, No. 4 (2012): pp. 143-154.
- [9] R.J. Kuo, C.H. Chen, Y.C. Hwang, "An intelligent stock trading decision support system through integration of genetic algorithm based fuzzy neural network and artificial neural network", Fuzzy Sets and Systems, Volume 118, Issue 1, 2001, Pages 21-45, ISSN 0165-0114, 10.1016/S0165-0114(98)00399-6.
- [10] Pare, S., Bhandari, A. K., Kumar, A., Singh, G. K., Khare, S. "Satellite image segmentation based on different objective functions using genetic algorithm: a comparative study." In 2015 IEEE international conference on digital signal processing (DSP) (pp. 730-734). IEEE.
- [11] Jayaraman, S., S. Esakkirajan, and T. Veerakumar. "Digital image processing", Mc Graw Hill India, 2009, ISBN 978-0070144798
- [12] Deborah, H., Arymurthy, A. M., "Image enhancement and image restoration for old document image using genetic algorithm", In 2010 Second International Conference on Advances in Computing, Control, and Telecommunication Technologies (pp. 108-112). IEEE.

# Using Sector Based Linear Regression in Epidemic Data

G. Nagy\*

\*Óbuda University, Alba Regia Technical Faculty, Institute of Geoinformatics

nagy.gabor@amk.uni-obuda.hu

ORCID ID: 0000-0001-9453-2291

**Abstract**—The statistical analysis and the machine learning are important tools of the research nowadays. In the last one and half year the importance of epidemic data and the analysis of this data has been increased as a result of the COVID-19 pandemic. This paper describes a research which uses Sector Based Linear Regression (SBLR), a robust linear regression for the analyzing and predicting with epidemic data.

**Index Terms**—robust regression, SBLR, Sector Based Linear Regression, COVID-19, epidemic data

## I. INTRODUCTION

The analysis of the collected data was very important at all times, but especially nowadays, when the computers can make highly difficult calculations for the better result. The international databases provide large amount of data about the COVID-19 epidemic, and we would like to discover the correlations and predict the numbers of following days.

### A. The analysis and prediction of epidemic data

The data of COVID-19 epidemic is published by many different authorities and organizations in the countries of the World. The data relates countries or lower regions spatial, and typically daily in time. The data collecting and integrating is a hard work, but fortunately there are repositories with the unified data. I use the data repository of the Centre for System Science and Engineering (CSSE) at John Hopkins University [1], [2].

This dataset can be downloaded from GitHub<sup>1</sup>. The dataset contains many CSV (coma separated values) files with different values (confirmed cases, deaths, recovered, etc) by date and country (or lower level region). The CSV is a simple and well usable format for the programs, which will be introduced in the remaining part of this article.

### B. The SBLR method

The Sector Based Linear Regression (SBLR) is an robust linear regression method [3], this is a generalized case of the Fitting Disc Method [4], which was developed for point cloud processing. The principle of SBLR is shown in two dimension in the Figure 1. The method looks for a line so, that this line divides the control points to two equal set in each sector (the right and the left side of the area).

The SBLR may be used with different quantiles, but in this paper I use only  $q = 0.5$ .

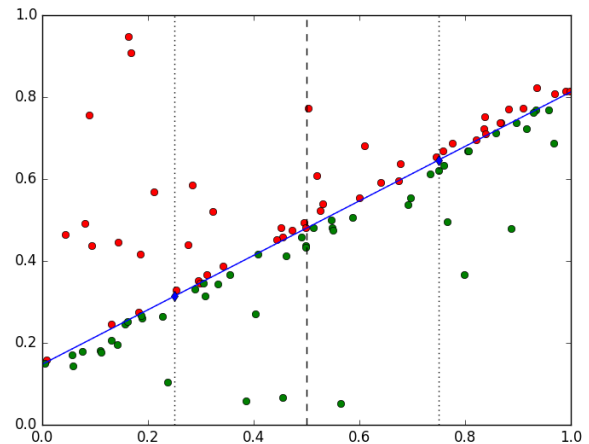


Figure 1. The principle of SBLR method. The half of the control points are above, and the another half are under the regression line in each sector. This is an robust regression, because the outlier control points do not modify significantly the regression line.

## II. LINEAR AND EXPONENTIAL REGRESSION

The epidemic waves have a phase when the growth is exponential. The prediction of the values is very important in this days.

The SBLR provides an linear regression method. The method can be applicable, if we use the logarithms of the values. The predicted values (for the following days) will be calculated by the exponent function.

This modification is suitable, if the dataset does not contain 0 values. In the analysis of this paper I selected time intervals without 0 data.

## III. DATA AND SOFTWARE

There is a Python [5], [6], [7] module, which has been implemented the SBLR method:

```

"""
Module for Sector Based Linear Regression
(See in: DOI: 10.14232/actacyb.23.4.2018.3)
Author: Nagy Gábor
"""

import numpy

def regnd(n):
    """The coordinates of the nodes of a regular n-dimensional hypertetrahedron,
    which centre is in the origin, and the distances
    of the nodes from the origin are 1"""
    if n==0:

```

<sup>1</sup><https://github.com/CSSEGISandData/COVID-19>

```

        return [[]]
    else:
        return [ [ y*(1-(1/n)**2)**0.5 for y in x]+[-1/n]\
                for x in regnd(n-1)]+[[0.0]*(n-1)+[1.0]]

def scaledl(lst, lm):
    """Scale a list of coordinates by lm"""
    return [ [ y*lm for y in x] for x in lst]

def lintr(lst, la, lb):
    """Calculate the linear transformation of the coordinates
    of the lst by x'=ax+b with the parameters of la and lb."""
    return [ [ la[i]+li[i]+lb[i] for i in range(len(lst[0]))] for li in lst]

def calctr(ptlst):
    """Calculate the transformation parameters for linear transform
    to (-1,...,-1)-(+1,...,+1) n-dimension cube every point of the lst"""
    nr=range(len(ptlst[0]))
    if len(ptlst)<2:
        return ([1 for i in nr], [-ptlst[0][i] for i in nr])
    mincoord=list(map(min, numpy.transpose(ptlst)))
    maxcoord=list(map(max, numpy.transpose(ptlst)))
    apar=[ 2/(maxcoord[i]-mincoord[i]) for i in nr]
    return (apar, [-1-mincoord[i]*apar[i] for i in nr])

def minidx(lst):
    """Return the index of the minimal value of the list."""
    wlst=list(lst)
    ret=0
    for i in range(1, len(wlst)):
        if wlst[i]<wlst[ret]:
            ret=i
    return ret

def linpar2cth(linpars):
    """Calculate centre heights from the linear parameters."""
    dim=len(linpars)-1
    ctcoords=[x*[1] for x in scaledl(regnd(dim), dim/(dim+1))]
    return (sum([x[i]*linpars[i] for i in range(dim+1)]) for x in ctcoords)

def cth2linpar(cths, chidx=-1, chcoord=[]):
    """Calculate linear parameters from the centre height."""
    dim=len(cths)-1
    ctcoords=[x*[1] for x in scaledl(regnd(dim), dim/(dim+1))]
    wcths=list(cths)
    if chidx>-1:
        ctcoords[chidx]=chcoord[:dim+1]
        wcths[chidx]=chcoord[-1]
    return list(numpy.linalg.solve(ctcoords, wcths))

def sbllr(ptlst, q=0.5):
    """Calculate linear equation to the pointlist by SBLR method"""
    dim=len(ptlst[0])-1
    ctps=scaledl(regnd(dim), dim/(dim+1))
    ctcoords=[x*[1] for x in ctps]
    ptsep=[[1] for x in range(dim+1)]
    pa,pb=calctr(ptlst)
    pa[-1]=1
    pb[-1]=0
    for pti in lintr(ptlst, pa, pb):
        ptsep[minidx((sum((pti[j]-ctps[i][j])**2 for j in range(dim)))\
                    for i in range(dim+1))].append(pti)
    if min(map(len, ptsep))<1:
        raise ValueError('Wrong distribution, empty sector!')
    cths=numpy.percentile([x[-1] for x in si], q*100 for si in ptsep)
    fullstep=0
    noch=0
    secid=0
    while noch<dim+1 and fullstep<100*dim+2:
        oldcth=cths[secid]
        cths[secid]=numpy.percentile((linpar2cth(cth2linpar(cths, secid, x))[secid]\
                    for x in ptsep[secid]), q*100)
        if abs(oldcth-cths[secid])>1E-5:
            noch=0
        else:
            noch+=1
            secid=(secid+1)%dim+1
            fullstep+=1
    retpar=cth2linpar(cths)
    return [retpar[i]*pa[i] for i in range(dim)]+\
        [sum([retpar[i]*pb[i] for i in range(dim)])+retpar[-1]]

```

This module can be downloaded from GitHub<sup>2</sup>.

The SBLR module provides linear regression in an  $n$ -dimensional space, but I use only the two dimensional case in this paper.

#### IV. TESTING THE METHOD

I use 28 days intervals from the exponential growth phases of the waves. This is four full week, the dataset contains four-point from every day of the week.

The data series, the regressed curve are shown in Matplotlib [8], [9] diagrams.

The Figure 2 shows the result of a regression. The orange line is an exponential curve, which has been fit to the last 28 days values marked by blue. The predicted curve is the red line, this is the continuation of the fitted line. Because this

<sup>2</sup><https://github.com/ngabor/sblr>

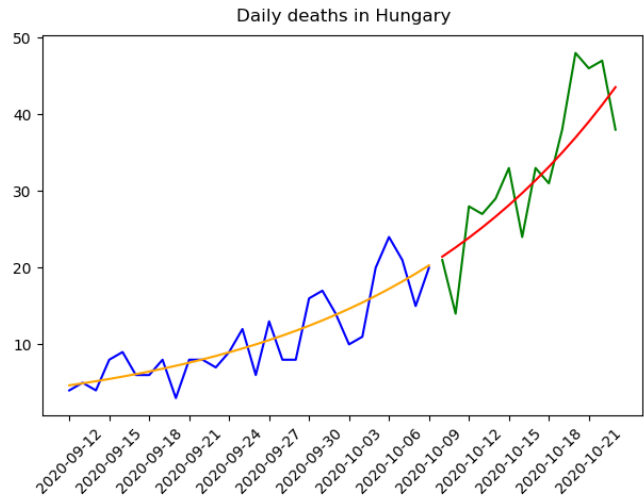


Figure 2. The predicted deaths in Hungary in the beginning of the second wave.

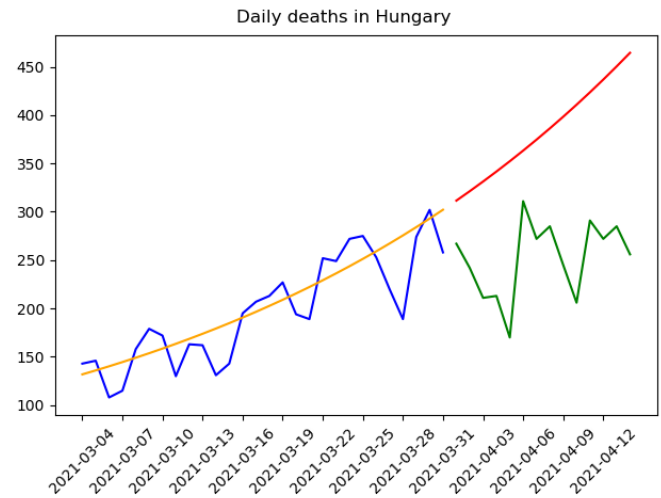


Figure 3. The predicted deaths in Hungary in the top of the third wave. The prediction is wrong, because the growth had stopped.

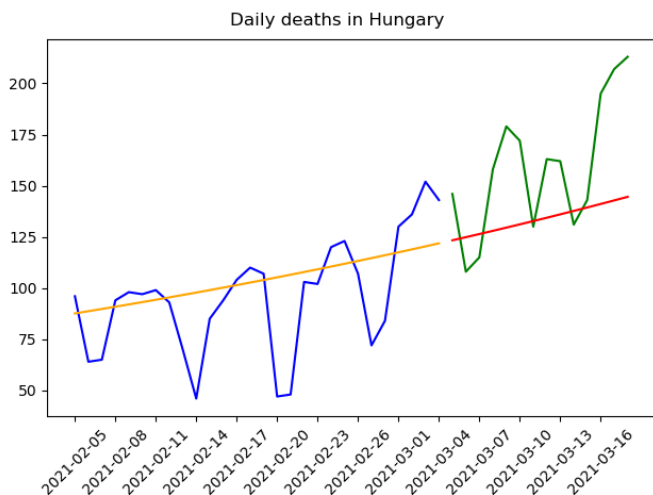
data is from the last year, I can draw the realized values by the green line.

The described method can predict only the exponential phase of a wave. The Figure 3 presents an unwell regression in the top of the third wave, when the growth was stopped.

#### V. CONCLUSION

The SBLR method is an robust linear regression method. This method may be applied with exponentially increasing case, if we use the logarithms of the values.

The described method can predict the values of the following days from the data of the previous period, but the predictions are correct only the exponential growth phase.



[9] J. D. Hunter, “Matplotlib: A 2d graphics environment,” *Computing In Science & Engineering*, vol. 9, no. 3, pp. 90–95, May-Jun 2007.

Figure 4. The predicted deaths in Hungary in the beginning of the third wave.

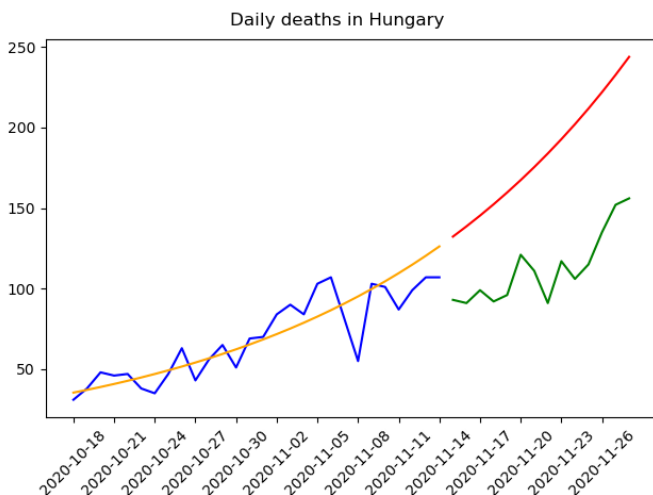


Figure 5. An unwell regression from the growing phase of the second wave.

### REFERENCES

- [1] J. CSSE, “Covid-19 data repository by the center for systems science and engineering (csse) at johns hopkins university,” 2020. [Online]. Available: <https://github.com/CSSEGISandData/COVID-19>
- [2] E. Dong, H. Du, and L. Gardner, “An interactive web-based dashboard to track covid-19 in real time,” *The Lancet infectious diseases*, vol. 20, no. 5, pp. 533–534, 2020.
- [3] G. Nagy, “Sector based linear regression, a new robust method for the multiple linear regression,” *ACTA CYBERNETICA*, vol. 23, no. 4, pp. 1017–1038, 2018.
- [4] G. Nagy, T. Jancsó, and C. Chen, “The fitting disc method, a new robust algorithm of the point cloud processing,” *ACTA POLYTECHNICA HUNGARICA*, vol. 14, no. 6, pp. 59–73, 2017.
- [5] G. Van Rossum *et al.*, “Python Programming Language.” in *USENIX Annual Technical Conference*, vol. 41, 2007.
- [6] T. E. Oliphant, “Python for scientific computing,” *Computing in Science & Engineering*, vol. 9, no. 3, 2007.
- [7] K. J. Millman and M. Aivazis, “Python for scientists and engineers,” *Computing in Science & Engineering*, vol. 13, no. 2, pp. 9–12, 2011.
- [8] G. Nagy, “Matplotlib in the geospatial analyzes,” in *12th International Symposium on Applied Informatics and Related Areas (AIS 2017)*, G. T. Orosz, Ed. Óbudai Egyetem, 2017, pp. 90–93.

**ORAL SESSION II.**

**Applied Informatics II.**

# Forced facial expression – the effect of different emotions and temporal patterns

Jozsef Halasz  
 Obuda University AMK,  
 Szekesfehervar, Hungary;  
 Pro Rekreatioe TOC,  
 Gardony, Hungary

[halasz.jozsef@amk.uni-obuda.hu](mailto:halasz.jozsef@amk.uni-obuda.hu)

Erika Peukert  
 Dept. of Psychiatry,  
 St. George Univ. Teaching Hospital,  
 Szekesfehervar, Hungary  
[peukert.erika@gmail.com](mailto:peukert.erika@gmail.com)

Edina Lukacs  
 Pro Rekreatioe TOC,  
 Gardony, Hungary  
[lukacs.edina@toparti.hu](mailto:lukacs.edina@toparti.hu)

Aniko Mahler  
 Pro Rekreatioe TOC,  
 Gardony, Hungary  
[mahlerne.kofner.aniko@toparti.hu](mailto:mahlerne.kofner.aniko@toparti.hu)

**Abstract**—In recent years, the importance of facial expression patterns has been recognized, e.g. in information society, neuroscience. In the present paper, forced facial expression patterns were studied by the means of the FaceReader 8.1 system. Human subjects were asked to mimic FEEST-related static facial expressions over 4 seconds each, and their expression was registered and analyzed. The temporal dynamics of a positive and negative valence expression, happiness and anger was analyzed, altogether with arousal data. General linear model was used to establish statistical differences. A significant interaction occurred between the content of input emotion (happiness/anger) and the temporal patterns (expressed anger, happiness, valence). The interaction was not significant in the case of the measured arousal. Our data indicate the importance of studying forced facial expression patterns in the interpretation of complex emotional stimuli.

**Keywords** — *emotions, facial expressions, recognition system, stimulus intensity.*

## I. INTRODUCTION

There is a growing interest for facial affect recognition systems in the field of computer sciences, market research, education and basic psychology/psychiatry research [1-6]. Advances in the facial affect recognition in recent years led to the development of facial affect recognition systems, among them the Noldus FaceReader [7]. Several types of affect recognition systems were introduced, and the long-term-goal of these systems is to help individuals with problems in social recognition [3,6]. Recognizing facial affect is a major component of social interactions, and mirrors several elements of the social recognition procedure. It is clear that facial affect recognition is accompanied by studying expression patterns. Thus, not only the expression to be recognized is getting

important, but studying natural or posing expression or social re-expression patterns are also getting more prominent [4, 5]. Originally, six basic universal emotions (anger, disgust, fear, happiness, sadness, surprise) were described as pan-cultural elements of facial affect [8]. In principle, the perception and interpretation of facial affect in humans is a time-dependent multilayer mechanism for each emotion [9].

Additional to its importance in the interpretation of human communicative signals, facial affect recognition systems might be considered as “social prosthetics” in vulnerable individuals [3]. Major psychiatric conditions affecting emotion recognition is autism spectrum disorder and antisocial personality disorder [10-15]. In these cases, long-term misinterpretation of social signals might result a more pronounced social dysfunction, but other psychiatric disorders, e.g. attention deficit hyperactivity disorder (ADHD), major depression are accompanied by social dysfunction [16]. Unfortunately, these studies did not target forced facial expression patterns, but studying these patterns might help to understand discrepancies in the circle of social functioning and therapeutic interventions [17-18].

Albeit FaceReader is validated for the recognition of the basic Ekman-like expressions, to our best knowledge, forced facial expression patterns were out of the scope of these studies [19-20].

The aim of the present study was to describe the detailed response profile of individuals by the means of the FaceReader system during forced facial expression patterns mimicking validated inputs of anger and happiness in a well-known stimulus database, the Facial Expression of Emotion: Stimuli and Test (FEEST). These data were used as technical preparations for studying preschoolers and their parents with certain psychopathologies both in terms of recognizing and expressing emotions.

## II. METHODS

The FEEST Emotion subtest is based on the six universal emotions described by Ekman and colleagues [8,21]. From the Ekman database, only faces expressing happiness and anger were used, altogether 11 faces (5 males, 6 females) with both emotions (22 stimuli). These faces were randomized, and a video input was created with 4 seconds of a particular stimulus face visible following 4 seconds of a blank screen. Three adults were asked to mimic the visual inputs as long as they see that on the screen. The study creates preliminary data for testing the usage of the forced expression test and to optimize data collection for applying to children and their parents in social context. The Noldus FaceReader system was originally developed for marketing applications [7], at present version 8.1 was used. Representative stimuli (anger and happiness) along with the surface of the FaceReader were presented in Figure 1 and 2. The FaceReader was used to analyze the videorecordings of the faces of the individuals during the forced expression test. General model was used with smoothening classification. 30 frames per seconds were analyzed, and data collection was performed ten times per seconds. Only four emotion related data types were collected (angry, happy, valence, arousal), 5280 data points for each emotions were used for the statistical analysis.

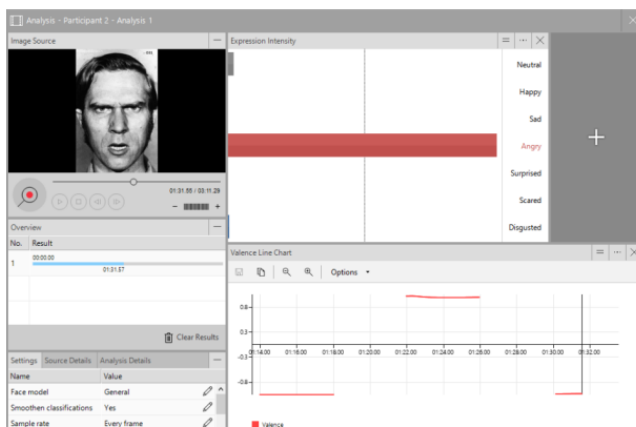


**Figure 1.** Representative stimulus face with the expression of anger. Participants were asked to mimic the expression as long as it was visible on the screen. Stimulus faces were on for 4 seconds, and a 4 second blank screen interval was present. FaceReader 8.1 screenshot.

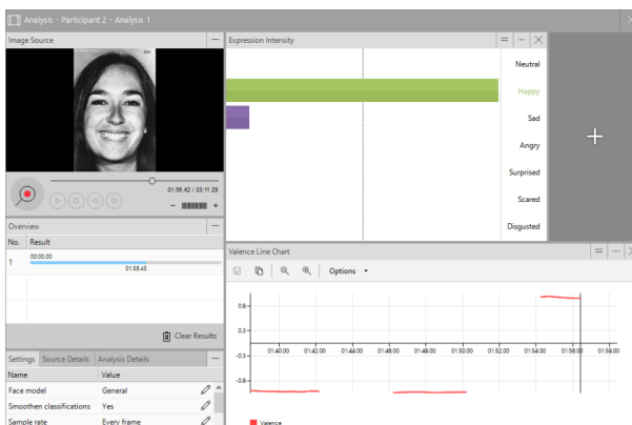


**Figure 2.** Representative stimulus face with the expression of happiness. Participants were asked to mimic the expression as long as it was visible on the screen. Stimulus faces were on for 4 seconds, and a 4 second blank screen interval was present. FaceReader 8.1 screenshot.

SPSS 20.0 was used to test the overall effect of the gender of the stimulus faces (male vs. female), stimulus type (anger vs. happiness) and the timing of the stimulus (during vs. over) (General Linear Model, GLM). Statistica 7.0 program was used to evaluate the timeline (per second, 4 seconds with stimulus on, 4 seconds with stimulus off) according to the stimulus type (GLM). Newman-Keuls post hoc comparisons were also run where appropriate.  $p < 0.05$  was considered as significant difference.

## III. RESULTS

In the detailed analysis, data loss was 2.8%. Gender and emotion interaction was present in the case of happy ( $F_{(2,5130)}=68.857$ ,  $p < 0.001$ ), angry ( $F_{(2,5130)}=18.541$ ,  $p < 0.001$ ), valence ( $F_{(2,5130)}=49.843$ ,  $p < 0.001$ ) and arousal ( $F_{(2,5130)}=38.526$ ,  $p < 0.001$ ) (Fig. 3).

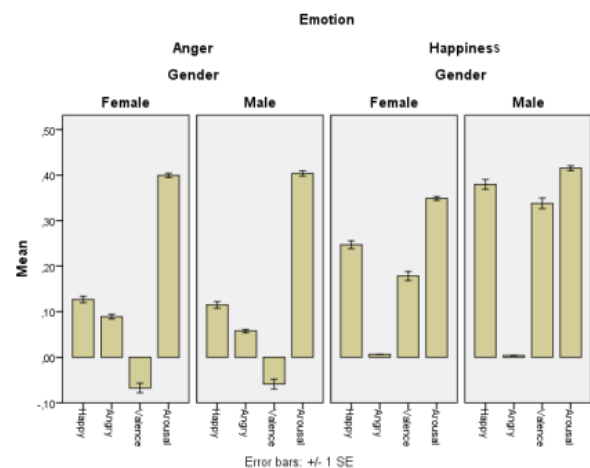


**Figure 3.** The overall effect of the gender and the emotion content of the stimulus faces during the study. X axis represent emotion content of the individuals with forced expressions. Y axis, arbitrary unit of the emotion content. Means and SE (standard error of the mean) are presented.

State (during input stimulus vs. over input stimulus) and emotion interaction was present in the case of happy ( $F_{(2,5130)}=773.366$ ,  $p < 0.001$ ), angry ( $F_{(2,5130)}=320.795$ ,  $p < 0.001$ ), valence ( $F_{(2,5130)}=1161.416$ ,  $p < 0.001$ ), but not in the case of arousal ( $F_{(2,5130)}=2.271$ ,  $p = 0.12$ ) (Fig. 4).

The 3-way interaction (gender, state and emotion) was also significant in the case of happy ( $F_{(1,5126)}=3.866$ ,  $p < 0.05$ ), angry ( $F_{(1,5126)}=8.856$ ,  $p < 0.003$ ), valence ( $F_{(1,5126)}=4.227$ ,  $p < 0.04$ ), but not in the case of arousal ( $F_{(1,5126)}=3.202$ ,  $p = 0.74$ ) (Fig. 5). Time and emotion interaction (but not gender interaction) was present in the case of happy ( $F_{(7,126)}=14.294$ ,  $p < 0.001$ ), angry ( $F_{(7,126)}=6.103$ ,  $p < 0.001$ ), valence ( $F_{(7,126)}=24.752$ ,  $p < 0.001$ ), but not in the case of arousal ( $F_{(7,126)}=0.560$ ,  $p = 0.44$ ) (Fig. 6-9).



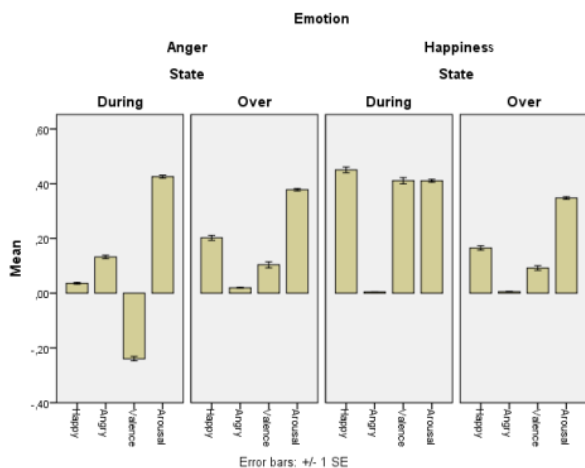


Figure 4. Summarized effect of the forced expression patterns by the two applied stimulus types (anger and happiness). During, average of the 4 seconds when the stimulus emotion was on; over, average of the 4 seconds when the stimulus emotion was off. Detailed statistics is described in the text.

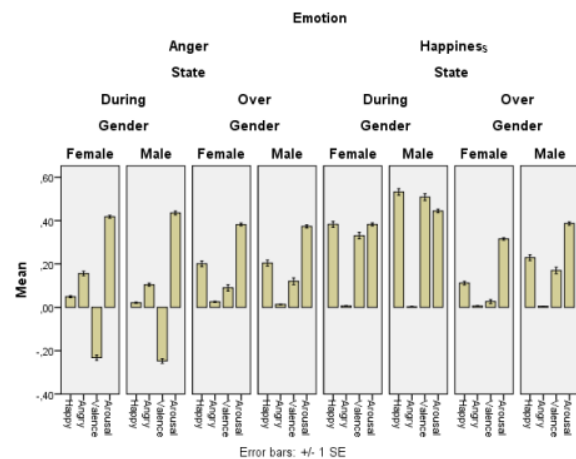


Figure 5. Summarized effect of the forced expression patterns by gender, the two applied stimulus types (anger and happiness) and state. During, average of the 4 seconds when the stimulus emotion was on; over, average of the 4 seconds when the stimulus emotion was off. Detailed statistics is described in the text.

IV. DISCUSSION

The main results of the present study were the following. First, unlike naturally expressed emotions or microemotions, long-lasting forced expressions have rebound effects, e.g. expressing anger accompanied by increased happy feelings afterwards. Second, a major gender, state and input stimulus interaction was observed in the case of happy, angry, and valence data. Third, arousal data were continuously high during the experimental setting, irrespective of the nature or the presence of the stimuli.

Emotion recognition systems are regularly more sensitive to happiness than to other emotions, like anger [22-24]. Busso et al reported higher sensitivity to happiness compared to anger recognition [23], irrespective of the methodology used. In a study where FaceReader was tested in relation with EMG activity, the highest correlation was achieved between the

activity of musculus zygomaticus activity and happiness labeling ( $r=0.72$ ), while smaller but still significant effect was achieved in the case of musculus corrigator activity and anger expression ( $r=0.55$ ) [25]. Overall, there are general differences in the sensitivity of recognizing distinct emotions in humans.

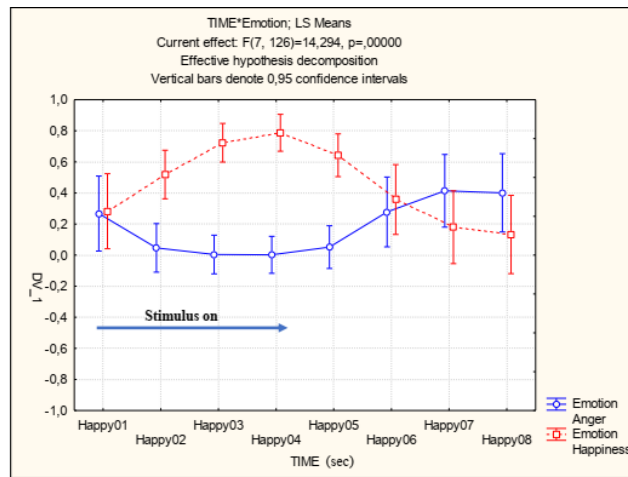


Figure 6. X axis represents emotion content (happy) of the individuals with forced expressions, timeline is presented, the 01-04 values (4 seconds) represent the stimulus (anger or happiness) on, while the 05-08 values represent the stimulus off (4 seconds). Y axis, arbitrary unit of the emotion content (happy). Means and 95% confidence intervals are presented.

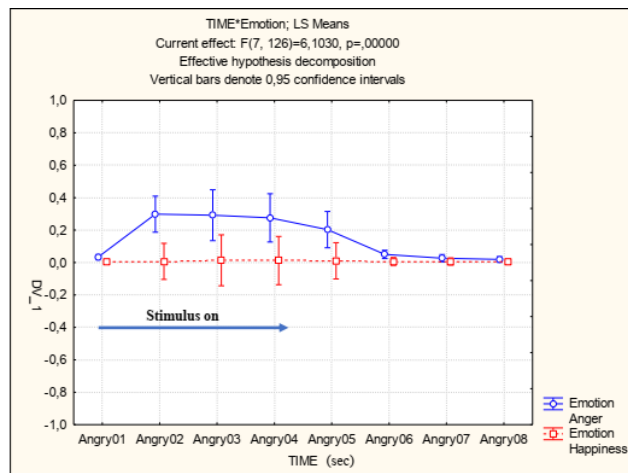
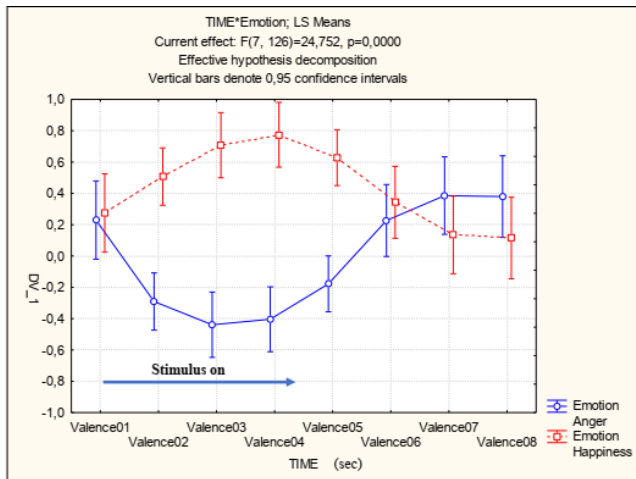


Figure 7. X axis represents emotion content (angry) of the individuals with forced expressions, timeline is presented, the 01-04 values (4 seconds) represent the stimulus (anger or happiness) on, while the 05-08 values represent the stimulus off (4 seconds). Y axis, arbitrary unit of the emotion content (angry). Means and 95% confidence intervals are presented.

Facial affect recognition might have major importance in the pathogenesis in certain psychiatric disorders [10-16]. Alterations described in the working of the amygdalo-prefrontal systems were described both in animal models [26-27] and in human studies [28-30]. Direct therapeutic processes targeting facial affect recognition are widely and beneficially used [11,12,15], albeit it is still questionable whether these processes might be able to modify core symptoms of the pathological conditions.

Philip et al reported subtle differences in response to facial expressions of real vs. virtual faces [31]. Facial electromyography revealed that rapid facial reactions were significantly stronger in the case of joy and anger when participants were presented with real faces compared with virtual ones. Interestingly, this effect was not present in the

case of sadness. As happiness and anger might have a major role in evolutionary processes (the 'angry male' and 'happy female' hypothesis), it is always important to study the effect of individual expressed emotion instead using emotion recognition or expression in general [32].



**Figure 8.** X axis represents emotion content (valence) of the individuals with forced expressions, timeline is presented, the 01-04 values (4 seconds) represent the stimulus (anger or happiness) on, while the 05-08 values represent the stimulus off (4 seconds). Y axis, arbitrary unit of the emotion content (valence). Means and 95% confidence intervals are presented.

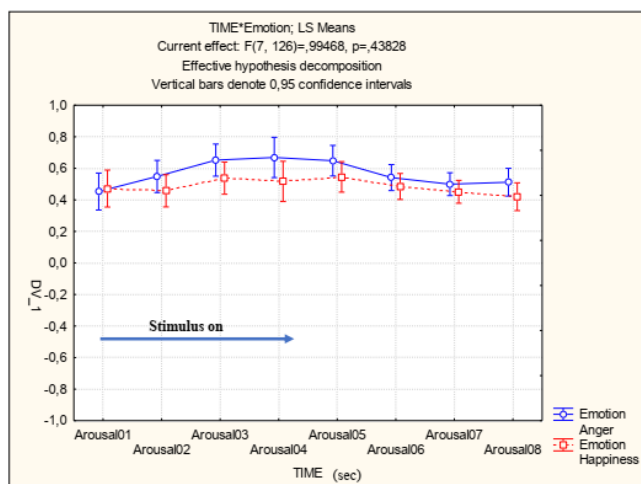


**Figure 9.** X axis represents emotion content (arousal) of the individuals with forced expressions, timeline is presented, the 01-04 values (4 seconds) represent the stimulus (anger or happiness) on, while the 05-08 values represent the stimulus off (4 seconds). Y axis, arbitrary unit of the emotion content (arousal). Means and SE (standard error of the mean) are presented.

Our results indicate that not only the type of the emotion, but the gender of the expresser and the timing of the stimuli might be crucial in the interpretation and in the re-expression. As we noted earlier, responding appropriately to the facial expression of others is a major factor in proper social functioning. It is widely acknowledged that understanding facial emotion expressions is critical, but unintentional and intentional self-re-expressions might cause troubles in social communication [33]. First, certain individuals need social prosthetics to help their interpretations, and the future of emotion recognition systems is to help these individuals [3,4,6]. Second, the recognition of emotions is not enough, but a proper re-expression is inevitable. Moreover, mimicking the expression during the recognition process might help the individuals in gaining better results in recognition [34,35].

Thus, these two sides can not be easily distinguished, what is clear, that people with autism spectrum disorder have multiple difficulties in this respect [11,36]. Posed vs. genuine expression can be used to help individuals with social difficulties [review: 37], but it is also unclear whether neurotypical subjects are able to distinguish properly the expression of individuals with autism spectrum disorder [38]. Thus, planning experiments all these things have to be taken into account. Our data on arousal indicate that between stimulus intervals were emotionally intensive for the subjects, and probably the effect has major importance when subject with behavioural problems would be tested. Our results also indicate to take the interstimulus intervals seriously, robust, overall analysis patterns for the whole timing of the studies would be inappropriate, but detailed framing is recommended.

The limitations of our study that only anger and happiness were used as stimulus emotions, and instead of dynamic, but long lasting emotions (e.g. slow emotions with reduced speed), a long static input was delivered to the subjects. The only advantage of static inputs were the clear cut latency data throughout the procedure. Using these inputs the effect of valence and arousal data could be interpreted, as these emotions are accompanied by high (opposite) valence and high arousal levels.

In a further step, we would like to assess the facial expression profile both in preschool children and their parents, also in natural settings and also during forced expression test. Understanding and controlling expression patterns might facilitate or disrupt dual communication signals. Later, we would like to discuss with couples their facial expression patterns to the emotions expressed by their children, and also in settings when their child is getting involved in a situation what might be emotionally intense to their parents. The process might have crucial importance in parent training that is considered as number one intervention for preschool children with ADHD or conduct disorder, but literature data is also indicating the usage of the procedure in children with autism spectrum disorder or attachment problems. An independent effect of perioral or eye region is also suggested, and an intervention study using action units (identical actions of independent facial muscles) is planned.

#### ACKNOWLEDGMENT

The authors declare no conflict of interest.

#### REFERENCES

- [1] B. Fasel, and J. Luetttin, "Automatic facial expression analysis: a survey", *Pattern Recogn.*, vol. 36, pp. 259–275, 2003.
- [2] I. Cohen, N. Sebe, A. Garg, L.S. Chen, and T.S. Huang, "Facial expression recognition from video sequences: temporal and static modeling", *Comp. Vis. Image Understanding*, vol. 91, pp. 160–187, 2003.
- [3] N. Samadiani *et al.*, "A Review on Automatic Facial Expression Recognition Systems Assisted by Multimodal Sensor Data", *Sensors*, vol. 19, art. E1863, 2019.

- [4] F. Zhang, T. Zhang, Q. Mao, and C. Xu, „Geometry Guided Pose-invariant Facial Expression Recognition”, *IEEE Trans. Image Process. Publ. IEEE Signal Process. Soc.*, 2020, doi: 10.1109/TIP.2020.2972114.
- [5] Y.-J. Hong, S. E. Choi, G. P. Nam, H. Choi, J. Cho, and I.-J. Kim, „Adaptive 3D Model-Based Facial Expression Synthesis and Pose Frontalization”, *Sensors*, vol. 20, no. 9, art. E2578, 2020, doi: 10.3390/s20092578.
- [6] B. C. Ko, „A Brief Review of Facial Emotion Recognition Based on Visual Information”, *Sensors*, vol. 18, art. E401, 2018, doi: 10.3390/s18020401.
- [7] Noldus Information Technology B.V., „FaceReader 8.0 Reference Manual”, Noldus GMB, The Netherlands, 2019.
- [8] P. Ekman, E.R. Sorenson, and W.V. Friesen, „Pan-cultural elements in facial displays of emotion”, *Science*, vol. 164, pp. 86–88, 1969.
- [9] R. Adolphs, „Recognizing emotions from facial expressions: psychological and neurological mechanisms”, *Behav. Cogn. Neurosci. Rev.*, vol. 1, pp. 21–62, 2002.
- [10] B. Chakrabarti, and S. Baron-Cohen, „Empathizing: neurocognitive developmental mechanisms and individual differences”, *Prog. Brain Res.*, vol. 156, pp. 403–417, 2006.
- [11] G. Golarai, K. Grill-Spector, and A.L. Reiss, „Autism and the development of face processing”, *Clin. Neurosci. Res.*, vol. 6, pp. 145–160, 2006.
- [12] O. Golan, and S. Baron-Cohen, „Systemizing empathy: teaching adults with Asperger syndrome or high-functioning autism to recognize complex emotions using interactive multimedia”, *Dev. Psychopathol.*, vol. 18, pp. 591–617, 2006.
- [13] S. Baron-Cohen, O. Golan, and E. Ashwin, „Can emotion recognition be taught to children with autism spectrum conditions?”, *Philos. Trans. R. Soc. Lond. B. Biol. Sci.*, vol. 364, pp. 3567–3574, 2009.
- [14] A.A. Marsh, and R.J. Blair, „Deficits in facial affect recognition among antisocial populations: a meta-analysis”, *Neurosci. Biobehav. Rev.*, vol. 32, pp. 454–465, 2008.
- [15] M.R. Dadds, Y. El Masry, S. Wimalaweera, and A.J. Guastella, „Reduced eye gaze explains "fear blindness" in childhood psychopathic traits”, *J. Am. Acad. Child Adolesc. Psychiatry*, vol. 47, pp. 455–463, 2008.
- [16] K. Borhani, and V. Nejati, „Emotional face recognition in individuals with attention-deficit/hyperactivity disorder: a review article”, *Dev. Neuropsychol.*, vol. 43, pp. 256–277, 2018.
- [17] R. Adolphs, „How should neuroscience study emotions? by distinguishing emotion states, concepts, and experiences”, *Soc. Cogn. Affect. Neurosci.*, vol. 12, pp. 24–31, 2017.
- [18] K. Dobs, I. Bülthoff, and J. Schultz, „Use and Usefulness of Dynamic Face Stimuli for Face Perception Studies—a Review of Behavioral Findings and Methodology”, *Front. Psychol.*, vol. 9, art. 1355, 2018, doi: 10.3389/fpsyg.2018.01355.
- [19] V. Terzis, C.N. Moridis, and A.A. Economides, „Measuring instant emotions during a self-assessment test: the use of FaceReader”, *Proceed. Measur. Behav.*, pp. 192–195, 2010.
- [20] V. Terzis, C.N. Moridis, and A.A. Economides, „Measuring instant emotions based on facial expressions during computer-based assessment”, *Pers. Ubiquit. Comput.*, vol. 17, pp. 43–52, 2013.
- [21] A. Young, D. Perrett, A. Calder, R. Sprengelmeyer, and P. Ekman, „Facial expressions of emotion- stimuli and tests (FEEST)”, Thames Valley Test Company, Bury St. Edmunds, UK, 2002.
- [22] S.V. Ioannou, A.T. Raouzaïou, V.A. Tzouvaras, T.P. Mailis, K.C. Karpouzis, and S.D. Kollias, „Emotion recognition through facial expression analysis based on a neurofuzzy network”, *Neural Networks*, vol. 18, pp. 423–435, 2005.
- [23] C. Busso, Z. Dheng, S. Yildirim, M. Bulut, C.M. Lee, A. Kazemzadeh, S. Lee, U. Neumann, and S. Narayanan, „Analysis of emotion expression using facial expressions, speech and multimodal information”, *ICMI, ACM-1-58113-890-3*, 2004.
- [24] Z. Zhang, M. Lyons, M. Schuster, and S. Akamatsu, „Comparison between geometry-based and Gabor-wavelets-based facial expression recognition using multi-layer perceptron”, *IEEE Int. Conf on Automatic Face and Gesture Recognition*, 1998.
- [25] T.J. D’Arcey, „Assessing the validity of the FaceReader using facial EMG”, M.A. Thesis, California State University, Chico, 2013.
- [26] J. Halász, M. Tóth, I. Kalló, Z. Liposits, and J. Haller, „The activation of prefrontal cortical neurons in aggression—a double labeling study”, *Behav. Brain Res.*, vol. 175, pp. 166–175, 2006.
- [27] J. Halász *et al.*, „The effect of neurokinin1 receptor blockade on territorial aggression and in a model of violent aggression”, *Biol. Psychiatry*, vol. 63, pp. 271–278, 2008.
- [28] A.A. Marsh *et al.*, „Reduced amygdala response to fearful expressions in children and adolescents with callous-unemotional traits and disruptive behavior disorders”, *Am. J. Psychiatry*, vol. 165, pp. 712–720, 2008.
- [29] A.P. Jones, K.R. Laurens, C.M. Herba, and G.J. Barker, „Amygdala hypoactivity to fearful faces in boys with conduct problems and callous-unemotional traits”, *Am. J. Psychiatry*, vol. 166, pp. 95–102, 2009.
- [30] R.J. Davidson, K.M. Putnam, and C.L. Larson, „Dysfunction in the neural circuitry of emotion regulation—a possible prelude to violence”, *Science*, vol. 289, pp. 591–594, 2000.
- [31] L. Philip, J.-C. Martin, and C. Clavel, „Rapid Facial Reactions in Response to Facial Expressions of Emotion Displayed by Real Versus Virtual Faces”, *I-Percept.*, vol. 9, 2018, doi: 10.1177/2041669518786527.
- [32] P. K. C. Tay, „The adaptive value associated with expressing and perceiving angry-male and happy-female faces”, *Front. Psychol.*, vol. 6, art. 851, 2015, doi: 10.3389/fpsyg.2015.00851.
- [33] J. Yi, P. Pärnamets, and A. Olsson, „The face value of feedback: facial behaviour is shaped by goals and punishments during interaction with dynamic faces”, *R. Soc. Open Sci.*, vol. 8, art. 202159, 2021, doi: 10.1098/rsos.202159.
- [34] A. E. Kowallik, M. Pohl, and S. R. Schweinberger, „Facial Imitation Improves Emotion Recognition in Adults with Different Levels of Sub-Clinical Autistic Traits”, *J. Intell.*, vol. 9, art. 4, 2021, doi: 10.3390/jintelligence9010004.
- [35] A. Wood, M. Rychlowska, S. Korb, and P. Niedenthal, „Fashioning the Face: Sensorimotor Simulation Contributes to Facial Expression Recognition”, *Trends Cogn. Sci.*, vol. 20, pp. 227–240, 2016.
- [36] K. Safar, M. M. Vandewouw, and M. J. Taylor, „Atypical development of emotional face processing networks in autism spectrum disorder from childhood through to adulthood”, *Dev. Cogn. Neurosci.*, vol. 51, 2021, doi: 10.1016/j.dcn.2021.101003.
- [37] P. J. Webster, S. Wang, and X. Li, „Review: Posed vs. Genuine Facial Emotion Recognition and Expression in Autism and Implications for Intervention”, *Front. Psychol.*, vol. 12, o. 653112, 2021, doi: 10.3389/fpsyg.2021.653112.
- [38] R. Brewer *et al.*, „Can Neurotypical Individuals Read Autistic Facial Expressions? Atypical Production of Emotional Facial Expressions in Autism Spectrum Disorders”, *Autism Res. Off. J. Int. Soc. Autism Res.*, vol. 9, 262–271, 2016.

# Review of knowledge base according to Information Technology Safety Awareness

Anikó Szarvák  
 Doctoral School of Applied Informatics and Applied  
 Mathematics  
 Óbuda University  
 Budapest, Hungary  
 szarvak.aniko@nik.uni-obuda.hu

Valéria Póser  
 Institute of Biomaterials and Applied Artificial Intelligence (BMI)  
 Óbuda University  
 Budapest, Hungary  
 poser.valeria@nik.uni-obuda.hu

**Abstract**— The majority of cyberattacks are targeting companies, government or service provider parties, but attacks and threats are not limited to these parties. Also, the most challenging in defense side to raise awareness of the employees, but these employees most of their time are people who enjoy the benefits of technology and uses it in their private life. Recently, according to IT Security Technology evolution, from Information System perspective, the human is the weakest link. This is supported by increased Social Engineering activity due pandemic reasons. This paper reviews the recent attacks and techniques according to increased e-commerce, internet and mobile activity. The goal of this review is to highlight how the usage of Information Technology and Information Communication Technology changed and review the connected fields, specially, the change in human side. This review defines new ways to achieve safe and secure usage through Information Technology Safety Awareness beyond Company Policy driven Information Security Awareness which is predefined in NIST SP-800-50 in 2003. The NIST standard suggests awareness training where it blurs compliance with corporate policy and basic, user knowledge. This review points out is that blending Information Technology Safety Awareness is problematic and straightening it up is a possible way to make user insecurity less of a problem.

**Keywords**— *Information Technology Safety Awareness, Information Communication Technology, human side*

## I. INTRODUCTION

Nowadays it is important to connect via Internet. Usage of PC-s, mobile handhelds and tablets are essential in personal life too, not only in work. Therefore, it is also important to be prepared personally for threats of Internet usage. In 20 years, communication technology has become an important part of our everyday lives. It stepped out from the boundaries of work. More research confirms that the velocity in the development of technology is not being followed by the human side at a sufficient speed.

Due the outstanding growth of e-commerce and mobile handheld activity, Europol [1] stated: “Criminal activities appropriating the COVID-19 outbreak have also gone mobile, with some instances of malware targeting Android devices.” In their warning on threats the areas such mobile usage, phishing, ransomware attacks are highlighted. We assume these areas are not only related to Covid-19 pandemic, but these threats are emerging in general according to private life Internet usage.

Mobile handheld device rise is undeniable. Guardian [2] stated in 2016, “PC sales have been in decline for years, while smartphones have reached at least 80% saturation within most

developed markets and have become the sole point of access to the internet for many in developing nations.”

In ENISA Threat Landscape 2020 - List of top 15 threats [3], Phishing is ranked as no. 3. In the report, ENISA states “Trend analysis of the phishing threat between January 2019 and April 2020. Phishing attacks ranked 3rd in the threat landscape, raising from the 4th position in 2018.” More interesting, in the detailed report [4] “667% increase in phishing scams in only 1 month during the COVID-19 pandemic”.

Phishing is just one of widely used Social Engineering (SE) attacks. In ENISA Threat Landscape, 5 of 15 threat is related to SE which means one third of the successful attacks are depends on human. These threats are the following:

- Malware,
- Phishing,
- SPAM,
- Identity theft,
- Ransomware.

Raising awareness is a must to reduce the risk of attacks. Instead of restricting the usage of the technology, users of the technology should be aware of the potential dangers, similar to driving car or using weapons. Importance of awareness is becoming more important as technology advances. Hence, as in physical life, the safeguards of IT are one step behind of it.

From various reports the tendency of cybercrime, both attack numbers and volume of loss increasing. According to the Internet Crime Complaint Center (IC3), there were U.S. \$1.3 billion in losses in 2018 due to Business Email Compromise (BEC) scams. [5]

Verizon’s 2018 Data Breach Investigations Report points out that email is the number one vector for both malware distribution (92.4 percent) and phishing (96 percent) stated by Cisco. [6] In Verizon’s 2020 Data Breach Investigation report points out that 22% of breaches involves Phishing as attack vector. [7]

In addition to the above collected reports and numbers, Purplesec [8] states “98% of cyberattacks rely on social engineering”. We assume, in most of the cases, only awareness, more precisely Information Technology Safety Awareness (ITSA) is the key defence tool what we – people – have. The knowledgebase of ITSA collects and summarizes the ways in which cybersecurity attacks can be detected for the average user and the possible ways to defend themselves.

## II. REVIEW OF CHANGE IN INTERNET USAGE

In telecommunication history, GPRS, 2G and 3G technologies supported the rise of cell phones connected to internet. IBM Simon is defined as first smartphone, released in 1994., then other cell phone companies stepped to this market. Nowadays smartphone mobile devices appearance dated to 2007, while Apple introduced the first iPhone. This means the smartphone technology is quite young, only 27 (14) years old.

We have to admit, the usage of Information Technology (IT) and Information Communication Technology (ICT) is changed in this decade. If we look back in time, 20 years ago we saw youngsters in the street listening Walkman or elders reading newspapers printed to paper, while they are using public transportation. Nowadays if we look around, we see people mostly a mobile in their hand. They are using instant messaging services, social network services or reading news, emails through it. Mobile started to spread in 1980. The statistics made by Areppim [9] shows that only in 36 years the mobile penetration earned 100% of the population of the world, based on the number of subscriptions. We note, it may be more if we count with mobiles without subscriptions. For a usage estimation, we calculated a growth on forecast data of subscriptions.

TABLE I. GROWTH ON SUBSCRIPTIONS

Millions of subscriptions per year		
2016	2020	%
7 418	7828	105,53%

We made a comparison on Internet usage based on infographics on “What happened in a minute on internet 2016” [10] and in 2020 [11]. We collected the same service usage numbers published in 2016 and 2020 and calculated the change of it.

TABLE II. GROWTH IN INTERNET USAGE

Internet service	Change in internet usage		
	2016	2020	%
Netflix, hours watched	69 444	764 000	1100,17
Facebook logon events	701 389	1 300 000	185,35
Google search	2 400 000	4 100 000	170,83
Youtube video viewed	2 780 000	4 700 000	169,06
E-mail sent	150 000 000	190 000 000	126,67
Tinder swipes	972 222	1 600 000	164,57

The percentages of the service usage between 2016 and 2020 shows significant growth at the examined services. We found it is less affected by the growth of mobile penetration and most affected by the spread of internet availability, worldwide. We assume, Netflix growth is distorted, compared to others due the company’s expansion policy and pandemic effect. Therefore, relying on other service usage growth, we estimate an average 163,3% on 5 years basis which is significantly higher than growth of mobile subscription penetration, where we found only 105,53%.

If we compare the growth of mobile subscription and the estimated average growth of service usage we can conclude, the usage of services is not depending on the number of the mobile subscriptions. Also, we assume, the services, like

Youtube, Netflix, Facebook, Tinder and other services are mostly used outside of the workplace.

### A. Cybersecurity treaths

The European Union Agency for Cybersecurity (ENISA) articulates in their research “List of top 15 threats” [12]: “During the next decade, cybersecurity risks will become harder to assess and interpret due to the growing complexity of the threat landscape, adversarial ecosystem and expansion of the attack surface.” We reviewed the listed threats according to the possible targets and have been made a classification whether these attacks are against companies or against people regardless of whether it may occur in connection with work or private life.

TABLE III. POSSIBLE TARGETS OF ATTACKS

Attack categories	Attack targets	
	Against Companies	Against People
Malware	x	x
Web based attacks	x	
Phishing	x	x
Web application attacks	x	
Spam	x	x
Distributed Denial of Service (DDOS)	x	
Identify theft	x	x
Data breach	x	
Insider threat	x	
Botnets	x	x
Physical manipulation, damage, theft and loss	x	x
Information leakage	x	x
Ransomware	x	x
Cyberespionage	x	x
Cryptojacking	x	x

This classification is based on the fact that the success of the attack requires assistance from user side. However, we admit, those people are more likely to be a target of an attack, who linked to key position at a company or in government, not only they are affected by for example identity theft. The table classifies the attack targets based on the assumptions above. According to the table, 10 of the ENISA’s top 15 attacks may targeting people who are not connected any companies, government. If we investigate the awareness from another perspective, people may not connect to any of Information Security Policies (ISP) maintained by companies, government, and they are not trained in Information Security Awareness too by companies or government.

These attacks are targeting people in their private life. Therefore, we assume the Security Awareness should not be relate only companies defined ISP. Security awareness should reach ICT users, generally. All of the users who has a personal computer, using mobile devices or wearables, accessing services via Internet must be educated against threats and attacks. We assume these fields are more related to general ICT usage instead of a company’s or government’s ISP and therefore the controls are not should be affected directly from an ISP rather it should be driven by ITSA, which addresses

private user's knowledge through tangible examples from their everyday life.

Since 2003, the NIST Special Publication 800-50 Building an Information Technology Security Awareness and Training Program [13] which is a fundamental document not only for federal agencies at United States of America but for IT security experts globally, a baseline standard for information security awareness trainings. This publication summarizes the areas that define the training topics, well thought out and comprehensive. But in the past 17 years, according to dramatic evolution in ICT, new threats showed up and cybersecurity threats become popular, natively against people, not only against companies or government or their stakeholders.

### III. PROTOTYPE OF ITSA

The prototype of ITSA collects cybersecurity attack samples which are perceptible by anybody who uses mobile handhelds or PCs. The awareness training built up to measure individuals' awareness. This measuring process is used to present the progress of the audience and highlight the fields with lack of awareness.

The goal of any kind of awareness is to handle risks and support the state of security as defined by Muha [14] "closed, full, continuous and proportionate protection is provided". From Data Privacy perspective, for individual users the protection of their data can be described with state of security as well as companies' business data protection.

If we count the fact, average people face with cybersecurity threats via a small screen, ITSA must address the following end-user related fields with topics discussed:

- Network knowledge – trusted networks connection  
Network knowledge area – trusted networks connection which is a key to build trust in the whole Internet. ITSA presents how easy to steal data through unencrypted connections, eavesdropping and man in the middle (MITM) attack. The goal with it to highlight the risk of untrusted network usage, for example free Wi-Fi services.
- Software knowledge area – Begin with the Software installation from non-secure source, across malicious code, spyware and trojans which are may installed with the permission of the user to PC or Mobiles, Tablets. The message for users is to be cautious with software downloaded from the Internet, specially from unknown source. Also, ITSA adds information on how to check software reliability and the permission handling of resources to the knowledgebase.
- Resource knowledge – ITSA collects privacy and security topics according to application installation and permission settings. Nowadays highlighted attack is the ransomware. In this area illustrated these kinds of attacks with use-cases in connection with fields of network, e-mail, WWW and Social Network. From Mobile perspective, banking malwares or other malicious code described in PC are relevant threats are presented here.
- Internet resource knowledge, such E-mail, World Wide Web (WWW) and Social Network (SN) usage – in this area ITSA highlights Phishing, SPAM and infected attachments which are key figures of an

attack. The main focus is on how many threat actors targeting and what are the most common points of an attack. Also, in this area, ITSA focusing on privacy considerations, threats on information share, visibility on web. In this area ITSA illustrates attacks with use-cases in connection with fields of network, e-mail, WWW and Social Network.

- Authentication credentials area – This section in ITSA contains the common problems of password weaknesses and draws attention on multi factor authentication topics. We address the same credential usage of multiple resources. This area presents risk according to same credential usage. Additionally, this area addresses weak credentials which is ease the attacker to access our data via e-mail, WWW or Social Network.

We reviewed the assets and services which are average users uses on daily basis. During the collection of ITSA knowledge base, we added the general SE related threats to end-user related fields. The collection of knowledge base points is showing use-cases in area to affected fields. With this matrix we defined five area to transfer knowledge on recent attacks. In ITSA we focus on why an end-user should be cautious and what an end-user can do to prevent an attack. Through all the cases we present the audience, we are going to strengthen them, they are able to do effective steps for their secure state.

ITSA addresses nearly the same topics which are addressed by ISA trainings based on ISP. The main difference is these ITSA trainings focus on how to do instead of company safety measures.

We note, the ISP's contains special use-cases and controls shaped to the company, therefore ISP based ISA is likely focus on what to do and what not to do. This kind of awareness trainings' goal is to direct the employee's behaviour. To achieve it they focus on the mitigation which is required by the company's IT security. The outcome is the attendees are familiar with cybersecurity terms. This is underpinned by a Pew Research Center survey [15] finds that Americans' understanding of technology-related issues varies greatly depending on the topic, term or concept. The majority of U.S. adults can correctly answer questions about phishing scams or website cookies. We assume these trainings are fails in long term because they affect the knowledge and the behaviour but not affects the attitude.

In contrast, the ITSA addressing the attitude. Through real life examples in connection with physical world can affect the attitude too. It is supported by the fact that people are touched with ransomware communication which connected to real-life ransom situation. It is usually phrased that Social Engineering (SE) attacks are addressing human weaknesses, such sympathy, helpfulness or cooperation, also these attacks are addressing naivety. If ITSA addresses attitude-change, we can also use the same human reactions, such sympathy, helpfulness and cooperation as strengths. Also, naivety can be addressed by attack operation examples which are illustrated by physical life attempts. ITSA presents cyberattack types connected to real-life actions; therefore, it is tangible for the audience.

All of the presented threats are described with physical life examples which are triggers defence reaction on the human side. We achieved good results before in similar case: "In a

case when we sent out a newsletter about ransomware and its capabilities of destruction flavoured emotionally, we got feedbacks from our end-users, full of understand of the risk and caution – awareness – on the topic. They highlighted they are touched by the message and they are felt the situation. The message sounded like this: “You can see kidnappings in movies [...] Imagine this could happen, kidnapping pictures of your loved ones, your family, from your computer.” [16]

We assume if end-users usually are not knowing what is happening behind the screen while using internet, reaching a website or using an application on mobile and what can happen while they are using it, they cannot be aware. Also, there is a common belief on personal computers and handhelds that if no one touches them, it does nothing. Based on these common believes, the ITSA focuses on the attitude but also includes two separate fields, the knowledgebase and the measuring process.

We agree the finding formulated by Bada et al. “The fact today is that security awareness as conceived is not working. Naturally, an individual that is faced with so many ambiguous warnings and complicated advice, may be tempted to abandon all efforts for protection, and not worry about any danger.” [17] This opened to us a new direction on ITSA development.

#### A. ITSA knowledgebase

“People know the answer to awareness questions, but they do not act accordingly to their real life” and “Simple transfer of knowledge about good practices in security is far from enough.” [18]. We agree with these findings, also we assume presenting the operation principles of specific attack is helpful. Knowing how an attack works can ease better understanding. Through this kind of knowledge transfer, we assume, we are able to raise knowledge on risk which may indicate better awareness through change in attitude.

“There is a need to separate ISP based ISA from the overall basic Information Technology Security Awareness. An independent definition of Information Technology Safety Awareness is knowledge or perception of a situation or a fact in Information Technology field or related area.” [16]

Additionally, ITSA is addresses risks through illustrative examples to connect ICT threats to real-life use-cases. This is necessary to bring closer these threats to the audience, make it concrete and tangible. This eliminates the shortcomings of most awareness training as described by Stewart et al.: “For information security awareness techniques to improve in effectiveness and efficiency it is clear that information security awareness content can’t be created from what the technical experts want to tell people, the contents of a technical standard or the prevailing best practice topics but rather the audience themselves that it seeks to influence and protect.” [19]

The goal is not to threaten the audience. This is supported by studies like Bada et al.’s article about cybersecurity awareness: “Threatening or intimidating security messages are not particularly effective, especially because they increase stress to such an extent that the individual may even be repulsed or deny the existence of the need for any security decision.” [17]

Beside the ITSA knowledgebase quite important to achieve behaviour change. Regular knowledge share scenarios are failing in some circumstances. Therefore, ITSA knowledge share follows a method, that links cybersecurity

threats with physical life conditions. The goal of ITSA is to connect cybersecurity threats to real-life risk and provoke defence reaction. ITSA is can be used by wide audience, anybody who have access internet, using PC or Mobile. ITSA implements an awareness training connecting ICT related threats to real-life risks to address defence reactions helps to change attitude instead of addressing knowledgebase or changing behaviour. Also, ITSA is applicable widely, from primary school, thus children are also affected by cyberattacks.

#### B. Measuring progress

The goal with this prototype of ITSA is to raise awareness with easily understandable examples. Therefore, during the awareness education, measuring the progress of the end-user side is indispensable. The measurement of the process has two separate questionnaires. To the attendees before and after the training the same image-based questions asked. The questionnaire not measuring the knowledgebase. The goal is to measure the change in the emotional reaction and the consciously or unconsciously reaction. The image-based questions illustrate the threats which are visible by average end-users.

In the questionnaire the images are not labelled. This is essential, because we want the end-users to react without any additional information, as it should happen in a real situation. In this case they are not influenced and not diverted in the direction of any reaction. They are on their own as it is usually the case when using ICT services. In addition to summarizing security awareness topics, ITSA aims to measure and address gaps based on measurement immediately for the audience. The goal with the measuring process is twofold. First, the audience get immediate feedback on their current state of awareness progress. Second, the level of security awareness of a group can be determined on the basis of aggregation. Based on these aggregated results targeted practices can be introduced to further raise of awareness.

#### C. Audience of ITSA

ITSA addresses general knowledgebase therefore, the threats may affect anybody who is connected once the internet, using mobile, applications, loading sites from world wide web, using Social Network sites and e-mails. Audience of ITSA can be anybody. The use-cases defined in ITSA is easily understandable and usable by end-users.

### IV. CONCLUSION

Awareness training topics suggested by NIST-SP 800-50 in 2003 are relevant today, however the environment is changed. The rise of ICT, PC and Mobile spread and wide usage escalated the cyberattacks too and the weakest link is defined as the people who are using it. Nowadays accessing internet is not a company related privilege, it is natively available for near anybody. In former time, while internet usage was only available through workplace, directing employees with ISP was relatively easy. Today, internet users are not prepared exactly the cyberattacks and their attempts are usually not directed by ISP or ISA.

Raising awareness is a must to reduce the risk and impact of cyberattacks. Instead of restricting the use of the technology, end-users of the technology should be aware of the potential dangers, similar to driving car or using weapons. Importance of awareness is becoming more important as technology advances hence, as in physical life, the safeguards

are one step behind of it. In this situation, risk reduction can be achieved by increasing security awareness.

ITSA topics collected and organized for average end-users. The collected and presented attack types are demonstrating the key points which are detectable by end-users. While it is connected to real life examples, direct emotional reaction may occur. This supported by the measuring process which gives direct feedback to the audience on their progress.

ITSA follows a knowledge share method where cybersecurity threats are linked with physical life events. Measurement process uses the appearance of possible cybersecurity attacks to collect the audience reactions and presents the results immediately for the audience.

#### ACKNOWLEDGMENT

Authors gratefully acknowledges the support of the Doctoral School of Applied Informatics and Applied Mathematics on this research.

#### REFERENCES

- [1] Europol Covid-19: Mobile Threats <https://www.europol.europa.eu/covid-19/covid-19-mobile-threats> Accessed: 2021. 05. 20.
- [2] Mobile web browsing overtakes desktop for the first time. <https://www.theguardian.com/technology/2016/nov/02/mobile-web-browsing-desktop-smartphones-tablets> 2016. Accessed: 2021. 05. 20.
- [3] <https://www.enisa.europa.eu/news/enisa-news/understanding-and-dealing-with-phishing-during-the-covid-19-pandemic> Accessed: 2021. 05. 20.
- [4] <https://www.enisa.europa.eu/topics/threat-risk-management/threats-and-trends/etl-review-folder/etl2020-phishing> Accessed: 2021. 05. 20.
- [5] [https://www.ic3.gov/Media/PDF/AnnualReport/2018\\_IC3Report.pdf](https://www.ic3.gov/Media/PDF/AnnualReport/2018_IC3Report.pdf) Accessed: 2021. 05. 22.
- [6] <https://www.cisco.com/c/dam/en/us/products/collateral/security/email-security/email-threat-report.pdf> Accessed: 2021. 05. 22.
- [7] J. Dolan: Psychology in Phising, IASP 470 Security System Capstone, 2017.
- [8] <https://purplesec.us/resources/cyber-security-statistics/#SocialEngineering> Accessed: 2021. 05. 25.
- [9] [https://stats.areppim.com/stats/stats\\_mobilexpenetr.htm](https://stats.areppim.com/stats/stats_mobilexpenetr.htm) Accessed: 2021. 09. 12.
- [10] <https://www.visualcapitalist.com/what-happens-internet-minute-2016/> Accessed: 2021. 09. 12.
- [11] <https://themarketingintrovert.com/content-marketing/internet-minute/> Accessed: 2021. 09. 12.
- [12] [https://www.enisa.europa.eu/publications/enisa-threat-landscape-2020-list-of-top-15-threats/at\\_download/fullReport](https://www.enisa.europa.eu/publications/enisa-threat-landscape-2020-list-of-top-15-threats/at_download/fullReport) Accessed: 2021. 03. 05.
- [13] National Institute of Standards and Technology - NIST: Building an Information Technology Security Awareness and Training Program. Wilson, M. and Hash, J. Computer Security Division Information Technology Laboratory. October 2003. <http://csrc.nist.gov/publications/nistpubs/800-50/NIST-SP800-50.pdf>
- [14] Muha Lajos: Az informatikai biztonság egy lehetséges rendszertana, 2008 [In.: Bolyai Szemle, XVII. évf. 4. szám, p.137-156., Budapest: ZMNE BJKMK, ISSN: 1416-1443]
- [15] M. Anderson and E. Vogels, “Americans and digital knowledge,” Pew Res. Center, Washington, DC, USA, Tech. Rep., 2019. [Online]. <https://www.pewresearch.org/internet/2019/10/09/americans-and-digital-knowledge/> Accessed: 2021. 05. 20.
- [16] A. Szarvák, V. Póser: Information Technology Safety Awareness – a review of regularly used terms and methods, AIS 2020, 15th International Symposium on Applied Informatics and Related Areas organized in the frame of Hungarian Science Festival 2020 by Óbuda University, 2020, pp. 107-111., ISBN 978-963-449-209-2
- [17] Maria Bada, Angela M.Sasse and Jason R. C. Nurse: Cyber Security Awareness Campaigns: Why do they fail to change behaviour?
- [18] Information Security Forum (ISF): From Promoting Awareness to Embedding Behaviours, Secure by choice not by chance, February 2014. <https://www.securityforum.org/shop/p-71-170>
- [19] Stewart, Geordie; Lacey, David: Death by a thousand facts: Criticising the technocratic approach to information security awareness, Information Management & Computer Security, Volume 20, Number 1, 2012, pp. 29-38(10) ISSN: 0968-5227



# Methods for High Precision Shutter Speed Measurements

Márk Rátosi

Department of Computer Science  
and Systems Technology  
University of Pannonia  
Veszprém, Hungary  
ratosi@dcs.uni-pannon.hu

Gergely Vakulya

Alba Regia Technical Faculty  
Óbuda University  
Székesfehérvár, Hungary  
vakulya.gergely@amk.uni-obuda.hu

Gyula Simon

Alba Regia Technical Faculty  
Óbuda University  
Székesfehérvár, Hungary  
simon.gyula@amk.uni-obuda.hu

**Abstract**—In this paper various methods are presented for measuring the shutter speed of cameras. Both classical methods for mechanical cameras and new methods for digital cameras are reviewed. Real measurements illustrate that the potential accuracy of novel methods is in the range of microseconds.

**Keywords**—shutter speed, exposure time, camera communication, equivalent sampling

## I. INTRODUCTION

In VLC (Visual Light Communication) systems the information is transmitted as modulated light. On the receiver side photodiodes, phototransistors, or other light sensitive devices are used. Camera communication (CamCom) systems implement VLC with cameras as receivers. The overall performance of such a system is highly determined by the parameters of the camera, especially the shutter speed (or exposure time) [1]. On most cameras shutter speed can be set to given presets, measurement of the real exposure times are beneficial. This paper gives a review of different camera shutter speed measurements.

## II. EXPOSURE TIME MEASUREMENT METHODS

### A. Direct method

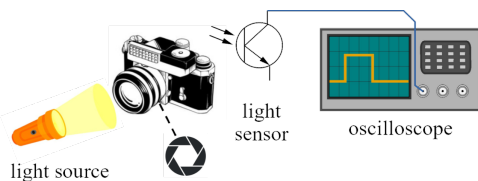


Fig. 1. Direct method using and oscilloscope.

In ISO standard 516 [2] a direct method is described to measure the shutter speed of either digital, or film cameras with mechanical, or electronic shutter. The described method uses the scheme shown in Fig. 1. The camera gets constant illumination through the lens and the light intensity is then measured behind the shutter with a photodiode or a phototransistor and an oscilloscope. The light sensor follows the change of the light intensity behind the shutter, the opening and closing events are visible as a rising and a falling edge

in the screen of the scope, making it possible to measure the time in between.

The solution is suitable for a wide range of cameras and shutter speeds, but unfortunately the disassembly of the camera is required to access the focal plane. Thus this method is only applicable during manufacturing and product testing.

The output signal of the light sensor clearly reveals the opening and closing events, and their difference gives a good estimate for the exposure time.

In [3] a good method is shown to measure the shutter time of film cameras replacing the film cartridge with the sensor. Unfortunately, in most digital cameras the focal plane is not accessible and the afore-mentioned procedures cannot be used.

### B. Motion blur based methods

Other solutions take advantage of the mostly undesired phenomenon called “motion blur“. Here photos are taken of objects with known speed (see Fig. 2). The shutter time can be calculated from the shape of the covered area. The radial marker (green line in Fig. 2) forms a filled arc on the photo, from the angle and the angular speed the shutter time can be calculated.

The most common angular speed of a turntable is

$$\omega = 33\frac{1}{3} \text{ RPM} = 33\frac{1}{3} \cdot 60 \text{ RPS} = 33\frac{1}{3} \cdot 60 \cdot 360 \text{ DPS}, \quad (1)$$

where RPM and RPS mean Revolutions Per Minute and seconds, respectively, and DPS stands for Degrees Per Seconds.

Let be  $\alpha$  be the central angle of the trace of on the photo taken of the turntable (green sector in Fig. 2). Then the exposure time  $\hat{S}$  can be calculated as follows:

$$\hat{S} = \frac{\alpha}{\omega}. \quad (2)$$

Measuring  $\alpha$  in the sub-degree range is difficult and exposure times longer than one revolution make the measurement ambiguous, giving this method a lower and an upper limit. Measurement range can be extended with variable angular speed. The detailed measurement method is described in [4] and further improved in [5].

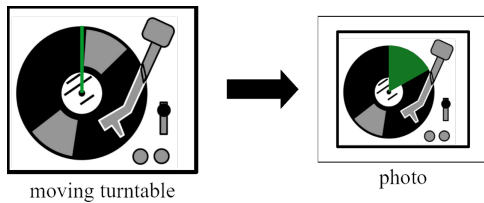


Fig. 2. Motion blur method with a turntable.

### C. Virtual movement based methods

This measurement method uses the trace of the electron beam in a CRT (Cathode Ray Tube) screen as a virtually moving object. However the naked eye can see a still image on the monitor, only a small portion illuminates at once, as the electron beam scans through it.

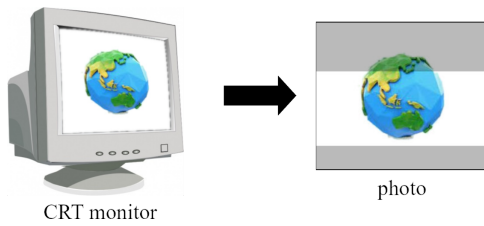


Fig. 3. Measurement using a CRT monitor.

The principle of the measurement method is shown on Fig. 3. The photo taken in the good moment from the monitor will contain a highlighted area, as shown in the right part of the figure. This is the part, where the beam hit the screen during the exposure. The most precise measurement can be achieved with this method, if the number of illuminated lines  $k$  is used instead of the area. Let be  $f_h$  is the horizontal sync frequency of the monitor. In case of standard  $640 \times 480$  60 Hz VGA mode  $f_h = 31.778$  kHz, determining the time of a single line to be  $t_h = 1/f_h$ . The exposure time can be calculate with the following formula:

$$\hat{S} = k \cdot t_h \quad (3)$$

More technical details can be found in [4]. The lower and upper bounds of the measurable exposure times are given by the time of a single line and the time of the entire screen. Instead of CRT monitors, alternatively the display of an oscilloscope can be utilized in a similar manner. In [6] a shutter speed measurement method is described, based on analog oscilloscopes.

### D. “Running“ LED based measurements

Replacing the physical movement with a logical one widens the possibilities in shutter speed measurement. In the setup shown in Fig. 4 an array of blinking LEDs is used, lighting up in series for equal times. From the the time of a single LED and the number of lit up LEDs on the photo the exposure time can be calculated. In [7] LED stripes of 100 LEDs are used, while the method [8] uses a  $10 \times 10$  matrix.

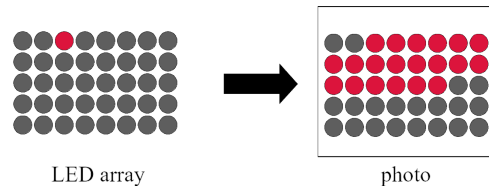


Fig. 4. Measurement device using an LED panel

The LEDs in the array light up after each other. Each LED is lit up for  $t_{LED}$ . A video frame showing  $k$  bright LEDs indicate an exposure time of

$$\hat{S} = t_{LED}k \quad (4)$$

Although this measurement method sounds straightforward at first, attention must be taken to the following conditions. First, the measurement device must be implemented so that turning on an LED and off the previous one must happen at the same time instant. Second, measurements can only be acceptable if there is at least video frame, where the illuminated LEDs are surrounded from both sides with at least one non-illuminated LED.

The experimental measurement device is based on a PIC16F876 microcontroller, running at 20 MHz clock speed, which drives 8 LEDs attached to the same 8-bit IO port, making it possible to manipulate the state of the 8 LEDs simultaneously, with a temporal resolution of  $0.2\mu s$ . With 8 LEDs exposure times between  $t_{LED}$  and  $6 \cdot t_{LED}$  can be measured, in discrete steps. Extending the time, when one of the LEDs in the middle is turned on, extends the measurement range.

### E. Equivalent sampling-based measurement

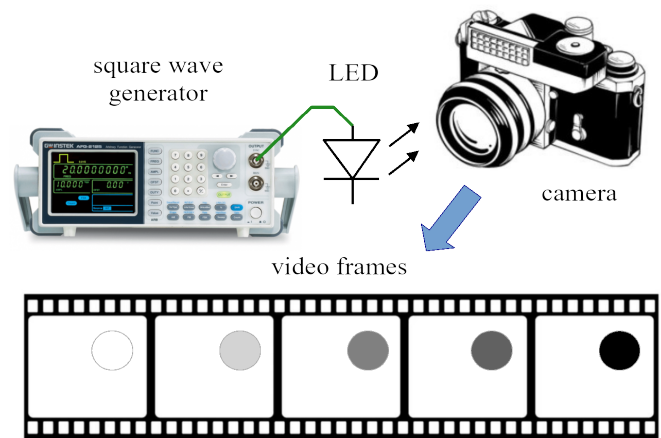


Fig. 5. The equivalent sampling-based method

The measurement setup, proposed in [9] is shown in Fig. 5. A square wave generator produces a square wave with 50% duty cycle, which drives an LED. Thus the light intensity  $x(t)$  of the LED is a periodic square wave with period of  $P$ , as follows:

$$x(t + P) = x(t). \quad (5)$$

The camera takes a series of pictures (in video mode) of the blinking LED, where the sampling interval of the camera is  $T_S$ . The blinking signal's frequency is selected so that  $T_S$  is *almost* an exact multiple of  $P$ , as follows:

$$T_S = nP + \Delta t, \quad (6)$$

where  $n$  is any integer and  $\Delta t$  is much smaller than  $T_S$ . Using (5), for two consecutive pictures taken by the camera the following equations are true:

$$x(k) = x(t_k) \quad (7)$$

and

$$x(k+1) = x(t_k + T_S) = x(t_k + nP + \Delta t) = x(t_k + \Delta t). \quad (8)$$

Thus it seems that the second sample is taken  $\Delta t$  time after the first sample. This is the well-known equivalent sampling [10], and  $\Delta t$  is the equivalent sampling interval. The phenomenon of equivalent sampling is illustrated in Fig. 6.

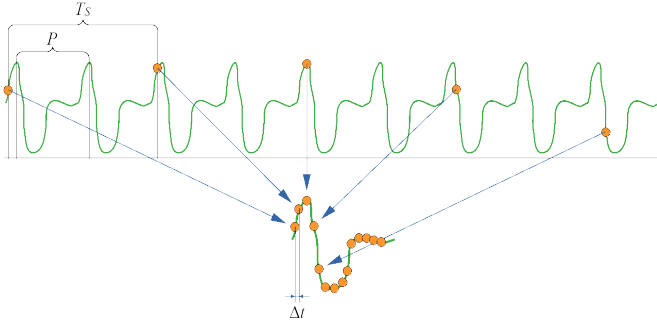


Fig. 6. Equivalent sampling of a periodic signal with equivalent sampling period of  $\Delta t$

According to the camera sampling model [9], shown in Fig. 7, the sensor of the camera integrates the incoming light intensity during the exposure time  $S$ . The nonlinearity  $\Gamma$  models the saturation of the signal at high intensities. The sampled signal  $x_S(k)$ , measured around time instant  $t_k$ , is the following:

$$x_S(k) = \Gamma \left( \alpha \int_{t_k - \frac{S}{2}}^{t_k + \frac{S}{2}} x(\tau) d\tau \right), \quad (9)$$

where  $S$  is the exposure time and  $\alpha$  is the gain of the camera. During the measurement, care is taken to operate the camera in a linear range, thus the output is the following:

$$x_S(t_k) = \alpha_0 + \alpha' \int_{t_k - \frac{S}{2}}^{t_k + \frac{S}{2}} x(\tau) d\tau, \quad (10)$$

The blinking signal's period is chosen so that the following constraint is fulfilled:

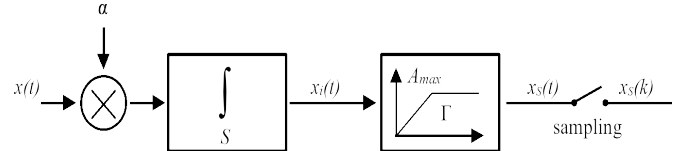


Fig. 7. Sampling model of the camera

$$\frac{P}{2} > S \quad (11)$$

In this case, since the input signal is a square wave, from (10) it follows that signal  $x_S(t)$  is a trapezoid. The period length of  $x_S(t)$  is  $P$  and the rising and falling times are equal to  $S$ , which is to be measured. Fig. 8. Illustrates the light intensity signal  $x(t)$ , while  $x_S(t)$  shows the effect of integral sampling through time  $S$ , and  $x_S(k)$  is the sampled version.

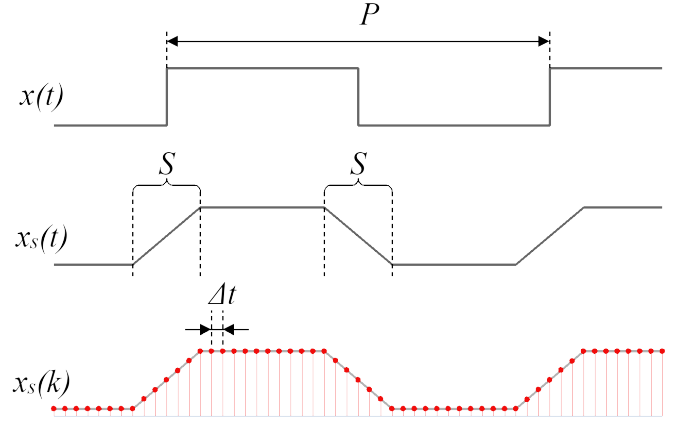


Fig. 8. The input square wave with period length of  $P$ , the integrated signal with exposure time of  $S$ , and the samples with equivalent sampling interval of  $\Delta t$ .

Let  $N_S$  be the number of samples in a rising edge of  $x_S(k)$ , and let  $N_P$  denote the number of the total samples in one period of  $x_S(k)$ , as shown in Fig. 8. The exposure time is estimated as

$$\hat{S} = \frac{N_S}{N_P} P. \quad (12)$$

In order to provide good resolution, small  $\Delta t$  values should be chosen: in this case the  $N_S$  and  $N_P$  become high. If  $\Delta t$  is high then values  $N_S$  and  $N_P$  are small and thus the resolution of  $\hat{S}$  is poor.

The measurement procedure is the following:

- 1) The generator's period length is set according to (6). The camera is set so that the measured signal does not saturate the camera.
- 2) The generator's period length is fine-tuned so that the video output of the camera shows a slowly blinking LED. After tuning the period length  $P$  is read.
- 3) The video stream, containing the blinking LED, is recorded.

- 4) The intensity signal  $x_S(k)$  of one pixel (e.g. the center of the LED) is extracted from the video.
- 5) The samples  $N_S$  and  $N_P$  are counted and the estimate  $\hat{S}$  is calculated according to (12).

### III. MEASUREMENTS

To illustrate the performance properties of the shutter speed measurement methods, two high-precision approaches were selected: a “running“ LED-based and an equivalent sampling-based method were utilized. The tested device was a high quality industrial Grasshopper3 Color camera of type GS3-U3-23S6C, produced by FLIR [11]. The camera has an RGB color sensor, and it was used with 30 FPS frame rate and 8 bit image depth. The camera can be set to predefined shutter speeds between  $5\mu s$  up to  $31.9s$ ; in our tests six values in the range between  $8\mu s$  and  $1ms$  were utilized.

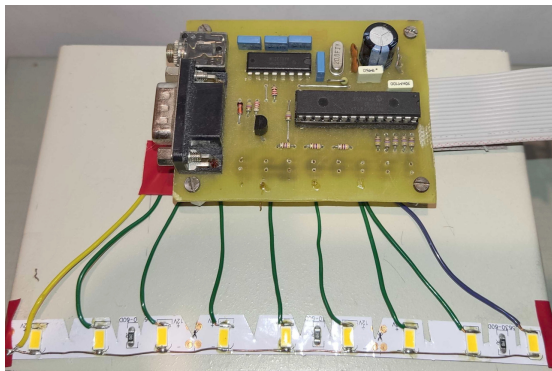


Fig. 9. Measurement setup for the “running“ LED-based method

The running LED-based device is shown in Fig. 9. Here the LED pattern was generated by a PIC16F876 microcontroller board, driving 8 LEDs. The on-time of each LED was configurable individually with time resolution of  $1\mu s$ . The estimated accuracy of the device, originating from the resolution and the accuracy of the timer, was  $\pm 1.5\mu s$ . The basic operation principle is the same as in devices [8] and [9], but the smaller number of LEDs is compensated by the possibility of the individual configuration of each LED.

The equivalent sampling-based measurement setup is shown in Fig. 10. Here the square wave was generated using an Arduino Due board. The blinking frequency was chosen to be approximately 120 Hz (providing  $P = 1/120s$ ), which is an integer multiple of the 30 FPS frame rate of the camera. The actual frequency was fine tuned in 5 millihertz steps.

The measurement results are shown in Table I. The nominal values were reported by the camera’s built-in software, the values  $\hat{S}_{LED}$  and  $\hat{S}_{EQS}$  are the measurement results by the “running“ LED and the equivalent sampling-based methods, respectively. The two methods provide results within  $1\mu s$ . Interestingly, the camera shows a constant  $6 - 7\mu s$  bias.

The operation of the equivalent sampling-based method is illustrated in Figs. 11 and 12. Fig. 11 shows a good measurement, where the camera operated in the linear operation range (color blue), while the other two measurements (red and

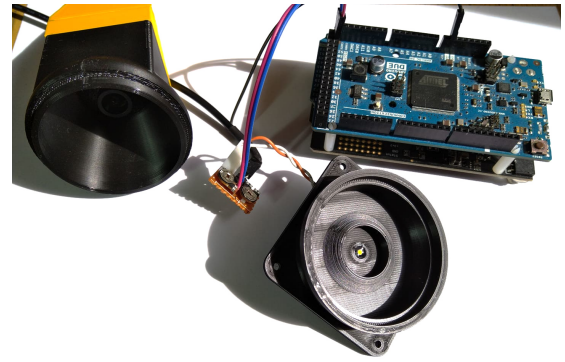


Fig. 10. Measurement setup for the equivalent sampling-based method: Camera with one half of the 3D printed cover (upper left corner), LED light source in center of half of the cover (bottom middle), Arduino Due as square wave generator (upper right corner).

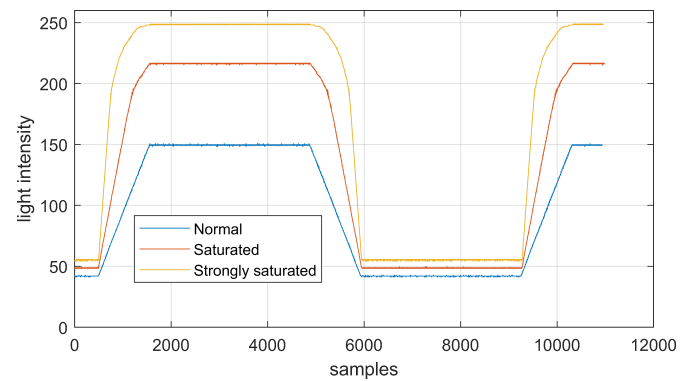


Fig. 11. Measurements with the tested camera taken in the linear range (blue curve) and with saturation (red and orange curves).

orange curves) show the effect of saturation. The trapezoid signal is apparent in the linear case, while it is distorted when the sensor is saturated, decreasing the measurement accuracy.

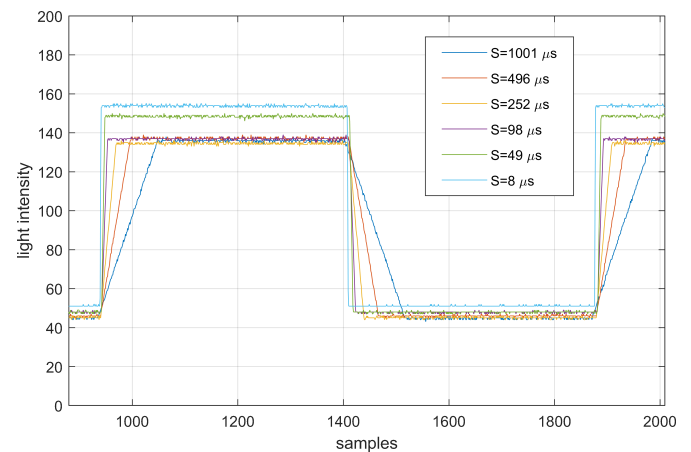


Fig. 12. Trapezoid diagrams of all measured exposure times of the camera. Legend shows the nominal  $S$  values.

In Fig. 12 measurements are shown with shutter speed values shown in Table I. All measurements were taken with the

same blinking frequency, thus the period length is the same for all cases. The length of the rising and falling edges are clearly different, and are proportional with the actual shutter speed.

TABLE I  
MEASURED EXPOSURE TIMES WITH THE "RUNNING" LED  
AND THE EQUIVALENT SAMPLING-BASED METHODS

Nominal $S(\mu s)$	f-stop	$\hat{S}_{LED}$ ( $\mu s$ )	$\hat{S}_{EQS}$ ( $\mu s$ )
1001	16	1008	1009.0
496	16	503	503.6
252	11	259	259.4
98	8	104	103.9
49	8	56	55.1
8	1.4	15	15.1

#### IV. SUMMARY

In this paper various methods were presented for camera shutter speed measurement. The operation principles were introduced for the direct, motion blur, virtual movement, "running" LED, and the equivalent sampling-based methods. The operation and performance properties of the latter two methods were also presented through the test of a high-end industrial camera. The measurement results indicate that these methods can provide accuracy in the low microsecond range.

#### REFERENCES

- [1] M. Rátosi and G. Simon, "Performance Analysis of the UFSOOK Protocol", in Proc. 2019 IEEE International Symposium on Measurements and Networking (M&N 2019), Catania, Italy, July. 8-10, 2019. pp. 1-6. doi: 10.1109/TWMN.2019.8805018
- [2] ISO 516:2019. Camera shutters — Timing — General definition and mechanical shutter measurements. International Organization for Standardization, 2019. Online: <https://www.iso.org/obp/ui/#iso:std:iso:516:ed-4:v1:en>
- [3] Y. Asakura, et al., "Exposure precision tester and exposure precision testing method for camera", U.S. Patent 5 895 132, Apr. 20, 1999.
- [4] Peter D. Hiscocks, "Measuring Camera Shutter Speed", Royal Astronomical Society, Toronto Centre, Canada, 2010. Online: <https://www.ee.ryerson.ca/~phiscock/astronomy/light-pollution/shutter-cal.pdf>
- [5] V. N. Budilov, V. I. Volovach, M. V. Shakurskiy and S. V. Eliseeva, "Automated measurement of digital video cameras exposure time", East-West Design & Test Symposium (EWDTS 2013), Rostov-on-Don, 2013, pp. 1-4. doi: 10.1109/EWDTS.2013.6673136
- [6] CCTVCAD Lab Toolkit. CCTVCAD Software. Perm, Russia, 2011. Online: [http://www.cctvcad.com/labtoolkit\\_help](http://www.cctvcad.com/labtoolkit_help)
- [7] L. Masson, F. Cao, C. Viard, and F. Guichard, "Device and algorithms for camera timing evaluation" in Proc. IS&T/SPIE Electronic Imaging Symposium, San Francisco, California, United States, 2014. doi:10.1117/12.2042161
- [8] Image Engineering: LED-Panel. Online: <https://www.image-engineering.de/products/equipment/measurement-devices/900-led-panel>
- [9] M. Rátosi, G. Vakulya, G. Simon, "Measuring Camera Exposure Time Using Equivalent Sampling", 2021 IEEE International Instrumentation and Measurement Technology Conference (I2MTC). IEEE, 2021.
- [10] G. Shize, S. Shenghe and Z. Zhongting, "A novel equivalent sampling method using in the digital storage oscilloscopes" in Proc. 1994 IEEE Instrumentation and Measurement Technology Conference, Hamamatsu, Japan, 1994, pp. 530-532 vol.2. doi: 10.1109/IMTC.1994.351901
- [11] FLIR Machine Vision Cameras. Online: <https://www.flir.com/browse/industrial/machine-vision-cameras/>

# Error Detection Methods in Photogrammetry

Tamas Jancso

*Institute of Geoinformatics, Alba Regia Technical Faculty, Óbuda University  
Pirosalma u. 1-3, Székesfehérvár, H-8000, Hungary  
jancso.tamas@amk.uni-obuda.hu*

**Abstract**— The error detection plays an important role in the photogrammetric evaluation process. Digital Photogrammetric Workstations (DPWs) are offering to cover the whole process starting from the camera calibration until gaining the ground coordinates of points for mapping, for 3D models and for producing orthophotos. To achieve the final products in the image evaluation with high accuracy, the error detection is an essential part in each step. The paper summarizes the error detection methods and solutions for correcting the final products in photogrammetry.

**Keywords**— photogrammetry, error detection, camera calibration, aerial triangulation

## I. INTRODUCTION

In the process of image evaluation gross errors could appear in photogrammetry. We can divide these errors into three groups, although a sharp limit between these groups doesn't exist [2]:

1. Large gross errors. Usually, we call them mistakes. The possible origin of these errors could appear in image or geodetic coordinates of points.

The origins of large gross errors in measuring the points:

- faulty replacement of point numbers,
- faulty replacement of coordinates,
- faulty identification of some common (tie) points in the common model,
- poor identification of points,
- the sign errors and confusion because of wrong direction of coordinate axes of geodetic and model coordinate systems,
- mistakes when typing the control data into file.

2. Gross errors of middle range. The origin of this error-type relates to the image and geodetic coordinates, too. Only the dimension of the error is smaller. here a new source of error can be a personal measurement error due to wrong interpretation or some errors in calculation of geodetic coordinates of control points.

3. Small gross errors. The origin of errors can be:

- a small mistake in observation and measurement of image point coordinates,
- a poor identification of tie and control points in image.

In this paper we deal with small gross errors only and to be more specific, we specify small gross errors by the formula (1).

$$4\sigma_0 \leq |\varepsilon_i| \leq 20\sigma_0 \quad (1)$$

Notation in (1):  $\varepsilon_i$  : gross error,  $\sigma_0$  : unit weight error.

Gross errors can occur in every step of an evaluation process bound to DPWs, but most of all we can collect gross errors during the orientation process, see Fig. 1.

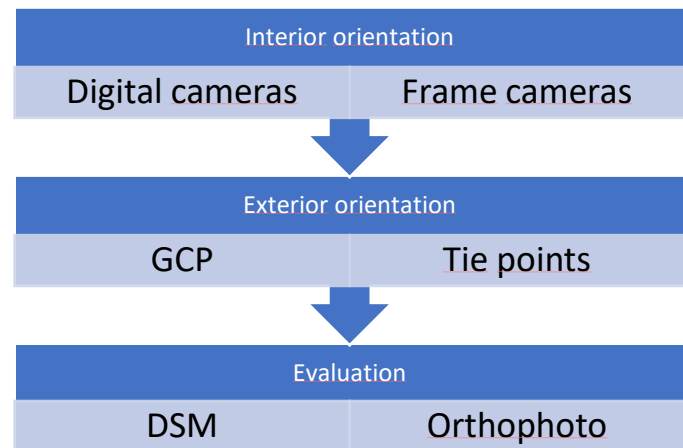


Figure 1. Evaluation process for a DPW [1]

During the interior orientation - for frame cameras – the photo coordinate system should be determined by the measurement of fiducial marks. This measurement can be automated based on an area-based image matching technique, but in rare cases the algorithm makes mistakes and misidentifies the fiducial marks, which leads to gross error.

The goal of the exterior orientation is to determine the ground coordinates of the exposure centre and the rotation angles of the camera for each photo. This procedure is also called as aerial triangulation. The whole algorithm is based on the bundle of rays built from the exposure centre, the image point and the associated ground point. During the calculations, we use ground control points (GCPs) and tie points. The GCPs can hold errors coming from the surveying calculations, and on the other hand, we can make mistakes (gross errors) during the measurement of these point in images.

The image matching algorithm is very fast and collects the tie points automatically, but among the collected points, we encounter gross errors, and it is not feasible to find them with manual inspection. If we detect these errors, then the sophisticated DSM (Digital Surface Model) and orthophoto production can be fully automatic and free from gross errors.

In this paper, we will have a closer look at the orientation process with attention to error detection.

## II. INTERIOR ORIENTATION

The task of the interior orientation is to find the camera constant, the coordinates of the principal point, the pixel size, the resolution, and the distortion parameters of the camera. Normally, these data are known for metric cameras summarized in the camera calibration report. In case of using scanned photos taken with frame cameras, the part of the interior orientation is to calculate the transformation parameters between the image and photo coordinate system. Usually, we use affine transformation for solving this task. The fiducial marks will play the role of common points between these coordinate systems. The photo coordinates of fiducial marks are known from the camera calibration report. Our task is to measure the pixel coordinates of these points. The measurement can be done manually or automatically by an area-based image matching algorithm with cross-correlation technique (see eq. (3)) [3]. In both cases, we can have faulty measurements and the large residuals will indicate gross error after the adjustment. The system of equations based on equations (2) is linear for the unknowns and can be solved directly [3], [4].

$$\begin{aligned} X &= a_0 + a_1x + a_2y \\ Y &= b_0 + b_1x + b_2y \end{aligned} \quad (2)$$

Notation in (1):

$X, Y$  : photo coordinates

$x, y$  : image (pixel) coordinates

$a_0, a_1, a_2, b_0, b_1, b_2$  : transformation parameters

The area-based image matching is frequently used also for the measurement of tie points necessary for the exterior orientation or DSM points for orthophoto production.

$$\rho = \frac{\sum_{r=1}^R \sum_{c=1}^C (g_1(r,c) - \mu_1)(g_2(r,c) - \mu_2)}{\sqrt{\sum_{r=1}^R \sum_{c=1}^C (g_1(r,c) - \mu_1)^2 \sum_{r=1}^R \sum_{c=1}^C (g_2(r,c) - \mu_2)^2}} \quad (3)$$

Where:

$g_1$  - the greyscale value of the pixel in the target area

$g_2$  - The greyscale value of the pixel in the search area

$r, c$  - row, column index

$\mu_1, \mu_2$  - Average grey values in the target and search areas

$R, C$  - number of rows and columns in the sample area

Let's see an example of an interior orientation based on fiducial marks. The image consisted of 8 fiducial marks and the measurement was done manually. The pixels size was 0.085 mm. The expected residual should be around one pixel or less after the adjustment. As we can see in Fig 2, at least one gross error should exist in the measurement, but among the residuals every fiducial mark indicates a large residual (0.144 mm). The overall standard deviation  $\sigma_0 = 0.208$  mm, which means approximately 2.5 pixel error.

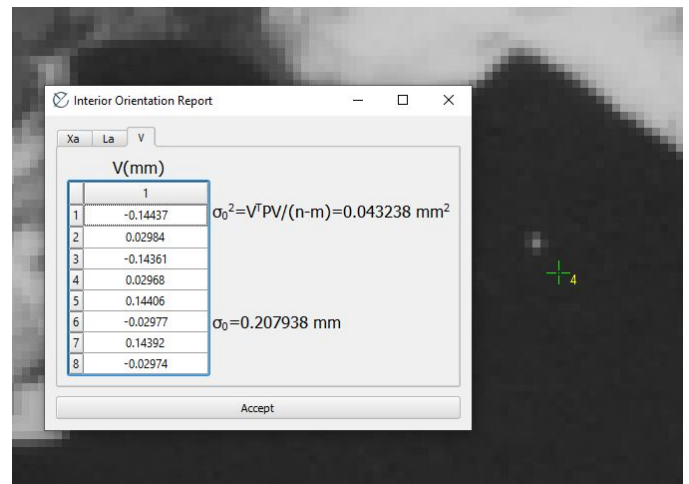


Figure 2. Residuals and standard deviation with gross error in fiducial mark no. 4

In general, it is easier to repeat the measurement and find the fiducial mark responsible for this error. By visual inspection, we can notice that the fiducial mark number 4 was measured incorrectly. After repeating the measurement, we significantly improved the standard deviation ( $\sigma_0 = 0.137$  mm) as it is visible in Fig 3.

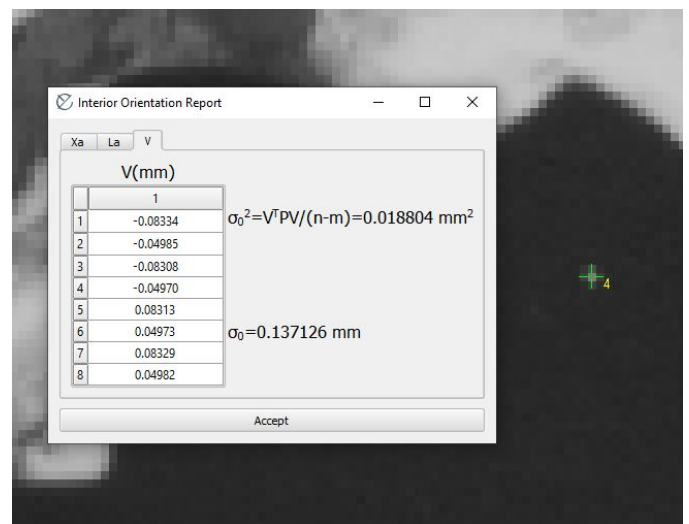


Figure 3. Residuals and standard deviation without a gross error

## III. EXTERIOR ORIENTATION

During the exterior orientation, the photo coordinates of tie points and control points can hold small gross errors. In addition, the geodetic coordinates of control points can have gross errors as well.

Methods for detecting small errors can be divided into two major groups:

- mathematical and statistical analysis of the results of the adjustment made by the method of least squares,

- robust estimation designed for processing of measurement results. These estimation methods are significantly less sensitive to gross errors than the least squares method.

In the following, some error filtering methods are briefly described [4].

The Data snooping method starts from the concept of reliability. The reliability reflects the degree of consistency in the measurements, and it expresses the extent of control in the adjustment. This depends on the number of redundant measurements and the geometric arrangement of the measured points. So, reliability puts in our hands a metric value by which we can determine the effectiveness in detection of gross errors.

Reliability can be derived from the  $\mathbf{Q}_{vv}$  equal to the covariance matrix of the residuals (4):

$$\mathbf{Q}_{vv} = \mathbf{Q}_{ll} - \mathbf{A} \cdot \mathbf{Q} \cdot \mathbf{A}^T \quad (4)$$

In formula (4),  $\mathbf{Q}_{ll}$  denotes the covariance matrix of the measurements, which is equal to the inverse of the weight matrix  $\mathbf{P}$ . The matrix  $\mathbf{Q}$  is  $\mathbf{N}^{-1} = (\mathbf{A}^T \cdot \mathbf{P} \cdot \mathbf{A})^{-1}$ .

Total redundancy of the equalization (number of redundant measurements) is written in (5) as:

$$r = n - u = \text{trace}(\mathbf{Q}_{vv} \cdot \mathbf{P}) = \sum r_i \quad (5)$$

In formula (5), the  $r_i$  values denote the diagonal elements of the  $\mathbf{R} = \mathbf{Q}_{vv} \cdot \mathbf{P}$  redundancy matrix as the redundancy of the given  $l_i$  measurement relative to the total  $r$  redundancy. The value of  $r_i$  can vary from 0 to 1. The value of redundancy is a relative number that expresses the extent to which a given measurement contributed ( $1 - r_i$ ) or did not contribute ( $r_i$ ) to the determination of the unknowns. A low value of redundancy indicates a weak configuration, making it more difficult to have control, but it is easier to have control at higher values. The  $\mathbf{R}$  redundancy matrix can be used to write a relationship between residuals  $\mathbf{v}$  and measurements  $\mathbf{l}$  (6):

$$\mathbf{v} = -\mathbf{R} \cdot \mathbf{l} \quad (6)$$

Thus, the equation (6) can also be written for the measurement of  $\Delta l$  wearing a gross error (7):

$$\Delta \mathbf{v} = -\mathbf{R} \cdot \Delta \mathbf{l} \quad (7)$$

Equation (7) allows the detection of gross errors because gross errors do not have large residuals when the redundancy value is low. According to Baarda's suggestion, the normalized residual can be used instead of the residual itself (8):

$$w_i = \frac{v_i}{\sigma_{v_i}} \quad (8)$$

The standard deviation of the residuals  $\sigma_{v_i}$  in formula (8) can also be calculated from the covariance matrix of the residuals or the redundancy value (9):

$$\sigma_{v_i} = \sigma_0 \sqrt{(\mathbf{Q}_{ll})_{ii}} = \sigma_0 \sqrt{(\mathbf{Q}_{vv} \cdot \mathbf{P})_{ii}} = \sigma_{l_i} \sqrt{r_i} \quad (9)$$

Based on Equation (9), it can be seen that  $w_i$  cannot be interpreted at  $r_i = 0$ , so error filtering is not possible in that case. Otherwise, gross errors can be detected as follows (10):

$$|w_i| \begin{cases} > k: \text{gross error} \\ \leq k: \text{no gross error} \end{cases} \quad (10)$$

The value of  $k$  in condition (10) can vary between 1.96 and 3.29 according to the corresponding statistical tests.

With the Data snooping method, we can only detect one gross error at a time, so the adjustment should be continued iteratively until all gross errors have been filtered out.

Robust estimators can be divided into two major groups:

- $L_p$ -norm estimators, where  $p$  denotes the power, and it can be between  $1 \leq p \leq \infty$ . If  $p = 2$ , then this corresponds to the least squares method. In the cases  $p = 1$  and  $p = \infty$ , the solution leads to linear programming. In photogrammetric practice, the  $L_1$  and  $L_2$  norms are most relevant.
- The adjustment method of least squares using weight functions that reduce the weights associated with gross errors.

The essence of this weighting-dependent iterative method is as follows:

The adjustment begins with the least squares method in the traditional way. However, in subsequent iterations, the observations receive a new weight ( $p'_i$ ) according to a specific weight function that includes residuals and other defined parameters. If the weight function is chosen correctly, the weights for gross errors will become smaller and smaller until they reach zero. When the iteration process is complete, the remaining errors will clearly indicate the points having a gross error.

Kruck suggests the following weight function (11), [4]:

$$p'_i = p_i \frac{tg\left(\frac{1-r_m}{c}\right)}{tg\left(\frac{1-r_i}{c}\right)} \quad (11)$$

The  $c$  in formula (11) is given empirically, for the redundancy values  $r_m$  is the average redundancy, which can be calculated by the following formula (12):

$$r_m = \frac{n-u}{n} \quad (12)$$

The weights become constant as the iterations progress, and a stability is reached, namely when  $r_i = r_m$  becomes true.



#### IV. CONCLUSIONS

As a summary we can say that a fully automatic gross error detection is not possible in every case. The error filtering process is working well only in those cases if the following conditions are fulfilled:

- the number of gross errors is not very high,
- large and medium size gross errors should be eliminated before the adjustment procedure,
- the sample (the number of measurements) is large enough to detect gross errors with statistical methods,
- the allowable random errors follow the normal (Gaussian) random error distribution,
- the geometric configuration of points participating in the adjustment should be favourable.

We can meet some conditions in the above list but not all ones. Therefore, the fully automatic error detection still remains

a task. On the other hand, we can see a very progressive development in this area thanks to the development of more sophisticated solutions for cloud services designed for processing of UAV images. Here the whole process is fully automatized, the user receives only the final products as orthophoto, DSM or DTM model.

#### REFERENCES

- [1] Jancso T., "Design of Software Modules for Serving DPWs", In: Orosz, Gábor (Ed.) AIS 2018 - 13th International Symposium on Applied Informatics and Related Areas, Székesfehérvár, Hungary, Óbuda University, Alba Regia Technical faculty, pp. 5-10., 2018.
- [2] Wang Z., "Principles of Photogrammetry", Beijing, Press of Wuhan Techn. Univ. of Surveying and Mapping, 1990.
- [3] Kraus K.: Photogrammetry, Geometry from Images and Laser Scans, Walter de Gruyter GmbH & Co. KG, Berlin, 2nd edition, ISBN 978-3-11-019007-6, 2007
- [4] T. Luhmann, S. Robson, S. Kyle and I. Harley: Close Range Photogrammetry, Whittles Publishing, ISBN 978-3-11-030269-1, pp. 97-103., 2014

**POSTER SESSION I.**  
**Applied Informatics**

# SMART PEDESTRIAN CROSSING FOR THE BLIND AND VISUALLY IMPAIRED

Dávid Fischer  
VisibleCrossing Kft.  
Székesfehérvár, Hungary  
[david.fischer@visiblecrossing.com](mailto:david.fischer@visiblecrossing.com)

Mátyás Marx  
Alba Regia Technical Faculty  
Óbudai University  
Székesfehérvár, Hungary  
[matyasmarx@gmail.com](mailto:matyasmarx@gmail.com)

Monika Pogátsnik  
Alba Regia Technical Faculty  
Óbudai University  
Székesfehérvár, Hungary  
[pogatsnik.monika@amk.uni-obuda.hu](mailto:pogatsnik.monika@amk.uni-obuda.hu)

**Abstract**— The aim of our research is to promote equal opportunities for the blind and visually impaired. It is indisputable that they can encounter challenges even in everyday traffic situations. An environment which is not unobstructed can make it impossible for a visually impaired person to approach it unaided. They are only able to use it independently when strict conditions are met in pedestrian crossing points without traffic control equipment. SafeXOne [1] is a smart pedestrian crossing system designed for roads without traffic control equipment. Our goal was to design an addition that supports the visually impaired in their orientation, mainly through a voice-based solution. It would allow for the proper recognition of the crossing point, i.e., the orientation of the individual. We want to help the visually impaired with supplemental light signals as well. In addition, we use the basic warning signals of the SafeXOne system to enhance security.

**Keywords**— *smart crossing, visually impaired, blind person, sound signal.*

## I. INTRODUCTION

### A. The goals of the project

As stated in the abstract, the main goal is to promote the safe inclusion of blind and visually impaired people in our public spaces. The project focuses on pedestrian crossings. Visually impaired people usually avoid places and routes that they consider unsafe. This may mean that a specific crossing point simply does not have any traffic control system established. In these situations, they can only rely on auditory cues. The system explained in this study offers a solution that enhances the safety of crossings and intersections that lack traffic lights.

### B. Overview of the SafeXOne system

The SafeXOne smart pedestrian crossing system is a newly created traffic safety tool. It was designed with easy installation in mind, so the road and sidewalk surfaces do not need to be broken up. This allows the application to be used widely and to be set up quickly. The system is comprised of four 1m tall rectangular poles, two at each side of the crossing. The poles that are on the same side make up an optical gate that uses infrared light to detect movement. This connection allows the system to notice a pedestrian crossing the road. The two types warning signals to oncoming vehicles are the bright yellow blinkers and the laser plane projected over the crossing at ankle height. Raspberry Pi modules realize controlling of the system. This includes network communications, data collection, and remote control.



Fig. 1. Demonstration of the SafeXOne system

Figure 1. is a still image of the functional simulation of SafeXOne. Here we can observe the design and the light signals that define the base system.

## II. BACKGROUND RESEARCH

### A. The number of visually impaired people in the population

Based on the data of the World Health Organization [2], the number of visually impaired people worldwide was estimated to be around 285 million (in 2010). This includes 39 million blind people and 246 million with less severe visual impairment. 82% of blind and 65% of visually impaired people were over the age of 50.

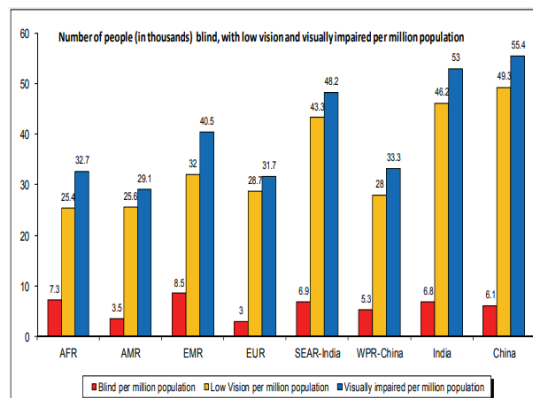


Fig. 2. Statistics of the number of visually impaired people (2010) [2]

Figure 2. visualizes the number of blind and visually impaired people according to geographical regions. It is clear that in the European region the proportion of these people is under the global average. Nevertheless, there were more than 26 million people living with visual impairment in the area at the time of the statistic.

According to the Hungarian Central Bureau of Statistics [3], [4], the population of Hungary in 2011 was 9,985,722. This included 82,484 visually impaired individuals, of which 9054 were blind. Around 61% of visually impaired and 53% of blind people are women. Furthermore, approximately 76% of visually impaired and 74% of blind individuals are over the age of 50. This illustrates that older persons are more likely to suffer from visual impairment. 15.6% of visually impaired and 18.9% of blind people live in the capital. In towns and municipalities, the proportion of visually impaired people is 64.3% whilst for blind people it is 61% [4].

Based on these statistics we can conclude that the vibrant capital city is not the most preferred choice of habitation for these individuals. The reasons for this phenomenon include the hard adaptation to the high local traffic that pose challenges for the mentioned groups.

## *B. Special circumstances related to the target group's daily traffic situations*

### *1) Types of visual impairment*

Several studies have been conducted to help improve the lives of visually impaired people. These studies unfold the way they sense their surroundings and their daily experiences [5]. Researching the topic can help us understand that even actions that seem mundane to us can be a challenge to a visually impaired individual. Their habits related to traversing traffic are greatly affected by the type of visual impairment that they have. The general cases are the following:

- Reduced sharpness: Most people are familiar with this concept. The main sufferers are the older generations.
- Limited field of vision (central): People with this sort of impairment can benefit from signals that they can detect with their peripheral vision.
- Limited field of vision (peripheral): Due to the loss of their peripheral vision, the individual cannot react to the other participants of traffic properly.
- Combination of reduced sharpness and limited field of vision
- Light sensitivity only: Individuals who can sense some light, for example identify the location of a strong light source.
- Complete blindness: This category includes people that cannot sense any light.

### *2) Daily traffic related challenges*

In the following section we explain the challenges a visually impaired person may face that seem simple for an able individual [5].

In an unknown intersection the most important information we need is which street we are in. This is rarely displayed in a format that an impaired person can make sense of. They often need to develop a mental map of their common routes that helps them track their location. They usually achieve this by counting housing blocks or intersections. In other cases, they may ask fellow pedestrians of their current whereabouts. A blind person has to process much information while crossing an intersection. They must figure out if their destination is straight ahead, or if they should make a turn. They need to be aware of the number of streets merging in

the intersection and the width of the road. They need to know whether the curb they reached is the other side or just a safety island. These parameters are readily available to an able person. Contrary to this, blind people cannot attain the same information as they can only use their hearing. Improper or missing information might even cause dangerous situations. Regarding the traffic control systems of the intersection, the blind person must be aware of the following:

- Type of the system
- Whether there is an integrated sound signal
- Whether the lamp is initiated by a button, and the location of that button
- Whether there is enough time available to properly analyze the orientation of the crossing before the lamp switches and they have to cross.
- Whether the specific equipment stops traffic completely or just partially.
- If a safety island is present, whether there is a second button to be pressed at the island.
- Whether there is any parallel traffic during their crossing of the road.

Attainment of all this information may be accomplished through listening to patterns across multiple signal cycles or searching for poles with buttons along the sidewalk.

Before a blind pedestrian crosses the road, they must be aware of their orientation to the crossing. Tactile ground surface indicators (if present) and auditory cues about the parallel traffic might aid the person.

In conclusion, any signal that may seem insignificant to people with normal vision can help a visually impaired individual tremendously, as they use any information that they possibly encounter.

## *C. Current solutions aiding the target group*

In this section, we take an overview of the already used assistance methods for visually impaired people. This helps us identify the most dangerous situations for the individuals and the existing solutions. Furthermore, knowledge of the current technology allows us to assess whether we can integrate some of it into our system.

### *1) General methods*

As an introduction, we shall list the simplest and oldest aiding techniques [5]. These are the following:

- Travel companion
- White cane
- Service dog

### *2) Remote control*

A more advanced method is the use of a four-button remote control that initiates various aiding equipment in Budapest, Hungary. This remote control helps visually impaired people find traffic control lamps, start speakers at public transport stops that tell them about the upcoming buses and trams, and the ATS systems. This is used for example at Metro line 4, where it helps them find the proper escalator [6].

### *3) Crosswatch*

Crosswatch [7] is a mobile phone application that helps blind people navigate at intersections using the camera of their phone. It uses machine vision to provide information to the

user about the location and orientation of the intersection. The program takes several pictures in a minute, which then the phone's processor analyzes, and notifies the user via a sound signal. Tests show that the application can provide useful information to the users. Therefore, it may become a viable solution in the future.

#### 4) ZebraRecognizer

ZebraRecognizer [8] is another application that uses the camera of a mobile phone. It helps the user locate the crossings by analyzing the painted road signs. It can calculate the distance to the crossing in meters and its relative position using real-time data. This information can help the person travel more safely.

### III. HEARING AND ENVIRONMENTAL NOISE

In order to produce an auditory signal that aids the target group well, we must consider the nature of hearing as a signal processing method. The signal must be clear and easy to identify. To achieve this, we also need to account for the noise composition and levels that are present at the application environment. In this section, we analyze traffic noise, the detection of auditory signals, and the characteristics of the signal to be used in our system, based on the previous information.

#### A. Traffic noise

The Environmental Noise Directive [9] of the European Union mandates the creation of noise maps and noise protection action plans every 5 years for specified areas. These areas are towns of more than 100,000 inhabitants, roads, railways, and airports above certain levels of annual traffic in each member state. This measurement program in Hungary was last conducted in 2017 [10].

We can learn important information from the noise maps comprised of the data [11]. The size of the specific town and the traffic levels of the particular road pose radically different expectations for the sound signaling system of the application.

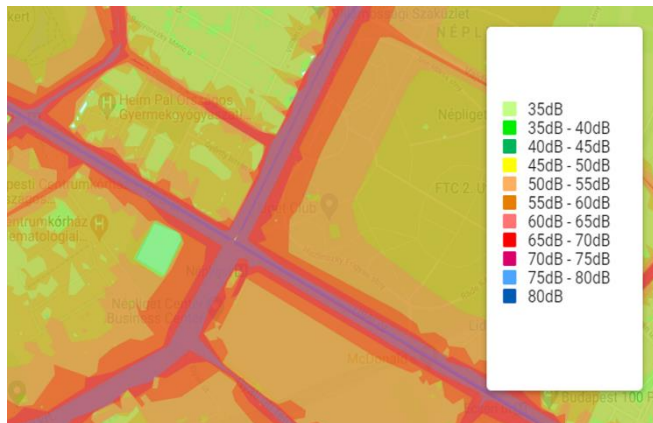


Fig. 3. The noise map of Budapest, Népliget area [11]

As it is clearly visible on Fig. 3, noise levels near a busy town road can exceed 75-80dB. In comparison, the same noise map for a less frequented small-town road (Fig. 4):

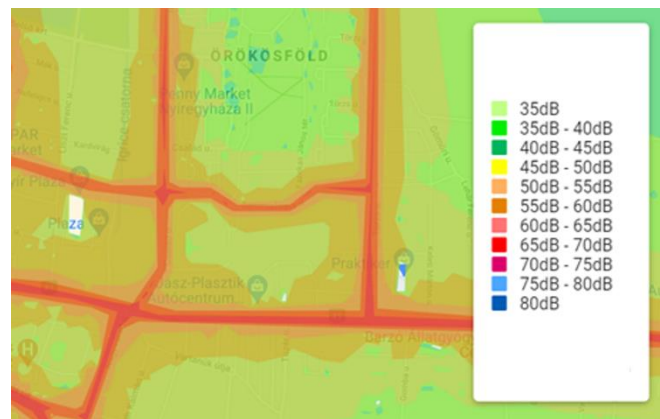


Fig. 4. Noise map of Nyíregyháza, area near Route 41 [11]

In a smaller town such as Nyíregyháza, noise levels rarely go above 70dB at the busiest roads.

It is clear, that the sound signaling system must be built in a way that it can be set up according to the noise levels of the specific application environment. This allows us to produce a signal that is loud enough to be identified, but not excessively loud, so that the system does not become irritating to the people living nearby.

Finding the lowest acceptable signal level is also important for low power consumption. Because of the logarithmic dB scale, raising the signal even just a few dBs require significantly more power (Table 1.).

TABLE I. RELATION OF SIGNAL LEVEL AND POWER REQUIRED  
REFERENCE: [12]

dB	Voltage	Power	Perceived loudness
+3	1.4X	2X	1.23X
+6	2.0X	4.0X	1.52X
+10	3.16X	10X	2X
+20	10X	100X	4X
+40	100X	10,000X	16X

The quadratic relation of the voltage and power is also obvious based on (1).

$$P = I^2 \cdot R = \frac{U^2}{R} \quad (1)$$

This must be considered when picking the suitable speaker.

#### B. Auditory signal processing

In this section, we look at the parameters of sound, mainly the ones assisting localization [14].

Based on three data, we can define the position of a sound source relative to the listener in a polar coordinate system. First one is the azimuth angle, second is the elevation angle, and third is the distance of the source.

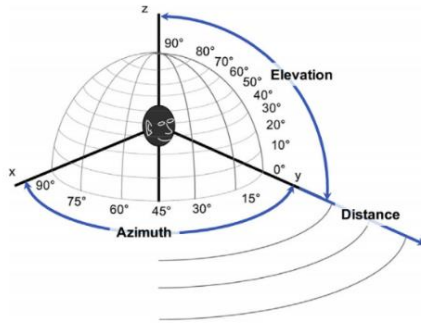


Fig. 5. Parameters of sound source localization [14]

One of the binaural cues used to determine the azimuth angle of a sound source is the Interaural Time Difference (ITD). We can observe this phenomenon on sound waves that have a wavelength greater than the diameter of the head (~17.5cm). In this range, the head causes the diffraction of the waves, and in turn, the two ears hear the sound at different times. This time difference can be expressed with Woodworth's equation (2):

$$\Delta t = \frac{r \cdot (\alpha + \sin \alpha)}{v} \quad (2)$$

Where  $r$  is the radius of the head in meters,  $\alpha$  is the azimuth angle in degrees ( $-90^\circ < \alpha < 90^\circ$ ), and  $v$  is the speed of sound in meters per second. ITD is the biggest at  $90^\circ$  incidence angle, as this is the case where the sound waves need to travel the most distance between the two ears. Using Woodworth's equation, we can calculate that this distance is  $2.57r$ . Taking  $r$  to be 0.0875 meters, we can use the basic equation for frequencies to see the maximal frequency in (3):

$$f_{\max} = \frac{v}{\lambda_{\min}} = \frac{343}{2.57 \cdot 0.0875} \approx 1525 \text{ Hz} \quad (3)$$

Where  $f_{\max}$  is the maximal frequency where ITD is still relevant, and  $\lambda_{\min}$  is the corresponding minimal wavelength. Thereby, 1525 Hz is approximately the biggest frequency where the phase-shift of the wave carries useful information for the brain regarding the location of the sound source.

The binaural cue that helps localization in the higher frequency range is the Interaural Intensity Difference, or Interaural Level Difference (IID/ILD). We can observe this phenomenon with sound waves that have a shorter wavelength than the diameter of the head. In this frequency range, the head blocks and reflects some of the acoustic energy (masking). This causes the two ears to perceive the sound with different intensities. Using the same approach as before, we can calculate the lowest frequency where the phenomenon is relevant ( $f_{\min}$ ) in (4):

$$f_{\min} = \frac{v}{\lambda_{\max}} = \frac{343}{0.175} \approx 1960 \text{ Hz} \quad (4)$$

In frequencies that are higher, the sound pressure level difference is the main information that helps localization of the sound source.

The distance of the sound source can be estimated using a variety of cues. For example, higher frequencies decay more over distance, and the ratio of direct and reverberant sound also carries information. Localization is easier for wide band sounds and sounds with a known frequency spectrum, such

as speech (for which we also have a larger basis of comparison). The binaural cues mentioned before can also help in some cases [14].

Localization in the direction of elevation is less important for our application, so we are not going to elaborate on that topic. It is also important to examine the perceived loudness of sounds. Sound pressure levels in decibels do not define the detectability of a sound completely. At different frequencies, we sense different sound pressure levels to be "equally loud". We can illustrate this using the equal loudness curves.

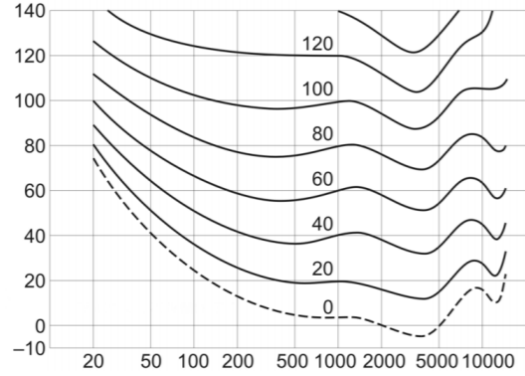


Fig. 6. Equal loudness curves (x=frequency in Hz, y=sound pressure level in dB) [15]

The perceived loudness in phons is equal to the measured sound pressure level in dBs at 1 kHz. 0 phons is the threshold of hearing. It is clear that different frequencies have a different threshold. We can also see that for example a 20 dB signal at 1 kHz and an 80 dB signal at 20 Hz are perceived to be equally loud [15].

We can see that the human hearing is quite sensitive below 1000 Hz, while localization is also adequate in this range [14]. Correlating with this assumption, other studies have shown that for traffic signal speakers 880 Hz is an ideal frequency, as it can be detected well in traffic noise, while walls and windows block it decently. This makes the signaling system more tolerable for the locals [16].

Still, we do not need to use only this single frequency. The properties of sound discussed in this section (frequency, sound pressure level) can be measured with proper instruments. Thereby, if we can integrate a suitable measuring device in our system (a certain microphone), then we can measure the aforementioned properties, and create a signal that is the most suitable for the given situation. It would allow us to dynamically alter our signal's traits, accounting for the level and composition of ambient noise in the given moment. This would make sure that the signal is loud enough, but only as loud as needed, and is not masked by the present frequencies of traffic noise. Human voice would also be a suitable signal, as our hearing is pronouncedly sensitive to it. This dynamic application method would make our system well suited to be implemented in a smart city concept. Based on the knowledge gathered in this section, we can conclude the following requirements for the sound signaling system to be implemented into our application:

- The system needs to monitor ambient noise dynamically.
- The selected speaker must be able to operate in a wide frequency band (for example the bandwidth of speech).

We need to select devices that meet these criteria.

#### IV. SELECTING THE DEVICES

##### A. The structure of the system

The sound signaling system needs five basic components. To measure the frequency composition and sound pressure level of the ambient noise, we need a microphone. To produce the suitable signal based on the measured data, we need a wideband speaker. The subsystems also need to communicate with one another, as there are four individual poles in the SafeXOne system. Furthermore, we want to utilize the remote control mentioned in the *Current solutions* section. A signal detection device is required to facilitate the communication with this tool. Last, but most importantly, we need to integrate programmable electronics to control all the equipment that make up the system.

##### B. Programmable electronics

Because of the local data processing, choosing the suitable programmable electronics also defines the range of the other devices that we can use. Some equipment may not be compatible with certain electronics, and the amount of data to be sent and processed is also a major factor. Thereby, it is important to select control electronics that can accommodate most modules without significant redesign and changes. This property is especially important for the prototype stage. The most widely used such devices are the Raspberry PI [17] and the Arduino [18] products.

The Raspberry PI is basically a low power computer. Even the simplest version can run a terminal-based operating system. From a data processing standpoint, this makes the device really strong. The downside of this strength is higher power consumption. Whether such high data processing capabilities are needed is also worth consideration.

Arduino is one of the most common programmable microcontroller brands. This is partially due to the reasonable pricing, but also the open-source hardware and software. This means that with proper skills and knowledge the modules can be modified to suit a specific application (for example, there are many robotics-specific modules). The software can also be expanded with self-written extension modules, in a remarkably easy manner. This allows for a wide selection of equipment to be integrated, which makes Arduino the basis of many similar projects [19], [20].

Based on all this information, we selected Arduino (Nano 33 IoT) for this stage of the project. The choice of other devices shall be based around this decision.

##### C. Local communication

The system is made up of four subsystems. This necessitates communication of these devices. This communication is required at the initiation of the system (when the pedestrian uses the remote control), so that all the units receive the signal. It is also necessary during data collection. This connection is needed as it would not be efficient to equip all four units with network communication and signal detection capabilities. There are many widespread and proven wireless local communication solutions, the most common ones being WIFI and ZigBee [21], [22], [23].

The ZigBee technology is oriented towards low consumption and good security. It is suitable for applications with small data traffic.

WIFI is a well spread local communication technology. There are many modules based on this solution. Some of these applications are optimized for quick data transmission, others for low power consumption, so the options are abundant.

The use of wired communication is not viable, as roads that have been built with EU funding cannot be reworked within five years after their completion [24].

At this stage of the project, selecting the local communication tool is not appropriate. After some testing, we can have a closer idea about the amount of data to be transmitted, as well as the necessary network speed. We can select the proper device based on these pieces of information later.

##### D. Speaker

The basic operating principle of loudspeakers is that they convert electrical power to the kinetic energy of a diaphragm. This diaphragm in turn moves the surrounding air particles, which we perceive as sound. There are many types of transducers used today (magnetostatic, piezoelectric, electrodynamic, etc.). For our application, we plan on using an electrodynamic loudspeaker. One of the main reasons behind this choice is the close proximity of Harman-Becker Automotive Systems LLC., and VisibleCrossing LLC. The goal is the closer collaboration of the two Székesfehérvár-based companies in the future.

An electrodynamic loudspeaker is remarkably simple, consisting of just eight main components [25]:

- Pole plate: A component of the magnet system. It helps channel the magnetic flux lines through the desired path.
- Magnet: Provides a permanent magnetic field. Its material is usually either ferrite or neodymium.
- Front plate: The third piece of the magnet assembly. Like the pole plate, its purpose is to channel the magnetic flux lines to the airgap.
- Voice coil: The current passing through the coil produces a magnetic field according to Lenz's law. The coil is placed in the permanent magnetic field of the magnet assembly, so the induced field of the coil will cause it to move. Altering the frequency of the current, we can produce sound.
- Spider: The main suspension part of the speaker. It makes sure that the coil returns to its original location after the current changes.
- Basket: It is the central frame of the speaker, to which all the subassemblies are connected.
- Cone: The diaphragm that radiates sound. It moves together with the voice coil, providing a larger surface to move enough air to produce adequate sound energy.
- Dust cap: It closes the center of the voice coil, protecting it from the outer elements. It is also part of the diaphragm sources and affects the speaker's sound reproduction capabilities.

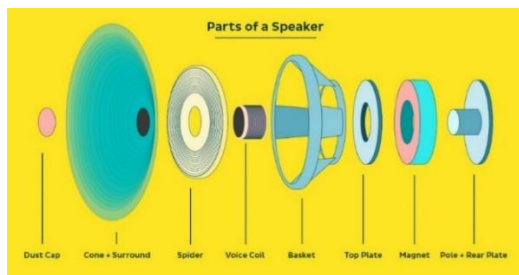


Fig. 7. Exploded view of an electrodynamic speaker [26]

This allows for an economical design with good power handling capabilities.

Certain supplemental elements may also be added to alter the sound pressure levels produced at different frequencies. Specific tonal imbalances in the frequency response can be corrected either actively (DSP software) or passively (with an RLC-circuit based filter). These solutions usually depend on the specific application. The device to be used in this certain project is not aimed to achieve the cleanest Hi-Fi sound, thereby, we might not need to resort to such extensions [25]. The directivity of the speaker might be of more interest. This can be affected using a grille or waveguide in front of the speaker [25]. The latter increases the directivity of the transducer, while it also raises the sound pressure level generated. This power increase is quite important for our far-field application. Using the industry standard measurement data of a speaker (sound pressure level at 1 meter, with 1 Watt input power) we can calculate the decrease of intensity over specific distances (5).

$$I = 20 \cdot \log_{10} \left( \frac{d_1}{d_0} \right) \quad (5)$$

Where 'I' is the decrease of intensity, 'd<sub>0</sub>' is the referenced distance from the speaker, and 'd<sub>1</sub>' is the distance from the speaker at which we want to know the decrease. Taking a general speaker with ~85 dB<sub>SPL</sub> sensitivity at d<sub>1</sub>=15 meters, we can see that the decreased intensity is only 62 dB with 1 Watt input power. If we check Table I., we can see that regaining this loss of more than 23 dBs would require over 100 times the power. With this in mind, the 4-5 dB increase provided by a waveguide can be very useful.

Based on our requirements, the speaker should be similar to ones used in AVAS (Acoustic Vehicle Alerting System) roles, in electric and hybrid powered cars. These speakers usually have a sensitivity of 80-85 dBs. Even more importantly, they can handle whether conditions very well, due to their original application. This must be considered, as our system is continuously operated outdoors, in varying environmental conditions.

### E. Microphone

One of the most important criteria of our project is to produce a sound that accounts for the dynamically changing ambient noise, so that the transferred information is always adequate to the pedestrian. To accomplish this, we need to measure the properties of the surrounding traffic noise. It is clear that perfect real-time measurement cannot be achieved, as the system's own sound generation and the measurement of ambient noise happens close by. The solution to this is that the sound to be produced would be defined based on data

collected before the specific time of initiation of the aiding signal (pressing the button on the remote control). To achieve this, we need to constantly store noise data for predefined stretches of time [27].

A microphone to be connected to programmable electronics is composed of two main parts. One is the microphone unit itself, the other is an amplifier circuit on a PCB board. The most often used microphone technology is that of an electret microphone. This is a capacitor-based transducer with a pre-polarized membrane, so there is no pretensioning needed. Due to its special makeup, its size can be particularly small. This is the reason why these microphones are the predominant choice for mobile phones. Setting the amplification correctly is key for this microphone type.

There are two main types of amplifier circuits used for this application. The first one is automatically set, where the circuit sets the gain dynamically, based on the sounds of its surroundings (mainly used for sound recordings). The second type can be manually adjusted, which allows for sound pressure level measurements, and comparison of the measured data. This second type would be suitable for our solution. The most adequate gain setup would be set based on future tests.



Fig. 8. MAX4466-based electret microphone with adjustable gain

With the reasons mentioned above in mind, we selected the MAX4466-based electret microphone with adjustable gain (Fig. 8.) [28].

### F. Logical composition

Figure 9. illustrates the proposed logical connections of the components in the system. There is a one-way data transfer towards SafeXOne. The early prototype would be designed to be simple, where SafeXOne takes part in the transfer of data through internet, and supplies power to the devices.

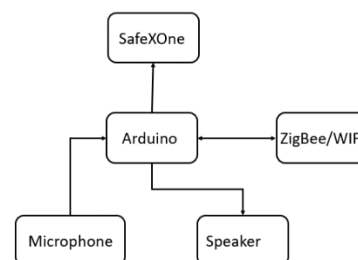


Fig. 9. Illustration of the system's logical composition

The local communication module would either be ZigBee or WIFI. This is the unit that is responsible for the internal communication of the system, providing two-way communication between devices. The microphone sends the



raw data to the Arduino module, which is responsible for the processing of this data. At the end of the sequence, the speaker produces the calculated signal.

## V. CONCLUSION AND FUTURE PLANS

To this point of our research, we collected the reasons and requirements that support the necessity of the proposed system and are needed for the creation of the prototype. The base idea is to upgrade the SafeXOne system with equipment that helps the orientation of visually impaired people at pedestrian crossing points and helps their navigation during the crossing.

To supply the necessity of the idea, we overviewed the types of visual impairment and the specific needs of aid for each type. We collected information on the existing aiding technologies, best practices in the area of traffic safety, some of which we may use to expand our system (supplemental light signal, tactile surface, etc.). We started designing the system after assessing the compiled knowledge.

In the following section of the project, we examined the question of hearing: the process of it, detection of auditory signals, sound source localization, and the information needed to select the proper aiding signal. These are all needed to select the right devices and optimize future tests and measurements.

After this research, we set up the requirements and defined the devices to be used. These are the programmable electronics, the local communication technology, the speaker, and the microphone. The devices were selected with the goal of creating a prototype and to conduct first round tests. For the programmable electronics, we selected Arduino, based on its flexible programming, as well as the open-source hardware and software. There are also some related existing solutions that further support this choice. The speaker would be a noise generator used in electric cars, based on its sensitivity, wide-band sound reproduction capabilities, and environmentally resistant structure. Last but not least, the microphone would be a MAX4466-based electret microphone with adjustable gain. This adjustment allows us to alter the amplifier circuit based on the conducted future measurements. The frequency range of the device is also suitable for our applications, while the simplicity and widespread use also makes acquiring the product easier.

The next step of the project is obtaining the parts for the prototype, composing the system, and conducting tests and measurements. The initial test would be conducted in controlled environments, while later the extension devices can be installed at currently operating SafeXOne pedestrian crossing sites.

## REFERENCES

- [1] M. Pogatsnik, D. Fischer, L. Nagy and S. Dora, "Autonomous pedestrian crossing in smart city environment," 2020 IEEE 24th International Conference on Intelligent Engineering Systems (INES), Reykjavik, Iceland, 2020, pp. 37-42, doi: 10.1109/INES49302.2020.9147188.
- [2] WHO, "Global data on visual impairment", URL: <https://bit.ly/3GhjvGM>, Download: 2021.02.18.
- [3] KSH, "Magyarország népességének száma nemek és életkor szerint" (Population of Hungary by sex and age), 2020 január 1. URL: <https://bit.ly/3C7Zx5G>, Download: 2021.02.18.
- [4] KSH, "A fogyatékkal élők helyzete és szociális ellátásuk" (The situation of people with disabilities and their social benefits) URL: <https://bit.ly/3vCSwaA>, Download: 2021.02.18.
- [5] NCHRP, "Accessible Pedestrian Signals: A Guide to Best Practices", URL: <https://bit.ly/2ZixwK0>, Download: 2021.02.18.
- [6] MVGYOSZ, "4 gombos távirányító látássérültek számára" (4-button remote control for the visually impaired), URL: <https://bit.ly/3jvsGk6>, Download: 2021.03.12.
- [7] V. N. Murali and J. M. Coughlan, "Smartphone-based crosswalk detection and localization for visually impaired pedestrians," 2013 IEEE International Conference on Multimedia and Expo Workshops (ICMEW), San Jose, CA, USA, 2013, pp. 1-7, doi: 10.1109/ICMEW.2013.6618432.
- [8] D. Ahmetovic, C. Bernareggi, A. Gerino and S. Mascetti, "ZebraRecognizer: Efficient and Precise Localization of Pedestrian Crossings," 2014 22nd International Conference on Pattern Recognition, Stockholm, Sweden, 2014, pp. 2566-2571, doi: 10.1109/ICPR.2014.443.
- [9] European Commission, "Environmental Noise Directive" URL: <https://bit.ly/3GhOHwi>, Download: 2021.02.26.
- [10] European Environment Agency, "Strategic noise maps (DF 4 and DF 8)" URL: <https://bit.ly/3m6PY1l>, Download: 2021.02.26.
- [11] Herman Ottó Intézet Nonprofit Kft. [Online]: Zajtérkép (Noise map) URL: <https://zajterkep.hu/index.html#>, Download: 2021.02.26.
- [12] Galen Carol Audio, "The Relationship of Voltage, Loudness, Power and Decibels", URL: <https://bit.ly/2XE5WXj>, Download: 2021.02.26.
- [13] L. Hodossy, „Elektrotechnika I.” (Electrotechnics I.) URL: <https://bit.ly/3GeXLC9>, Download: 2021.02.26.
- [14] M. Risoud, J.-N. Hanson, F. Gauvrit, C. Renard, P. E. Lemesre, N.-X. Bonne, C. Vincent, "Sound source localization" (2018), URL: <https://bit.ly/3E7gHDr>, Download: 2021.03.14.
- [15] P. Antal, T. Tóth, "Elektronikus tananyagok tervezése (Design of electronic study materials) (2014), URL: <https://mek.oszk.hu/14100/14163/pdf/14163.pdf>, Download: 2021.03.15.
- [16] M. Niewiarowicz, A. Furmann: Localization of Acoustic Signals Used in Sound Emitters at Pedestrian Crosswalks (2012) URL: <https://bit.ly/3GfKU2z> Download: 2021.02.15.
- [17] [Online] „Raspberry Pi website” URL: <https://www.raspberrypi.org/>, Download: 2021.03.11.
- [18] [Online] „Arduino webpage” URL: <https://www.arduino.cc/>, Download: 2021.03.11.
- [19] J. Sarik and I. Kymissis, "Lab kits using the Arduino prototyping platform," 2010 IEEE Frontiers in Education Conference (FIE), Arlington, VA, USA, 2010, pp. T3C-1-T3C-5, doi: 10.1109/FIE.2010.5673417.
- [20] T. H. Nasution, M. A. Muchtar, I. Siregar, U. Andayani, E. Christian and E. P. Sinulingga, "Electrical appliances control prototype by using GSM module and Arduino," 2017 4th International Conference on Industrial Engineering and Applications (ICIEA), Nagoya, 2017, pp. 355-358, doi: 10.1109/IEA.2017.7939237.
- [21] A. D. Deshmukh and U. B. Shinde, "A low cost environment monitoring system using raspberry Pi and arduino with Zigbee," 2016 International Conference on Inventive Computation Technologies (ICICT), Coimbatore, India, 2016, pp. 1-6, doi: 10.1109/INVENTIVE.2016.7830096.
- [22] Cs. Faragó, "ESP8266 chip", URL: <http://faragocsaba.hu/arduino-esp8266>, Download: 2021.04.05.
- [23] European Commission, „European Innovation Partnership - ZigBee”, URL: <https://bit.ly/3b0v9uC>, Download: 2021.04.14.
- [24] EU, "Green Public Procurement Criteria for Road Design, Construction and Maintenance", URL: <https://bit.ly/3E3FqGg>, Download: 2021.09.01.
- [25] Based on internal documentations owned by Harman International Corp.
- [26] Rory Seydel (Landr), "How do speakers work: Understanding Audio Reproduction" URL: <https://blog.landr.com/how-do-speakers-work/> Download: 2021.04.07.
- [27] A. Yavilevich, „Arduino sound level meter and spectrum analyzer” URL: <https://bit.ly/3ppPFkm>, Download: 2021.04.05.
- [28] Adafruit, „Electret Microphone Amplifier - MAX4466 with Adjustable Gain” URL: <https://www.adafruit.com/product/1063> Download: 2021.04.05.

# UAV based navigation system for forest fires monitoring

Daniyar Kaliyev

*School of Information Technology and Intellectual Systems*

*D.Serikbayev East Kazakhstan Technical University*

Ust-Kamenogorsk, Kazakhstan  
[daniyar.1996.samarka@gmail.com](mailto:daniyar.1996.samarka@gmail.com)

Olga Shvets

*School of Information Technology and Intellectual Systems*

*D.Serikbayev East Kazakhstan Technical University*

Ust-Kamenogorsk, Kazakhstan  
[olga.shvets75@gmail.com](mailto:olga.shvets75@gmail.com)

György Györök

*Alba Regia Technical Faculty Óbuda University,*

Budapest, Hungary  
[gyorok.gyorgy@amk.uni-obuda.hu](mailto:gyorok.gyorgy@amk.uni-obuda.hu)

**Abstract** — In recent years, large amount of forest has been destroyed by fires, bringing terrible consequences for the environment and society. It is important that firefighters possess an increased situational awareness about the fire spread, in order to act appropriately to prevent the fire to an uncontrollable size. Recent advances in UAV technology shows promising applications for UAVs to detecting and monitoring forest fires. Therefore, one of the most important issues is UAV's flight navigation system. In this study, we suggest a structural diagram of the UAV navigation system, which is based on radio control from a ground control panel using geolocation system. This approach provides effective application of UAV, both in automatic and manual modes by means of onboard navigation and control equipment. The results shows that the use of UAVs is an effective way of combating a fire situation in addition to existing methods and technologies for solving operational problems of fire detection.

**Keywords** — *aerial fire monitoring, forest fire, UAV, navigation system.*

## I. INTRODUCTION

In recent years there have been a significant number of wildfires that have devastated millions of hectares of forest. In addition to destroying local flora and fauna, these fires also destroy infrastructure and, unfortunately, sometimes result in human casualties among fire brigades and civilians who may be accidentally surrounded by fire. Thus, early detection and real-time fire surveillance are two key factors that allow firefighters to act appropriately to keep fires from reaching unmanageable proportions. There is a need for a less costly and more efficient way to accomplish the forestry tasks previously performed by aviation. In this regard, of particular interest are unmanned aerial vehicles of various technical equipment and flight ranges.

Unmanned aerial vehicles (UAVs) are becoming even more important for environmental monitoring, on the one hand, providing data from remote and inaccessible areas, and on the other, reducing the cost of conducting necessary research using traditional field methods, while increasing operational efficiency. Photo and video recordings obtained with the help of unmanned aerial vehicles, both with conventional and special cameras, give a complete picture of forest massifs and their condition, including information on the species and heights of trees and their exact location in accordance with the coordinates of the GPS and Glonass navigation systems, which, of course, is necessary for effective and sustainable forest management.

UAVs with computer-based remote sensing systems are an increasingly becoming an attractive and realistic option. The use of UAVs in the fire systems solves a number of problems associated with the lack of staff, the inaccessibility of areas, the need to minimize the impact of human presence, when

carrying out forestry work to determine the operational and current data on the fire.

The use of UAVs at the moment is limited to special cases when solving production tasks, mainly in an experimental manner. Relevant is the development of theoretical foundations and practical techniques for organizing the effective use of UAVs for detecting forest fires with the definition of flight paths, parameters of information and command lines of communication. In addition, it is important to have spare power units or a device for recharging them in the field, as well as the required number of the most demanded spare elements of the UAV [1].

The modern level of technology has greatly expanded the capabilities of UAVs as an autonomous system of various structural forms of design and purpose. Thanks to the use of various cameras and prompt automated processing of the obtained information, such vehicles can be used to monitor the state of forests, roads, the effectiveness of forest management activities [4]. The use of computer vision technology in the remote monitoring system using UAVs will automatically detect fires in real time and warn about them. The processing of data received from the UAV makes it possible to determine the places of fire occurrence, as well as to quickly and correctly determine the coordinates of the place of fire occurrence and mark them on the terrain map. This article discusses the use of navigation control system of UAVs, which allow to perform flights for monitoring and detection of forest fires.

## II. SYSTEM DESIGN

### A. System description

One of the most important issues in the use of UAVs for forest fire control and suppression of forest fires is the development of flight paths and flight control systems. At the same time, the built-in navigation equipment of the UAV and automatic course and vertical stabilization devices on the basis of direction gyroscope and position sensors allow to keep the body in a stable state and thus provide acceptable accuracy in determining the coordinates and direction of the forest fire on the terrain map [3]. Various methods are proposed for the precise georeferencing of UAV images, implemented by additional use of GPS navigators as part of the receiver, increasing the overlap of images [2].

Each forest fire must be monitored from the air from the moment of its detection until its complete elimination in order to take prompt action. In order to detect hidden fires, forest fires are circled 4-5 times a day. Range of fire location depends on height of observation, weather and smoke level. For the solution of this problem it is optimal to use UAVs with the flight range from 2 km to 10 km and with the flight time of 20...60 min, that corresponds to the ground patrolling.

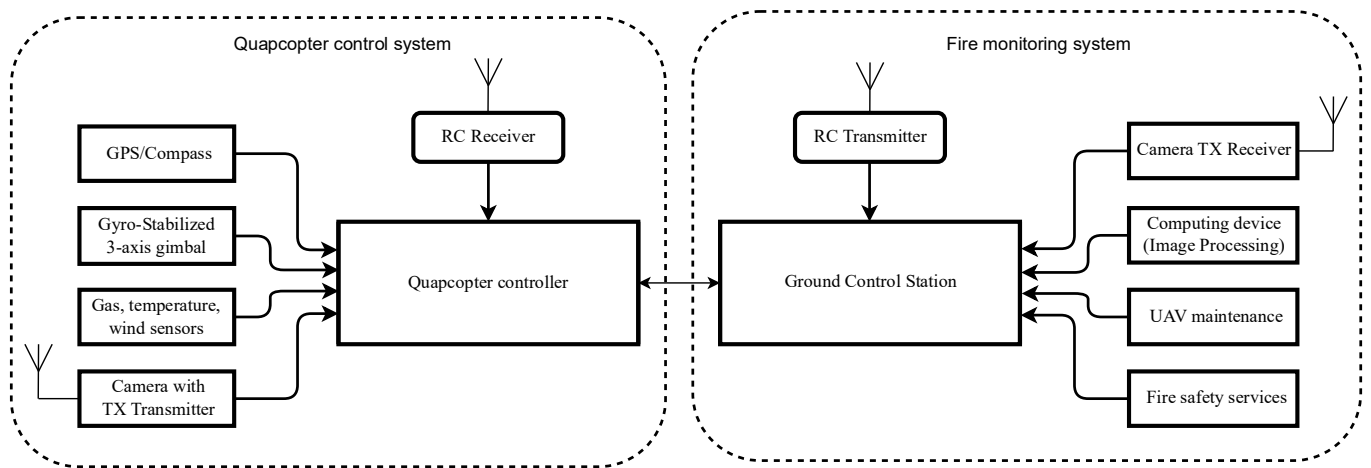


Fig. 1: Basic architecture UAV-aided navigation system communications

The UAV navigation system under development is based on radio control from the ground console by the operator and the use of a satellite navigation system, which determines navigation parameters with high accuracy. The proposed system is designed for real-time monitoring, which collect data from sensors and cameras using the UAV. The schematic of UAV based navigation system is shown in Figure 1.

### B. Ground Control Station

The Ground Control Station (GCS) acts as the central control point during UAV flights and provides the necessary capabilities to plan and execute safety-related tasks. The GCS performs functions such as flight mission planning, processing of received data (video images), modules for mobile and satellite control, and displays to track all progress. The GCS also generates alarm commands based on safety system warnings.

During flight, the UAV is controlled manually in radio control mode and automatically through onboard navigation and control equipment, which includes [8]:

- satellite navigation receiver, which provides reception of navigation information from GLONASS and GPS systems;
- an airborne communication system operating in a certain frequency range for transmitting UAV commands, streaming video and photo images;
- sensor system for determining spatial orientation by course and vertical, stabilization and motion parameters of the UAV;
- air signals system ensuring measurement of altitude and flight speed.

The onboard navigation system must ensure that the UAV [8]:

- flight along a set route (the route assignment is made with the coordinates and altitude of the route turning points);
- change the route setting or return to the start point and fly around the specified point on command from the ground control point;
- automatic takeoff, flight and landing at the operator's command at the ground control point.

To achieve these goals, the UAV-based forest fire monitoring and detection system includes the following: 1) various frames and sensors, including global positioning system (GPS) receivers, inertial measurement units (IMUs), and digital cameras; 2) specific algorithms for monitoring, detection, diagnosis, and prediction; 3) GNC guidance, navigation, and control systems for both single and multiple

UAVs; and 4) multiple UAV localization and control systems for optimal cover of fire areas [6].

### C. UAV

Currently on the market there are a plenty of UAVs of different classes, with completely different technical characteristics [9]. Let us formulate the basic requirements with the goal we are considering: the device must have an electric drive, good flight characteristics, a quality video camera and at the same time the lowest possible price. When choosing a UAV, we mainly took into account such aspects as the possibility of transporting sensors that allow monitoring a fire, together with a computer. In our case we propose to use quadcopters, because their advantages are compactness, the ability to take off and land under fairly limited conditions, the capability to change the flight speed up to zero (hover mode) for detail images [5]. The position of the UAV in latitude, longitude and altitude is determined by the controller based on the global positioning system (GPS) signal. The controller also provides the three Euler, pitch, roll, and yaw angles needed to determine the position of the UAV.

### D. Sensors

Collecting sensors data is cheap and effective way of monitoring forest fires in a secure. Nowadays, a wide variety of sensors are available, and many of them are reliable enough to help authorities respond quicker and make decisions. Temperature sensor can be useful to keep the drone in a safe zone, and this means that if the temperature is superior to a threshold, the drone should not keep the path. Besides that, it gives important information to the firefighters.

Gas sensors (also known as gas detectors) detects and identify different types of gasses. The measurements can be useful to detect the fire, for example, measuring abnormal concentration carbon dioxide.

Wind sensors with anemometer measures the wind speed, and it presents useful information for firefighters, since wind speed affects forest fires in a significant way.

Also, there are several required embedded drone sensors. The combination of accelerometer and gyroscope sensors is very useful to estimate the speed of the drone. Barometer is necessary to estimate and keep the drone altitude.

### E. Creating UAV flight mission

The flight path is set using the Mission Planner software for autonomous UAV flight. For our applications, the Mission Planner software is excellent (Figure 2). This program is an

open-source control center for the autopilot of different types of UAVs. With this program, various configurations and fine-tuning of the UAV can be selected for optimal performance; also, individual flight missions can be planned, tracked, stored, and downloaded to the autopilot with conventional point-and-click waypoint entry on Google maps or other online services[10].

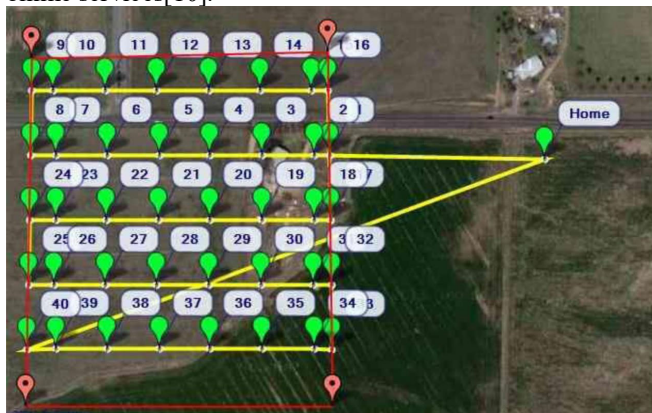


Fig. 2: Mission Planner flight plan

There are several recommended measures when performing a flight operation. The starting point should be chosen as high as possible relative to the intended route with a minimum distance from the objects under investigation to increase the useful operating time and achieve maximum results. It is necessary to determine the direction of the route relative to the ground control station and make sure there are no obstacles in this direction to ensure direct radio visibility. The landing site is selected near the starting point, taking into account the possibility of visual control of the UAV landing by the operator.

### III. ALGORITHM OF MONITORING OPERATION

#### A. Data collecting

In the first monitoring phase, the UAV takes off and begins surveillance of the target area, transmitting high-resolution images in real time to the ground station. The control points of the UAV flight are indicated on the satellite image along with coordinates in which the status of the drone is displayed. The UAV begins surveying by following the route and begins scanning the area, transmitting video images to the station. The detected event is recorded and the information is transmitted in real time to the base station. This stage also provides infrared and thermal data to simulate fire behavior and environmental parameters. The UAVs also pick up smoke and gases and transmit the information to the ground station.

#### B. Monitoring

The monitoring phase is responsible for collecting environmental parameters, scanning the target area, detecting the fire, and responding after detection. The UAV operation is programmed from the ground station and continues to explore for scanning until an event is detected in the allotted time. For this purpose, the UAV establishes several communication channels between the satellite and the ground station.

#### C. Data analysis and image processing at ground station

Control of the UAV is in the ground station, and information is transmitted to the ground station for real-time analysis for decision making. The ground station is directly connected to the UAV and the satellite system. The video

image data from the UAV is processed by a computing device (personal computer), applying image processing algorithms to detect the fire. They include:

- Image preprocessing techniques are used to improve the accuracy of data processing by changing its brightness and contrast, removing noise and sharpening the image, etc.
- Motion detection techniques such as background subtraction are used to detect fire and smoke motion in the video by analyzing the differences in the images of the video frames.
- Color detection based on RGB and HSI color models are widely used at the first step to extract fire-like pixels. This reduces the search space for further processing with more computationally expensive detection algorithms.

In case a fire is detected by the input image, a firefighting team from the ground station makes a plan to extinguish the fire [6].

#### D. The operation of the proposed architecture

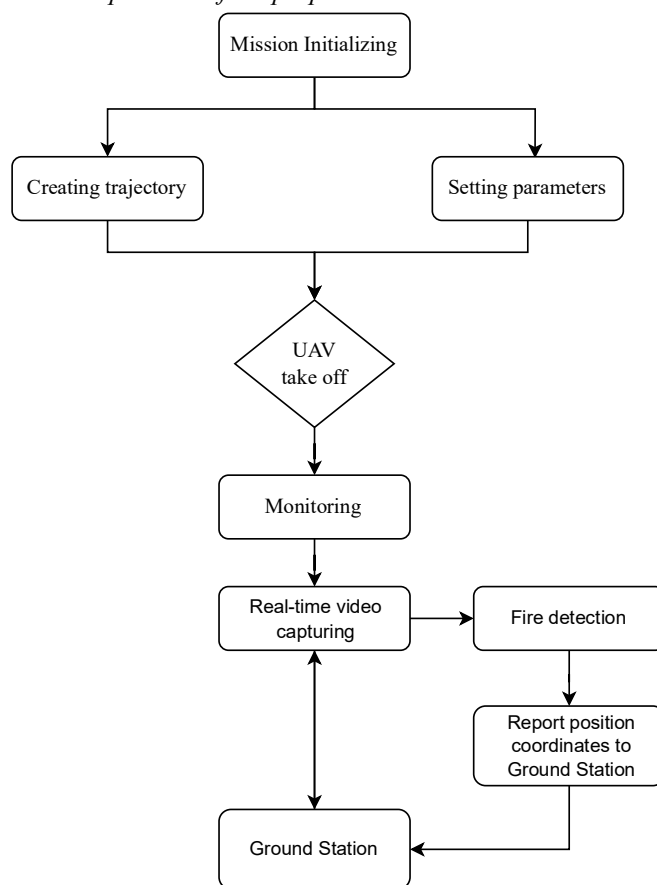


Fig. 3: Algorithm of operation of the UAV fire detection system

The operation of the proposed event detection system is shown in Figure 3. In the initial stages, the ground station sends mission development requests by setting parameters and UAV flight paths to monitor the target area. The monitoring map of the area generates UAV flight paths according to the mission, and then this information is transmitted with updated parameters to the ground station. As soon as the connection is established and the conditions for the UAV flight are satisfied, the UAV takes off and begins to take high-resolution images. During flight, the UAV begins scanning the marked area, transmitting data to the ground station in real time via the communication channels between the UAV and the ground

station as well as with the satellite. The resulting information is transmitted to the ground station for real-time processing. In the last stages, the data collected from the UAV is analyzed at the ground station, which continuously monitors the data for fire detection, and whenever a detection occurs, the UAV will transmit coordinates to the ground station to confirm the information. Based on this data, a decision on further operations will be made. When a fire is detected, the geolocation must be accurately known to the firefighting crews in order to act quickly and effectively in the extinguishing process. The geolocation of the fire can be calculated by knowing the coordinates and position of the UAV, as well as the distance between the UAV and the fire itself.

#### IV. CONCLUSION

UAVs are increasingly used in practice as a tool for monitoring and early detection of fires. In this article we have presented UAV based monitoring system for fire detecting. The proposed structure of the system provides the requirements to the accuracy and safety of UAV flights. It is safe to say that the use of UAVs can significantly reduce the cost of detecting forest fires. Therefore, there is a need for additional research and development of integrated solutions for monitoring, detection and control of forest fires. Among the future works of this research is the technical implementation of the proposed method and the conduct of field tests to optimize the system. Thus, we can expect further developments in this area in the future.

#### REFERENCES

- [1] Zmarz A. Application of UAV in forestry to acquire image data, WULS-SGGW, Warszawa 2011.
- [2] Stöcker, C., et al., Review of the current state of UAV regulations. *Remote sensing*, 2017. 9(5): p. 459
- [3] Chi Yuan, Youmin Zhang, Zhixiang Liu, A Survey on Technologies for Automatic Forest Fire Monitoring, Detection and Fighting Using UAVs and Remote Sensing Techniques, *Canadian Journal of Forest Research*, 2015.
- [4] Joaquim Sousa, Pedro Gamboa, Aerial Forest Fire Detection and Monitoring Using a Small UAV, *International Congress on Engineering — Engineering for Evolution*, Volume 2020..
- [5] M. A. Akhloufi, N. A. Castro, A. Couturier, M. A. Akhloufi, N. A. Castro, and A. Couturier, "UAVs for wildland fires," in *Autonomous Systems: Sensors, Vehicles, Security, and the Internet of Everything*, 2018, vol. 10643, no. May, pp. 1–14.
- [6] Merino L., Caballero F., Martínez-de-Dios J.R., Maza I., Ollero A. An Unmanned Aircraft System for Automatic Forest Fire Monitoring and Measurement. *Journal of Intelligent & Robotic Systems*, 2012, vol. 65, pp. 533–548.
- [7] L. Zhang, B. Wang, W. Peng, C. Li, Z. Lu, and Y. Guo, "Forest fire detection solution based on UAV aerial data," *Int. J. Smart Home*, vol. 9, no. 8, pp. 239–250, 2015.
- [8] G. F. M. Center(GFMC), "Firebird 2001 Fire Fighting Management Support System", 2001.
- [9] E. Pastor, C. Barrado, P. Royo, E. Santamaria, J. Lopez, and E. Salami, "Architecture for a helicopter-based unmanned aerial systems wildfire surveillance system," *Geocarto Int.*, vol. 26, no. 2, pp. 113–131, 2011.
- [10] Ardupilot Mission Planner: <https://ardupilot.org/ardupilot/index.html>.

# The Applicability of ROS in the Use of Unmanned Combat Aerial Vehicles

János Sári  
 Alba Regia Technical Faculty  
 Óbuda University  
 Székesfehérvár, Hungary  
[sari.janos1999@gmail.com](mailto:sari.janos1999@gmail.com)  
 ORCID: 0000-0001-8861-3300

Károly Széll  
 Alba Regia Technical Faculty  
 Óbuda University  
 Székesfehérvár, Hungary  
[szell.karoly@amk.uni-obuda.hu](mailto:szell.karoly@amk.uni-obuda.hu)  
 ORCID: 0000-0001-7499-5643

**Abstract**— Thanks to the technological advancement in the past few years the Unmanned Aerial Vehicles (UAVs) have developed immensely. It is inevitable to use UAVs for surveillance, reconnaissance and intelligence purposes in modern warfare. As a result of their high efficiency using more than one UAV in a mission has become incredibly widespread. Of course, drones required not only professionals on the field but also experts in the lab. Numerous algorithms are needed to enhance the UAV’s intelligence in guidance, navigation, and control. One of the possibilities to upgrade drones in order to fulfil the requirements is the Robot Operating System (ROS). This paper introduces the possibilities of ROS based on its capabilities.

**Keywords**— UAV, ROS, framework, military

## I. INTRODUCTION

Unmanned Aerial Vehicles (UAVs) can be found in many industries and environments due to their versatility. Of course, for UAVs to operate properly, it is essential to use and operate devices that can meet the different criteria. The resulting complex system is known as UAS (Unmanned Aircraft System) which has adopted by the Federal Aviation Administration (FAA). UAS include not only the Ground Control Station (GCS) and the Unmanned Aircraft but also the Command and Control Link/Data Link. In 1998 NATO started a standardization process in order to unify the unmanned control systems and help enable UAS interoperability. As a result, STANAG 4568 has been created which clarifies the definition of data link interface, control interface and Human and Computer Interfaces within NATO (see Fig. 1.).[1][2][4]

In modern warfare using UAVs are not only inevitable but also essential in order to aid soldiers and protect human life. Drones can be controlled remotely or can fly autonomously (based on a pre-programmed flight plan); also, they are capable of operating individually and in swarms. Nowadays it can be risky to use one drone for a specified mission because of the new threats that have emerged in the recent years (EMP attacks, hijacking, Data link spoofing, jamming) [16]. Due to this, research in the field of swarm intelligence and artificial intelligence is becoming increasingly important.[9]

One way to enhance UAS while maintaining the efficient development is using software like ROS (Robot Operating Systems). ROS not only provides hardware abstraction and low-level device control but also message-passing between processes for system.[7]

In this paper the integrability of ROS in UAS is investigated. After a brief description about the possible

ways of grouping drones and the UAVs used in military, the basics of ROS will be discussed connected to the topic. The following sections describe the vulnerabilities of Robot Operating Systems, the problems that might arise, the solutions, and the basic requirements of a ROS based UAV.

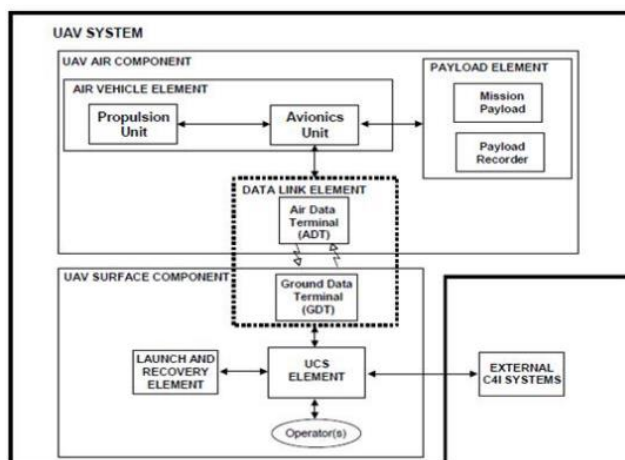


Fig. 1: Possible UAS Architecture (STANAG 4586) [3]

## II. CLASSIFICATION OF UAVs

The classification of the Unmanned Aerial Vehicles can be done in several ways due to their universal use and diversity. There are differences in size (micro), design (VTOL, tilt-wing, HTOL) and also in the incorporated energy source (battery, fuel cells). Of course, as technology continues to evolve, new types will emerge, sometimes forming entirely new groups (see Fig. 2.). [6][8]

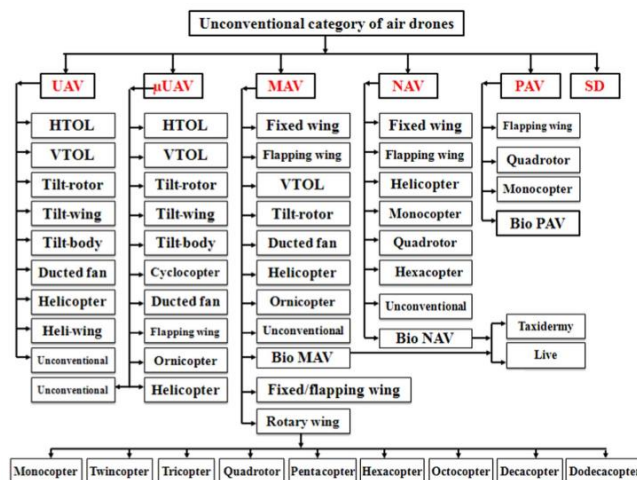


Fig. 2: Various types of UAVs [8]

### III. UAVs FOR MILITARY PURPOSES

As we mentioned UAVs can be used for different kind of military purposes: surveillance, reconnaissance, intelligence etc. They can also intervene on the battlefield either indirectly using precision guided munitions controlled by an operator or directly by dropping or firing these munitions autonomously.[14][15]

The history of the first military Unmanned Aerial Vehicle dates back to the Second World War. The result of the competition between France and the US was the Voisin BN3 biplane which was able to fly for about 100km. However, UAVs were not used for surveillance purposes until 1973, during the Vietnam War.[14][15]

Although a classification of unmanned aerial vehicles has been presented above, a classification as function is preferred for military use. On this basis we can distinguish:

- Target and Decoy UAVs
- Reconnaissance UAVs
- Combat UAVs
- Research and Development UAVs
- Civil and Commercial UAVs

The different classifications clearly define the difficulty or the risks of the mission and its purpose. Of course as technology evolves, these groups are also expanding. One such application – that has been explored by the authors as well – is the deployment and use of various UAVs to enhance the security and runway safety of military airfields. [14][15]

Using drones with thermal imaging camera can improve the accuracy of weather mapping. With the image analysis of images along the runway UAVs can help to detect the presence of foreign object debris (FOD) on the surface (runway), such as fallen parts of the aircraft or a flock of birds. Furthermore, changes in the condition of surfaces, cracks and icing can be detected (see Fig. 3).[9]

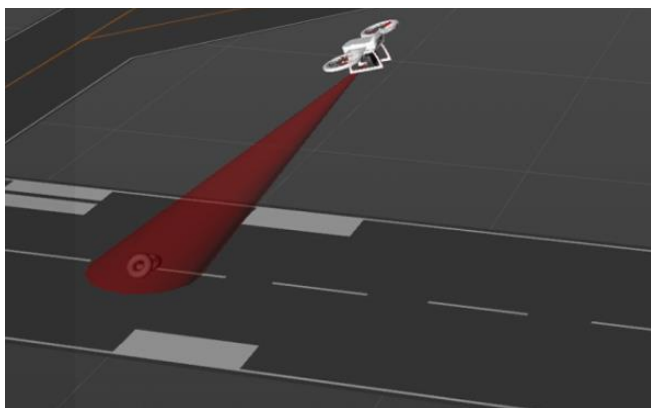


Fig. 3: Use of unmanned aerial vehicle as a FOD seeker

### IV. ROBOT OPERATING SYSTEM (ROS)

The Robot Operating System, or ROS, is a framework widely used in robotics. It is an open source; American-developed; meta-operating system that uses libraries to build, write and run codes across multiple computers. It has the advantage of having many pre-built features such as face recognition, motion tracking, robot control, route planning etc. ROS is mainly based on Linux, C++ and Python

programming languages. The applications created in ROS are called nodes (see Fig. 4.) (master, publisher, and subscriber). The communication between nodes is implemented by the ROS system itself. [1][7]



Fig. 4: ROS structure

In case of asynchronous communication in ROS, the preferred model is the publisher-subscriber model. The advantages of this model are:

- Any code can publish a message to any topic.
- Any node can subscribe to any topic.
- Multiple nodes can publish to the same topic.
- Multiple nodes can subscribe to the same topic.
- A node can publish to multiple topics.
- A node can subscribe to multiple topics.

In order to support different kind of programming languages ROS include a client library. Of course for other purposes for example hardware control, transmission and reception, visual space controlling; ROS has its own relevant component: hardware interface, communication, simulation tools (see Fig. 5.).



Fig. 5: Components of ROS [7]

As we mentioned ROS is an open source, meta-operating system which allows us to use it in the field of unmanned aviation. In a structure where ROS is implemented into an UAV or UAS, the aforementioned pub-sub model is usually adopted for communication. In this case the master node helps in the information exchange process between the two other nodes. [1]

To make the communication process easier between small drones a protocol so called MAVlink is used. It follows a modern hybrid publish-subscribe and point-to-point design pattern. Thanks to the diversity of ROS, the possibilities offered by MAVlink can be exploited by MAVROS (see Fig. 6.). In fact MAVROS is a MAVlink expandable communication node. [5]

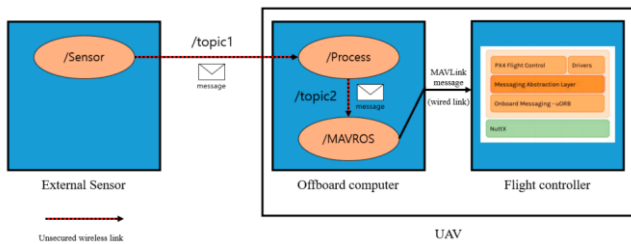


Fig. 6: A possible structure of a ROS-based UAV [1]

As we mentioned there are many disadvantages using ROS in UAVs. The weak points are the possibility of jamming, Data link spoofing and in extreme cases hijacking [16]. Of course software developers are aware of the risk factors. Due to this users are advised to create a restricted access to the network, and not disclosing the ROS master. It can be achieved by establishing isolated hosts, networks, or using firewalls. Additional problems can be caused by the formation of abnormal or infinite loops. For this reason a timer tool called Watchdog is implemented in ROS which monitors the CPU and intervene when loops may occur. [1][7]

Because of the vulnerability of the systems it is easy to break into the network. Attacks like false data injection can easily lead to total collapse. Unfortunately the weaknesses of the master node (for example the master node does not check whether the node making the request is a normal node or a malicious node) are the main reason why this can happen. [1]

## V. HOW TO SECURE ROS

Apart from the mentioned solutions there are many other options for securing our ROS system. In the following we would like to present two alternatives that have become quite popular in the recent days.

### Encryption

Many studies show that ROS-Encryption is not an idea to be rejected. Ciphred communications in ROS requires just a little more overhead of CPU performance but it provides a much more secure flow of information.

The number of algorithms which can be used for encryption has increased significantly in the past years. Nowadays cryptographic algorithms AES (Advanced Encryption Standard) are preferred over DES (Data Encryption Standard) due to their speed and reliability. Algorithms like AES converts data in plaintext to an uninterpretable form which is called the ciphertext.[20]

### Secure-ROS

Secure-ROS provides alternative versions of core ROS packages that enable secure communication between ROS nodes. Secure-ROS uses IPsec (Internet Protocol Security) in transport mode and modified versions of the ROS master (rospy, roscpp) to ensure secure communication. The user only can specify authorized subscribers and publishers to topics at run time.[19]

## VI. THE BASIC REQUIREMENTS FOR ROS BASED UAVS

The first and most important task is to check whether the integration of the drone into ROS is even possible. This step is crucially important because complete ROS systems can be very expensive, and due to this they are not always cost-

efficient. Thankfully, the mentioned problem can be solved easily with ROS plugins. An additional solution is the use of ROSBRIDGE, which provides a JSON API to ROS functionality for non-ROS programs (the client does not have to install ROS).[12][13]

The second step is the correct choice of the frame and the propeller. The size, structure and the material of the frame have a significant influence on the flight characteristics. The properties of the propeller will mainly affect the lifting power. To study the behavior of the propeller and the frame, it is worth creating a simulation environment. This can be done with software like Ansys (see Fig. 7.) which is a numerical fluid dynamics software that discretises continuous operations in space and time. [11]

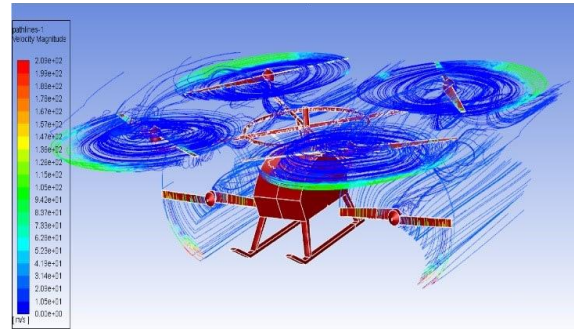


Fig. 7: A possibility of a UAV Ansys simulation [10]

As already mentioned, drones or UAVs can also be distinguished by the energy source they use. For small unmanned aircrafts, as shown in Figure 3, lithium polymer batteries are the preferred choice. Compared to lithium-ion, these types are more resistant to overcharging and less likely to leak electrolyte. Another feature is that they are much lighter than their predecessors, thanks to the special polymer.

A further necessary condition is the existence of engines. The number and the power of engines are mainly affected by the goal which we want to achieve. Of course, it is not enough to install the engines themselves, they also need to be synchronized. In case of small drones the brushless engines are more common due to their durability and performance.

Other essential components of drones are the various control elements such as Electronic Speed Controller, Flight Controller, Manual Control Unit etc. (see Fig. 8.) In the case of embedded system, the applications of fault-tolerant redundant solutions are recommended [17], [18].



Fig. 8: Example of drone main parts



## VII. CONCLUSION

The experience of recent years suggests that unmanned aircraft will become more widespread in the coming years. Of course, this will influence many civilian and military areas as well. UAS will become more complicated, but hopefully the communication between drones becomes easier. But of course this requires a system that can effectively manage the parties involved in the communication process. According to the current state of technology, one such solution could be ROS.

The use of ROS in military drones is not always advantageous, as can be seen above, but it offers a very practical solution thanks to its ease of use and simplicity. It is easy to see that systems such as ROS would be able to innovate, this branch of warfare, but we assume that ROS itself will only be used by underdeveloped forces.

This study not only presents the classification of drones and their system architecture, but also takes a new look at the application of unmanned aerial vehicles using ROS.

## ACKNOWLEDGMENT

The authors thankfully acknowledge the financial support of this work by the Howmet Aerospace Foundation, the Arconic Foundation, and the project no. 2019-1.3.1-KK-2019-00007 implemented with the support provided from the National Research, Development and Innovation Fund of Hungary, financed under the 2019-1.3.1-KK funding scheme.

## REFERENCES

- [1] Hyojun Lee, Jiyoung Yoon, Min-Seong Jang, Kyung-Joon Park: A Robot Operating System Framework for Secure UAV Communications, *Sensors* 2021, 21, 1369. [CrossRef]
- [2] Suraj G. Gupta, Mangesh M. Ghonge, Dr. P. M. Jawandhiya: Review of Unmanned Aircraft System (UAS), *International Journal of Advanced Research in Computer Engineering & Technology (IJARCET)* Volume 2, Issue 4, April 2013
- [3] Michael Chanda, Julee DiPlacido, John Dougherty, Richard Egan, John Kelly, Trent Kingery, Daniel Liston, Douglas Mousseau, James Nadeau, Theodore Rothman, Lisa Smith, Michael Supko: Proposed Functional Architecture and Associated Benefits Analysis of a Common Ground Control Station for Unmanned Aircraft Systems, *NAVAL POSTGRADUATE SCHOOL MONTEREY, CALIFORNIA*, Available online: <https://www.researchgate.net/publication/265528436> (accessed on 25.10.2021)
- [4] Mário Monteiro Marques: STANAG 4586 –Standard Interfaces of UAV Control System (UCS) for NATO UAV Interoperability, *STO-EN-SCI-271*, Available online: <https://www.sto.nato.int/publications/STO%20Educational%20Notes/STO-EN-SCI-271/EN-SCI-271-03.pdf> (accessed on 25.10.2021)
- [5] MAVlink: MAVLink Developer Guide, Available online: <https://mavlink.io/en/> (accessed on 25.10.2021)
- [6] Adnan S. Saeed, Ahmad Bani Younes, Chenxiao Cai, Guowei Cai: A survey of hybrid Unmanned Aerial Vehicles, [CrossRef]
- [7] YoonSeok Pyo, HanCheol Cho, RyuWoon Jung, TaeHoon Lim: ROS, Robot Programming, From the basic concept to practical programming and robot application, Dec 22, 2017, ISBN: 979-11-962307-1-5
- [8] M. Hassanalain, A. Abdelkefi: Classifications, applications, and design challenges of drones: A review, [CrossRef]
- [9] Vas Tímea, Békési Bertold, Sári János, Kele Katalin, Magyar Martin, Szabó Richárd: A mesterséges intelligencia alkalmazhatósága a modern kori repülésben, *Repüléstudományi Közlemények*, 33. évfolyam (2021) 1. szám 5–18., DOI: 10.32560/rk.2021.1.1
- [10] Ansys simulation. Available online: <https://www.fiverr.com/cfd828/do-cfd-simulation-ud-with-ansys-fluent> (accessed on 25.10.2021)
- [11] Sári János, Beneda Károly, Kavas László: Repülőgép-hajtóművek égéstereinék áramlástanai vizsgálata számítógépes szimulációban, *REPÜLÉSTUDOMÁNYI KÖZLEMÉNYEK (1997-TŐL)* 32 : 3 pp. 93-103. , 11 p. (2020) [CrossRef]
- [12] Rosbridge. Available online: [http://wiki.ros.org/rosbridge\\_suite](http://wiki.ros.org/rosbridge_suite) (accessed on 25.10.2021)
- [13] Pluginlib. Available online: <http://wiki.ros.org/pluginlib> (accessed on 25.10.2021)
- [14] John W.R. Taylor, John F. Guilmartin: Unmanned aerial vehicles (UAVs). Available online: <https://www.britannica.com/technology/military-aircraft/Unmanned-aerial-vehicles-UAVs> (accessed on 25.10.2021)
- [15] Jack Brown: TYPES OF MILITARY DRONES: THE BEST TECHNOLOGY AVAILABLE TODAY Available online: <https://www.mydronelab.com/blog/types-of-military-drones.html> (accessed on 25.10.2021)
- [16] Judit Takács MÓDNÉ: The importance and development of safety awareness with soft skills in industrial environment, *OPUS ET EDUCATIO: MUNKA ÉS NEVELÉS* 8 : 3 pp. 314-323. , 10 p. (2021)
- [17] Györök György, Beszédes Bertalan. Fault-tolerant Software Solutions in Microcontroller Based Systems. In: Orosz, Gábor Tamás (szerk.) AIS 2017 - 12th International Symposium on Applied Informatics and Related Areas organized in the frame of Hungarian Science Festival 2017 by Óbuda University : Proceedings. Székesfehérvár, Magyarország : Óbudai Egyetem (2017) 204 p. pp. 7-12. , 6 p.
- [18] György Györök, Bertalan Beszédes. Adaptive optocoupler degradation compensation in isolated feedback loops. In: Szakál, Anikó (szerk.) IEEE 12th International Symposium on Applied Computational Intelligence and Informatics (SACI 2018). Temesvár, Románia : IEEE Romania Section, IEEE Hungary Section (2018) 604 p. pp. 167-172. , 6 p.
- [19] Secure ROS. Available online: [https://sri-csl.github.io/secure\\_ros/](https://sri-csl.github.io/secure_ros/) (accessed on 25.10.2021)
- [20] Doczi, R.; Kis, F.; Suto, B.; Poser, V.; Kronreif, G.; Josvai, E.; Kozlovsky, M. Increasing ROS 1.x Communication Security for Medical Surgery Robot. In Proceedings of the 2016 IEEE International Conference on Systems, Man, and Cybernetics (SMC), Budapest, Hungary, 9–12 October 2016

# Acceleration Measurement Experiments in Dairy Cattle

Éva Hajnal  
Alba Regia Technical Faculty  
Óbuda University  
Székesfehérvár, Hungary  
[hajnal.eva@amk.uni-obuda.hu](mailto:hajnal.eva@amk.uni-obuda.hu)

Gergely Vakulya  
Alba Regia Technical Faculty  
Óbuda University  
Székesfehérvár, Hungary  
[vakulya.gergely@amk.uni-obuda.hu](mailto:vakulya.gergely@amk.uni-obuda.hu)

Péter Udvardy  
Alba Regia Technical Faculty  
Óbuda University  
Székesfehérvár, Hungary  
[udvardy.peter@amk.uni-obuda.hu](mailto:udvardy.peter@amk.uni-obuda.hu)

Levente Kovács  
Hungarian University of Agriculture  
and Life Sciences  
Gödöllő, Hungary  
[Kovacs.Levente@uni-mate.hu](mailto:Kovacs.Levente@uni-mate.hu)

**Abstract**— The great challenge of our time is monitoring of the condition of our farm animals, which is made possible by IoT technologies. This segment of agriculture is called IoF, Internet of Farms. This article presents the preliminary experiments in bolus sensor development. Many physiological and behavioral characteristics of cattle can be monitored by recording and analyzing data from an external three-axis accelerometer placed on the cattle's body.

**Keywords**—IoF, accelerometer, dairy cattle, data science

## I. INTRODUCTION

Automation and digitalization are trends in animal husbandry today[1]. This process is often referred to as IoF, Internet of Farms [2]. This covers that animals are instrumented with different sensors, allowing them to be monitored continuously. This innovation not only helps livestock farms to manage their workforce, but also helps farms to keep their animal welfare in focus, including good health, housing conditions and the management of heat stress, which is increasingly affecting animals as a result of global warming. In the case of dairy cattle, we often speak of sensors placed on the legs, neck, tail, or rectum, or possibly combinations thereof [1]–[9]. External sensors placed on the animal are very problematic in animal husbandry because they are picked up by the animals or can be damaged during their daily movement. To prevent this, boluses placed in the rumen of cattle have also recently appeared. With the development of technology, the goal would be to develop tools that can accompany the life of an animal, perform complex measurements and often provide complex analysis of the condition of animals. In line with this trend, we performed experiments to investigate which physiological and behavioral characteristics of dairy cattle can be identified with a three-axis accelerometer. The ultimate goal is to develop a bolus that can perform complex measurements and complex analysis from the measured data, helping to detect estrus, heat shock, the onset of calving, and to assess overall animal welfare. One of the planned components of this complex measuring instrument is the three-axis accelerometer, which, together with the experimental device, would be

introduced into the rumen of cattle. In the preliminary experiments, unfortunately, neglecting the movements of the rumen, the sensors were placed to the side of the cattle and tried to collect as many behaviors that could be identified with an accelerometer. Thus, our research question was what elementary behaviors and events can be collected using a bolus sensor, which can be the input data of a complex evaluation system, even including artificial intelligence solutions.



Figure 1. Sensor unit with 3 axes accelerometer

## II. METHODS

The experiments were performed on the Etyek farm. The identifiers (ear numbers) of the cows used in the experimental set-up were recorded. In all cases, the experiment was performed with healthy dairy cows.

### Experiment I.

Devices used for the first experiment: Sensor unit with Bosch BMA180 three-axis acceleration sensor, in which the sample rate can be adjusted between 20 Hz and 2400

Hz and sensitivity can be adjusted between 1 G and 16 G. Wireless communication was implemented the 802.15.4 protocol with 250 kbps in the 2.4 GHz band. The sampling frequency was 600 Hz. The unit was powered from an 18650 LiIon cell.

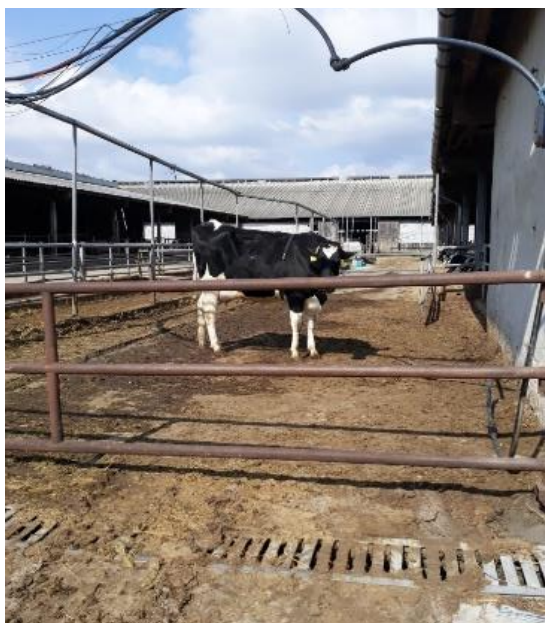


Figure 2 Dairy cow in the 1st experiment in a paddock. The sensor is attached to the side with a strap.

The receiving side: it was a 2.4 GHz data radio, the data was recorded with a laptop. Meanwhile, video was recorded with a GoPro Hero 3 camera, and video and accelerometer measurements were time-synchronized. The structure of the measured data set is shown in Figure 3.

..1, ..1618991182.550546449, ..2464, ..3947, ...676, ..1578
..1, ..1618991182.550546449, ..2465, ..3949, ...707, ..1620
..1, ..1618991182.550546449, ..2466, ..3955, ...727, ..1686
..1, ..1618991182.550546449, ..2467, ..3946, ...721, ..1695
..1, ..1618991182.550546449, ..2468, ..3936, ...738, ..1737
..1, ..1618991182.550546449, ..2469, ..3914, ...716, ..1766
..1, ..1618991182.550546449, ..2470, ..3901, ...701, ..1834
..1, ..1618991182.550546449, ..2471, ..3869, ...733, ..1888
..1, ..1618991182.550546449, ..2472, ..3837, ...727, ..1940
..1, ..1618991182.550546449, ..2473, ..3810, ...697, ..1983
..1, ..1618991182.550546449, ..2474, ..3804, ...669, ..2037

Figure 3: Data format: Sensor ID, Timestamp, Buffer serial number, Acceleration in X, Y and Z directions

In a group, 16 data have the same timestamp, the time distribution of measurements is uniform, but the data is congested and several packets are lost, so a subsequent correction was required, the steps of which

- Chronological backward timestamp correction according to the buffer sequence number
- Possible interpolation of missing data based on buffer sequence numbers
- Modify the timestamp with a constant value, align it with the video.

Unfortunately, the noise of the measurements was very large, so in each case it was necessary to correct this,

which was solved by averaging the data of the 16-member data buffer sent in units. With this we were able to get a roughly smoothed baseline.

During the data processing, the time synchronization of video recording had to be solved. During recording, synchronization points were added to the video, then a visible timestamp is added to the frames.

During the statistical processing of the data, the timestamp of the data records had to be corrected based on the buffer number, as in several cases congestion developed on the receiving side and the storage of the data was delayed. In addition, several data packets were lost, which were replaced by linear interpolation based on the existing data if the statistical processing algorithm could only process a complete data set.

When processing the video, the video was manually annotated according to the observable behaviors. These are: standing, walking, rumination, stepping, other, Unobservable behaviors: lying, drinking, eating, extreme movements.

In the statistical processing, the resulting vector was calculated, from which - histograms were made Block-by-block scattering and its evaluation is the blending of motion information and video.



Figure 4 Lying data logger with the cattle ID

#### Experiment II.

Animal: three cattle, identified by ID wearing on the ears that were in a stable within the Etyek farm during the experiment

Methodology: The experimental device was strapped to the animal and the data from the device were recorded for 2 days, in parallel, the lying position counter (HOB0 Pendant G Data Logger unfiltered, Onset Computer

Corp., Bourne, MA) [9] attached to the legs of the animals recorded the lying position for all three animals. Device: Measuring instrument is the same as described in the experiment 1<sup>st</sup>. Sampling frequency was 300Hz, data was recorded with a Raspberry Pi 3B computer with the settings and data format described in the experiment 1<sup>st</sup>. During the processing, no video was made, but we were able to separate the time spent by each animal with lying with help of the recorded data series provided by the lying position counter. Thus, this series of measurements is suitable for separating the lying position from other movements.

### III. RESULTS AND DISCUSSION

As a result of the first experiment, a set of data with acceleration values and timestamps was available, as well as video recording for the same period, which was manually categorized by behavior, distinguishing between standing, walking, stepping, ruminant, and other categories. The streamed graph of the measured data set was copied to the video recording. Figure 5 shows the measurement result. The image of the current video corresponds to the value of 0s in the graph. The graph in Figure 5 shows the standard deviation within the data buffers containing 16 data. In the graphs, standing and walking behavior can be well separated. The area below the graph characterizes locomotor activity. Unfortunately, rumination cannot be identified with these studies. Feeding and drinking were not available for the cow in the paddock, so eating and drinking behavior patterns could not be observed.

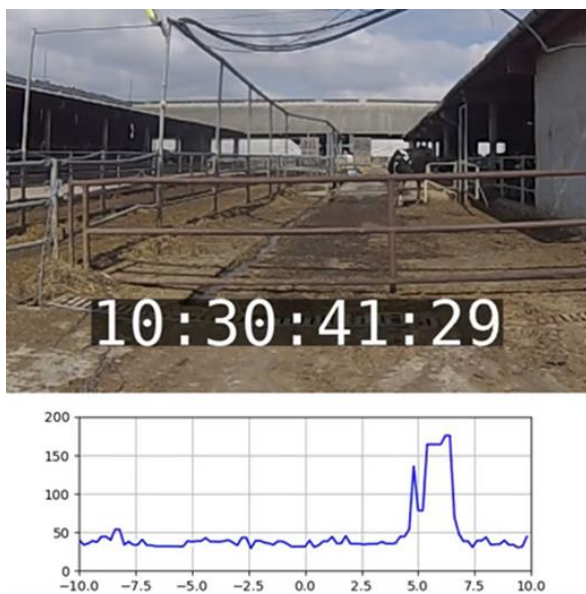


Figure 5 The timeline and the graph made from the sensor data stream were added to the video taken in the paddock.

As this paddock does not give the cow enough comfort, the cow remained standing throughout the study period. Thus, it was not possible to detect the lying position either.

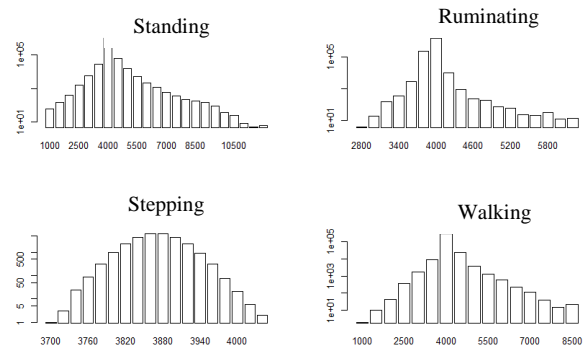


Figure 6 Histogram of the resultant acceleration values for four different modes of motion

The resultant acceleration from the acceleration values measured on the three axes was calculated. The resultant acceleration values were plotted on a histogram. Due to the setting of the device, the possible values of the resultant acceleration were in the range of 0-8000. Figure 6 shows that the histograms have also maximum for the three forms of motion at 4096, namely standing, ruminating and walking. The value of 4096 corresponds to a value of 1G of the ground gravity acceleration. Because the animals have a fairly large body weight, they perform the movements with relatively small relative accelerations. Only stepping as a behavior can be distinguished from other movements based on a histogram because the resulting acceleration averages 3850, which corresponds to 0.94G. From the histogram, it can be seen that the 2-fold standard deviation is within the intervals of 1000 and 7000. Thus, it will not be necessary to change this initial setting during the subsequent setting of the sensor.

Figure 7 shows the result of the second experiment. In this experiment, it was possible to observe the acceleration values measured in the lying position of the animal. The figure shows the acceleration values measured on the y and z axes. Acceleration values measured in lying position are indicated in green and those measured in other body positions are indicated in red. Besides a few outliers, red and green points, corresponding to the two categories, can be linearly separable. Unfortunately, as no additional sensors were available and no video capture was possible, it was no way to identify additional behavioral categories on the measured data set. The basis for position identification is that the angle of inclination of the sensor attached to the side of the animal is 20-30 ° when lying down.

Since the position of the sensor has changed at lying, this position could be separated from the other body positions. In the experiment, the sensor rotates when the cattle lying down.

Unfortunately, the sensor placed on the animal can be moved. In this case, the consecutive horizontal and non-horizontal positions can be distinguished because the angle of inclination of the sensor changes, but it is not possible to assign absolute acceleration values to the

lying position or the other positions. Unfortunately, in the case of a rumen bolus, a similar case must be occurring. In the rumen of the animal, the sensor can move easily. With proper techniques, the sensor can be mounted around roughly one axis, the vertical axis, but this can make it difficult to detect the position later on.

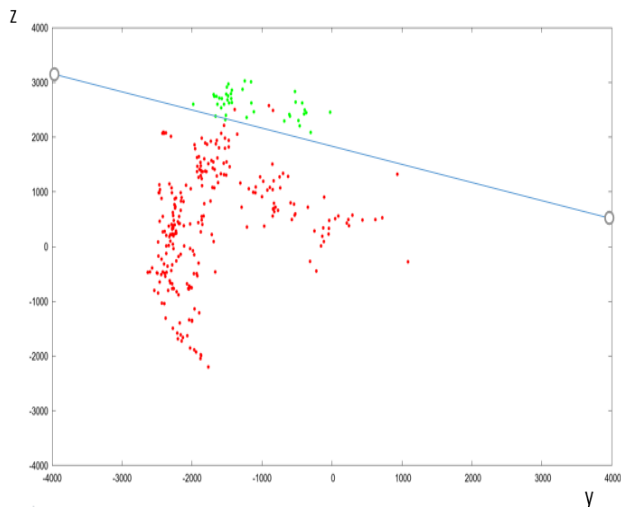


Figure 7 The horizontal and vertical positions can be clearly distinguished by considering the acceleration values measured along the y and z axes.

#### IV. CONCLUSION

The article reviews and evaluates preliminary experiments of a rumen bolus accelerometer sensor. The sensor should make it possible to identify individual movements and behaviors. Based on this, the locomotor activity and activity of the experimented animals can be precisely determined and quantified. In subsequent experiments, some important health and animal husbandry characteristics of the animal can be identified on this basis. As well as on the basis of additional sensor data and other information collected about the animals, using data analysis methods that also use artificial intelligence. The primary goal is the accurate and rapid identification of health problems, estrus and parturition. In the presented experimental setup, the following forms of movement could be identified: standing, walking, stepping in a standing position, lying down. Eating, drinking, rumination, and increased locomotion activity indicating estrus were not detected in this experiment. The interpretation of the experiments was disturbed by the fact that the sensor was fixed to the side of the animal, so that the position of all three axes of the accelerometer relative to the animal was constant during the experiments. Later, it can be expected that the sensor can move freely in the rumen of the animal, with a maximum of one vertical axis that can be fixed in the absolute sense. In the next phase of the research, it is worth placing some bolus sensors in the cow's rumen and extracting native, measured data from it, as well as for a short time. A short time is a period of about 30 days because it contains at least one cycle of estrus of the cow.

It is a good idea to follow the experiment with external validation tools. Ideally, this could mean making a video with a suitable camera system. Based on this, the behavior of the cow can be accurately categorized. Less valuable but usable results can be obtained by equipping the cow involved in the bolus experiment with bed counting, ruminant, and estrus sensors. In the first case, all important behaviors (standing, walking, lying, jumping, ruminating, eating, drinking) can be identified, while in the second case, only a reduced number of categories can be evaluated.

#### ACKNOWLEDGMENT

I would like to thank the help and the effort of colleagues and students. The financial support of this paper was from 2020-1.1.2-PIACI-KFI-2020-00109 grant. We would like to thank the director of Etyek Farm, namely Gergely Áron Simon, for the help in conducting the experiments.

#### REFERENCES

- [1] H. El Bilali, F. Bottalico, G. Ottomano Palmisano, and R. Capone, *Information and communication technologies for smart and sustainable agriculture*, vol. 78. 2020.
- [2] C. Michie *et al.*, "The Internet of Things enhancing animal welfare and farm operational efficiency," *J. Dairy Res.*, vol. 87, no. S1, pp. 20–27, 2020.
- [3] A. W. Hamilton *et al.*, "Identification of the Rumination in Cattle Using Support Vector Machines with Motion-Sensitive Bolus Sensors."
- [4] C. H. Knight, "Review: Sensor techniques in ruminants: More than fitness trackers," *Animal*, vol. 14, no. S1, pp. S187–S195, 2020.
- [5] T. H. Swartz, M. L. McGilliard, and C. S. Petersson-Wolfe, "Technical note: The use of an accelerometer for measuring step activity and lying behaviors in dairy calves," *J. Dairy Sci.*, vol. 99, no. 11, pp. 9109–9113, 2016.
- [6] J. Q. Gu, Z. H. Wang, R. H. Gao, and H. R. Wu, "Cow behavior recognition based on image analysis and activities," *Int. J. Agric. Biol. Eng.*, vol. 10, no. 3, pp. 165–174, 2017.
- [7] L. Kovács, V. Jurkovich, M. Bakony, O. Szenci, P. Póti, and J. Tőzsér, "Welfare implication of measuring heart rate and heart rate variability in dairy cattle: Literature review and conclusions for future research," *Animal*, vol. 8, no. 2, pp. 316–330, 2014.
- [8] B. Jiang, X. Yin, and H. Song, "Single-stream long-term optical flow convolution network for action recognition of lameness dairy cow," *Comput. Electron. Agric.*, vol. 175, no. April, p. 105536, 2020.
- [9] D. N. Ledgerwood, C. Winckler, and C. B. Tucker, "Evaluation of data loggers, sampling intervals, and editing techniques for measuring the lying behavior of dairy cattle," *J. Dairy Sci.*, vol. 93, no. 11, pp. 5129–5139, 2010.

# Photovoltaic Panel Failure Prediction Using a Thermal Imaging Camera

Bertalan Beszedes<sup>1</sup>, György Györök<sup>1</sup>

<sup>1</sup> Óbuda University, Alba Regia Technical Faculty, Budai Str. 45, H-8000 Székesfehérvár  
{beszedes.bertalan, gyorok.gyorgy}@uni-obuda.hu

**Abstract** — The aim of the study - based on domestic and foreign sources - is to show the inspection possibilities of thermal imaging cameras which used in industrial and civil areas. During the introduction of the topic, this paper will introduce the most important metrological requirements and practical knowledge of thermography. The paper focuses on photovoltaic panel inspection and failure detection. The paper will discuss the monitoring possibilities. Some common thermal camera operator errors, accuracy and credibility of the measurements are also presented.

**Keywords** — thermal imager, heat camera, IR camera, PV inspection, photovoltaic panel inspection, PV error detection, photovoltaic panel error detection

## I. INTRODUCTION

With the help of thermography, it is also possible to check the quality required during the production of photovoltaic cells and to check the solar panels during operation. This article discusses the condition assessment of solar panels in more detail. The advantage of this solution is that high-power solar parks can also be inspected in a short time, thus increasing operational reliability.

Examination of the electrical parameters (characteristic curve) of solar panels or strings shows a deterioration in efficiency, but the location of the fault and the type of fault cannot be determined. The thermal imaging test can be used to determine the location of the fault and to determine the type of fault.

Thermographic condition assessment helps in fault prediction, economical operation and maintenance. The thermographic examination also covers the electrical cables, connections and equipment, the rise of their temperature above the operating value indicates the location of the fault. For solar cells, however, more knowledge is needed to perform a more complex study.

## II. THEORETICAL BACKGROUND

Before inspecting and evaluating solar cells and panels, it is a good idea to review their operation in order to understand the causes of thermal effects that indicate fault phenomena.

The solar cell is a pn junction, the photons of the incoming solar radiation pass through the n-type layer, and then, giving off their energy in the depletion region, they generate free charge carriers. The charge carriers carry work as they pass through the load.

The internal photoelectric effect can be achieved with both thick-layer (single-crystal silicon, polycrystalline silicon) and thin-film (amorphous silicon) technology. The testing of compound semiconductor or electrolyte-based solar cells is not substantially different from the testing of silicon-based solar cells.

The voltage achievable with a solar cell is approximately 0.5V. By connecting the cells in series, the voltage of the module can be increased, thus increasing the efficiency of energy transmission. If one of the cells connected in a row fails or is shaded, the efficiency of the whole row is reduced. Within the solar panel, the solar cells connected in series are divided into substrings. The substrings are connected in parallel with a bypass diode. In the event of a substring failure, the solar panel will

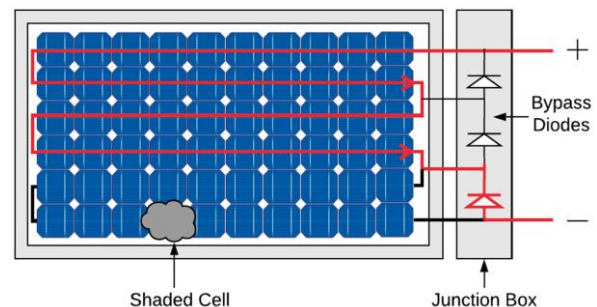


Figure 1: Solar panel bypass diode [1]

remain operational with reduced capabilities (Fig. 1).

Fig. 2 shows the different connection options between PV modules and PV inverters. Based on power output, location, reliability, cost and efficiency system properties, there are four main topologies.

The central topology connects several thousands of PV panels to one inverter. PV array has hundreds of PV strings connected in parallel, and each string has hundreds of PV panels connected in series. The string topology connects one PV string with one inverter. The multistring topology connects one PV string to a dc–dc converter, and then a few dc–dc converters are connected to one inverter. The module integrated topology connects one inverter to one PV panel.

## III. TYPICAL FAULTS AND ERRORS

Faults in solar systems lead to inefficiencies and other more serious faults. The causes of the fault can be traced back to the manufacturing, transport, installation, operation and environmental causes.

Electrical fault, due to their nature, is contact fault, short circuit and incorrect polarity. Control faults include non-optimal operating point operation and bypassed strings or modules. Cell-level defects are caused by fractures, cracks, cell aging, their typical form of failure is short circuit, open circuit, PID (Potential-Induced Degradation).

Electrical and mechanical faults indicate improper transport and installation. Inefficiencies are typically the result of poor design, shading by vegetation or contaminants, and are rarely caused by aging alone.

Visually perceptible inclusions, color deviations, delamination are not significant defects. The oxidizing

effect of water penetrating along fractures, dents, and hairline cracks, as well as short circuits and open circuits in the silicon layer, cause a significant loss of power. Defects that are not visible to the naked eye can only be detected by indirect instrumental testing.

#### IV. MEASUREMENT SUGGESTIONS

In the case of thermographic inspection of all equipment, direct sunlight should be avoided. It is worth avoiding due to the reflection of solar radiation as well as the effect of heat.

However, intense sunshine is required to perform outdoor measurements on solar cells. To detect a fault, it is necessary to have temperature differences caused by the fault. The detection of the error phenomenon is made more difficult by the surface reflection of the panels, but the choice of a professional examination angle helps the observation. [3]

The cell or panel being tested must meet the following criteria. The test must be in loaded operating condition. The minimum power of solar radiation must be at least  $600 \text{ W / m}^2$ . Cloud cover should be less frequent than cumulus clouds (2/8 Cumulus). The test object must be free of precipitation. The wind speed is a maximum of 20-29 km / h (4 Beaufort). During the test, the irradiance shall not exceed a rate of change of 10% / min. If this happens, the measurement can be resumed after a settling time of 10 minutes. [4]

For thermographic condition surveys, compliance with general criteria is also the default, such as ensuring proper viewing angle and resolution, and professional documentation of the measured equipment and measurement.

The inspection of electrical elements can reveal undersized, overloaded, oxidized, damaged, faulty cables and connections, as well as faulty electronic equipment.

Examination of solar cells and panels can reveal faults in the contacts between the cells (increased resistance, open circuits). The error signal can be the temperature rise indicated by the bypass diode between the substrings or the blocking diode between the modules, the temperature difference of the unloaded, polarity faulty, short circuited, shaded cells. The effects of cracks, microcracks, fractures and other degradation can be indicated. [5]

Thermal camera testing of solar cells is more expensive than electroluminescence testing, but the need to break the joints of the panels and the need for external power supply can be avoided. Thermography allows for quick in-service inspection.

When inspecting large systems with thermal imaging, it is also necessary to comply with occupational safety regulations. In the case of high-voltage equipment, the safety distance must be taken into account, and the measuring location must be chosen carefully from the point of view of thermal reflection.

#### V. MEASUREMENT DIFFICULTIES

When performing a measurement, the greatest difficulty is the proper examination and evaluation of sunny reflecting surfaces. Measurements can be made with long-wave bolometer thermal imagers, knowing that the angle of observation greatly influences the measurement results (Fig. 3). The emission factor of the measured surface also

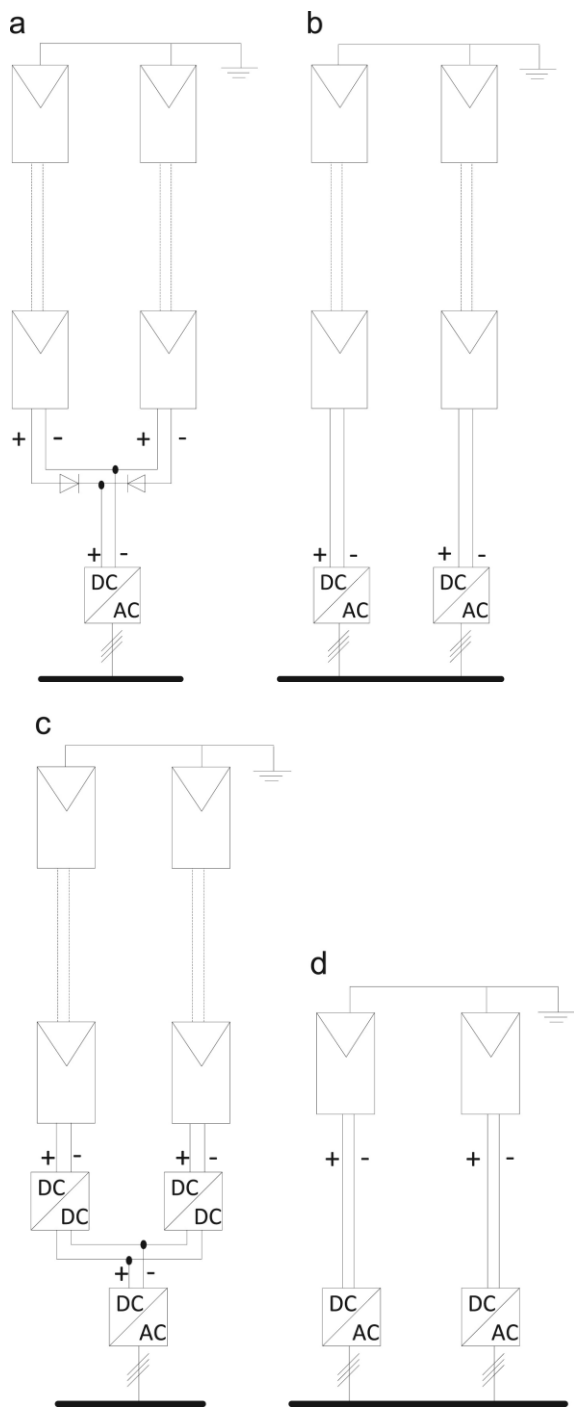


Figure 2: PV inverter topologies: central (a), string (b), multistring (c), and module integrated (d) [2]

depends on the viewing angle and the temperature of the tested glass surface.

At PV module thermograms that are two source of radiation. The first is the black body radiation from the module the second is the reflected environmental radiation (Fig. 4). The thermal inspection needs the PV module surface temperature without the influence of the environmental radiation. The black body equivalent temperature of the sky must be subtracted from the thermal image of the module.

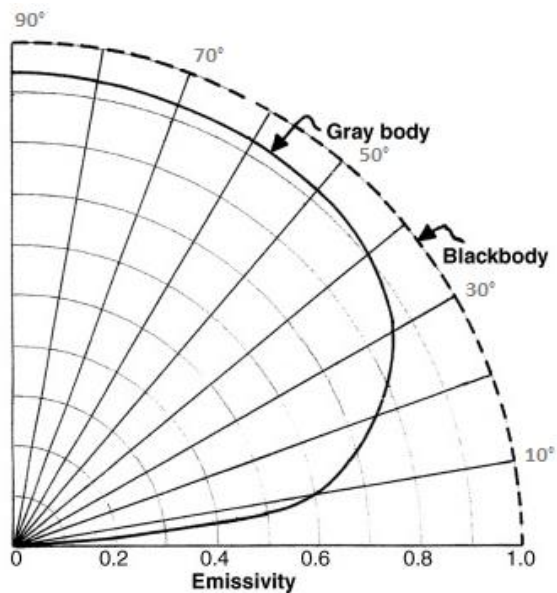


Figure 3: Thermal image with angle-dependent reflections [6]

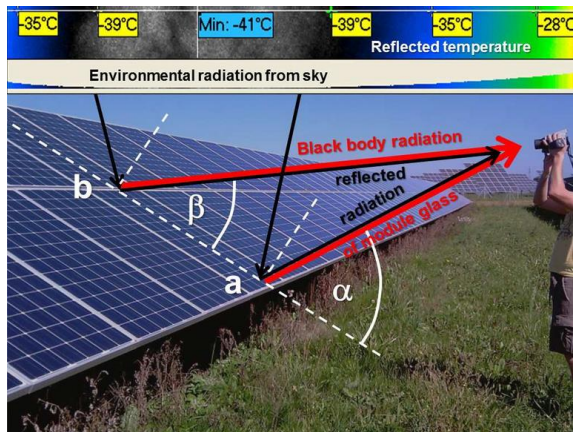


Figure 4: Observation angle for thermal camera measurement [7]

If the angle of inclination of the solar panels (relative to horizontal) is  $45^\circ$  and the angle of incidence of solar radiation during the measurement is  $50^\circ$ , the angle of observation must be kept below  $40^\circ$  (below  $85^\circ$  with respect to the surface of the module) to avoid reflection.

To keep the emission factor of the glass surface of the solar panel at an acceptable value, the angle of observation must be kept above  $30^\circ$  relative to the surface of the solar module.

The relatively low resolution of thermographic measuring instruments also limits the measuring distance. The loss of a cell results in a change in the thermal image with a surface area corresponding to its size. The cell contacts and solders also cause local temperature changes ( $\sim 3 \times 3$  cm), the detailed thermal image is justified for their detection.

## VI. PROPOSED THERMAL IMAGER

Due to the temperatures to be measured, it is advisable to choose a long-wave thermal imager. Emission factors for reflective glass surfaces, on the other hand, justify the use of medium-wave thermal imagers with a filter, but the temperatures to be measured are low. [8]

Temperatures between  $20^\circ\text{C}$  and  $100^\circ\text{C}$  are expected to be measured. It is advisable to choose lower-priced, long-wave ( $7..8\mu\text{m} - 12..14\mu\text{m}$ ), matrix or scanning type, bolometer thermal imagers. The use of medium-wave photon detector thermal imagers is in most cases uneconomical. [9]

The measuring range must be at least between  $-20..0^\circ\text{C}$  and  $150..250^\circ\text{C}$ . The lower level of the lower limit of the measuring range provides a lower level of image noise. The resolution should be higher than  $320 \times 240$  pixels, the proposed lower limit is  $640 \times 480$  pixels. [10]

The geometric resolution should be 2 mrad or less. Display the smallest area to be detected by at least 3 pixels. The modest geometric resolution results in a inspection point close to the surface to be measured, which would lead to shading of the solar panel. [11]

The resolution in the temperature range should be a minimum of 80mK, but a value of 50mK or better is recommended. Fault locations on solar panels are expected to show significant temperature differences, but thermal cameras with better temperature resolution are able to provide evaluable results even at lower irradiations. [12]

The frequency of the image refresh rate is not relevant for installed thermal imagers (scanning thermal imagers), a minimum image refresh rate of 50Hz (matrix thermal imagers) is recommended for manual testing, and a minimum image refresh rate of 120Hz for aerial photographs (microbolometer thermal imagers). [13]

The speed of the scan is increased by the presence of a function with autofocus and enabling composite imaging. Surveying larger areas is aided by the ability to save GPS coordinates and take continuous shots. [14] [15]

If the limit value is exceeded, the automatic alarm function greatly facilitates scanning troubleshooting, and the possibility of thermal image mounting reduces the time of post-production. [16] [17]

Work is accelerated by the use of models that allow lens replacement. [18]

## VII. PRACTICAL EXAMPLES

Thermal camera monitoring of solar modules can be done from a tripod, mobile platform, or a telescopic pole or UAV can be used. [19] In all cases, keep in mind that in order to measure correctly, the panels cannot be shaded for extended periods of time (Fig. 8). [20] [21]



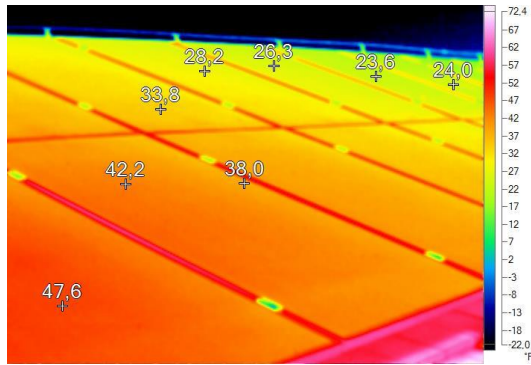


Figure 5: Incorrect observation angle

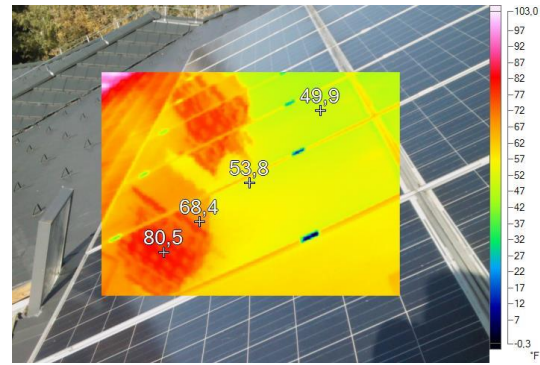


Figure 8: Incorrect measurement due to shaded PV panels

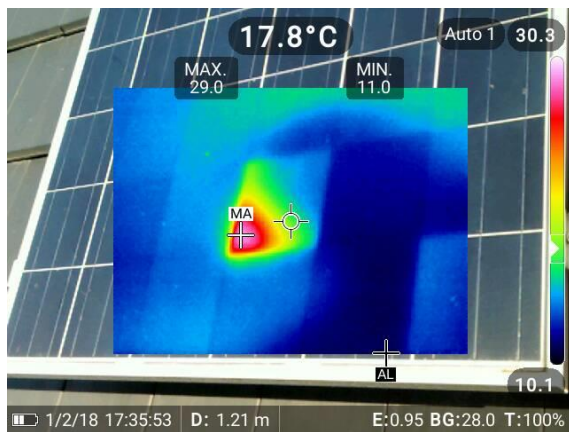


Figure 6: Starting solar cell short circuit

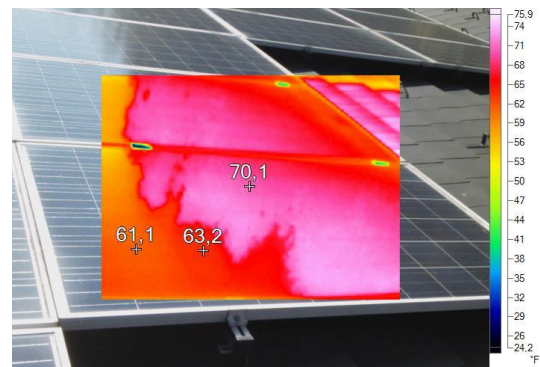


Figure 9: Incorrect measurement due to environmental reflection

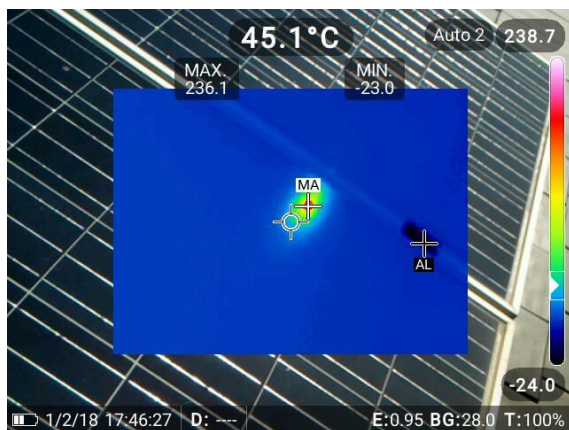


Figure 7: Inclusion due to manufacturing defect

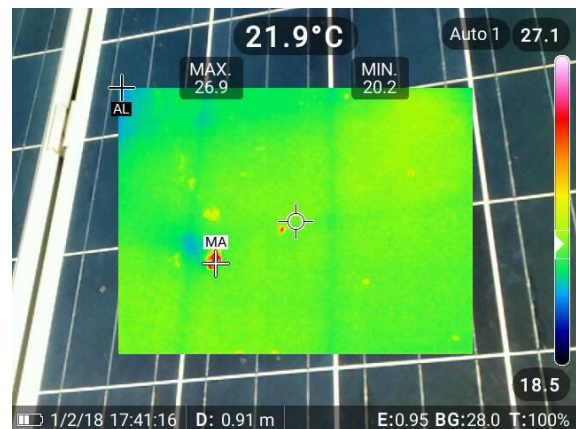


Figure 10: Warming due to pollution

If reflection is suspicious in the measurement (Fig. 9), you may want to change the angle of observation. If the measured surface temperature changes, the reflection is real, it is necessary to add a new observation point in order to eliminate the reflection. If the measured surface temperature does not change, the thermal image is correct. [22] [23]

Figure 6 shows a partial cell temperature increase, it is predicting a solar cell short circuit. Point heating of the inclusion due to a manufacturing defect, it will not cause a

failure later (Fig. 7). Figure 10 shows warm spots due to surface pollution, it is recommended to clean the surface to prevent efficiency loss. Figure 11 and Figure 12 shows two different inspection angles about slightly increased temperature terminal boxes. The phenomenon refers the imperfection of electrical connections and predicts their failure.

#### CONCLUSION

The article attempts to introduce some typical mistakes that can be made during thermographic measurements and

how to eliminate them. This paper proposes some further useful measuring recommendations for reducing measurement errors in the area of thermal imaging diagnostics. Related to photovoltaic panels, the proposed techniques are makes more reliable measurements. The authors are convinced about the high industrial usability of the shown adjustments.

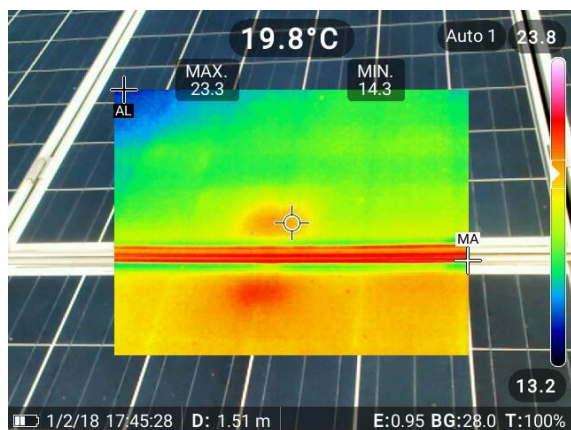


Figure 11: Warming due to pollution

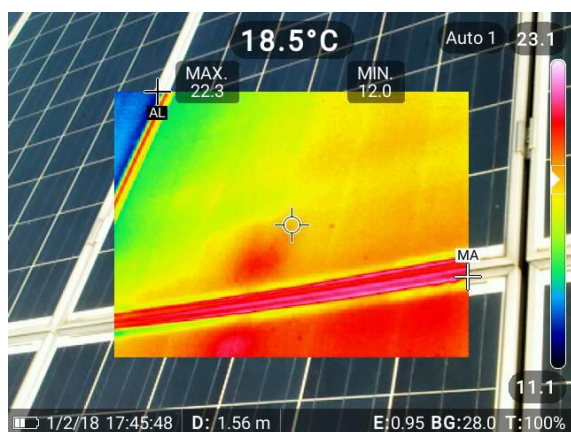


Figure 12: Warming due to pollution

#### REFERENCES

- [1] Vieira RG, de Araújo FMU, Dhinish M, Guerra MIS. A Comprehensive Review on Bypass Diode Application on Photovoltaic Modules. *Energies*. 2020; 13(10):2472. <https://doi.org/10.3390/en13102472>
- [2] Ana Cabrera-Tobar, Eduard Bullich-Massagué, Mònica Aragüés-Peñalba, Oriol Gomis-Bellmunt. Topologies for large scale photovoltaic power plants. *Renewable and Sustainable Energy Reviews*. Volume 59. 2016. pp. 309-319. ISSN 1364-0321. <https://doi.org/10.1016/j.rser.2015.12.362>.
- [3] Picault D, Raison B, Bacha S. Guidelines for evaluating grid connected PV system topologies. In: 2009 IEEE international conference on industrial technology. IEEE; 2009. p. 1–5. Gippsland, VIC. <http://dx.doi.org/10.1109/ICIT.2009.4939505>
- [4] L. Hassaine, E. Olias, J. Quintero, V. Salas. Overview of power inverter topologies and control structures for grid connected photovoltaic systems. *Renew Sustain Energy Rev*. 30 (2014), pp. 796-807. <https://doi.org/10.1016/j.rser.2013.11.005>
- [5] Z. Zeng, H. Yang, R. Zhao, C. Cheng. Topologies and control strategies of multi-functional grid-connected inverters for power quality enhancement: a comprehensive review. *Renew Sustain Energy Rev*, 24 (2013), pp. 223-270. <https://doi.org/10.1016/j.rser.2013.03.033>
- [6] Kirk J. Havens, Edward J. Sharp. Thermal Imaging Techniques to Survey and Monitor Animals in the Wild. Chapter 6 – Emissivity. Academic Press. 2016. pp. 89-99. ISBN 9780128033845. <https://doi.org/10.1016/B978-0-12-803384-5.00006-3>.
- [7] Jaeckel, Bengt & Weinreich, Bernhard & Buerhop, C. & Jahn, Ulrike. (2016). Outdoor Non-Destructive Infrared Thermography of Photovoltaic Modules and Plants for Inspection: IEC 62446-3. 32nd European Photovoltaic Solar Energy Conference and Exhibition At: Munich. June 2016.
- [8] Györök György, Beszédés Bertalan, “Using thermal imaging cameras to test electrical systems,” in IEEE International Conference and Workshop in Óbuda on Electrical and Power Engineering : IEEE CANDO-EPE 2018, 2018, pp. 147–152.
- [9] John G. Webster. The measurement, Instrumentation, and Sensors Handbook. ISBN: 0-8493-2145-X. ISSN: 1523-3014. 1999
- [10] J.M. Lloyd, Thermal Imaging Systems, New York, Plenum Press, 1975, 20-21. pp.
- [11] Gerald C. Holst. Common Sense Approach to Thermal Imaging. 2000. 370. p.
- [12] Rahne Eric. Thermográfia – elmélet és gyakorlati mérés technika. Invest-Marketing Bt. 650. p. 2018. ISBN: 9789638740168
- [13] Györög, Györök ; Bertalan, Beszédés. Mistakes that can be Made During Thermographic Measurements and How to Avoid them. In: Orosz, Gábor Tamás (szerk.) AIS 2019 : 14th International Symposium on Applied Informatics and Related Areas organized in the frame of Hungarian Science Festival 2019 by Óbuda University. Székesfehérvár, Magyarország : Óbudai Egyetem (2019) pp. 159-162. , 4 p.
- [14] GYÖRÖK, György, et al. Multiprocessor application in embedded control system. In: 2012 IEEE 10th Jubilee International Symposium on Intelligent Systems and Informatics. IEEE, 2012. p. 305-309.
- [15] G. Györök and L. Simon, “Programozható analóg áramkör megszakításos alkalmazása mikrovezérlő környezetben,” in Alkalmazott informatika és határterületei, Székesfehérvár, Magyarország: Óbudai Egyetem, 2009, p. 1–4.
- [16] G. Györök and L. József, “The effect of cyclic thermal stresses in the life of PET shrink’s heating body,” in 8th IEEE International Symposium on Applied Machine Intelligence and Informatics (SAMI 2010), A. Szakál, Ed. Herlany, Szlovákia, 2010, p. 1–4.
- [17] G. Györök and L. József, “A Special Case of Electronic Power Control of Induction Heating Equipment,” in Acta Polytechnica Hungarica, vol. 11, no. 5, 2014, pp. 235–246.
- [18] Ladislav Fozo, Rudolf Andoga and Radovan Kovacs, "Thermodynamic cycle computation of a micro turbojet engine," in: CINTI 2016. - Danvers : IEEE, 2016 P. 000075-000079. - ISBN 978-1-5090-3909-8
- [19] Rudolf Andoga, Ladislav Madarász, Ladislav Fözö, Tobiáš Lazar and Vladimír Gašpa, "Innovative approaches in modeling, control and diagnostics of small turbojet engines," in: Acta Polytechnica Hungarica. Vol. 10, no. 5 (2013), p. 81-99. - ISSN 1785-8860
- [20] Maroš Komjátý, Ladislav Fözö and Rudolf Andoga, "Experimental identification of a small turbojet engine with variable exhaust nozzle," in: CINTI 2015. - Danvers : IEEE, 2015 P. 65-69. - ISBN 978-1-4673-8519-0
- [21] György Györök, Számítógép perifériák, Óbudai Egyetem, OE AREK 8003 ISBN 978 615 5018 57 2, Budapest, 2013.
- [22] Károly Artúr, Elek Renáta, Haidegger Tamás, Széll Károly, Galambos Péter. Optical flow-based segmentation of moving objects for mobile robot navigation using pre-trained deep learning models. In: IEEE (szerk.) 2019 IEEE International Conference on Systems, Man and Cybernetics (SMC). Piscataway (NJ), Amerikai Egyesült Államok : IEEE (2019) pp. 3060-3066. , 7 p.
- [23] Redjimi Hemza, Galambos Péter, Tar József, Széll Károly. The Effects of Simultaneous Noise and Missing Information in Fixed Point Iteration-based Adaptive Control. In: IEEE (szerk.) 2019 IEEE International Conference on Systems, Man and Cybernetics (SMC).Piscataway (NJ), Amerikai Egyesült Államok : IEEE (2019) pp. 1430-1435. , 6 p.

# Diverse approach of Cybersecurity culture in Education

Judit Módné Takács  
 Alba Regia Technical Faculty  
 Obuda University  
 Szekesfehervar, Hungary  
[modne.t.judit@amk.uni-obuda.hu](mailto:modne.t.judit@amk.uni-obuda.hu)

Monika Pogatsnik  
 Alba Regia Technical Faculty  
 Obuda University  
 Szekesfehervar, Hungary  
[pogatsnik.monika@amk.uni-obuda.hu](mailto:pogatsnik.monika@amk.uni-obuda.hu)

Nikoletta Tolner  
 Alba Regia Technical Faculty  
 Obuda University  
 Szekesfehervar, Hungary  
[tolner.nikoletta@amk.uni-obuda.hu](mailto:tolner.nikoletta@amk.uni-obuda.hu)

**Abstract**— Cyberspace has become a required living space in modern society in the 21st century. Technological developments at the global level increase social vulnerability. Human is a critical element in creating security. Creating complete safety is an impossible mission, so the emphasis should be on resilience and prevention. There is an increased need for safety awareness and training development, which should be extended to all relevant participants to increase resilience. In this process, education could be effectively involved and provide long-term problem-solving. For Z and Alpha generation young people, cyberspace is their natural medium. However, it is far from comfortable living space for the generation that prepares, mentors, and educates them. Without the development of a proper cybersecurity culture, all participants are exposed to dangers, which could only be promoted through cooperation and proper cyber hygiene. The perpetual cyber threat that affects our everyday lives has also rewritten the expectations of the necessary competencies, skills, and abilities in recent years. There is a growing demand for security professionals in this rapidly evolving digital world. Education, on the other hand, cannot support this need, so it needs complete reform. IT education does not adequately support the development of digital and STEM competencies. The issue of safe living needs to be addressed regardless of gender, ethnicity, profession, or education. Thus, education requires special attention, including effective teaching methods that can adapt to the needs of the generation and the effective development of cyber defence and cyber-attack prevention capabilities.

**Keywords**— *cybersecurity, education, security culture, cybersecurity professions.*

## I. MAIN AREAS OF CYBERSECURITY, PAST AND PRESENT IN EDUCATION

Cyber security, cyberspace or even cyberculture has been a part of our lives for a very long time. These concepts involved are often unclear, closely related, but still difficult to define. Because the daily life of a 21st-century person is already taking place in cyberspace, social life and business relations push traditional communication channels into the background. There are several reasons for this progress, cost-effectiveness, changed habits, generational differences, and rapid technological development. The further training of our digital society from a cyber security and material point of view has become critical, an integral part of which is the cyber hygiene capability of those involved and its development. [1] In this way, education is a priority for national security and business economics.

The European Parliament's proposal for a resolution on cyber defence (2018/2004 (INI)) [2] draws attention to similar issues. The motion highlights that “*resilient cyberspace requires impeccable cyber hygiene*” and emphasizes that a 21st-century cyber defence education and training system would significantly reduce threats.

The European Network and Information Security Agency identify five main areas that define cyber security: security and protection of the communication system, operational security, safety of stored and transmitted data and information, physical security of the system, protection against cyber threats. [3]

## II. KEY CONCEPTS

The list of concepts related to the topic is very diverse and long. Consider some relevant, clearer terms in cybersecurity.

### A. Cybersecurity

The National Cybersecurity Strategy [4] defines the cybersecurity concept and its relationship with education in Hungary in 2013 as follows: “*Cybersecurity is the continuous and planned use of political, legal, economic, educational and awareness-raising and technical tools to address risks in cyberspace, transforming cyberspace into a reliable environment for the smooth functioning and operation of social and economic processes, ensuring an acceptable risks level in cyberspace.*” Examining the educational side, they want to achieve the field of cyber security by integrating IT into education.

In 2020, Magyar Közlöny (Hungarian Gazette) published the renewed National Security Strategy. This paper outlines the concept of security in a much more complex way, including cyber security. An important fact appears in this document, the higher education and information technology sector's key role. There are no specific points of contact with education, only the formation and development of citizens' sense of responsibility and security-minded thinking as a strategic interest appears as a strategic goal. [5]

### B. Cyber resilience

Cyber resilience is the ability to continuously achieve the desired result, despite the unfavourable cyber events surrounding it, to achieve an adequate level of security for the organization and individual. The main difference between cybersecurity and cyber resilience is alternately a difference

in approach. *"Resilience is built into organizations and IT systems, rather than added as separate functions."* [6]

*"Cyber resilience is the most important feature of any cyber system, especially during the transition to the sixth technological stage and related Industry 4.0 technologies."* [7]

Because cyberattacks are a very serious threat worldwide. Besides, preventing cyber-attacks, organizations focus on an immediate and consistent cyber-attack response (they can minimize disruptive effects on operations). This capability can be called cyber-resilience. [8]

### C. Cyber hygiene and Cyber security culture

There are also several definitions on the Internet to define this concept, but there is no clear definition. Maennel et al [9] attempted to gather definitions of Cyber Hygiene by researching the scientific literature. Finally, the authors of this article suggest a definition of cyber hygiene: *"Cyber hygiene is a set of practices aimed at protecting from negative impact to the assets from cyber security-related risks."* So cyber hygiene exists in different forms. It is understood from the creation, control, and maintenance of the online security of individuals and organizations, considering their risk assessments and the technologies they use.

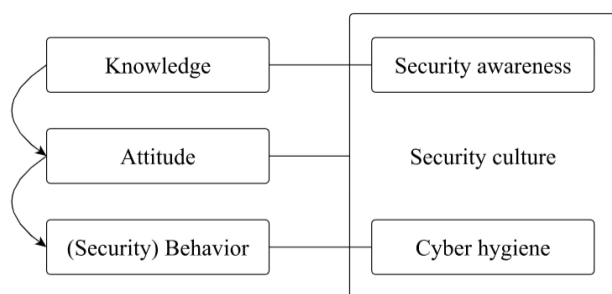


Fig. 1. Cyberhygiene and related terms [9]

Others see cyber hygiene to encourage users to have a safe online presence. The presence of cyber hygiene persuades individuals to follow processes to protect themselves and others. From this perspective, the focus is on user awareness and training. [10]

In another view, *"Cyber hygiene is the establishment and maintenance of an individual's online safety. It is the online analogue of personal hygiene and encapsulates the daily routines, occasional checks and general behaviours required to maintain a user's online "health".*" [11]

Overall, therefore, cybersecurity culture includes cybersecurity awareness, safe behaviour, and cyber hygiene. [9]

### III. CYBER SECURITY EDUCATION IN THE 21ST CENTURY, TAKING INTO ACCOUNT Z GENERATIONAL SPECIFICITIES

#### A. Cyber security education in Hungary

Nowadays - the epidemic situation has also contributed to this - we live a big slice of our lives in cyberspace. We work online, study, bank, buy, do business. There are daily attacks in this space, whether against individuals or larger groups, states. For our security, it is important to keep up with cybercriminals and prepare for and even prevent attacks.

However, this requires properly trained professionals and increased security awareness for all participants in cyberspace. Security itself is part of digital competencies, but its weight has appreciated over the past year and a half. Based on the European Union Reference Framework (2006), 8 key competencies have been identified, one of them is digital competence.

According to Ferrari [12], "digital literacy can be broadly described as the confident, critical, and creative use of ICT (information and communication technologies) to achieve goals in the areas of work, employment, learning, leisure, social inclusion and/or participation. Digital literacy is a transversal key competence which as such enables the acquisition of other key competences (e.g., language, mathematics, learning to learn, cultural awareness). "According to Yuhyun Park [13], there are 7 important basic digital skills:

1. digital literacy,
2. digital communication,
3. digital emotional maturity and intelligence,
4. digital security,
5. knowledge of digital rights,
6. our digital "individuality"
7. digital use ("use" includes digital healthcare, community activity and other off-screen activities).

Demand for IT professionals, including cybersecurity professionals, has doubled in the last 5 years. [14, 15, 16] NET Internetkutató és Tanácsadó Kft has prepared a comprehensive labour market survey on behalf of the Ministry of Innovation and Technology, IVSZ and the Government Informatics Development Agency. The research carried out under the Economic Development and Innovation Operational Program (Ginop) surveyed 3,140 companies, 2,159 IT professionals, 1,785 high school and 2,170 drop-out students, and analysed almost 11,000 job advertisements. Research shows that the demand for IT professionals will exceed the number of professionals issued by educational institutions for years to come. In our rapidly changing world, the development of information technology is constantly rewriting needs, and educational institutions are unable to respond immediately to these rapidly changing needs. In the following, we will look at the trainings in the field of information security and cyber security in Hungarian higher education (Source <https://www.felvi.hu>, and the websites of the universities, <http://uni-obuda.hu/>; <https://www.uni-nke.hu/>; <https://www.elte.hu/>; <https://gdf.hu/>).

NATIONAL UNIVERSITY OF PUBLIC SERVICE Faculty of Military Science and Military Training

- Basic training course in military infocommunication: The aim of the training is to train military info-communication specialists.
- Undergraduate course in International Security and Defence Policy: The training is mainly in the fields of national defence, military, and security. During the training, students will learn how to analyse and evaluate professional problems in security policy and defence issues, and how to create organizational conditions.
- Undergraduate course in national security for those belonging to the personnel of the Military National Security Service or the reconnaissance professional officers of the Hungarian Armed Forces, as well as

the personnel of the special operational forces and the professional organizations cooperating with them. The aim of the training is to train national security experts for special-purpose national security services, as well as other clients, who can effectively fulfil the requirements and tasks of their jobs in the organizations of the national security field using their up-to-date theoretical and practical knowledge.

- Master's Degree Program in Défense Infocommunication Systems Design: The aim is to train professional and civilian professionals who are suitable for the Hungarian Armed Forces, law enforcement agencies, national security services, defence administration, and the wider defence sphere - especially those cooperating with NATO systems, the secure operation of its infocommunication systems, including the design, organization, management, supervision and control, and the provision of conditions for cooperation between such systems.
- Master's Degree Program in International Security and Défense Policy: The aim of the course is to train professionals who are able to work in the activities and international relations of the defence administration system, especially NATO, the EU, the UN and the OSCE, as well as countries and partners with Hungary.
- Master's degree program in National Security: Graduates are trained to prepare current security and defence policy and special strategic analysis, to assess security and crisis situations, and to professionally apply the human resources, special tools and methods required for effective professional activity.

#### NATIONAL UNIVERSITY OF PUBLIC SERVICE Faculty of Law Enforcement

- Crime-Cyber Investigation Specialization: During the training, students get to know the basics of the operation of information systems, the IT, special legal, forensic, and criminal service knowledge necessary for the detection and proof of cybercrime.
- Master's degree in security management: the aim of the training is to train security managers who, in cooperation with state and municipal law enforcement, security and security management professionals, can develop and operate integrated (physical and information) security systems for private entities and public institutions. fully manage the area within an organization or as an external service provider.
- Civil Master's Degree Program in Civil Security: the aim of the training is to train national security professionals who are suitable to perform managerial and expert tasks in the administrative, military, law enforcement, scientific sectors, and to assess, analyse and solve national security problems based on their professional knowledge and practical skills.

#### NATIONAL UNIVERSITY OF PUBLIC SERVICE Faculty of Political Science and International Studies

- Master's Degree Program in Cyber Security: The program is primarily aimed at training professionals in the public service who are responsible for cyber security and who plan to work in the field of international relations, information security of state and municipal organizations, and protection of critical IT systems. In addition to these, of course, students are also prepared for market challenges. After acquiring the basic legal and IT knowledge in the field, students get acquainted with the basics of security organization, risk assessment and physical protection, and the basics of information security.
- Further training in electronic information security management: The main goal of the training is to transfer the professional competencies necessary for the performance of the tasks of the persons responsible for the security of the electronic information system defined in Act L of 2013 on electronic information security of state and local government bodies and to develop a security-conscious approach.

#### UNIVERSITY OF ÓBUDA Donát Bánki Faculty of Mechanical and Safety Engineering

- Bachelor's degree in safety engineering: The aim of the training is to train safety engineers who are suitable for the operation and maintenance of the equipment of safety systems, the introduction and application of related new technologies.
- Master's Degree Program in Security Engineering: The aim of the training is to train security engineers who, can design, organize, operate, perform maintenance tasks, through their acquired high-level technical, IT and organizational knowledge, as well as the related skills.
- Specialized in-service training: A form of training based on a bachelor's and master's degree (or a college or university degree under the previous system) that provides training for specific tasks without changing the level of the degree.
- Information Security Engineer / Specialist: the aim of the training is to provide interdependent, up-to-date professional knowledge and marketable knowledge to professionals working in jobs related to information security.

#### UNIVERSITY OF ÓBUDA János Neumann Faculty of Informatics

- Cyber Security Engineer / Specialist: The curriculum includes modern IT security procedures and their application possibilities; IT security risk analysis; general characteristics of threats in cyberspace; methods and tools for detecting and neutralizing IT incidents; methods and possibilities of IT security modelling and complex examination; aspects and possibilities of cyber defence; etc.

#### GÁBOR DÉNES COLLEGE

- Data protection and information security manager: During the training, students acquire the knowledge elements necessary for the management of the data protection and information security monitoring system supporting corporate economic security.

#### EÖTVÖS LORÁND UNIVERSITY Faculty of Law

- Data security and data protection lawyer: the aim of the training is to prepare lawyers in the field of data security, data protection, freedom of information and legal data management, private data management, building on the practice of NAIH, and the proper conduct of litigation and non-litigation.
- Data Security and Data Protection Law Specialist: the aim of the training is to prepare holders of a degree entitling them to internal data protection responsibility activities, based on the practice of NAIH, to recognize and manage legal problems in the field of data security, data protection, freedom of information and public and private data management.

### B. Z generational specificities

After a more thorough study of the training topics, we can see that these trainings do not affect every single area of information security and cyber security. The core business of the school largely determines which segment of cybersecurity is given priority during training. Somewhere the study and knowledge of the legal background is important, elsewhere the IT background is stronger. It would be very important to make this area attractive to applicants. The age of those entering education also greatly influences who chooses this field. Generational differences, different basic skills influence the choice.

For the purposes of this paper, we will focus only on Generation Z [17]. This is the age group most represented in university education today. There are several definitions of generational boundaries. According to Pais [18] members of Generation Z were born between 1996 and 2009. This generation is characterized by the author as follows: “They live their lives connected to the Internet, sort of wired”. Their excellent intellect and highly advanced problem-solving ability are associated with an excellent technical sense that generates a strong practical need.” Tari [19] classifies young people born between 1995 and 2009 into Generation Z. McCrindle (2014) [20] considers the age group born after 2000 to be Generation Z. This generation is also called “digital natives”. They do not know life without the World Wide Web. For them, using a computer, a smartphone, the World Wide Web is a completely natural thing. This generation poses new challenges to educators because they are unwilling to accept traditional methods, they want to acquire knowledge in interactive, interesting lessons. Members of the generation use technical innovations with ease, but their safety awareness is inadequate. They are not fully aware of the dangers in cyberspace. Coercive measures caused by the COVID epidemic included the implementation of education online. The transition from attendance education to online education had to be resolved so quickly that the issue of security was not much addressed. Young people who had previously used the online space for other purposes were suddenly forced to live in this space almost their entire lives. There are many sources of danger in cyberspace that most young people find difficult or unnoticed. It would be important for safety awareness to appear in education and have a much greater weight. According to a survey, 60% of 8–12-year-olds were exposed to some form of cyber risk during online education [21]. More than 84% of school-age children were involved in online education worldwide. These children and their parents, as well as the teachers who teach them, also need to develop their

digital competencies. There are aspirations and regulations for these at the international level.

## IV. NEEDED COMPETENCIES AND SKILLS FOR A CYBERSECURITY SPECIALIST

### A. Security awareness in the light of digital competencies

The Comprehensive Framework for the Assessment of ICT Competences [22] defines five main areas of competence:

1. Accessing, evaluating, and managing information and data
2. Sharing information and communicating
3. Transforming and creating information and digital content
4. Problem-solving in a digital context and computational thinking
5. Appropriate use of ICT (online security, safety and risk awareness and skills)

Online security competencies include the appropriate use of ICT in multiple environments and platforms. With increased information sharing, students need to be aware of how to handle and protect personal information. Basic security knowledge includes the use of strong passwords, anti-virus measures, and the protection of personal information.

Decision-makers’ interest in assessing students’ ICT-related safety and security competencies is reflected in the widespread inclusion of such competencies in school curricula in education systems. As the use of ICT in the classroom and beyond becomes more common, a wide range of issues related to online safety are being included in school curricula. These online security topics include safe online behaviour, privacy, cyberbullying, downloading, copyright, safe use of cell phones, and contact with strangers. It is becoming increasingly important to integrate online security practices into ICT education, in addition to understanding existing knowledge of security and safety issues related to ICT access and use [24], [25].

Among the competencies, stress tolerance and resilience appear little in the literature as important elements. Stress tolerance is much needed because of the ability to respond appropriately in an emergency cybersecurity situation. Resilience is the ability to adapt to changing situations, which is important for proper adaptation to security situations.

### B. Needed skills for a cybersecurity specialist

Based on the description of the Cyber Security Guide [23], the following are typical for a cybersecurity professional. A cybersecurity professional takes care of the security of the company and its employees in cyberspace. They ensure continuous monitoring of systems, secure operation, and protection against attacks by software and hardware devices. They are also responsible for training and educating employees, passing on their experience and strengthening safety awareness. They design and implement firewalls and security systems by the latest security standards. “*People in this role are often hired as much for their soft skills as their technical ability.*” [23]

Needed skills include, in addition to the appropriate level of training, good communication skills, teamwork, the ability to work in an “emergency”, stress tolerance and problem-solving skills, the ability to adapt to the needs and attitudes of

employees, a kind of flexibility skills. Rapid response, analytical thinking, and continuous learning skills are essential in this field.

*"In terms of skills, experience, and general mindset, a cybersecurity specialist needs to be like a Swiss Army knife of the digital world. A person in this role needs to be multi-disciplinary and adaptable to a wide variety of situations."*[23]

## V. SUMMARY AND FURTHER RESEARCH

Our study was prepared with the aim of assessing the literature, clarifying the most important conceptual issues and directions in the field of IT competencies, including IT security knowledge, for our empirical research.

Although IT competencies are highlighted in many documents, education at BSc, MSc and specialist training levels is provided at several universities in Hungary, but education in this important area is not yet sufficiently represented in lower and secondary institutions. In the case of the growing Z and alpha generation, the priority development of these competencies is necessary, especially regarding the development of the soft skills required for the development of a safety awareness attitude, safety culture, resilience, and cyber hygiene. In addition, in a later study, it would be worthwhile to examine the proportion of students graduating from the training places listed in the article in the field of IT security. How can I compensate for the lack of IT security specialist companies in Hungary? What methods do companies and organizations use to fill the gap?

## REFERENCES

- [1] Fekete-Karydis K., Lázár B.: A kibévédelmi stratégiák fejlődése, kibévédelmi kihívások, aktualitások (2.): Az Európai Unió kibévédelmi szabályozása 2013-tól napjainkig (Development of cyber defense strategies, cyber defense challenges, current events (2.): European Union cyber security regulation from 2013 to the present) *Honvédségi Szemle: A Magyar Honvédség Központi 147. évfolyam: 2019/5. szám pp. 60-72., 13 p.* (2019) URL: <https://kiadvany.magyarhonvedseg.hu/index.php/honvszemle/article/view/224> (Last viewed: 2021.08.12)
- [2] Az Európai Parlament állásfoglalására irányuló indítvány a kibévédelemről (Motion for a european parliament resolution on cyber defense) (2018/2004(INI)) (2018) URL: [https://www.europarl.europa.eu/doceo/document/A-8-2018-0189\\_HU.html](https://www.europarl.europa.eu/doceo/document/A-8-2018-0189_HU.html) (Last viewed: 2021.08.25).
- [3] Beláz A., Berzsényi D.: Kibévédelmi Stratégia 2.0 – A kibévédelmi stratégiai irányításának kérdései. (Cyber Security Strategy 2.0 - Issues of Strategic Management of Cyber Security) *Elemzések. Budapest, Stratégiai Védelmi Kutatóközpont* (2017). URL: <https://bit.ly/3C2zWuS> (Last viewed: 2021.09.19)
- [4] 1139/2013. (III. 21.) Kormányhatározat Magyarország Nemzeti Kibévédelmi Stratégiájáról, 5. és 10/g pont (Government Resolution on Hungary's National Cyber Security Strategy) URL: [https://2010-2014.kormany.hu/download/b/b6/21000/Magyarország\\_Nemzeti\\_Kibévédelmi\\_Strategiaja.pdf](https://2010-2014.kormany.hu/download/b/b6/21000/Magyarország_Nemzeti_Kibévédelmi_Strategiaja.pdf) (Last viewed: 2021.09.10)
- [5] 1163/2020. (IV.21.) Kormányhatározat Magyarország Nemzeti Biztonsági Stratégiájáról. (Government Decision on the National Security Strategy of Hungary.) URL: <https://magyarkozlony.hu/dokumentumok/6c9e9f4be48fd1bc620655a7f249f81681f8ba67/megtekintes> (Last viewed: 2021.09.19)
- [6] Björck F., Henkel M., Stirna J., Zdravkovic J.: Cyber Resilience – Fundamentals for a Definition. In: Rocha A., Correia A., Costanzo S., Reis L. (eds) *New Contributions in Information Systems and Technologies. Advances in Intelligent Systems and Computing*, vol 353. Springer, Cham.(2015) DOI: [https://doi.org/10.1007/978-3-319-16486-1\\_31](https://doi.org/10.1007/978-3-319-16486-1_31) (Last viewed: 2021.08.27.)
- [7] Sergei P.: Cyber Resilience, *River Publishers* (2019)
- [8] Sepúlveda Estay D. A., Sahay R., Barfod M. B., Jensen C. D.: A systematic review of cyber-resilience assessment frameworks, *Computers & Security*, Volume 97, (2020), 101996, ISSN 0167-4048, DOI: <https://doi.org/10.1016/j.cose.2020.101996>, (Last viewed: 2021.08.27.)
- [9] Maennel K., Mäses S., Maennel O.: Cyber Hygiene: The Big Picture. In: Gruschka N. (eds) *Secure IT Systems. NordSec 2018. Lecture Notes in Computer Science*, vol 11252. Springer, Cham. (2018) DOI: [https://doi.org/10.1007/978-3-030-03638-6\\_18](https://doi.org/10.1007/978-3-030-03638-6_18), (Last viewed: 2021.08.27.)
- [10] Pflieger L., Sasse M. A., Furnham A.: From weakest link to security hero: Transforming staff security behavior, *Journal of Homeland Security and Emergency Management*, vol. 11, no. 4, pp.489–510, (2014)
- [11] Vishwanath, A., Neo, L.S., Goh, P., Lee, S., Khader, M., Ong, G., & Chin, J.E.: Cyber hygiene: The concept, its measure, and its initial tests. *Decis. Support Syst.*, 128. (2020)
- [12] Ferrari A., 2013, Report EUR 26035 EN [https://www.deaweb.hu/images/bongeszde/digcomp\\_teljes\\_hun\\_1512\\_31.pdf](https://www.deaweb.hu/images/bongeszde/digcomp_teljes_hun_1512_31.pdf), (Last viewed: 2021.08.27.)
- [13] Yuhyun Park: 8 digital life skills all children need and a plan for teaching them. World Economic Forum, Global Agenda, 2016, <https://bit.ly/2Zcgbmw> (Last viewed: 2021.08.26.)
- [14] XXI. Fialat Műszaki Tudományos Ülésszaka, 2016. Kolozsvár, 313–316. <http://hdl.handle.net/10598/29092>; Security awareness in context of digital competence: Nyikes Zoltán, Óbudai Egyetem, Biztonságtudományi Doktori Iskola, (Last viewed: 2021.08.26.)
- [15] Berzsényi D.: The Human Side of Cybersecurity, *Nemzet és Biztonság 2017/2. szám 54–67.* <https://bit.ly/3aWvlyy>; (Last viewed: 2021.08.27.)
- [16] Csutak, Zs.: Kibévédelmi kihívások a 21. században. In: Móra Akadémia, (5). pp. 360-375. (2018); <https://bit.ly/3C250uU>; (Last viewed: 2021.08.27.)
- [17] Molnár L. – Kovácsné Havelant Kinga Digitális kompetenciák a Z-generációban; Észak-magyarországi Stratégiai Füzetek XVIII. évf. 2021 különszám, [https://www.strategiaifuzetek.hu/files/216/SF-2021-k\\_136.pdf](https://www.strategiaifuzetek.hu/files/216/SF-2021-k_136.pdf); (Last viewed: 2021.08.29.)
- [18] Pais E. R. (2013) Y és Z generáció mint a jövő munkavállalói. <http://docplayer.hu/2100822-Y-esz-generacio-mint-a-jovo-munkavallaloi.html>, (Last viewed: 2021.08.29.)
- [19] Tari A.: Z generáció TERICUM KÖNYVKIADÓ. ISBN:9789639633926, Nyelv:MAGYAR, Kiadás éve:2011.
- [20] The ABC of XYZ: Understanding the Global Generations, October 2018, Mark McCrindle, ISBN: 978 0 9924839 0 6
- [21] Joshua A. Jackman, Douglas A. Gentile, Nam-Joon Cho & Yuhyun: Addressing the digital skills gap for future education, Published: 11 March 2021 <https://www.nature.com/articles/s41562-021-01074-z>
- [22] OECD (2018): Pisa 2021 ICT Framework
- [23] Cybersecurity Guide: How to Become a Cybersecurity Specialist (2021). URL: <https://cybersecurityguide.org/careers/security-specialist/> (Last viewed: 2021.09.23)
- [24] Károly A., Elek R., Haidegger T., Széll K., Galambos P. (2019): Optical flow-based segmentation of moving objects for mobile robot navigation using pre-trained deep learning models. In: IEEE (szerk.) 2019 IEEE International Conference on Systems, Man and Cybernetics (SMC) Piscataway (NJ), pp. 3060-3066.
- [25] Redjimi H., Galambos P., Tar J., Széll K. (2019): The Effects of Simultaneous Noise and Missing Information in Fixed Point Iteration-based Adaptive Control. In: IEEE (szerk.) 2019 IEEE International Conference on Systems, Man and Cybernetics (SMC). Piscataway (NJ), pp. 1430-1435.

# Analysis of a Prime-Representing Constant

G. Nagy\*

\*Óbuda University, Alba Regia Technical Faculty, Institute of Geoinformatics

nagy.gabor@amk.uni-obuda.hu

ORCID ID: 0000-0001-9453-2291

**Abstract**—Fridman et al [1] have described an irrational constant, which can be used to generate a sequence of all of the prime numbers. This paper gives a program, which can calculate this constant in arbitrary precision, and presents some analysis with the calculated data.

**Index Terms**—prime numbers, prime-representing constant, Python

## I. INTRODUCTION

Fridman et al describes a sequence in [1]. If the  $i$ th element of the sequence of prime numbers denoted by  $p_i$ , the described sequence is determined by these expressions:

$$f_1 = \sum_{k=1}^{\infty} \frac{p_k - 1}{\prod_{j=1}^k p_j} \simeq 2.92 \quad (1)$$

$$f_i = \lfloor f_{i-1} \rfloor (f_{i-1} - \lfloor f_{i-1} \rfloor + 1) \quad (2)$$

The described  $f$  sequence connects to the sequence of prime numbers, because:

$$p_i = \lfloor f_i \rfloor \quad (3)$$

The first element of the sequence is an irrational constant, which can generate the sequence of prime numbers by the equations (2) and (3). All  $\lfloor f_i \rfloor$  is a prime number, and this method provides all of the prime numbers.

## II. THE TEST PROGRAM

I have developed a Python [2], [3], [4] program for calculating the prime-representing constant, and doing some calculations with this number.

```
"""
A program for calculating the prime generator constant with
arbitrary precision, and check the sequence of generated numbers.
(See in DOI:10.1080/00029890.2019.1530554)
Author: Nagy Gabor
"""
```

```
#module imports
```

```
#the decimal module for calculating with arbitrary precision
import decimal
```

```
#the log function from the math module
from math import log
```

```
#some simple functions for prime numbers
```

```
def isprime(n):
    for i in range(2, int(n**0.5)+1):
        if n%i==0:
            return False
    return True
```

```
def nextprime(n):
    i=n
    while True:
        i+=1
        if isprime(i):
            return i
```

```
#Set the number of decimal digits
decdig=1000 # modify this number to change the precision
decimal.setcontext(decimal.Context(prec=decdig+2))

#Set the limits of the increase
qlim=decimal.Decimal(0.1)**(decdig+3)

#Calculate the prime generator constant
c=decimal.Decimal(0)
denominator=1
p=2
while True:
    q=(p-1)/decimal.Decimal(denominator)
    if q<qlim:
        break
    c+=q
    denominator*=p
    p=nextprime(p)
#The prime generator constant is rounded to the required precision
#(the calculation works with two more digits)
c=round(c, decdig)
#Print the value of the prime generator constant
print(f'The prime generator constant with {decdig} digits:')
print(c)

#Calculate the sequence until the first number which is not prime
#the initial list with the first element of the sequence
f=[c]
while True:
    #calculate the next element of the sequence
    f.append(int(f[-1])*(1+f[-1]%1))
    #end the iteration, if the last element is not correct
    if int(f[-1])!=nextprime(int(f[-2])):
        break
#calculated the list of generated primes
#(the last element of the f list is not correct)
pl=[int(x) for x in f[:-1]]
#print the result
print(f'\nThis number provides {len(pl)} prime numbers:')
print(' '.join((str(pj) for pj in pl)))
print(f'The first wrong number: {int(f[-1])}')
print(f'\nThe count of prime's decimal digits:', sum([len(str(pj)) for pj in pl]) )
print(f'\nThe sum of primes's logarithms (base=10):', sum([log(pj, 10) for pj in pl]))
```

This sample program can be downloaded from GitHub<sup>1</sup>.

The programs use the decimal Python module. This module provides decimal objects, which represents an number with arbitrary decimal digits. In the first step the program calculate the prime-representing constant ( $f_1$ ) by the equation (1). This equation contains an infinite summation. The program calculate the elements of this summation until the increase will be less than a limit, which is less than the required precision.

This program can calculate the value of the prime representing constant with arbitrary precision. The first 1000 digits are:

```
2.920050977316134712092562917112019468002727899
32142671977268253310773377212776612419017811231
75837422983388595531013766557907893508590053204
58879066450802184292252411229314474766432726781
35940161193093481787115189352526460357537952181
08130464201677079773895702501118038092826861786
58154888032203367829269125018738690914047486202
26129121622736838982992945558789156975535538705
18739251538181607957171434240446633933138827942
```

<sup>1</sup><https://github.com/ngabor/primegenconst>



63272129485703450548197999040464926096485197137  
 63913013768679285321042395712078626139752461367  
 42059302377616384076898261130632683169598660539  
 41841083990772474014702698539309967440776095857  
 59049691130821855859902170542405345175550582796  
 53606079314120316578636254109249073897393328606  
 72772227778457834272139260508254028067617639389  
 06299645073523384311614730916065503649336668524  
 71602529082686731529397629219137499668462799308  
 53615755759049885203735106436548610543326144375  
 30514732349448181398754438855296110963025921245  
 99095044825003663535855619587169625921692456215  
 563334172710729

III. ANALYSIS OF THE CONSTANT

The prime-representing constant is an irrational number, the program can calculate this number only an arbitrary but finite precision. (In the sample program this precision is determined as the decimal digits of the number.) When anybody calculates the sequence from an approximate value, only the first part of the calculated sequence equals to the sequence of prime numbers.

The question arises that what is the connection between the precision (the numbers of decimal digits) and the length of the list of the correct generated prime numbers.

The program calculates the sum of the decimal based logarithm of the correct generated prime numbers. The Table I contains the result of these calculation with some different decimal digits from 10 to 10000.

The results of  $\sum_{i=1}^n \log_{10} p_i$  are very close to the numbers of decimal digits. The sums of the decimal digits of the correct generated primes are typically greater than the decimal digits (the precision) of the prime-representing constant.

IV. CONCLUSION

The sequence described [1] can generate the total sequence of prime numbers, but the practical application is limited by the precision of the calculations.

The size of information is very similar in the approximated prime-representing constant and in the sequence of primes, which can be generated by the approximated constant.

REFERENCES

[1] D. Fridman, J. Garbulsky, B. Glecer, J. Grime, and M. T. Florentin, "A prime-representing constant," *The American Mathematical Monthly*, vol. 126, no. 1, pp. 70–73, 2019.  
 [2] G. Van Rossum *et al.*, "Python Programming Language." in *USENIX Annual Technical Conference*, vol. 41, 2007.  
 [3] T. E. Oliphant, "Python for scientific computing," *Computing in Science & Engineering*, vol. 9, no. 3, 2007.  
 [4] K. J. Millman and M. Aivazis, "Python for scientists and engineers," *Computing in Science & Engineering*, vol. 13, no. 2, pp. 9–12, 2011.

Table I  
 THE PRIME-REPRESENTING CONSTANT IS CALCULATED WITH DIFFERENT DECIMAL DIGITS ( $d$ ), AND LOOK FOR THE LAST ELEMENT OF THE SEQUENCE ( $f_n$ ), WHICH PROVIDES A CORRECT PRIME NUMBER ( $p_n$ ). THE SUM OF THIS PRIME'S DECIMAL DIGITS AND 10-BASED LOGARITHM ARE ALSO CALCULATED. THIS TABLE PRESENTS SOME EXAMPLE BETWEEN 10 AND 10000.

$d$	$p_n$	$n$	sum of decimal digits	$\sum_{i=1}^n \log_{10} p_i$
10	31	11	18	11,3
20	53	16	28	19,51
30	83	23	42	32,43
40	103	27	52	40,38
50	131	32	67	50,72
60	157	37	82	61,55
70	181	42	97	72,73
80	197	45	106	79,59
90	227	49	118	88,92
100	257	55	136	103,22
200	487	93	250	200,71
300	727	129	358	300,86
400	967	163	460	400,33
500	1201	197	591	503,44
600	1447	229	719	603,31
700	1657	260	843	702,19
800	1889	290	963	799,68
900	2129	320	1083	898,81
1000	2371	351	1207	1002,75
1500	3533	494	1779	1498,44
2000	4679	633	2335	2000,42
2500	5849	768	2875	2502,86
3000	6983	898	3395	2997,81
3500	8191	1028	3915	3502,21
4000	9337	1155	4423	4002,91
4500	10457	1279	4969	4498,26
5000	11689	1403	5589	4999,68
5500	12799	1526	6204	5502,49
6000	13921	1646	6804	5997,62
6500	15131	1767	7409	6501,33
7000	16229	1886	8004	7000,52
7500	17431	2005	8599	7503,48
8000	18523	2122	9184	8001,32
8500	19777	2239	9769	8502,46
9000	20939	2355	10349	9002,25
9500	22051	2471	10929	9504,8
10000	23167	2585	11499	10001,2

**POSTER SESSION II.**

**Robotics and Industrial Applications**

# Hand Gesture Controlled Robot

Dávid Bárándi  
Alba Regia Technical Faculty  
Óbuda University  
Székesfehérvár, Hungary  
[barandidavid@stud.uni-obuda.hu](mailto:barandidavid@stud.uni-obuda.hu)

Károly Széll  
Alba Regia Technical Faculty  
Óbuda University  
Székesfehérvár, Hungary  
[szell.karoly@amk.uni-obuda.hu](mailto:szell.karoly@amk.uni-obuda.hu)  
ORCID: 0000-0001-7499-5643

**Abstract**— Robot manipulators in factories are usually used in automatic mode, running a pre-written program. My goal with this project was to be able to control the robot manipulator in real time with hand movements. This would allow in the future, by using augmented reality and a mobile robot manipulator, to work in places that would be dangerous for human life (e.g., chemical environment, extreme cold/hot environment.)

**Keywords**—robotics, ROS, automation, industry 4.0, hand detecting and tracking, collaborative robot, OpenCV, Mediapipe

## I. INTRODUCTION

Many examples in modern robotics show that, in some cases, seamless and real-time control is needed. In many cases it is difficult to control a robot with a keyboard or with the control panel of the robot itself. Gesture-based robot control is where a human can control the robot with hand movements and does not need to enter numerical values with a keyboard or control panel. This is suitable for controlling any robot in areas where human operation is not feasible for safety reasons [1]– [3]. So, you can control the robot safely in front of a TV or PC [4].

Thanks to the development of the Robotics Laboratory at the Alba Regia Faculty of Technology of Óbuda University, students will gain access to the most common industrial robots and collaborative robotics in industry. The collaborative robot in the lab can be used by any student to extend, develop, and test different ideas [5]– [8]. The collaborative robot is a Universal Robots UR5 e-series 6 degrees of freedom multifunctional co-robot.

## II. PROBLEM DESCRIPTION

I have taken the following aspects into account in the design:

- Implementation with minimum hardware requirements
- Plug n play with any webcam and universal robots
- 3D movement with a webcam
- Integrating OpenCV into ROS

The main problem was caused by the different Python versions. OpenCV and Mediapipe only works with Python3, while ROS Melodic uses Python2. The reason for choosing ROS Melodic over the newer ROS Noetic (which already supports Python3) is that the Universal Robots GitHub page for the package recommends Ubuntu 18.04, which only runs ROS Melodic.

## III. STRUCTURE OF THE ENVIROMENT

The project only required a Universal Robots UR5 e-series collaborative robot and a webcam. For image processing, I used the Open-Source Computer Vision Library (OpenCV) with Python3, and for hand recognition and tracking, I used Mediapipe developed by Google, also with Python3. Mediapipe was chosen because we wanted to track not only the hand itself, but also the hand points, to allow for the description and teaching of gestures in the future (see Figure 1. )

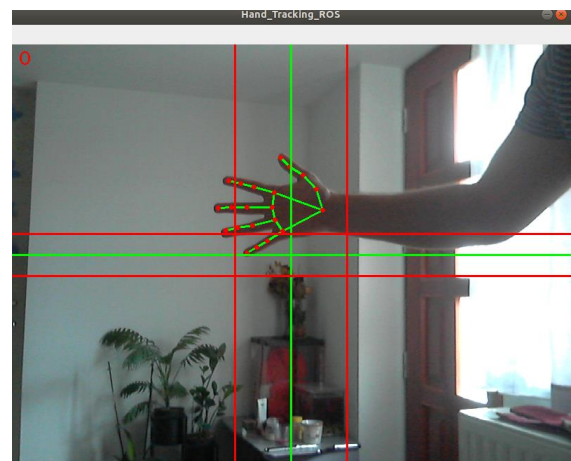


Figure 1. Hand recognition with OpenCV and Mediapipe

### Universal Robots UR5e

Technical Data of UR5-e (see Figure 2. ):

- Maximum reach: 850 mm
- Weight with cable: 20.6 kg
- Maximum payload: 5 kg
- Degrees of freedom: 6

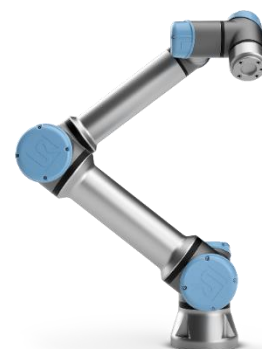


Figure 2. UR5e

## IV. STRUCTURE OF THE PROGRAM

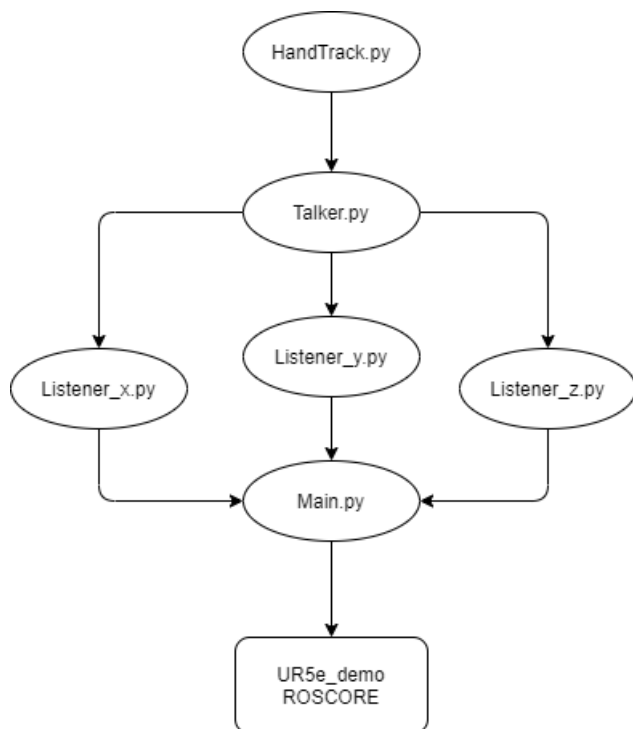


Figure 3. Structure of the program

The developed system uses live video stream for gesture recognition. It monitors in real time the position of the points on the hand and issues movement commands to the robot based on this information. The proposed technique Robot system operation is divided into four subsections:

- Setup ROS environment
- Hand detection with OpenCV and MediaPipe
- Processing data from hand detection
- Sending motion commands to the robot

## A. Setup ROS environment

Robot Operating system (ROS) is a flexible framework for creating robot programs. Every ROS project needs a central core on which to hang other nodes that perform complex tasks. For this project, I used the Universal Robots factory package as the core. The package includes Moveit and Rviz (see Figure 5. ), a visualization environment that allows me to easily design the path needed to move the robot and Rviz was used for one of the safety elements.

## B. Hand detection with OpenCV and MediaPipe

The project is based on the HandTrack.py file (see Figure 3. ). To detect the hand, I used the open-source computer vision library (OpenCV) and MediaPipe. OpenCV can be used to draw lines on the camera image so that I can draw the origin point and the threshold zone, where the robot stops moving when the tracked point is reached. For hand recognition and tracking I used MediaPipe, which is an open-source Python package developed by google which is perfect for hand recognition. It places a landmark of 21 points on the recognized hand, the points of which I used to control the robot (see Figure 4. ).

## C. Processing data from hand detection

The data from HandTrack.py is collected by the Talker.py (see Figure 6.) file and passed to the Listener files. The Talker.py file is the publisher node which is the transition between Python2 and Python3. The subscriber nodes are the Listener nodes. These files decide whether the robot should move in a positive or negative direction on a given axis, and they also define the size of the step per instruction and the threshold zone (marked with red lines, see Figure 1. ). Listener\_z.py is the file where the initial length of the segment between point 1 (WRIST) and point 12 (MIDDLE\_FINGER\_TIP) is defined (see Figure 4. ). If the length of the segment increases by a factor of 1.2 during hand tracking, the robot moves in a positive direction, if it increases by a factor of 0.8, the robot moves in a negative direction on the axis. Here it is important that the hand is in front of the camera when starting the Main.py file, because only then can the length of the section be recorded, otherwise the robot will only move on 2 axes.

## D. Sending motion commands to the robot

The Main.py file (see Figure 7. ) is responsible for the movement commands. The starting position and the orientation of the TCP are defined here. In addition, the Main.py file collects the data returned by the Listener files and sends it to the robot, which executes it in the form of a motion. The program's motion, designed with state and executed with the real robot's state, is displayed in Rviz, so that we can even remotely control the robot manipulator after modeling the robot's environment.

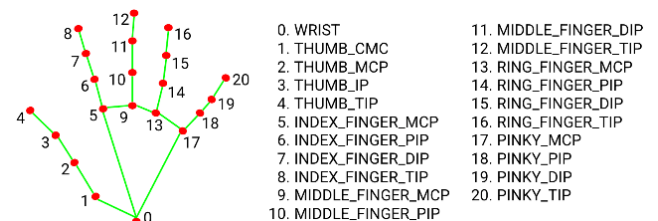


Figure 4. Mediapipe hand landmarks

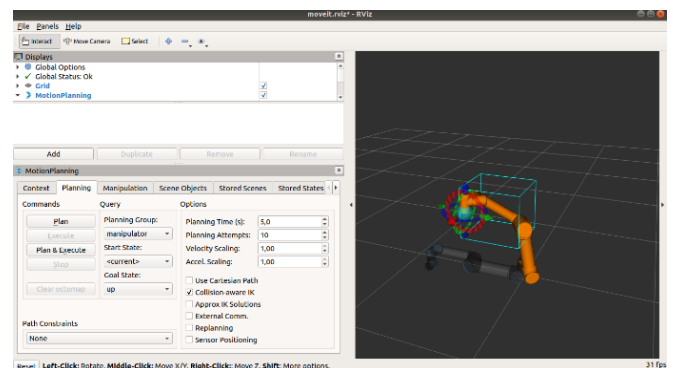


Figure 5. UR5e in Rviz

```

dr0id@dr0id-ThinkPad-L440: ~
File Edit View Search Terminal Tabs Help
roscore http://dr0id-ThinkPad-L440:11311/ x dr0id@dr0id-ThinkPad-L440: ~ x
dim: []
data_offset: 0
data: [0.182, 0.3, 0.355, 0.264, 0.306, 0.043, 0.239, 0.013]
[INFO] [1632752576.613902]: layout:
dim: []
data_offset: 0
data: [0.162, 0.307, 0.326, 0.192, 0.281, 0.042, 0.215, 0.014]
[INFO] [1632752578.039807]: layout:
dim: []
data_offset: 0
data: [0.156, 0.318, 0.325, 0.203, 0.266, 0.046, 0.207, 0.016]
[INFO] [1632752579.460439]: layout:
dim: []
data_offset: 0
data: [0.162, 0.322, 0.331, 0.208, 0.278, 0.049, 0.213, 0.02]
[INFO] [1632752580.888231]: layout:
dim: []
data_offset: 0
data: [0.158, 0.321, 0.327, 0.203, 0.274, 0.04, 0.207, 0.002]
[INFO] [1632752582.308224]: layout:
dim: []
data_offset: 0
data: [0.156, 0.319, 0.325, 0.198, 0.271, 0.04, 0.205, 0.005]
    
```

Figure 6. Talker.py during running

```

root@dr0id-ThinkPad-L440: /home/dr0id
File Edit View Search Terminal Tabs Help
/home/dr0id/catkin_ws/s... x dr0id@dr0id-ThinkPad-L4... x root@dr0id-ThinkPad-L44... x
position:
x: 0.81725
y: 0.1914499999961
z: -0.00549100003927
orientation:
x: 3.38932338369e-12
y: 0.707106781259
z: 0.707106781114
w: 7.30837588403e-14
position:
x: 0.81725
y: 0.1914499999961
z: -0.00549100003927
orientation:
x: 3.38932338369e-12
y: 0.707106781259
z: 0.707106781114
w: 7.30837588403e-14
Pose1_OK
OK
(Y: ', -0.35700000000000004, 0.005)
(Z: ', -0.037999999999999998, 0.005)
(X: ', 0.2229708501127445, 0.24401844192601513, -0.01)
    
```

Figure 7. Main.py during running

## V. SAFETY FUNCTIONS

During testing, the robot follows unpredictable trajectories after losing track of the hand. Three main safety features were implemented to avoid unexpected trajectories. First, the robot's workspace was virtually constrained. This was solved within Rviz by creating a simple safety cage. We were able to limit the range of motion sufficiently so that the robot cannot damage its environment. When the robot reaches the green wall, it stops automatically (see Figure 8). Secondly, when the program detects too much movement at the hand between two image refreshes, it stops immediately. This is necessary because if the detection of the hand is incorrect, the robot may receive incorrect data which can lead to unpredictable movement paths and possible collisions. Finally, when the camera loses hand tracking it sends a 0 value to the robot so that the robot stops moving, so there is no need to stop the program in case of signal loss.

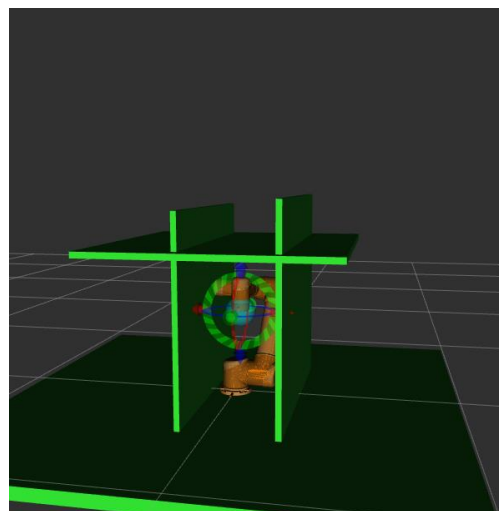


Figure 8. UR5e in Rviz with the safety cage

## VI. PROBLEMS DURING PROJECT AND OPPORTUNITIES DEVELOPMENTS

The project has encountered several problems. The main problem with 3D movement is that only the distance between 0 and 12 points is observed, so a fist strike is enough to move the robot. To solve this problem, we need to replace the webcam with a Microsoft Kinect V2 [5]– [9], which is capable of depth sensing, which would solve this problem. The other big problem is software optimization. The software currently works at a very low FPS. The consequence of this is that it is not possible to make fast movements with the hand because it loses tracking, this should be optimized in the future. One possible solution could be to rework the structure of the program and include Kinect Studio if Kinect V2 is used. This would allow faster movements and tracking on the robot side. With Kinect Studio, it would be possible to program and teach dedicated gestures [3], [14] and hand signals, which would facilitate working with a collaborative robot. Another solution could be to re-implement difficult computational parts/modules in C++, e.g., with python bindings. The use of Leap Motion for higher accuracy was considered, but we could not test and implement this because Leap Motion is not available at the university.

## VII. CONCLUSION

The document presents a preliminary project for scientific studies and research. The robot can be controlled by hand gestures in the following ways. The robot will move along the x, y and z axes depending on the quarter of the camera image in which the tracked point on the hand (see Figure 4. ), in this case point 0 WRIST, is located and the length of the segment between point 12 MIDDLE\_FINGER\_TIP and point 0 WRIST increases or decreases compared to the initial length recorded at startup. The experimental results show that with shorter steps and higher robot speed, a less skilled, more fluid and more accurate movement can be achieved. In the future, we would like to replace the webcam with a Kinect V2 or a Leap Motion sensor for more accurate hand detection. Furthermore, we would like to rewrite the more resource-intensive modules or, if necessary, the whole program in C++ to achieve higher performance.

## ACKNOWLEDGMENT

The authors thankfully acknowledge the financial support of this work by the Howmet Aerospace Foundation, the Arconic Foundation, and the project no. 2019-1.3.1-KK-2019-00007 implemented with the support provided from the National Research, Development and Innovation Fund of Hungary, financed under the 2019-1.3.1-KK funding scheme.

## REFERENCES

- [1] “Gesture-controlled user interfaces, what have we done and what’s next? | Request PDF.” [https://www.researchgate.net/publication/228815683\\_Gesture-controlled\\_user\\_interfaces\\_what\\_have\\_we\\_done\\_and\\_what’s\\_next](https://www.researchgate.net/publication/228815683_Gesture-controlled_user_interfaces_what_have_we_done_and_what’s_next) (accessed Oct. 15, 2021).
- [2] “Gesture-controlled user interfaces, what have we done and what’s next? | Request PDF.” [https://www.researchgate.net/publication/228815683\\_Gesture-controlled\\_user\\_interfaces\\_what\\_have\\_we\\_done\\_and\\_what’s\\_next](https://www.researchgate.net/publication/228815683_Gesture-controlled_user_interfaces_what_have_we_done_and_what’s_next) (accessed Oct. 15, 2021).
- [3] J. L. Raheja, R. Shyam, U. Kumar, and P. B. Prasad, “Real-time robotic hand control using hand gestures,” *ICMLC 2010 - The 2nd International Conference on Machine Learning and Computing*, pp. 12–16, 2010, doi: 10.1109/ICMLC.2010.12.
- [4] D. Ionescu, B. Ionescu, C. Gadea, and S. Islam, “An intelligent gesture interface for controlling TV sets and set-top boxes,” *SACI 2011 - 6th IEEE International Symposium on Applied Computational Intelligence and Informatics, Proceedings*, pp. 159–164, 2011, doi: 10.1109/SACI.2011.5872992.
- [5] M. Pogatsnik and R. B. Kendrovics: Communication and Reading Comprehension among Informatics and Engineering Students, 2020 IEEE 18th World Symposium on Applied Machine Intelligence and Informatics (SAMI), Herlany, Slovakia, 2020, pp. 235-240, doi: 10.1109/SAMI48414.2020.9108764.
- [6] Módné Takács Judit, Pogátsnik Monika: The online learning from the students’ perspective, In: Szakál, Anikó (szerk.) 2021 IEEE 19th World Symposium on Applied Machine Intelligence and Informatics (SAMI), Budapest, Magyarország : IEEE Hungary Section (2021) 507 p. pp. 00027-00032. , 6 p.
- [7] György Györök, Bertalan Beszédes. Artificial Education Process Environment for Embedded Systems. In: Orosz, Gábor Tamás (szerk.) 9th International Symposium on Applied Informatics and Related Areas - AIS2014. Székesfehérvár, Magyarország : Óbudai Egyetem, (2014) pp. 37-42. , 6 p.
- [8] Pogátsnik Monika: Dual education: connecting education and the labor market, *Opus et Educatio* Volume 8. Number 3., pp. 304-313, DOI: <http://dx.doi.org/10.3311/ope.466>
- [9] Y. Liu, M. Dong, S. Bi, D. Gao, Y. Jing, and L. Li, “Gesture recognition based on Kinect,” *6th Annual IEEE International Conference on Cyber Technology in Automation, Control and Intelligent Systems, IEEE-CYBER 2016*, pp. 343–347, Sep. 2016, doi: 10.1109/CYBER.2016.7574847.
- [10] M. R. L. Varshini and C. M. Vidhyapathi, “Dynamic fingure gesture recognition using KINECT,” *Proceedings of 2016 International Conference on Advanced Communication Control and Computing Technologies, ICACCCT 2016*, pp. 212–216, Jan. 2017, doi: 10.1109/ICACCCT.2016.7831632.
- [11] E. P. Ghonge and M. N. Kulkarni, “Gesture based control of IRB1520ID using Microsoft’s Kinect,” *Proceedings of the 2nd International Conference on Communication and Electronics Systems, ICCES 2017*, vol. 2018-January, pp. 355–358, Mar. 2018, doi: 10.1109/CESYS.2017.8321298.
- [12] Y. Wang, C. Yang, X. Wu, S. Xu, and H. Li, “Kinect based dynamic hand gesture recognition algorithm research,” *Proceedings of the 2012 4th International Conference on Intelligent Human-Machine Systems and Cybernetics, IHMSC 2012*, vol. 1, pp. 274–279, 2012, doi: 10.1109/IHMSC.2012.76.
- [13] C. W. F. Cueva, S. H. M. Torres, and M. J. Kern, “7 DOF industrial robot controlled by hand gestures using microsoft kinect v2,” *2017 IEEE 3rd Colombian Conference on Automatic Control, CCAC 2017 - Conference Proceedings*, vol. 2018-January, pp. 1–6, Jan. 2018, doi: 10.1109/CCAC.2017.8276455.
- [14] R. C. Hsu, P. C. Su, J. le Hsu, and C. Y. Wang, “Real-Time Interaction System of Human-Robot with Hand Gestures,” *2nd IEEE Eurasia Conference on IOT, Communication and Engineering 2020, ECICE 2020*, pp. 396–398, Oct. 2020, doi: 10.1109/ECICE50847.2020.9301957.

# Dynamic Arc Stabilization Options for Gas Metal Arc MIG/MAG Robot Welding

István Elek Kiss  
Alba Regia Technical Faculty  
Óbuda University  
Székesfehérvár, Hungary  
istvanelekkiss@gmail.com

Dr. Károly Széll  
Alba Regia Technical Faculty  
Óbuda University  
Székesfehérvár, Hungary  
szell.karoly@amk.uni-  
obuda.hu  
ORCID: 0000-0001-7499-5643

**Abstract** - As the number of welding experts and the cost of automation are reduced, the use of robotics is becoming increasingly important in this field. The purpose of this article is to introduce the automation of the production of a given component as a use case for university studies and experimental settings for further research. The part had previously been welded by hand, but the growing annual order number has necessitated robot welding. The article presents a new welding device that uses a robotic arm equipped with relevant sensors.

**Keywords**—MIG/MAG welding, robot welding, welding sensors, digital education

## I. INTRODUCTION

Nowadays, the number of skilled welders is declining. In order to perform quality work, the presence of welding robots is becoming more widespread, in both manufacturing and development areas. [1]

Improving production with a welding robot in most cases does not mean improving the equipment, but improving the production environment. For example, it is a common applicability advantage to repair a welded part device for proper quality production. [2] However, this solution is in most cases too expensive, time consuming and does not even provide adequate quality.

When using sensors for robotic welding [3](see Fig. 1.), it is advisable to use a non-contact welding seam tracking system. The intelligent laser sensor (SLS) must be mounted so that it faces the welding gun. The SLPr (Smart Laser Probe) (see Fig. 2.) is responsible for positioning the welding head and also for the welding wire to be in the correct connection. This intelligent laser probe, for most simple straight seams, offers significant benefits in terms of quality and productivity.



Fig. 1: Robot welding with sensor

The second section of the paper describes the basics of the problem of a welding robot like fixing the workpiece, the coordinate systems of the robot arm and welding.[4] The focus of the third section is the design of the welding jig mentioning those topics which might be important in education. The fourth section introduces a simulation environment for robot Smart Laser Probe which is a completely new and fairly effective approach to seam tracking. Leveraging the latest in electronics and digital technology, SLPr raises seam tracking to a better level of standard system performance.[5]



Fig. 2: Smart Laser Probe

## II. TYPICAL APPLICATION

Smart Laser Probe is the tracking system of choice for machine welding applications such as:

- Welding lathes for air, water and all types of cylindrical tanks
- Linear machines, such as side beam, travel carriage and seam welders
- Gantry welders, such as railway wagon side and roof welders
- Simple column and boom applications

Key Features of SLPr include:

- Very high-quality, high-resolution image generation by exploiting several novel and unique design features

- Fully digital system in incorporating a completely up-to-date control structure
- User friendly operator interface
- Wide range of standard sensors and interface options for different applications.[6]

If the sensor is used during welding, the programming time is significantly shortened, and the position of the seam can be determined more precisely. I would like to explain this by an example (see Fig. 3.). Welding must be performed on an arc marked in blue.[7]

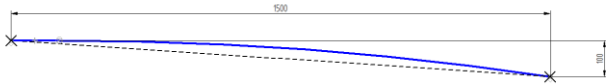


Fig. 3: Programming line by sensor

P1- the starting point of welding P2 is the end point of welding When programming, I record point P1 as the starting point where the robot will start welding. Point P2 is the end point where the welding is completed. If the sensor is switched off, the welding robot connects the two points in a straight line, so the robot would follow the dotted line. By switching on the sensor, the robot takes into account the “pattern” of the given welding radius, thus following the actual welding arc between the two points.

### III. PROBLEM DESCRIPTION

As shown in Figure 4., the sensor is attached to the welding gun. One of the biggest disadvantages of Smart Laser Probe is that there is approx. 80 mm constant distance. [8]

Based on these, the robot will not actually start welding at point P1 (figure 3.), but 80 mm forward. We program a specific welding dimensions and determine the tolerance range.

As there is an 80 mm difference between the detection line and the actual welding point, the deformation due to welding is not detected by the robot within this section. This phenomenon is a problem because even in this range, a few tenths of a mm of deformation occurs due to heat input from welding. After determining the position of the workpiece, the next step was to design the fixation.

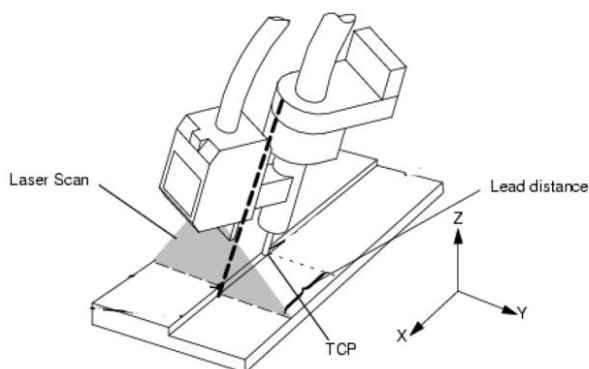


Fig. 4: Head with attached sensor

### IV. PROPOSAL

The proposed solution to the aforementioned error is to use an arc sensor. [9]

Through Arc Seam Tracking (TAST) allows the robot to follow the welding seam vertically, the distance between the gun and the workpiece, observing changes in the welding current.

The information provided by TAST allows the system to adjust the robot trajectory to remain the center of the weld in the joint. The path of the robot can be set to the weaving plane and the vertical plane (z direction of the tool). You can use vertical tracking with or without subsequent subtracking, with or without weaving (see Fig. 5.). [10]

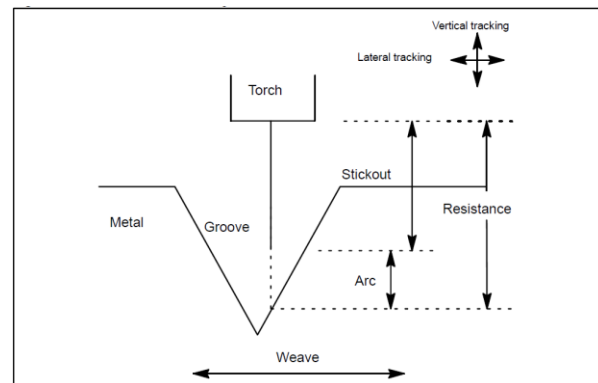


Fig. 5.: Sub tracking

The use of the six-point method for property racks are recommended to adjust the tool frame. When jogging in the tool, the z + coordinate should move along the gun nozzle and be away from work. The following requirements should be met for successful tracking:

- The material thickness should be greater than 2 mm.
- Grooves should have a consistent included angle of 90 degrees or less.
- Fillet joint scan have a maximum included angle of 90 degrees and must have at least 5 mm leg length.
- The minimum weave width must be three times the diameter of the electrode or greater.
- Tack weld, leg size, should be less than or equal than half the weld size, if possible, and concave in profile.
- The actual weld seam should deviate less than 15 degrees rotation from the taught weld seam.
- The torch must be positioned close to the center of the weld seam at the start of the weld (Touch Sensing might be necessary).
- Outside corner and lap joint fillets must use a weave width of 2 mm less than the base metal thickness.
- Fit up of the joint (gap) must be with in normal (blind) welding robot tolerances. Ideally, gaps should be consistent along the weld path
- Base metal must be ferrous or have a resistance greater than mild steel.
- TAST uses SINE type weaving only.



See Figure 6. for recommended weld joint configurations that can be used with TAST.

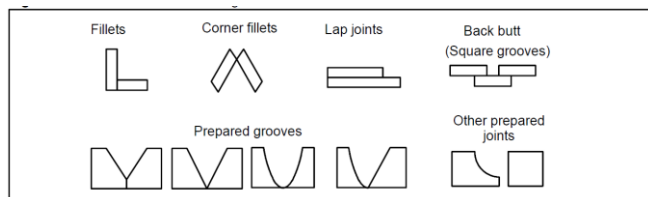


Fig. 6.: Recommended weld joint

When welding with sensors, the best solution is to use multiple sensors. In some cases, it is preferable to use an optical sensor. However, there are cases where the arc tracking sensor is the best solution. [11]

The general experience is that within a complex welded structure, and even on a given product, there are welded joints where the simultaneous use of several sensors is the most appropriate solution. [12]

Robot welding, developed with sensors, is an excellent solution for the production of more complex structures with the right quality.

At the same time, of course, the robot environment (figure 6.), such as the welding devices and jigs around the robot, must be improved. This is necessary because not everything can be solved by developing sensors alone. [13]

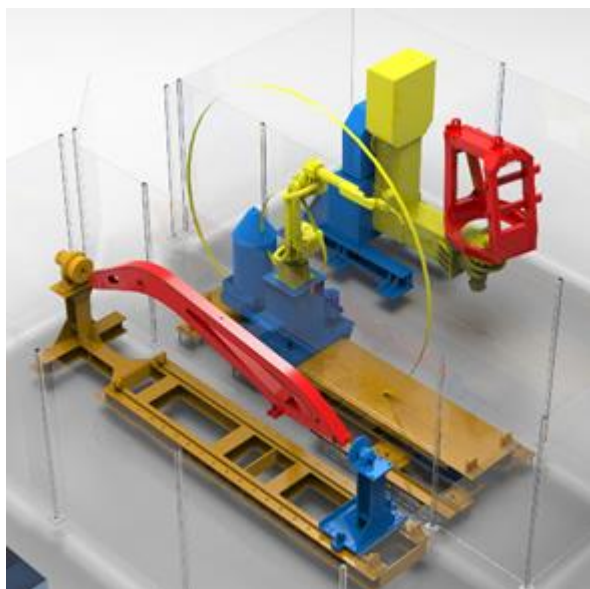


Fig. 7.: Robot environment with devices and jigs

One of the best solutions for deformation in the heat zone is still that the device for securing the welded structure is properly designed and manufactured. [14]

The device must take care that the part is not deformed during welding. After all, the right sensor follows the deformation, but this deformation may not meet the drawing specifications.

We can use very reliable, commercially available welding devices (see Figure 8.), but we can also use special,

individually designed welding jigs (see Figure 9. and 10.) for the right quality.



Fig. 8.: Commercially available welding device



Fig. 10.: Individually designed welding jig

## V. CONCLUSION

Robot welding is a major advance in the production of welded structures. [15] Robots need to be further developed in order to weld complex structures to the right quality. In the world today, it is a common fact that the development of robot welding is exhausted in the development of welding jigs. This in itself is not enough. Appropriate sensor programming is also required.[16] Of course, proper work safety must always be kept in mind during the design and manufacturing processes. [17]

The most important condition for this progress is that we learn to use robots in addition to sensors, as the result of this development may be that we can develop and manufacture more complex welded structures in the right quality.

## VI. ACKNOWLEDGEMENT

The authors thankfully acknowledge the financial support of this work by the Howmet Aerospace Foundation, the Arconic Foundation, and the project no. 2019-1.3.1-KK-2019-00007 implemented with the support provided from the National Research, Development and Innovation Fund of Hungary, financed under the 2019-1.3.1-KK funding scheme.

## REFERENCES

- [1] T. Lei, Y. Huang, H. Wang, and Y. Rong, "Automatic weld seam tracking of tube-to-tubesheet TIG welding robot with multiple sensors," *Journal of Manufacturing Processes*, vol. 63, 2021, doi: 10.1016/j.jmapro.2020.03.047.
- [2] M. Bejlegaard, T. D. Brunoe, and K. Nielsen, "A changeable jig-less welding cell for subassembly of construction machinery," in *IFIP Advances in Information and Communication Technology*, 2018, vol. 535. doi: 10.1007/978-3-319-99704-9\_37.
- [3] J. Fan, F. Jing, L. Yang, L. Teng, and M. Tan, "A Precise Initial Weld Point Guiding Method of Micro-Gap Weld Based on Structured Light Vision Sensor," *IEEE Sensors Journal*, vol. 19, no. 1, 2019, doi: 10.1109/JSEN.2018.2876144.
- [4] J. Wu, R. Zhang, and G. Yang, "Design and experiment verification of a new heavy friction-stir-weld robot for large-scale complex surface structures," *Industrial Robot*, vol. 42, no. 4, 2015, doi: 10.1108/IR-01-2015-0009.
- [5] S. K. Lee, W. S. Chang, W. S. Yoo, and S. J. Na, "A study on a vision sensor based laser welding system for bellows," *Journal of Manufacturing Systems*, vol. 19, no. 4, 2000, doi: 10.1016/S0278-6125(01)80004-2.
- [6] T. F. C. Berninger, T. Slimak, T. Weber, and D. J. Rixen, "An external stabilization unit for high-precision applications of robot manipulators," 2020. doi: 10.1109/IROS45743.2020.9341454.
- [7] S. F. Gao, X. H. Tang, P. Q. Xu, and S. Yao, "A seam tracing system based on an active optical vision sensor," *Cailiao Kexue yu Gongyi/Material Science and Technology*, vol. 14, no. SUPPL., 2006.
- [8] D. Li, H. Chen, Y. Sheng, and L. Yang, "Dual-station intelligent welding robot system based on CCD," *Measurement Science and Technology*, vol. 30, no. 4, 2019, doi: 10.1088/1361-6501/ab02d7.
- [9] Y. Zou and X. Chen, "Hand-eye calibration of arc welding robot and laser vision sensor through semidefinite programming," *Industrial Robot*, vol. 45, no. 5, 2018, doi: 10.1108/IR-02-2018-0034.
- [10] J. H. Du, J. X. Deng, K. J. Huang, J. S. Huang, and X. Lei, "Seam tracking system based on rotating arc sensor for robot arc welding," *Journal of Discrete Mathematical Sciences and Cryptography*, vol. 21, no. 6, 2018, doi: 10.1080/09720529.2018.1534354.
- [11] P. Kah, M. Shrestha, E. Hiltunen, and J. Martikainen, "Robotic arc welding sensors and programming in industrial applications," *International Journal of Mechanical and Materials Engineering*, vol. 10, no. 1. 2015. doi: 10.1186/s40712-015-0042-y.
- [12] A. Kafi and T. A. Kovács, "Arc Sensor Parameter Optimisation for Robot Welding," in *Lecture Notes in Mechanical Engineering*, 2021, vol. 22. doi: 10.1007/978-981-15-9529-5\_44.
- [13] L. Yang, E. Li, T. Long, J. Fan, and Z. Liang, "A Novel 3-D Path Extraction Method for Arc Welding Robot Based on Stereo Structured Light Sensor," *IEEE Sensors Journal*, vol. 19, no. 2, 2019, doi: 10.1109/JSEN.2018.2877976.
- [14] J. Le, H. Zhang, and X. Q. Chen, "Realization of rectangular fillet weld tracking based on rotating arc sensors and analysis of experimental results in gas metal arc welding," *Robotics and Computer-Integrated Manufacturing*, vol. 49, 2018, doi: 10.1016/j.rcim.2017.06.004.
- [15] Y. Xu *et al.*, "Welding seam tracking in robotic gas metal arc welding," *Journal of Materials Processing Technology*, vol. 248, 2017, doi: 10.1016/j.jmatprotec.2017.04.025.
- [16] J. Le, H. Zhang, X. Q. Chen, and G. Xiong, "Rectangular fillet weld tracking by robots based on rotating arc sensors in gas metal arc welding," *International Journal of Advanced Manufacturing Technology*, vol. 93, no. 5–8, 2017, doi: 10.1007/s00170-017-0633-2.
- [17] Judit Takács Módné: The importance and development of safety awareness with soft skills in industrial environment  
OPUS ET EDUCATIO: MUNKA ÉS NEVELÉS 8: 3 pp. 314-323., 10 p. (2021)

# Mobile Robot Environment for SLAM

Albin Nátrán  
Alba Regia Technical Faculty  
Óbuda University  
Székesfehérvár, Hungary  
[natran.albin@stud.uni-obuda.hu](mailto:natran.albin@stud.uni-obuda.hu)

Károly Széll  
Alba Regia Technical Faculty  
Óbuda University  
Székesfehérvár, Hungary  
[szell.karoly@amk.uniobuda.hu](mailto:szell.karoly@amk.uniobuda.hu)  
ORCID: 0000-0001-7499-5643

**Abstract**— The paper introduces a mobile robot system in a virtual environment. The mobile robot can travel autonomously and implement SLAM by using sensor data. The system is prepared for later hardware implementation for benchmarking different SLAM algorithms.

**Keywords**—mobile robot, SLAM, virtual

## I. INTRODUCTION

One of the main areas of research in recent decades has been the navigation of mobile robots. Its main criteria are good and precise localization. The most common localization technology is GNSS (Global Navigation Satellite System). This system ensures the absolute position of the Earth with excellent accuracy. However, the accuracy of a system is greatly influenced by environmental factors such as a cave, city, or tunnel. The resulting error can result in inaccuracies of up to meters, which is not acceptable for autonomous navigation of a mobile robot. Therefore, they need to represent their environment in some form. The starting point for this can be a 2D map. This map can consist of geometric features, but even more complex objects. With this consistent map, the mobile robot will be able to detect free spaces, obstacles and landmarks.

This type of localization approach is called simultaneous localization and mapping (SLAM). SLAM is the process by which a robot or robotic system uses sensors to create a map of its surroundings and at the same time estimate its position. From this information, the mobile robot can plan its own route without human intervention.

SLAM can be created with several complex algorithms that create different maps. However, there is no standard for comparing maps. Therefore, it would be worthwhile to develop a method that allows the comparison of different algorithms. [1]

## II. HARDWARE

The basis of the robot is an iRobot Roomba 605. Roomba is very good at creating a robust platform with useful accessories. The systems they provide may operate for years. It is outstandingly good in terms of parts support. The Roomba 605 is an omni robot. It has a very good weight distribution. Its wheels are driven by two separate motors and can be turned by a spherical wheel. It has a built-in IR and bumper sensors. Can be integrated into ROS. Numerous research and hobby developments have already been done with this model. There is also a model called Create which is designed specifically for robotic developments. [4]

Roomba alone is not able to meet the defined criteria. Therefore, a Lidar-based sensor must be added. In this project the RPLIDAR A1M8 had been chosen.

There is only one essential component left which is the controller The Raspberry Pi 3 B + is the most appropriate. It supports Ubuntu and ROS. It has built-in Wi-Fi which can be used as communication protocol (see Fig. 1.). [2]

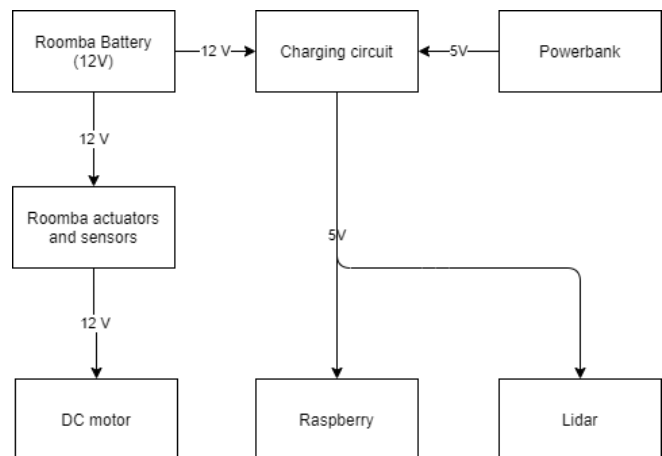


Fig. 1: Structure of the elements

## III. SIMULATION

Due to the high computational demands of the simulation, a personal computer was chosen as the basic hardware. ROS partially supports Debian, Gentoo, Mac OS X, Arch Linux, Android, Windows, and Open Embedded. However, ROS's primary operating system is Ubuntu. The three most popular distribution is the Indigo, Kinetic and Jade Turtle. [3]

ROS Indigo and Kinetic are currently widely supported distributions. Indigo is the most stable version; however, essential packages are missing from it. Jade Turtle is the latest version, but because of that it is least stable. The kinetic distribution of ROS offers a trade-off between the two versions. Therefore, the best choice is the Ubuntu 16.04 (LTS) with ROS Kinetic distribution. [3]

CoppeliaSim proves to be a remarkably better choice than its peers. It has an integrated development environment and fast algorithm development capabilities. [5]

The simplest way to describe this simulation environment is a three-tier model. The hardware is in the first layer. The second layer is the operating system that manages the hardware and the application layer which in the simulation runs. It is important to note that the simulation must be designed in such a way that it can be considered a real robot by another program. Therefore, no other layer or communication protocol is required in that case.

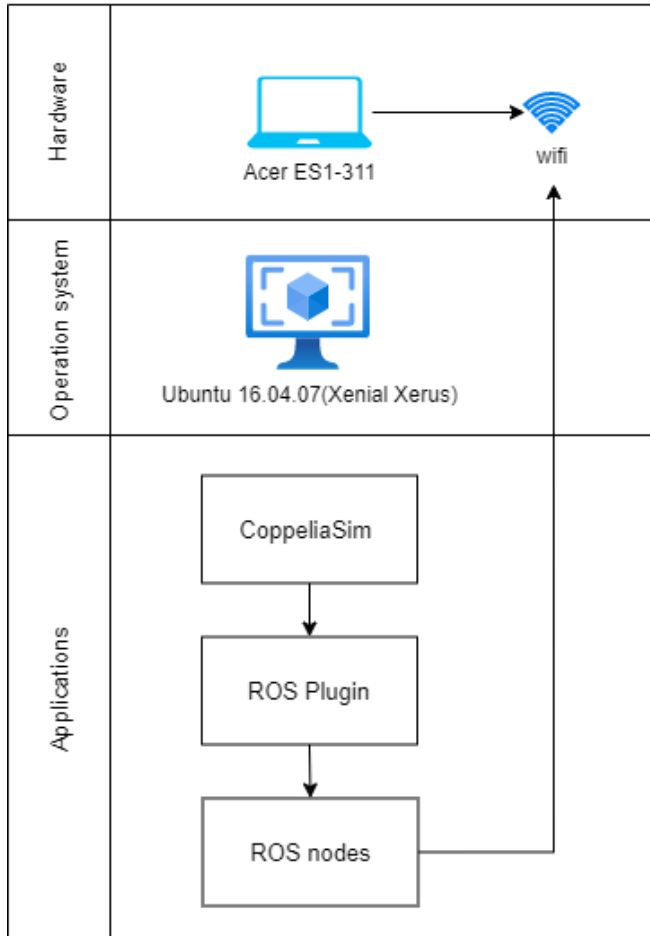


Fig. 2: Structure of the simulation

Following the example of the physical mobile robot, a virtual mobile robot was built. It's easy to create a new model, but it's important to keep in mind that the goal is to create a model that looks good, provides a well-optimized, and stable simulation.

The scene objects were divided into two groups. The first group includes the objects needed to build a mobile robot. The second group is environmental objects, which include walls, obstacles, and other objects.

In a new scene one opportunity is to model individual shapes from primitive shapes. In this case, shapes are well optimized and can be handled dynamically by the simulation program. However, these shapes do not reflect the shape of the robot. Therefore, the already completed 3D models were used. This makes it as accurate as possible externally. After importing, the scales are needed to be set and each shape named.

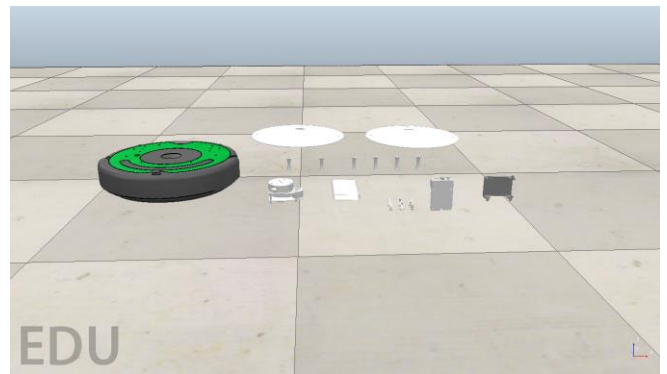


Fig. 3: Model elements

All the shapes required for the external appearance of the mobile robot are visible. To easily handle forms, grouping is required. There are three groups. The first is Roomba, the second is Platforms and the third is Lidar. After compilation and grouping of all the forms, the model is complete. However, it is not yet suitable for simulation. Pure shapes must be created from these shapes.

After creating the pure shapes, the model became very complex in structure. Each triangle in the simulation requires a calculation therefore the program becomes very slow. The model needs to be simplified. The number of triangles must be reduced. This can be done by using the Decimation function. There are also triangles inside the model, these are not necessary elements for simulation, which can be deleted by the Extract inside of selected shape function.

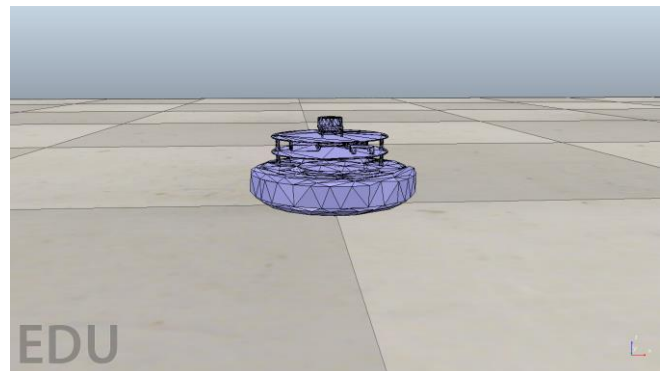


Fig. 4: Simplified model

The original model contained about 25,000 triangles. After simplifications, that number dropped to only 5,000. Further simplification is also possible using the Shape edit mode. However, the goal is not to oversimplify.

To get nearly the same point cloud when testing the virtual and real mobile robots, a test track is necessary. For the first tests a common apartment was chosen.

The test environment is a 56 square meter panel apartment, the layout of which can be seen in Figure 5. The CoppeliaSim model library contains almost all the elements needed to model the apartment.



Fig. 5: Environment

The scene consists of three main rooms. The first is the living room and dining room, followed by the hallway and finally the bedroom. For the mobile robot to be able to detect walls and obstacles, each object is defined as a dynamic element. When the simulation starts, the doors open automatically at a 90-degree angle.

Hierarchy design is an important element of simulation. It facilitates to make a logical connection between each element. The Roomba is located at the top followed by the platforms and finally the Lidar.

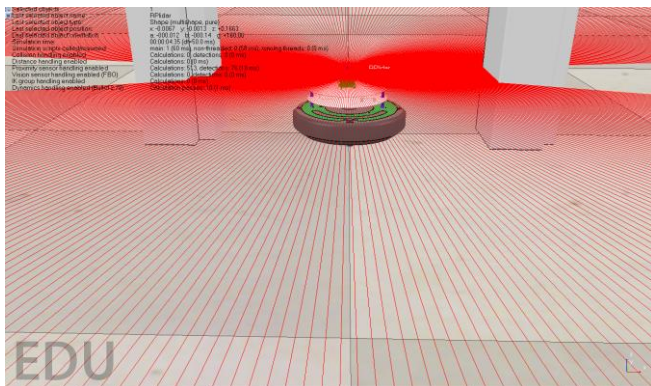


Fig. 6: Simulation

#### IV. CONTROL ALGORITHM

Once the real and virtual mobile robot is complete, the design of the control module followed. It was realized in Matlab environment. Control of the robot can also be solved on the personal computer, which is running the simulation, however, its resources were not sufficient to perform both tasks at the same time. Therefore, a dedicated PC was used as a ROS master. The PC is running Windows 10 operating system. Supported by Matlab.

The program code is divided into four parts. In the first part, the blocks responsible for ROS communication can be found. The second part is the collision avoidance block. The third part is the Navigation block and the last is the SLAM implementation blocks.

Avoiding obstacles is one of the key issues for mobile robot systems. It must include some kind of collision avoidance. It is necessary to implement an algorithm that detects the obstacle and stops the robot. It then avoided the obstacle and progressed towards his goal. Topics provide the necessary information to develop the algorithm.

A custom block was also implemented. It has a total of five input parameters. Two of these cannot be linked to ROS. The first is the maximum speed. Basically, between -1 and 1. Speed values can be specified. However, with this solution we can also reduce and increase this value. The other is the emergency stop, in case of unwanted operation of the robot we can stop immediately. The other inputs are the known Topics. At the output, the Topics are transmitted necessary for the robot to move and the motion ban, which indicates if there is an obstacle near the robot. The emergency stop can take two values. 0 does not require a stop, the robot is working properly. A value of 1 indicates when a stop is required. [6]

If there is no collision, control is passed to the navigation block. Basically, the logic uses permutation of input values to detect and avoid collisions. An example of this is if the right bumper sensor has sent a value of 1 but another sensor has zero then there is an obstacle on the right side of the robot. In this case, the robot shifts to reverse and begins to turn left. After a value of 0 is repeated for all sensors, it transmits control. [6]

If the mobile robot were equipped with an accurate location system, there would be no need for a navigation block. The robot would always know its position. However, this is not possible for the reasons mentioned.

There are several options for navigation. The most common method is to use localization points. In this case, the robot knows its surroundings and has an accurate map. To get from the starting point to the specified destination, a route planning algorithm is needed that calculates the optimal route.

Another method is to focus only on avoiding a collision. The robot is constantly moving forward, if it detects an obstacle, it will dodge and continue its journey. The biggest disadvantage of this is that the crawl time cannot be determined. It can easily turn out that the robot is unable to find a way out of a room and gets stuck. Therefore, this method can only be used effectively in open spaces.

It is important for the robot to be able to map even unknown environments. Thus, a navigation form was necessary that facilitates it. As a result, an algorithm was chosen that follows the walls.

The algorithm is based on odom Topic. Based on the Lidar data and orientation, the distance to the wall can be determined and the degree of orientation error can be determined from this. If the error rate is 0, the robot travels parallel to a wall. If this value is non-zero, a correction is required. The Lidar has  $0^\circ$  and  $360^\circ$  viewing angles that can be narrowed down dynamically to get the best results. After determining the orientation error, it must be defined which wall the robot will follow. The easiest way is to find the nearest wall. [6]

Complementing the two indices with the necessary orientation. The difference between the measured and the required orientation gives the amount of error that has not yet been evaluated. The two sub-systems contain the necessary data structural changes. Based on the obtained data, a Matlab function block calculates the required speed and direction.[6]

Matlab is a great help in creating SLAM. There is an official Matlab example program that can implement SLAM from Lidar point cloud data. However, to do this, the full point cloud data structure must first be established.

There are two possible solutions to this problem. First, the Matlab example program can be used with different SLAM algorithms on a pre-saved point cloud. In this case, the map can only be compiled after the robot has gone through the entire test track. It also follows that its usability can only be evaluated after that. Since the robot uses a ROS framework, the other option is to use standalone ROS Nodes. This solution is more efficient as different algorithms can be applied simultaneously.

#### V. CONCLUSION

The paper introduced a simulation environment that is based on an iRobot Roomba hardware platform. The system is based on ROS framework, CoppeliaSim simulation environment and Matlab. The implemented environment is prepared for the hardware implementation with the purpose of testing relevant SLAM algorithms.

#### ACKNOWLEDGMENT

The authors thankfully acknowledge the financial support of this work by the Howmet Aerospace Foundation, the Aronic Foundation, and the project no. 2019-1.3.1-KK-2019-00007 implemented with the support provided from the National Research, Development and Innovation Fund of Hungary, financed under the 2019-1.3.1-KK funding scheme.

#### REFERENCES

- [1] L. Joseph és J. Cacace, Mastering ROS for Robotics Programming - Second Edition, 2018.
- [2] „What is Raspberry Pi?,” [Online]. Available: <https://www.raspberrypi.org/help/what-%20is-a-raspberry-pi/> (accessed on 25.10.2021)
- [3] G. Staples, „ROS Distributions,” 11 06 2020. [Online]. Available: <http://wiki.ros.org/Distributions> (accessed on 25.10.2021)
- [4] „iRobot Roomba 605,” 2021. [Online]. Available: <https://www.irobotthailand.com/en/shop/irobot-roomba-605/> (accessed on 25.10.2021)
- [5] „Coppeliaslim User Manual,” Coppeliaslim, 2021. [Online]. Available: <https://www.coppeliarobotics.com/helpFiles/> (accessed on 25.10.2021)
- [6] „Robotic System Toolbox,” 2021. [Online]. Available: <https://www.mathworks.com/products/robotics.html> (accessed on 25.10.2021)

# Automation of EDM Machines

Márk Liszi  
Alba Regia Technical Faculty  
Óbuda University  
Székesfehérvár, Hungary  
[liszi.mark@stud.uni-obuda.hu](mailto:liszi.mark@stud.uni-obuda.hu)

Károly Széll  
Alba Regia Technical Faculty  
Óbuda University  
Székesfehérvár, Hungary  
[szell.karoly@amk.uni-obuda.hu](mailto:szell.karoly@amk.uni-obuda.hu)  
ORCID: 0000-0001-7499-5643

**Abstract**— The automation of metal working machines is usually done for cycle time reduction and for the increase of capacity and precision. This project was started mainly to reduce the downtime between the installation of parts onto the machine. Also, the working conditions next to an electric discharge machine can be harmful to the human body in a long-term period. Collaboration of human and industrial robot will be used to create a semi-autonomous production cell of four electric discharge machining (EDM) machines.

**Keywords**—robotics, manufacturing, automation, industry 4.0, electric discharge machines, industrial robot, robot cell

## I. INTRODUCTION

With the use of electric discharge machining (EDM)[1], [2] we must agree with the fact, that the material remove rate is far not as fast as we are used to with CNC machines. Consequently, companies trying to fit as many workpieces into the machines as possible and they are making a mistake there. It is self-evident that they are trying to maximize their productivity but with the oversized fixtures they make the pallet and workpiece change longer. Especially if they cannot run another pallet because the short of space.

With the creation of an autonomous robot cell, we will try to reduce our downtimes caused by the change of the workpiece and the fixture. Dual education gives us the opportunity to use the resources of the university and also the industrial environment [11]. Thus, our solution can be implemented in simulation and in real-world as well. This paper focuses on the simulation environment.

## II. MACHINED PARTS

The workpieces are made of nickel-based superalloys. The electrodes what we are using for material removal are made of graphite. During the machining process relatively huge amount of metal is removed. Also, a thin layer of graphite is burned down from the electrode in each discharging process. The volume of the waste material creation under a full machining session creates about a bucket (5 liters) of sludge.

These workpieces can be found more than twenty different shapes within the area of the factory. For our project we will care about the three most identical. The smallest, the largest and the heaviest composition (see Fig. 1.).

TABLE I. MAIN PARAMETER OF WORKPARTS

Workpieces' parameters			
Part name	Overall dimension	Weight/piece	Pieces / fixture <sup>a</sup>
Part1	156x79x30 mm	1,1 kg	24
Part2	170x367x244 mm	40 kg	2
Part3	488x610x235 mm	53 kg	1

<sup>a</sup>. According to the current fixtures.

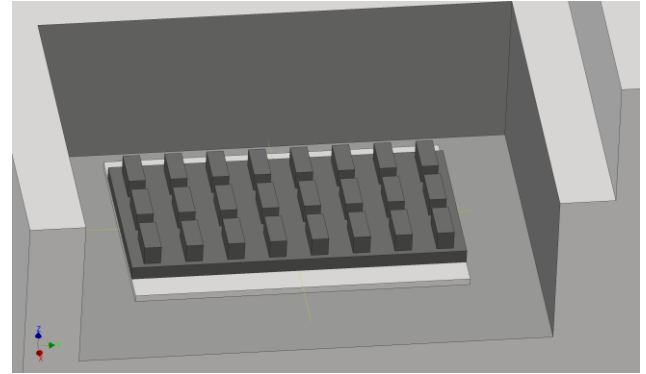


Fig. 1. The model of the largest fixture installed onto the EDM machine

According to the previously mentioned sludge accumulation the use of a conventional zero-point system is impossible. Previous experiences show that most type of commercially available zero-point sets are not sealed enough to handle this amount of waste material. While they are properly separate the dielectric liquid and all solid particles in it if the two segments are attached. As soon as the spigot is moved out of the clamp, sludge and dust can enter the clamping system (see Fig. 2.). Furthermore, the manual cleaning process were not precise enough and small amount of solid particle could get inside the clamping unit from the spigots.

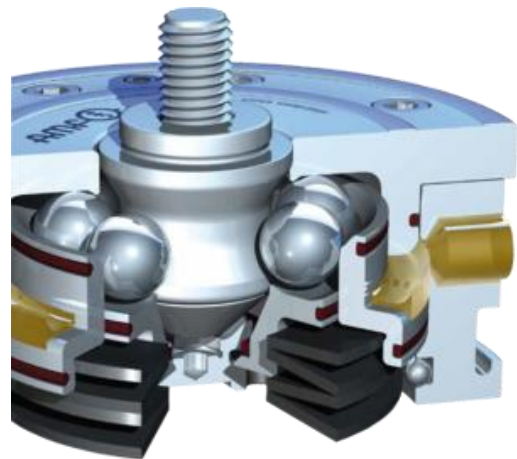


Fig. 2. Cross section of an conventional spigot-clamp assembly [9]

## III. DOWNTIMES

Currently the change of parts in the fixture happens while the fixture is installed onto the EDM machine. After the finished parts has been taken out from the fixture, the operators have to clean up its place for the next unmachined part.

In case of installing another fixture to the machine the operators first must have the zero point of the pallet.

The following table shows the downtimes caused by the three most inefficient fixture/part change.

TABLE II. MOST UNEFFICIENT PART CHANGES

Downtimes			
Part name	Part1	Part2	Part4
Number of machined parts	24	6	8
Part change/setup time	1:00:00	0:30:00	0:40:00
Electrode change/setup time	0:15:00	0:10:00	0:05:00
Overall setup time	1:15:00	0:40:00	0:45:00
Machine work time	2:40:00	3:00:00	2:00:00
Cycle time	3:55:00	3:40:00	2:45:00
Downtime percentage	31,90%	18,20%	27,30%

b. All time values should be read as hh:mm:ss.

It is visible that the downtime rate is about an average of 26% in these cases.

IV. ELEMENTS OF THE ROBOTIC CELL

First of all, to eliminate as much downtime as possible, we would like to use custom, self-made pallets. The currently used fixtures would be implemented into the new pallets. A relatively small size pallet would accommodate 6 to 8 pieces from the smallest parts and only one from the largest (see Fig. 3. and 4.).

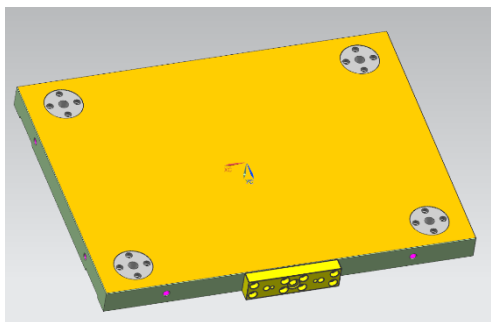


Fig. 3. Bottom side of the custom pallet

TABLE III. MAIN PARAMETERS OF PALLET

Custom pallet	
Material	EN AW-5083 / AlMg4,5Mn0,7
Dimensions	600x450x40 mm
Weight	31 kg

These pallets should be installed with self-centering cones for easier zero-point measurement. The simple fitting geometry provides easier cleaning too. Since the pallets should be made of aluminum to be lightweight, clamping inserts should be used where the pallets will be fixed by the hydraulic clamp.

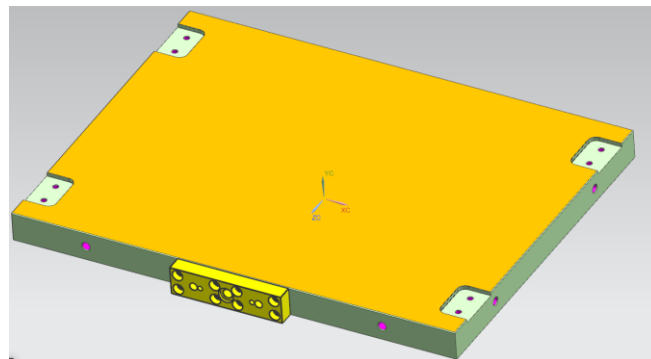


Fig. 4. Top side of the custom pallet

For the pallet handling we would like to use EROWA's RCS5 GripperLink system which is a pneumatic operated coupling with optional electric feedback (see Fig. 5.). The allowed payload for this gripper is 250 kg (F2) and can handle up to 610 Nm of torque in the center of clamping (M1). [10]

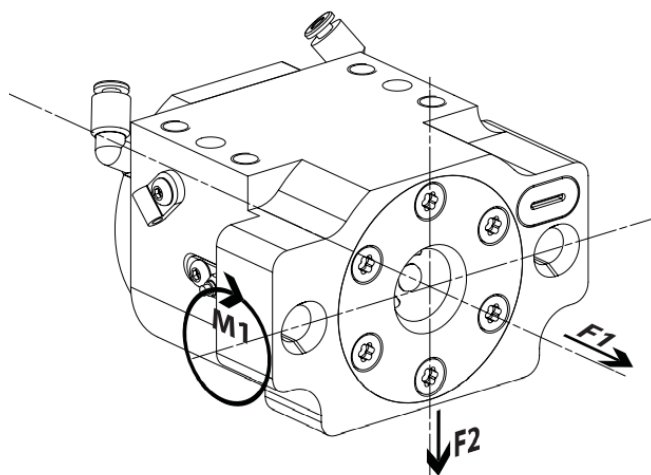


Fig. 5. Allowable maximum payload of robot side RCS5 Gripperlink

For smaller electrodes we would like to use EROWA Gripper S what can be directly attached to the RCS5 robot side GripperLink. This is a very simple two finger, form and force fitting gripper.

Both the pallets and the electrodes should be identified with RFID chips. [3]–[5]

V. LAYOUT CONCEPTS

At the first step of the layout design, we had to consider the environment and all its obstacles. The most important aspect was the crane. It limited our free space because all the four EDM machines should be able to be planted with the crane in case of manual operations (see dashed red line in Fig. 6.).

Furthermore, we had to give enough space for the transfer operations, such as workshop carriages and forklifts. Also we had to leave enough space around the machines for maintenance and cleaning purpose.



A. Layout A

According to the first concept the machines would be placed around the robot (see Fig. 6.). This way the neighbor machines shouldn't be moved. Implementing this plan, we would need the shortest rail. Otherwise, to keep at least one machine manually operatable the robot should be able to bend over the wall of the EDM machine. This also means that in this case the pallet should be attached to the robot along its short side. However, the allowable payload would let us to move pallets this way the additional stress wouldn't be favorable. Thus, the pallet storage systems size would be very limited, and hard to access in case of a manually operated machine.

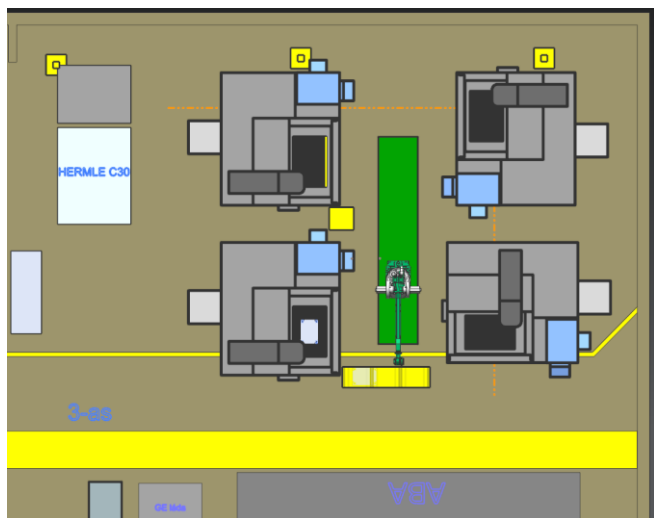


Fig. 6. The first concept of the cell

B. Layout B

In this case the machines are placed very similarly but rotated 90 degrees clockwise (see Fig. 7.). Also, a passageway should be created on the wall, between the 3rd and 4th facility. At the other end of the rail a square shaped storage system should be created. The bottom left machine would be the one that is ready for manual operations, but it still requires to pick the pallets along its longer side and to place it to the machine table over its side.

Although, this plan would ensure all the slots for the pallets that we required, the length of the linear rail would be unbearably long.



Fig. 7. Second conception of the cell

C. Layout C

The third layout was the most preferred (see Fig. 8.). In this case the EDM machines are horizontally planted next to each other. In front of them the linear rail takes place the

overall length of which is 12 meters. Behind the rail the pallet and electrode storing system would be placed. With this concept, an about 1 meter wide “corridor” could be left behind the machines, where the operators can empty the slung cartridge. Also, the sequential separation of the machine is available for manual operation. Not to mention, the cell won't be inside the working area.

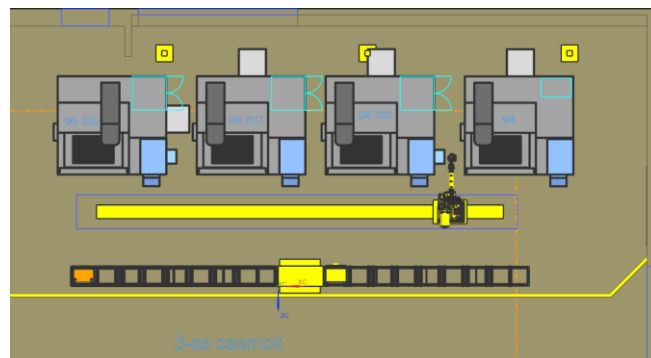


Fig. 8. The most favored layout

The pallet storage system is currently designed as a welded frame which is 6 meters long, 3,5 meters high and 600mm wide (see Fig. 9.). With these dimensions the system could accommodate about 80 pallets equipped with the tallest workpieces on it.

The feed of the storage system would be executed by the robot. The operators should plant the filled and checked pallet to a dedicated slot, next to the system. From this place the robot takes it and places it onto one of the previously defined shelves.

Also, the same method should be applied to the electrodes.

Outside the cell a workplace should be created where the operators can previously install the workpieces into the pallet.

After that a Coordinate Measuring Machine (CMM) should be used to ensure the correct installation of the parts and to obtain main information of the filled pallet. Such as zero points. [6]

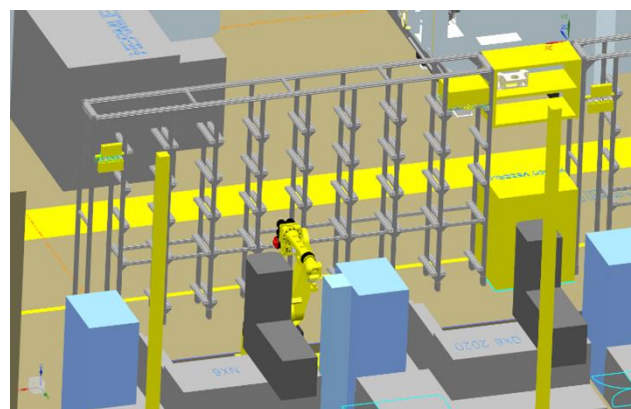


Fig. 9. The pallet storage shelves

VI. ROBOTIC CELL

With the help of Fanuc Hungary, we found that the Fanuc R-2000iC/165F could be an optimal choice for our application. [7]

This is one of the most commonly used type of industrial Fanuc robot due to its great price/performance ratio. Featuring its following properties:

TABLE IV. MAIN PARAMETERS OF ROBOT

R-2000iC/165F	
Controlled axes	6
Repeatability <sup>c</sup>	±0,05 mm
Payload	165 kg
Maximum reach	2655 mm

<sup>c</sup> Based on ISO9283.

Both its impressive payload and reach makes it available for the palletizing functions, while the 6 joint makes the electrode change easier.

For the linear rail system, a Hungarian company could be in our help. They are specialized for making welding jigs and mounting appliances for automation and robot systems. The 12 meters long rail could be built up from 6 pieces two-meter-long segments. This way the rail can be extended, so the cell can easily be adapted for the future needs.[8]

The production cell should obey all occupational safety rules. Not only simulated walls and restricted areas should control the robot's work area, but from every side the cell should be enclosed with safety fence.

Moreover, additional safety systems, such as area scanners and monitoring switches would be advised to use where human interference could happen.

For the synchronized work of each element in the cell we are planning to use Siemens S7 PLC with a 10-inch HMI. The network communication of the production cell should be maintained with PROFINET connection.

In the era of industry 4.0 in case such a valuable system the implementation of predictive maintenance is also recommended [12].

## VII. RETURN ON INVESTEMENT

The overall projects capital requirement is 350.000 EUR what according to our calculations, in case of all 4 machines working 24 hours a day and 7 days a week with an hourly rate of 34 EUR per machine, and an average 30% of downtime, it would take about 1,5 years to return. Calculated with an 80% of exploitation because of the summer downtime, holidays, maintenance and other unforeseeable downtimes.

## VIII. CONCLUSION

The paper introduces the automation of four EDM machines. The main requirements as decrease of downtime, cost effective solution, ergonomic workplace are fulfilled and discussed through several layouts. The return on investment of the proposed solution would is 1,5 years.

## ACKNOWLEDGMENT

The authors thankfully acknowledge the financial support of this work by the Howmet Aerospace Foundation, the Arconic Foundation, and the project no. 2019-1.3.1-KK-2019-00007 implemented with the support provided from the National Research, Development and Innovation Fund

of Hungary, financed under the 2019-1.3.1-KK funding scheme. The authors would like to express their gratitude to those who have provided their help in the various experiments. The research has been supported by Alba Creo Kft. and H.T.M. Tool Manufacturing Company.

## REFERENCES

- [1] Y. Li, W. Hou, J. Xu, and H. Yu, "An investigation on drilling micro holes in different processes using micro-EDM," *2016 IEEE International Conference on Mechatronics and Automation, IEEE ICMA 2016*, pp. 1283–1288, Sep. 2016, doi: 10.1109/ICMA.2016.7558747.
- [2] Y. Li, W. Yu, J. Xu, and H. Yu, "A comparative investigation of micro-EDM drilling capability for Ti-6Al-4V alloy against austenitic stainless steel SUS 316," *2016 IEEE International Conference on Mechatronics and Automation, IEEE ICMA 2016*, pp. 1612–1616, Sep. 2016, doi: 10.1109/ICMA.2016.7558805.
- [3] B. Du *et al.*, "Intelligent verification system based on rfid smart electricity meter," *Proceedings - 8th International Conference on Instrumentation and Measurement, Computer, Communication and Control, IMCCC 2018*, pp. 1542–1547, Jul. 2018, doi: 10.1109/IMCCC.2018.00318.
- [4] S. Jeon, M. Choi, G. Kim, and B. Hong, "Localization of pallets based on passive RFID tags," *ITNG2010 - 7th International Conference on Information Technology: New Generations*, pp. 834–839, 2010, doi: 10.1109/ITNG.2010.193.
- [5] H. Borstell, J. Kluth, M. Jaeschke, C. Plate, B. Gebert, and K. Richter, "Pallet monitoring system based on a heterogeneous sensor network for transparent warehouse processes," *2014 Workshop on Sensor Data Fusion: Trends, Solutions, Applications, SDF 2014*, Nov. 2014, doi: 10.1109/SDF.2014.6954718.
- [6] C. Prasse, J. Stenzel, B. Rudak, F. Weichert, H. Muller, and M. ten Hompel, "Low cost contour check of loading units using PMD sensors," *Proceedings of the International Conference on Sensing Technology, ICST*, pp. 477–482, 2013, doi: 10.1109/ICSENST.2013.6727699.
- [7] J. Tian, J. Zhao, H. Zhao, Z. Li, and Z. Hu, "Research and development of palletizing robot structure and control system," *2019 IEEE International Conference on Real-Time Computing and Robotics, RCAR 2019*, vol. 2019-August, pp. 316–321, Aug. 2019, doi: 10.1109/RCAR47638.2019.9043989.
- [8] N. Shen, Y. Wu, J. Li, N. Lu, and J. Yao, "Path planning based on the analytical inverse kinematics of the rail-mounted industrial robot for continuous-trajectory tracking," *Proceedings - 2020 12th International Conference on Intelligent Human-Machine Systems and Cybernetics, IHMSC 2020*, vol. 1, pp. 273–276, Aug. 2020, doi: 10.1109/IHMSC49165.2020.00068.
- [9] Zero point system cross section. Available online: <http://www.kirschnerhidraulika.hu/zero/> (accessed on 25.10.2021)
- [10] EROWA RCS5 Gripperlink. Available online: <https://www.erowa.com/en/products/gripper-rcs-5-erowa-lift/pd/046162/?c0=26240?favourites=add> (accessed on 25.10.2021)
- [11] Pogátsnik Monika: Dual education: Connecting education and the labor market. *Opus et Educatio* Volume 8. Number 3..pp. 304-313, <http://dx.doi.org/10.3311/ope.466>
- [12] Manhertz G., Gardonyi G., Por G.: Managing measured vibration data for malfunction detection of an assembled mechanical coupling, *INTERNATIONAL JOURNAL OF ADVANCED MANUFACTURING TECHNOLOGY* 75 : 5-8 pp. 693-703. , 11 p. (2014)

# Monitoring Of The State Of A Person At Hazardous Work

Olga Shvets  
IT and intelligent system  
sub-department  
East-Kazakhstan

Technical University  
Ust-Kamenogorsk, Kazakhstan  
olga.shvets75@gmail.kz

Bauyrzhan Smakanov  
IT and intelligent system  
sub-department  
East-Kazakhstan

Technical University  
Ust-Kamenogorsk, Kazakhstan  
bauka.10.10@mail.ru

Zhanerke Bakatbayeva  
IT and intelligent system  
sub-department  
East-Kazakhstan

Technical University  
Ust-Kamenogorsk, Kazakhstan  
zhanerke.25@mail.ru

**Abstract**—The relevance of increasing the level of safety of the population at work is obvious today. A special place is occupied by work associated with increased danger in the case of monotonous, routine work, when a person ceases to adequately control the situation due to fatigue or distraction of attention, for example, when guarding objects in front of monitors of security cameras, when the driver of a vehicle is driving for a long time, etc. The use of modern digital technologies in this area is a promising area of research. The results of the work are aimed at improving the safety of people engaged in monotonous activities in real time using neural networks. Application area is operational monitoring of the state of a person at hazardous work, for example security of objects or driver of a vehicle. In this study, the design of an intelligent system for monitoring a person's condition during hazardous work (awake or asleep) is considered.

**Keywords**—neural networks, emotions recognition, software development

## I. INTRODUCTION

Currently, there is a rapid growth in the use of video surveillance systems, which is explained by a wide range of tasks solved by such systems and the constantly increasing availability of surveillance and communication facilities. Video surveillance systems are used in a wide variety of areas: monitoring of road transport systems, security and law enforcement, unmanned aircraft, control of production processes, as well as in many other areas. A person, his life and health are the highest value. The analysis of industrial accidents, injuries, accidents, as well as occupational diseases shows that the main reason for them is non-compliance with safety requirements, human ignorance of man-made hazards and methods of protection against them. The use of video surveillance systems allows you to analyse the behaviour of the observed objects, increase the efficiency of their control, the reliability and quality of the results obtained, and provide support in decision-making. With the development of computer methods for processing visual information, intelligent video surveillance systems capable of automatically analysing incoming information are becoming more and more attractive. Computerization of the process allows dramatically increasing the scale of monitoring and reducing the use of human resources, while increasing the reliability and impartiality of observation.

## II. IMAGE PROCESSING FOR RECOGNIZING HUMAN EMOTIONS

There are two approaches to the recognition of human emotions based on the use of neural networks. The classical approach to the problem of classification of emotions is based on the classification of key points of the human face.

The location of key points fixes hard and non-rigid deformations of the face due to head movements and facial expressions. Algorithms such as PDM, CML, AAM, DPM, or CNN can be used to obtain key points of a human face [3, 6]. The next stage of recognition in the classical approach is the classification of key points. Support vector machines are well suited for the classification of key points. At the moment, the problem of finding key points is quite well studied and there are a large number of algorithms that allow you to obtain key points with accuracy sufficient for further classification by these points of human emotions. But, to use the classic approach, it is necessary that the position of the face in the image be aligned. An alternative to using the classical approach is the approach based on convolutional neural networks. A convolutional neural network is architecture of artificial neural networks aimed at efficient pattern recognition, aimed at the operation of calculating a new value of a selected pixel, taking into account the values of the surrounding pixels. Convolutional networks are a good basic solution for classifying various visual data, which was used in this work.

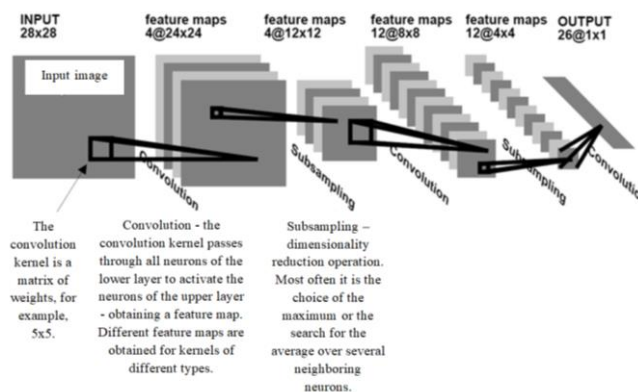


Fig. 1. Network architecture, Yann LeCun [6]

The convolution kernel, which is a square  $n * n$  matrix, is used to calculate the value. When processing images, matrices of RGB-channels of pixels in rectangular coordinates are used as initial ones. Image filtering is one of the most fundamental operations of computer vision, pattern recognition, and image processing.

The convolutional neural network (CNN, LeNet) was introduced in 1998 by French researcher Yann LeCun as an extension of the neocognitron model [6] (see Figure 1).

The convolutional network model used consists of three types of layers:

- convolutional layers,

- subsampling layers and
- layers of a "normal" neural network - perceptron (see Figure 2).

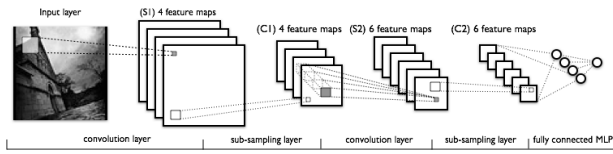


Fig. 2. Example of a Diagram of a convolutional network [6]

The first two types of layers form the input feature vector for the multilayer perceptron. The network can be trained using gradient methods.

The convolution operation can be described by the following formula [1, 4, 6].

$$(f * g)[m, n] = \sum_{k, l} f[m - k, n - l] \cdot g[k, l] \quad (1)$$

Here  $f$  is the original image matrix;  $g$  is the kernel (matrix) of the convolution.

Depending on the method of processing the edges of the original matrix, the result may be smaller than the original image, the same size or larger.

The convolutional layer implements the idea of local receptive fields, i.e. each output neuron is connected only to a certain (small) region of the input matrix and thus simulates some of the features of human vision.

In a simplified form, this layer can be described by the following formula.

$$x^l = f(x^{l-1} * k^l + b^l) \quad (2)$$

Here  $x$  is the output of layer  $l$ ,  $f()$  is the activation function,  $b$  is the shift coefficient, and the symbol  $*$  denotes the operation of convolution of the input  $x$  with the kernel  $k$ .

At the same time, due to edge effects, the size of the original matrices is reduced.

$$x_j^l = f\left(\sum_i x_i^{l-1} * k_j^l + b_j^l\right) \quad (3)$$

Here  $x_j^l$  is the feature map  $j$  (output of layer  $l$ ),  $f()$  is the activation function,  $b_j$  is the shift coefficient for the feature map  $j$ ,  $k_j$  is the kernel of convolution number  $j$ ,  $x_i^{l-1}$  is the feature map of the previous layer.

Using a subsampling layer can improve the recognition of zoomed samples (reduced or enlarged). Layers of this type reduce the size of the input feature map (usually by a factor of 2). This can be done in different ways, in this program the method of selecting the maximum element (max-pooling) was used - the entire feature map is divided into cells of 2x2 elements, from which the maximum by value are selected. Formally, the layer can be described as follows.

$$x^l = f(a^l \cdot \text{subsample}(x^{l-1}) + b^l) \quad (4)$$

Here  $x$  is the output of the layer  $l()$  is the activation function,  $a$ ,  $b$  are the coefficients,  $\text{subsample}()$  is the operation of sampling local maximum values.

The last of the types of layers is the layer of a "regular" multilayer perceptron (MLP), it can be described by the following relationship.

$$x_j^l = f\left(\sum_i x_i^{l-1} \cdot w_{ij}^{l-1} + b_j^{l-1}\right) \quad (5)$$

Here  $x^l$  is the output of layer  $l$ ,  $f()$  is the activation function,  $b$  is the shift coefficient,  $w$  is the matrix of weight coefficients.

Consider the topology of a 7-layer convolutional network, the order of which is described below.

- input layer - image matrix;
- convolutional layer - a set of matrices of the same type (feature maps);
- subsampling layer – the previous set of matrices reduced by 2 times;
- convolutional layer – the previous set of matrices is combined into one in accordance with the scheme for connecting layers, then a new set is generated;
- subsampling layer – the previous set of matrices reduced by 2 times;
- MLP layer – the previous set of matrices is expanded into a vector and processed as MLP;
- MLP layer (output).

In this case, neurons (feature maps) of the second subsampling layer and the third convolutional layer are selectively connected, i.e. according to the adjacency matrix, which is specified as a network parameter. For a network with the number of feature maps in the second layer 7 and 9 in the third layer, it may look like this (see Table 1).

TABLE I. AN EXAMPLE OF AN ADJACENCY MATRIX OF CONVOLUTIONAL LAYERS CONNECTIONS

N	1	2	3	4	5	6	7	8	9
1	1	0	0	0	0	1	1	1	0
2	1	1	0	0	0	0	1	1	1
3	1	1	1	0	0	0	0	1	1
4	0	1	1	1	0	0	0	1	1
5	0	0	1	1	1		0	0	1
6	0	0	0	1	1	1	0	0	0
7	0	0	0	0	1	1	1	0	0

Thus, each output map is formed by a partial sum of the results of the convolutions of the input maps, for each such partial sum its own set of convolution kernels.

In order to ensure the full flow of mental processes, a person must be in a state of wakefulness. Only in conditions of optimal wakefulness can a person [3, 5]:

- the best way to receive and process information;
- recall the necessary electoral communication systems;
- program activities;
- exercise control over activities;
- correct errors;
- maintain the chosen direction of activity.

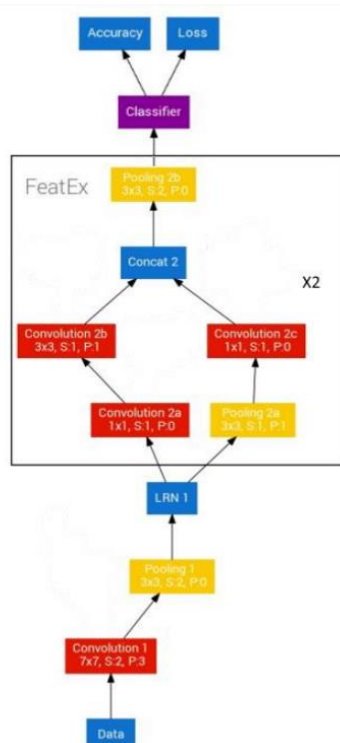


Fig. 3. Architecture of the model

There are the following levels of wakefulness: extreme level of tension, active wakefulness, and calm wakefulness.

The movements of the driver's head, describing its position at any moment in time, can be obtained using a static 2D image from the camera. In order to determine the position of the driver's head, which is not strictly parallel, but at a certain angle to the plane of the smartphone camera, Euler angles are calculated that describe the rotation of an object in three-dimensional Euclidean space. Angles of turning the head to the left or to the right, as well as tilting forward or backward, can be applied when a distraction of the driver's attention is detected, or a situation where the driver is "nodding", that is, it becomes difficult for him to keep his head in the normal position, respectively. When detecting the state of weakened attention of the driver, the determination of the position of his head relative to the body is used. In the first case, a situation is considered in which the driver's head should be directed directly in the direction of movement of the vehicle. The driver has identified signs of a weakened attention if his head is not looking at direction of vehicle movement for more than 1.5 seconds.

### III. SOFTWARE

Let's start processing images (photographs) to identify a state other than wakefulness (sleep or falling asleep).

In the "Path to the folder with the source still frames of the video stream" field, specify the path to the folder with the source images. Then it is required to indicate a description of the person's states according to the figure, for example, a person is awake or a person is asleep (see Figure 4).

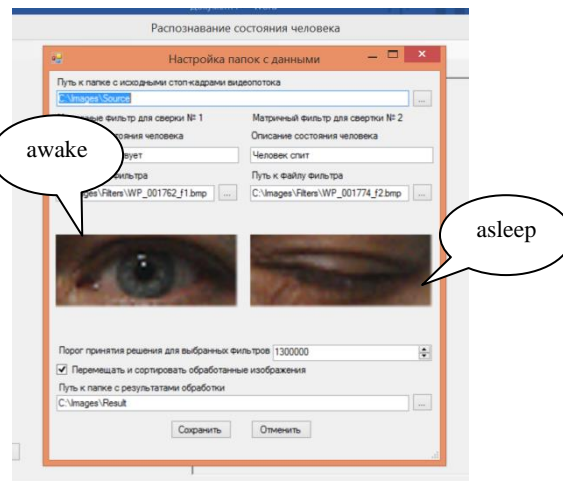


Fig. 4. Program settings window

Select filters from the Images \ Filters folder according to the picture. To do this, press the button "Start recognition" (see Figures 5, 6).

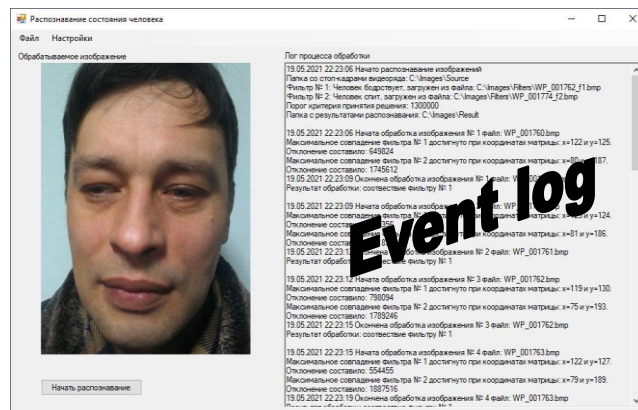


Fig. 5. Checking for compliance of the image with filter 1

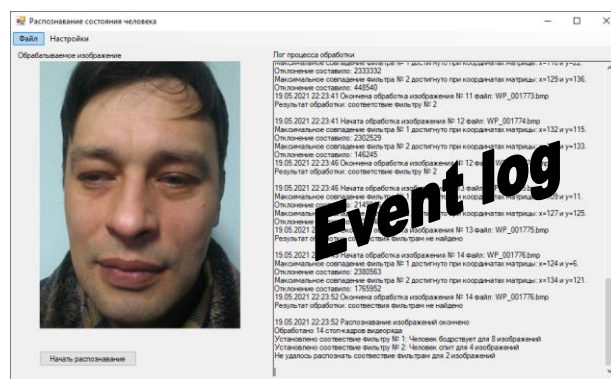


Fig. 6. Checking for compliance of the image with filter 2

During the recognition process, the current recognized image is displayed in the left part of the window. In the right part of the window there is a log of the recognition process. The log displays information about the number of still frames of the video sequence, matches filter 1 (a person is awake) or filter 2 (a person is sleeping / falling asleep). If the freeze frame is not recognized as one of the filters, the message is displayed: "Failed to recognize the matching filters for <number> images."

14 test images are shown as an example: 8 with open eyes (matching filter 1), 4 with closed eyes (matching filter

2) and 2 with narrowed eyes (not matching filters) (see Figure 7).

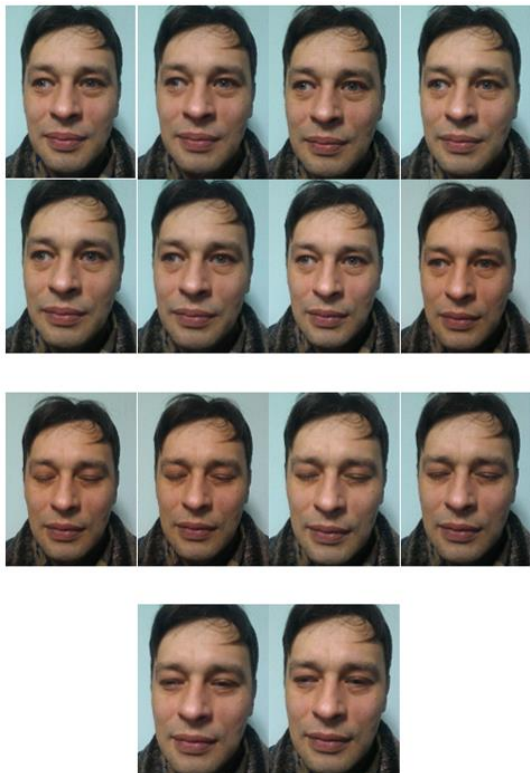


Fig. 7. Test images (photos)

The recognition accuracy of the test set of images is 100%. The program is customized for a specific person, which is also an additional advantage and a guarantee of the accuracy of state recognition. When changing an employee (driver, security guard), we can change the set of images, or add to the database.

#### IV. CONCLUSION

The monitoring of dangerous driver behaviour is based on the processing and analysis of driver images read from the smartphone camera in the vehicle cabin. It includes the detection of facial characteristics describing the condition and position of the eyes and mouth, the direction and movement of the driver's head.

It was developed intelligent system for monitoring the state of a person during hazardous work by Shvets O, Shokarev A., Bakatbayeva Zh. It was received a certificate on data registration in the state register of copyrighted objects of the Republic of Kazakhstan No. 18410, from June 04, 2021 (see Figure 8).

We are going to continue the research and to add more emotional states in the software, not only awake and asleep, but also extreme level of tension, active wakefulness, calm wakefulness, stress and fatigue.



Fig. 8. A certificate on data registration in the state register of copyrighted objects of the Republic of Kazakhstan No. 18410, from June 04, 2021 (Shvets O, Shokarev A., Bakatbayeva Zh.)

All the considered methods and algorithms are implemented in a software package in the C # programming language.

#### ACKNOWLEDGMENT

Part of the research was carried out with the support of the East-Kazakhstan technical university.

#### REFERENCES

- [1] L. Alzubaidi, J. Zhang, A. J. Humaidi, A. Al-Dujaili, Ye Duan, O. Al-Shamma, J. M. Santamaria, M. A. Fadhel, M. Al-Amidie, L. Farhan, Review of deep learning: concepts, CNN architectures, challenges, applications, future directions, Journal of Big Data No. 8(1), March 2021, 74 p.
- [2] N. Xu, B. Price, S. Cohen, T. Huang, Deep image matting, Proceedings of the IEEE Conference on Computer Vision and Pattern Recognition, 2017, pp. 2970-2979.
- [3] R. Logan, G. B. Williams., M. Ferreira da Silva, A. Indani, N. Scholnicov, A. Ganguly, S. J. Miller, Deep Convolutional Neural Networks With Ensemble Learning and Generative Adversarial Networks for Alzheimer’s Disease Image Data Classification, Frontiers in Aging Neuroscience, V. 13, 2021, p. 497, URL=<https://www.frontiersin.org/article/10.3389/fnagi.2021.720226>, DOI=10.3389/fnagi.2021.720226.
- [4] R. Patel, S. Patel, A Comprehensive Study of Applying Convolutional Neural Network for Computer Vision, International Journal of Advanced Science and Technology 6(6), 2020, pp. 2161-2174.
- [5] W. Xu, J. He, Y. Shu, H. Zheng, Advances in Convolutional Neural Networks, Advances and Applications in Deep Learning, Marco Antonio Aceves-Fernandez, IntechOpen, 2020, DOI: 10.5772/intechopen.93512, Available from: <https://www.intechopen.com/chapters/73604>.
- [6] Y. LeCun, L. Bottou, Y. Bengio, and P. Haffner, Gradient-based learning applied to document recognition., Proceedings of the IEEE, november 1998, 86(11), pp. 2278-2324.

**POSTER SESSION III.**

**Geodesy and Geoinformatics**

# Establishment of GNSS calibration network

Eszter DULEBA  
 Institute of Geoinformatics  
 Óbuda University, Alba Regia  
 Technical Faculty  
 Székesfehérvár, HUNGARY  
 duleba.eszter@gmail.com

Gergely LÁSZLÓ  
 Institute of Geoinformatics  
 Óbuda University, Alba Regia  
 Technical Faculty  
 Székesfehérvár, HUNGARY  
 laszlo.gergely@amk.uni-obuda.hu

Zoltán TÓTH  
 Institute of Geoinformatics  
 Óbuda University, Alba Regia  
 Technical Faculty  
 Székesfehérvár, HUNGARY  
 toth.zoltan@amk.uni-obuda.hu

**Abstract—** It is important to always have measuring equipment which most important parameters and errors are known. For GNSS receiver antennas one of the crucial information for high precision measurement is the location of the true phase center, in relation of its theoretical location. To determine this, a calibration network is necessary. In this paper the process of establishing such network will be presented.

## I. INTRODUCTION

It is important to know that the GNSS receivers we want to use for extreme accuracy (sub cm) measurement are calibrated or not. Doing calibration is possible on certified places but if we want it for technical reasons, it is possible to create our own calibration network, which can give the same benefits, but without certification [1] [2].

## II. GNSS SYSTEMS

The Global Navigational Satellite System is able to perform positioning, timing and navigation by being in contact with “artificial moons” if their position is known. Based on this, we can create a reference system from which we can later extract the necessary data. The operation of GNSS gives us access to different raw data, which we can store for our purposes or possibly further process. These raw measurement materials can be phase values, code distances



Figure 1. NAVSTAR GPS



Figure 2. GLONASS logo

or doppler numbers [4].

There are different base-systems within GNSS systems.

The GPS system (Fig. 1.) was created and maintained by the United States in the 1970s. Once completed, its primary task was to meet military needs using 24 active satellites.

GLONASS (Fig. 2.) is the result of developments in Russia (first launch occurred in 1982, during the Soviet era),

its structure is similar to its American counterpart and can be considered of a similar standard [5].

Europe has not lagged its competitors either, creating the Galileo project in 2005 [6] [7] [8].

This proprietary satellite positioning system provides EU Member States with positioning independent of the other systems.

Nowadays, the development of technology has brought inevitable needs and upgrades. As a result, they started to build a modern location network in Hungary as well, to provide real-time corrections for applications in need of more precise positions.

## III. CALIBRATION

The cornerstone of this research was the process of calibration. By performing the calibration, a connection was established between the actual properties provided by the measuring device and the actual quantity to be measured. During calibration, the measurements are performed by comparison with a special, standard quantity. The standard is an extremely accurate value. After the process is completed, a calibration certificate and reports could be prepared [12].

It is important to distinguish between authentication and calibration. Certification is a legal, i.e. official activity, which can be performed only by authorized persons, for which an official document, a certificate of authentication is issued. In contrast, calibration can even be performed by the owner of the device, for example, if the manufacturer requires periodic calibration to enforce the warranty or guarantee [13].

When calibrating GNSS antennas, we are talking about creating a model that determines the position of its phase center. The location of the phase centers of the various antennas is usually given by the manufacturers relative to a reference point. This value should be used in calculations to reduce the potential for error [14].

GNSS calibration begins with a 6-hour measurement where the measured results are processed in 30-minute parts because the National Authority (Lecher Tudásközpont) requires the longer measurements to break down to fast static-like portions, to calculate standard deviation between them [15]. So the measurement was processed in 12 parts. Vector calculations were performed for these measurements



to obtain the components, average them, and plot the differences between the averaged value and the value considered correct from the result, between all the possible combinations of the three pillars and the reference permanent stations

#### IV. ESTABLISHING CALIBRATION NETWORK

The created network is located on the top of the southern wing of Institute of Geoinformatics. Three pillars were placed there during its construction (we can id them as: East-Central-West), because it is on ideal place if we want to conduct orientational measurements. On the pillars - as a center - a hilti nail was fixed (Fig. 3.). These have limited use (with the help of a pillar stand only) to centrally place a



Figure 3. – The top of the pillar

GPS receiver or even a total station on them.



Figure 4. – Receiver on the pillar

Therefore, in addition to the existing marks, an eccentric standard threaded instrument screw has been built into the

pillar, which is suitable for placing an instrument base on them.

The network was determined in two ways, the first was by GPS technology. 3 Leica 500 GPS receivers were placed on the 3 pillars (Fig. 4.).

At least one of the receivers measured continuously over a 6-hour time interval, while the other two typically operated on each pillars for a minimum of 3-4 hours (the duration was limited due to the capacity of the batteries), in paralell of course with the permanent station called Székesfehérvár.

The measurement itself could have been done by using only one GPS receiver, measuring 6 hours at the eastern point, for example, then obtaining a vector between the eastern point and the Székesfehérvár point, then measuring 6 hours at the western point, thus obtaining a vector between the western and permanent station and so on, but if its possible to use multiple numbers of identical receivers it is favorable to perform the measurements at the same time on all so to reduce any errors that could arise otherways [18].

In addition to reducing the combined measurement time of the network (one measurement period lasting more than 6 hours each), it also had the advantage that discreate vectors were obtained for the three pillars not only from Székesfehérvár, also between them. This is also more advantageous, because in this way superfluous measurements are availabel for all determinations, so by equalization it is possible not only to determine the network points coordinates, their reliability values also [17].

These measurements were performed for three consecutive days. During the establishment of the network, the measurements with GPS receivers took place at different times of the day on all three days to reduce errors caused by unfavorable satellite constellations, which can occur some time of every day, so by changing time of day the satellite geometries were also different for every measurement. There were of course overlaps between thr 6 hours periods, but the starting time of the measurements were fundamentally different.

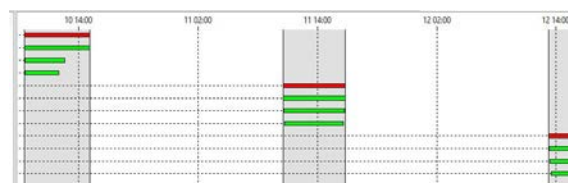


Figure 5. – Intervals of the receivers

The first measurement period was started on September 10, 2020 ~ 8:30. An instrument (KEL) and SZFV were then measured until 15:05, KOZ until 12:35, and NYU until 11:58. The second measurement day, September 11, 2020, started at ~ 10:30. Then, table shows (10. figure), the measurements were successful at almost the same intervals (~ 6 hours). In the third period, on September 12, 2020,

receivers were started around 13:15. Here, similar durations were as in the first period (Fig. 5-6.).

Point Id	Start	End	Durat...	Height ...	Antenna Type
SZFV	09/10/2020 08:29...	09/10/2020 15:05...	6h 36' ...	0.0000	AR20 LEIM
KEL	09/10/2020 08:31...	09/10/2020 15:05...	6h 34' ...	0.1765	AT502 Pillar
KOZ	09/10/2020 08:34...	09/10/2020 12:35...	4h 00' ...	0.1752	AT502 Pillar
NYU	09/10/2020 08:36...	09/10/2020 11:58...	3h 21' ...	0.1770	AT502 Pillar
SZFV	09/11/2020 10:32...	09/11/2020 16:48...	6h 16' ...	0.0000	AR20 LEIM
KEL	09/11/2020 10:34...	09/11/2020 16:48...	6h 13' ...	0.1765	AT502 Pillar
KOZ	09/11/2020 10:38...	09/11/2020 16:44...	6h 06' ...	0.1752	AT502 Pillar
NYU	09/11/2020 10:42...	09/11/2020 16:33...	5h 51' ...	0.1770	AT502 Pillar
SZFV	09/12/2020 13:15...	09/12/2020 19:18...	6h 03' ...	0.0000	AR20 LEIM
KEL	09/12/2020 13:17...	09/12/2020 19:18...	6h 00' ...	0.1765	AT502 Pillar
KOZ	09/12/2020 13:22...	09/12/2020 17:41...	4h 18' ...	0.1752	AT502 Pillar
NYU	09/12/2020 13:28...	09/12/2020 17:39...	4h 11' ...	0.1770	AT502 Pillar

Figure 6. – Durations of the receivers

In the first step, these results were calculated one day at a time. To perform the vector calculation and equalization, Leica Infinity software suit was used, It should also be mentioned that the vector calculation was performed with the RTKlib open source processing program.

V. PROCESSING

The raw measurement results were read from the receivers and downloaded from the permanent station were loaded in RINEX format into the Leica Infinity program for all 3-day static measurements. Four RINEX files were available for every day. One contained the results of the Székesfehérvár permanent station and the other were the measurements on the pillars. The header of a measurement is shown on the following, 7. figure:

```

KEL_2540.20o - Jegyzetömb
Fájl Szerkesztés Formátum Nézet Súgó
| 2.11 OBSERVATION DATA G RINEX VERSION / TYPE
LEICA GEO OFFICE 8.4 12-9-20 21:05 PGM / RUN BY / DATE
OBSERVER / AGENCY
KEL MARKER NAME
KEL MARKER NUMBER
0 REC # / TYPE / VERS
ANT # / TYPE
4119992.8080 1372038.0850 4656165.3127 APPROX POSITION XYZ
0.1850 0.0000 0.0000 ANTENNA: DELTA H/E/N
L1PhaOff: 0.0683 L2PhaOff: 0.0712 COMMENT
1 WAVELENGTH FACT L1/2
4 C1 L1 P2 L2 # / TYPES OF OBSERV
2020 9 10 6 31 30.0000000 GPS TIME OF FIRST OBS
2020 9 10 13 6 0.0000000 GPS TIME OF LAST OBS
18 LEAP SECONDS
21 # OF SATELLITES
COMMENT
G 1 962 962 952 952 PRN / # OF OBS
G 2 0 0 0 0 PRN / # OF OBS
G 3 747 747 747 747 PRN / # OF OBS
G 4 349 349 342 342 PRN / # OF OBS
    
```

Figure 7. – The header of a measurement

As a result, 18 vectors (6 from each day) with their 3-3 components were calculated ( $\Delta x$ ,  $\Delta y$  and  $\Delta z$ ). The 6 vectors were constructed according to the following scheme (based on Figure 9): KEL-SZFV, KOZ-SZFV, NYU-SZFV, KEL-KOZ, KOZ-NYU, KEL-NYU. Since redundant

measurements were preset, it was possible to adjust the GNSS network.

The adjustments were performed both as a free network and also as a fixed network. In the latter case, the coordinates of the permanent station were accepted as fix. In the first case, all coordinates can get corrections, in the second case the permanent station does not. The latter solution will be considered final at a later date

VI. ESTABLISHMENT OF A HORIZONTAL AND ELEVATION NETWORK WITH MEASURING STATION AND LEVEL

Precise leveling was also performed on the pillars. The relative height difference between each was determined by standard, precise-level leveling method with a precision of 0.1 mm.

The pillars were also measured at 4 locations (screws, nails and 2-2 points on the concrete surface of the pillars), of which we used only three in our measurement.

VII. HORIZONTAL NETWORK

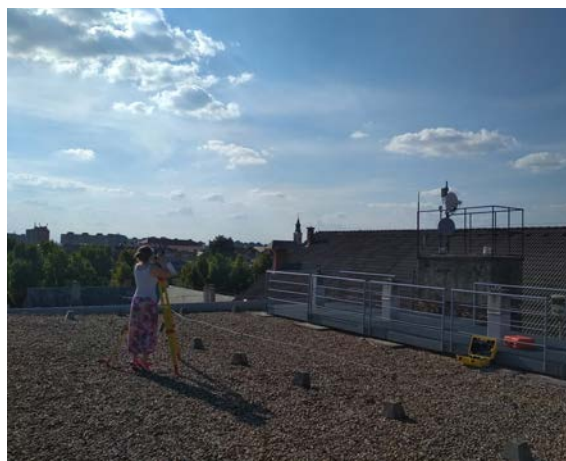


Figure 8. –Top of the GEO – Measurements with Geomax

Measurements were performed with a Geomax total station on the three pillars and one external point (Fig. 8-9.). Direction and distance measurement were performed in one round in one telescope face. The measurement was conducted from an excentric position to reflector prisms placed on the pillars at the precise horizontal location of the GNSS receivers, and also to points on the permanent station. The surrounding points with known EOVS coordinates (typically church towers) were also included in the definition of the network, so that we can later use them to clearly insert the network into the EOVS system. The network was adjusted as a free network.

The calculation was performed with GeoCalc. GeoCalc is a Desktop GIS application that can read GIS data stored in different digital formats, different projection a system,

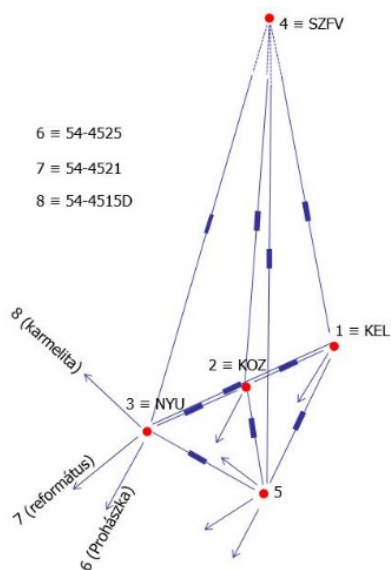


Figure 9. – The free network

and display them as thematic maps, print them in a suitable format [17]. As a result, we obtained coordinates and mean errors.

The network was also adjusted as a vertical network, so that the height of the middle point was captured (-2.3694m). This deviation, as mentioned before, follows from the eccentricity of the phase center that was identified as a deviation in the vertical sense (Fig. 10).

	Wild csúcs	Csavar	Hírti	Pillér-festő
	Helyi Magasság			
1	99.7047	99.5382	99.5329	99
2	99.7032	99.5358	99.5319	99
3	99.7226	99.5519	99.5489	99

Figure 10. – Vertical network results

## VIII. CONCLUSIONS

In the sense of having precise measurement tools, it is not always necessary to find a company which offers certified solutions for calibrations. In many cases it is possible to make similarly precise calibrations by and for ourselves by creating a suitable location. In this paper a case was presented in which a custom built GNSS calibration network was established, measured and the results were adjusted with high precision so in the future conducting GNSS antenna calibration would be possible any time.

## IX. REFERENCES

- [1] Dr. Busics György Műholdas helymeghatározás 1. TAMOP elektronikus jegyzet (NyME 2010) [https://regi.tankonyvtar.hu/hu/tartalom/tamop425/0027\\_MHM1/ch01s02.html](https://regi.tankonyvtar.hu/hu/tartalom/tamop425/0027_MHM1/ch01s02.html)
- [2] GNSS (Global Navigation Satellite System) vevő egységek és használatuk. 2019. 05. 25. <https://newtechnology.hu/gnss-global-navigation-satellite-system-vevo-egysegek-es-hasznalatuk/>
- [3] And Standing Up Straight (New Zealand's new gravity-based vertical datum) <http://blogs.lincoln.ac.nz/gis/2016/08/28/and-standing-up-straight/>
- [4] Dr. Busics György Műholdas helymeghatározás 2., GNSS alaprendszerek TAMOP elektronikus jegyzet (NyME 2010) [https://regi.tankonyvtar.hu/hu/tartalom/tamop425/0027\\_MHM2/ch01s02.html](https://regi.tankonyvtar.hu/hu/tartalom/tamop425/0027_MHM2/ch01s02.html)
- [5] WikiPedia – GLONASS (en) szócikk <https://en.wikipedia.org/wiki/GLONASS>
- [6] Galileo next-gen satellites on the horizon (SpacewatchEurope) <https://spacewatch.global/2020/08/galileo-next-gen-satellites-on-the-horizon/>
- [7] Post-Brexit UK won't use EU Galileo satellite system (News) <https://www.dw.com/en/post-brexit-uk-wont-use-eu-galileo-satellite-system-british-pm-says/a-46533333>
- [8] A Galileo életre kel! (Európai Bizottság) [https://ec.europa.eu/commission/presscorner/detail/hu/IP\\_16\\_4366](https://ec.europa.eu/commission/presscorner/detail/hu/IP_16_4366)
- [9] Dr. Busics György Műholdas helymeghatározás 6., Passzív GPS hálózatok, statikus technológiák (NyME 2010) [https://regi.tankonyvtar.hu/hu/tartalom/tamop425/0027\\_MHM6/ch01s03.html](https://regi.tankonyvtar.hu/hu/tartalom/tamop425/0027_MHM6/ch01s03.html)
- [10] Dr. Busics György Műholdas helymeghatározás 7., Aktív GNSS hálózatok és szolgáltatásaik (NyME 2010) [https://regi.tankonyvtar.hu/hu/tartalom/tamop425/0027\\_MHM7/ch01s04.html](https://regi.tankonyvtar.hu/hu/tartalom/tamop425/0027_MHM7/ch01s04.html)
- [11] Geomatikai közlemények III. Sopron, 2000.
- [12] A méretarány-tényező néhány alkalmazásáról a földmérésben – Dr. Busics György 2019/4 <http://edit.elte.hu/xmlui/static/pdfjs/web/viewer.html?file=http://edit.elte.hu/xmlui/bitstream/handle/10831/43487/GK.2019.4.3-DOI.pdf?sequence=1&isAllowed=y>
- [13] K-GEO Kalibráló Laboratórium honlapja <http://lechnerkozpont.hu/oldal/k-geo>
- [14] Kozmikus Geodéziai Observatórium, Lechner Nonprofit Kft. honlapja. <https://www.sgo-penc.hu/obszer.php#section2>
- [15] Geodéziai hálózatok (K-GEO) [https://www.sgo-penc.hu/geo\\_halozatok.php](https://www.sgo-penc.hu/geo_halozatok.php)
- [16] GeoCalc ismertető: <https://www.geocalc.hu/>
- [17] János, Katona Parcel analysis for the general application of remote sensing monitoring In: Orosz, Gábor Tamás (szerk.) AIS 2019 : 14th International Symposium on Applied Informatics and Related Areas organized in the frame of Hungarian Science Festival 2019 by Óbuda University Székesfehérvár, Magyarország : Óbudai Egyetem, (2019) pp. 69-70. , 2 p.
- [18] Katona, Janos ; Gulyas, Margit Horoszné Determination of factors modifying land value based on spatial data In: Drótos, Dániel; Vásárhelyi, József; Czap, László; Ivo, Petráš (szerk.) Proceedings of the 19th International Carpathian Control Conference (ICCC 2018) Piscataway (NJ), Amerikai Egyesült Államok : IEEE, (2018) pp. 625-628. , 4 p.

# Increasing urban development efficiency through land value capture mechanisms

János Katona

Óbuda University Alba Regia Technical Faculty  
Székesfehérvár, Hungary  
[dr.katona.janos@uni-obuda.hu](mailto:dr.katona.janos@uni-obuda.hu)

Andrea Pödör

Óbuda University Alba Regia Technical Faculty  
Székesfehérvár, Hungary  
[andrea.podor@uni-obuda.hu](mailto:andrea.podor@uni-obuda.hu)

**Abstract**— In Hungary, value capture basically relies on recurring forms. Real estate tax and real estate transfer tax are regulated by law. In addition, municipalities can levy local taxes, such as real estate tax for buildings, real estate tax for lands and communal tax. In Hungary the investors have very few obligation to public value. Therefore, in the settlements with an increased population, the local governments are in a difficult position in terms of the basic tasks (e.g. kindergarten, health care). Municipalities are heavily dependent on subsidies and the local business tax. There is a need for a complex value capture method that excludes speculation and expects greater social involvement from investors. Examining foreign examples, the study seeks answers to increase development efficiency.

**Keywords**— value capture, urban development,

## I. INTRODUCTION – LAND VALUE CAPTURE

Land value capture refers to fiscal instruments through which public authorities can capture increases in properties values that are unrelated to actions of land owners. [1]

Land value capture is a policy approach that enables communities to recover and reinvest land value increases that result from public investment and other government actions. Also known as “value sharing,” it’s rooted in the notion that public action should generate public benefit. The potential advantage of land value capture is that the revenue from, for example, a tax can be used to fund public projects that may subsequently increase the net return (rent) to the landowners. [2]

The term public value capturing comprises a wide range of methods that public authorities can use to capture part of the land value increment from landowners. There are basically two major groups of land valuation methods: recurring forms and non-recurring forms.

### A. Recurring forms of public value capture

- **Taxation:** The land value may be used in addition to the value of the buildings. Alternatively, only the land value or the profitability of the real estate may be used. Generally, professional valuation experts create maps of land values which have to be actualized in a certain interval. The valuation of the buildings is done by a simplified version of the cost approach multiplying the useable area of the buildings by price per square metre which is listed in a valuation table.
- **Tax rates:** Countries use a system of different rates distinguishing between plot and constructions, use of the plot and/or buildings (e.g. living or commercial use) or built or unbuilt plots. It can also be used continuous progression and Extraordinary tax for unbuilt plots.

### B. Non-recurring forms of public value capture

- **Fees or levies:** Many countries use fees or levies to recoup development costs (e.g. costs of infrastructure).
- **Tax or levy on planning gains:** A certain percentage of the added land value created by zoning is captured. Generally, the collected funds are dedicated to determined public purposes.
- **Flexible building rights or transferable development rights:** Different models which imply exceptions to the general use regulations in favour of investors or property owners who paid a certain amount of money exist. The allowed exceptions and financial considerations are generally regulated in legal norms. In doing so, the core of the urban planning will be conserved in spite of more flexible building rights.
- **The “real estate consortium” or “conjoint urbanisation” or “land readjustment”:** The public authorities and private land owners aspire a co-operation for the urban development of former rural areas by exchanging ownership rights on land. After the development the land owners get back a plot which has the same value as the plot before the development. Due to the increasing prices per square meter will remain a part of the developed area with the municipality. These plots may be used for social housing programmes or other public functions. Another option is a payment in cash for the development benefits.
- **Negotiated development:** The developer prepares the plan jointly with the municipality. Nevertheless, the municipality should take into account all private and public interests before the approval of the plan. It has to be avoided that the financial aspects compromise the public interest of good planning. The affected area can be (complete or partial) property of the developer or municipality. Generally, the developer is responsible for the construction of the infrastructure.
- **Urban development or redevelopment measures:** those measures by means of which an area is substantially improved or transformed with the purpose of eliminating urban deficits.
- **Interim acquisition or land banking:** The build-up of land stocks is oftentimes used in municipalities to have available plots for public objectives within urban development. Afterwards, a part of the plots may be sold to maintain the stock balance by a so-called “revolving land stock”
- **Contract models or developer obligations:** The agreement of certain duties of the private partner in return to subsequent building rights is an alternative to

interim acquisition (Munoz-Gielen and van der Krabben 2019b). The most common duties are the provision of the needed area for the infrastructure or provision of plots for social, public or ecological objectives. [3]

## II. INTERNATIONAL PERSPECTIVE ON LAND VALUE CAPTURE

The tools listed in the introduction are used in different variations by each country. The following subsections present some typical solutions.

### A. German model

Municipalities shall collect charges for the recoupment of otherwise unrecoverable public expenditure on local public infrastructure in accordance with the GFBC. In consequence the landowners have to provide the land for the technical infrastructure and have to pay for the construction. The amount of land / money depends on the regulation of the legally binding land use plan. On the other hand, local governments have the option to increase the PVC by urban contracts. Tools used in Germany:

- Recoupment charge for local infrastructure
- Land reallocation
- Urban development measure
- Interim acquisition
- Contract models (urban contracts)
- Real estate tax
- Real estate transfer tax

### B. Baltic countries: Latvia, Estonia, Lithuania

A concept (term) of value capture (PVC or LVC) and definition of it is not recognised in any formal source, however, the tools for capturing increase of land value due to development processes by public authorities can be identified. Tools:

- Planning fees and development fees are not introduced, but a lot of costs have to be covered by developer during the development process
- Development agreement: implementation of a detailed plan
- Development agreement: charge (fee) for local infrastructure
- Capital gain tax
- Real property tax in Latvia. Land tax in Estonia and Lithuania

### C. Swedish model

No formal term/concept found in any formal source but it is topical to political and an academic debate, however tools introduced/stipulated straight into legal acts and its amendments:

- Recoupment charge for local infrastructure
- Development agreement: charge (fee) for internal infrastructure and since 2015 also for parts of external infrastructure
- Land allocation: land transfer to developer
- Capital gain tax
- Annual property tax

### D. Swiss model

Compensation of planning related advantages for balancing the planning system financially (legitimized by justice). “Cantonal legislation shall regulate appropriate

compensation procedures for major advantages and disadvantages resulting from planning under this Act. Planning advantages shall be compensated for at a rate of at least 20 per cent.”

- Compensation: Compensating unearned advantages to cross-finance undeserved disadvantages (expropriation, rezoning, etc.)
- No tools under development procedure recognised
- No taxation related to real estate/property

## III. TOOLS OF PUBLIC VALUE CAPTURE IN HUNGARY

In Hungary, the urban land-use planning and urban development is laid down by the Act LXXVIII of 1997 on the formation and protection of the built environment. The amendment of Government Decree 253/1997. (XII. 20.) on the national requirements regarding town planning and construction contains legislation details concerning settlements such as the requirements of urban planning, building placement or building regulations. One of the most important urban planning means is the settlement structure plan which determines the urban structure, the urban use, and the structure of utility networks. The settlement structure plan contains each and every unit of the land use. General requirements concerning all zones are specified in the Government Decree; local building codes can also supplement these requirements. The development plan should contain the origin (e. public money, tender money etc.) and the rate of the possible resources. [4][5]

### A. Recurring forms of public value capture

In Hungary, the recurring forms can be divided into real estate tax, here local regulations can differentiate the tax into 2 forms, one is for buildings and another for lands. The third recurring form is the municipal tax. There are real estate transfer tax and the capital gain tax are in case of sale of the real estate.

1) *Real estate tax for buildings*: One type of locally levied tax is the building tax. The municipality is the one who can introduce the tax in its area of jurisdiction. The building tax covers several types of real estate, not just the house, and even the taxpayer can be multiple, as a property can have more than one owner.

In the area under the jurisdiction of the local government, a tax must be paid - in accordance with the local government decree - on the buildings as well as on the non-residential buildings and parts of buildings such as the garage.

Municipalities publish on their website who and how much tax they have to pay. Taxpayers must create a declaration form.

The tax liability arises when a building permit has been issued for the building and the permit has become final in the following year. In the same way, the application for continuance creates the tax liability. Otherwise, any changes related to the taxation of the structure must be reported to the municipal tax authority within 15 days. The obligation to pay the building tax, on the other hand, ceases when the building is demolished.

Cases of construction with tax exemption:

- emergency housing,
- room for healthcare provided by a general practitioner

- a facility used exclusively for the storage of radioactive waste and the storage of spent nuclear fuel (under the Atomic Energy Act)
- a building for animal or plant production according to the real estate register or a storage building related to these activities (eg fertilizer storage barn, greenhouse, crop storage, seed storage), provided that the building is used by the taxable person for its intended purpose in connection with animal husbandry or plant growing activities.

The building tax is calculated per square meter and may vary from place to place. There are municipalities where buildings for residential purpose are not subject for taxation.

Those, who is registered in the land register, but also the beneficiary or the holder of the registration of another right will be a taxable person.

As of January 1, 2018, the provision according to which the owner of the advertising medium can be weighted with a bulding tax is in force. The tax base can be used for the publication of advertising media, calculated in square meter - with an area of two decimal places - 12,000 HUF / m<sup>2</sup>.

2) *Real estate tax for lands*: One form of tax that can be levied not by the state but by the municipality on real estate covered by the regulation. The land tax is one of the local taxes that many municipalities have introduced. The land is by law the area where there is no building. The concept of a plot/land includes several types of real estate, yet there are exceptions, after which there is no taxation. The municipality should announce on their website wether they are introduced this type of tax or not.

The owner(s) and others with registered property rights who are registered in land registry will pay the tax.

Exemption from land tax under the Local Taxes Act:

- a part of land of the same size as the useful floor area of the building or building part on the land,
- land inside of the municipal area land under agricultural cultivation, form 1.01.2017
- 50% of the taxable area of the land under construction,
- forest inside of the municipal area
- land which is under construction ban
- a security and safety area (zone) belonging to the taxable person's product manufacturing plant, established by law or official regulation, provided that at least 50% of the taxable person's annual net turnover in the tax year preceding the tax year comes from the sale of his own product.

There are two ways to calculate. On the one hand, it can be based on a square meter, that is, if the floor area of the plot is the basis for the land tax, the law can define the highest value per square meter, which the local government can request at the land tax address, recently this is 200 HUF. The other way is to calculate the land tax by the adjusted turnover value of the land. If the local government decides otherwise, the land tax can be a maximum of 3% of the adjusted turnover value. What is the adjusted turnover value? 50 percent of the market price of the plot.

3) *Municipal/Communal tax*: The communal tax is defined in the local tax legislation. There are taxes that every municipality is allowed to dictate on locals or who have a

business in their territory. The purpose of local taxes, such as the communal tax, is also to establish the management of the local government and to help its independent operation.

The municipalities obliged to announce on their website the regulation and the rate of communal tax. The bulduing and land owners have to pay this type of tax.

The municipal tax payment is related to the building tax and land tax payment. There is also communal tax on an apartment lease, which is shared equally by the tenants, unless it is agreed in the contract who is the taxable person.

The amount of the tax is determined by the local government taking into account the amount of the upper limit multiplied by the product of the changes in the consumer price level between 2006 and 2003 and the second year before the tax year. Therefore it varies greatly from settlement to settlement. [6]

4) *Real estate transfer tax*: Hungarian legislation prescribes that all incomes are taxable, and tax shall be payable on acquisition. In other words, after the sale of a property, tax has to be paid by both the old owner and the new one. With the tax payment, the citizen proportionally contributes to both national and social tasks. The rate of the tax is uniformly 4 % of the purchase price, above 1 milliard forint 2% but maximum 200 million forints. There are allowances, the most important ones are the followings:

- replacement purchase: if we sell our property and buy another one in 3 years, we have to pay tax after the difference of the value of the two properties – in case the newer one is more expensive.
- tax allowances for the youth: people under the age of 35 can ask for tax allowance if they buy their first property and the total value of the property exceeds 15 million forints
- tax allowance for a new-built property
- tax exempt: people are exempt from paying tax if the property changes the owner who are married or close relatives

5) *Capital gain tax*: Hungary currently has a 15% flat-rate personal income tax. The method of the calculation is the following:

- selling price – purchase price – eligible costs: tax base
- the amount of tax payable: tax base x 0,15
- The tax base decreases over the years and after 5 years it is 0.

#### B. *Non-recurring forms*

According to Act LXV of 1990 on municipalities, the municipalities are responsible for providing local public transportation, district heating, water utility management and ensuring parking areas. Since a lot of settlements would not be able to supply the basic tasks individually, they are invited to tenders by The Ministry of Interior of Hungary. These tenders can be used for building or renovating day nurseries, kindergartens or hospitals. [7]

1) *Fee for construction of infrastructure*: Although one of the tasks of municipailies is to provide utility services, citizens need to pay a contribution for wiring. Both the

service provider and the municipality can ask citizens to pay a contribution. This is a one-time fee. The rate of the fee is determined by the representative body of the municipality; the costs of the investment can be passed on the citizens partly or fully by the municipality. Municipality carry out investments with the help of tenders.

Providing sewer utility services does not belong to the basic tasks of a municipality but in case of its construction, the municipality oblige people to wiring.

The municipalities develop local road network as much as possible financially; typically, they do not ask residents to pay a contribution. [8]

2) *Development according General Urban Planning Legislation*: The means for the long-term goals of urban development is the urban development concept, and the means for the implementation of medium-term goals is the integrated urban development strategy. These documents are based on consensus, and they help the implementation of the improvements. Moreover, the the amendment of Government Decree 253/1997. (XII. 20.) on the national requirements regarding town planning and construction also contains general regulations for property investments. One of these regulations is to ensure a defined number of parking space specified in the local building code for residential and holiday units, but it is mandatory to accommodate a maximum of one car. Opinions are divided on whether one parking space per apartment is enough, but everyone agrees that their number should be regulated. According to some interpretations, this number is appropriate, as the means of solving transport problems is not the car, but public transport.

It is common to support the rehabilitation of brownfield sites. For instance the value added tax of a property built newly in brownfield sites is 5% instead of 27%. Thematic programmes have been determined for the development of brownfield sites. The strategy sets out the following four key objectives:

- To eliminate functional deficits by the preference of economically rational mixed land use and by the expansion of green field system
- To develop the support of sustainable economic growth
- To minimize barriers for renewal to support temporary utilization

The investments will return over time in the form of taxes, rents, and public land use fees.

It is important to bear in mind the protection of the public interest in case of modifications to the plan financed by the undertakings. [9]

3) *Development according Special Urban Planning*: The protection of private property is essential in Hungary, as well; therefore in all cases, a consensual solution is supported. However, there are priority investments where state intervention is needed. The Act LIII of 2006 is on the acceleration and simplification of the implementation of the investments that are tremendously important for National Economy. The following categories are laid down in the Act:

- Tremendously important case for National Economy
- Tremendously important transport infrastructure investment for National Economy
- Tremendously important investment

The act accelerates the official procedures required for construction and their judicial review. [10]

4) *Cooperative development by urban contracts*: There are several ways in which the government and the municipalities are trying to curb realty sector speculation. According to the changed tax law, the property transfer tax is extra high, 90 percent for real estate declared inland and the law on PIT (personal income tax) also taxes the income from the transfer of real estate. Furthermore, more and more municipalities are thinking of a property contribution from the owners in exchange for the increase in value. [11]

More and more urban development companies are being set up in Hungary. The urban development company receives remuneration specified in the agency contract by the municipality for the operative management of the planning and implementation of urban developments and for their operating costs. The remuneration needs to be set in the most financially efficient way and it needs to encourage the urban development company to achieve the highest possible proportion and amount of direct urban development revenue so that the costs of an urban development can be lower for the public sector.[12]

#### IV. SUMMARY

The tax rate for real estate is 4%. This is an average value in the European Union. This type of tax and the associated tax rate are accepted. No change is required.

Hungary currently has a 15% flat-rate capital gain tax. In European terms, this rate is among the lowest. At the same time, VAT is the highest, which nuances the overall picture. The Constitution enshrines the right of local governments to own and state revenue. However, this constitutional provision does not mean that all statutory tasks must be covered by a state budget contribution. This financial source is provided by a combined system of own resources and central budget contributions. An important new practice on the part of municipalities is to impose an extra high sales tax on real estate declared to be inland.

Due to the high tax at the international level, the social acceptance of land value capture in Hungary is low. Although more and more municipalities are introducing legally allowed local taxes, the real solution may be the tool of cooperative development by urban contracts.

As there is a correlation between decentralization and economic efficiency, the freedom of local governments must be maintained. At the same time, there is a need for a legal framework that supports land value capture. If they are not endowed with satisfactory political and financial power, they run the risk of losing their economic position, from the perspective of both capital, labor, and external companies. In the spirit of social responsibility, expectations must be set for real estate developers.

As in Germany, in Hungary the tax legislative power can also belong to the state and the local government, the German model can be a good example in terms of value capture rate as well as public space provide.

#### REFERENCES

- [1] Oppio et.al., "OECD (2017)", The Governance of Land Use in OECD Countries Policy Analysis and Recommendations, 2018
- [2] Medda, F. & Modelewska, M., "Land Value Capture as a funding source for urban investment: the Warsaw Metro System", UCL QASER Lab, ERNST & YOUNG: Better Government Program 2009-10., 2010

- [3] Hendricks, A. et. al., “Public value capture of increasing property values – What are unearned increments?” In: Erwin Hepperle, Rober Dixon-Gough, Reinfried Mansberger, Jenny Paulsson, Jozef Hernik and Thomas Kalbro (eds.), *Land Ownership and Land Use Development – The Intergration of Past, Present and Future in Spatial Planning and Land Management Policies*, vdf Hochschulverlag, pp. 257-282. K. Elissa, “Title of paper if known,” unpublished., 2017
- [4] Katona, J., “The role of GIS in spatial planning”, In: Orosz G.T.; Petőné Csuka I. (szerk.), *15th International Symposium on Applied Informatics and Related Areas organized in the frame of Hungarian Science Festival 2020 : AIS 2020, Székesfehérvár, 2020*. pp 85-88
- [5] Szalavetz, A., “Upgrading and value capture in global value chains in Hungary: More complex than what the smile curve suggests.” In *Foreign Direct Investment in Central and Eastern Europe, 2017*. pp. 127-150
- [6] Bor, G., Tóth, Z., László, G., “Low-cost distance measuring methods and their investigation for BIM modeling”, In: Orosz, Gábor Tamás (szerk.) *AIS 2019 : 14th International Symposium on Applied Informatics and Related Areas organized in the frame of Hungarian Science Festival 2019 by Óbuda University Székesfehérvár, Magyarország : Óbudai Egyetem, (2019) pp. 54-60. , 7 p. Közlemény:30922468*
- [7] László, G., Földváry, L., “Determination of 3D surface deformation for the 2018 Oaxaca earthquake using InSAR” In: Bacsaárdi, László; Kovács, Kálmán (szerk.) *Selected papers of the 5th International Conference on Research, Technology and Education of Space (HSPACE 2019) Budapest, Magyarország : Magyar Asztronautikai Társaság, (2019) pp. 17-22. Paper: HSPACE2019-FP-18 , 5 p. Közlemény:31134921*
- [8] Balázsik, V., Tóth, Z., Abdurahmanov, I., “Analysis of Data Acquisition Accuracy with UAV”, *INTERNATIONAL JOURNAL OF GEOINFORMATICS 17 : 1 pp. 1-10. , 10 p. (2021)*
- [9] Harnos, L., “A városfejlesztés és a lakáspiac kapcsolata Sopronban”, In: Csanádi-Bognár, Sz.; Fata, I.; Kromják, L. (szerk.) *Határtalan tudomány. Tanulmánykötet a Magyar Tudomány Ünnepe alkalmából., Tomori Pál Főiskola, 2019, pp. 75-82.*
- [10] Tóth, Z.; Mélykúti, G., Barsi, Á., “Digitális videokamera kalibrációja” *GEOMATIKAI KÖZLEMÉNYEK / PUBLICATIONS IN GEOMATICS 8 pp. 297-302. , 6 p. (2005)*
- [11] Alhusain, O., Tóth, Z., Rakusz, Á., Almási, L., Farkas, B., “Vision-based System for Quality Control of Some Food Products”, *ISPRS JOURNAL OF PHOTOGRAMMETRY AND REMOTE SENSING 35 pp. 477-482. , 6 p. (2004)*
- [12] Dietz, F., “Integrált Városfejlesztési Stratégia, Budapest”, 2011, 192 p.



# Application development supporting orthophoto documentation

Gergely LÁSZLÓ  
Institute of Geoinformatics  
Óbuda University, Alba Regia  
Technical Faculty  
Székesfehérvár, HUNGARY  
[laszlo.gergely@amk.uni-obuda.hu](mailto:laszlo.gergely@amk.uni-obuda.hu)

Gabriella BOR  
Department of Orthophotogrammetry,  
Envirosense Hungary Ltd.  
Debrecen, HUNGARY  
[gabriella.bor@envirosense.hu](mailto:gabriella.bor@envirosense.hu)

Grégory LUCAS  
Department of Orthophotogrammetry  
Envirosense Hungary Ltd.  
Debrecen, HUNGARY  
[gregory.lucas@envirosense.hu](mailto:gregory.lucas@envirosense.hu)

Csaba LÉNÁRT, Phd.  
Remote Sensing Centre  
University of Debrecen  
Debrecen, HUNGARY  
[lenart.csaba@unideb.hu](mailto:lenart.csaba@unideb.hu)

**Abstract**— We have developed a GIS algorithm that can support the project application processes with automatic and accurate GIS results that can be used for the planning and post-flight implementation documentation of orthophoto projects. The tools aim at easing the documentation of orthophotography projects both in the planning phase and after the completion of data acquisition, by providing qualitative information within the form of maps.

The flight planning software available on the market have limited output capacities -they can output the photo footprints with correction based on terrain elevation- but they do not offer the capacity to extensively document photogrammetry project as it is expected in some state level applications. To cover this gap we have developed the three different following tools: 1) a tool issuing tables with the percentage of overlap between adjacent images; 2) A tool generating a map of the effective resolution where the variation of the resolution can be appreciated and 3) a tool targeting the buildings inclination that issues a map with the leaning percentage at each location. The two last solutions include corrections made from the terrain elevation.

In this paper we aim to present our solutions for these practical problems.

**Keywords**—*orthophoto, photogrammetry, GIS, application development, maps*

## I. INTRODUCTION

In parallel with the constant increase with the accuracy requirements, there is a growing need with the documentation of the quality of photogrammetry projects. New descriptors are requested to characterize the advanced products at the diverse phase of a project (planning and acquisition).

Flight planning software that are in use today cover the most common requirements, but they do not offer advanced options to meet some of the newest requirements. So, there are areas of application where such advanced software features do not yet exist.

A photogrammetry project starts with an appropriate planning. and many aspects need to be considered in order to properly prepare a flight plan.

In order to obtain the proper results, in addition to technical requirements, it is necessary to know the accuracy

and method of the subsequent processing procedure, as well as the expected conditions of the flight. A computational error made at this stage can make processing difficult or even completely impossible. To create a proper flight plan, it has to be considered:

1. Aircraft performance specifications
2. Measuring camera parameters
3. The type of product to be manufactured
4. Terrain conditions
5. Accuracy requirements
6. Processing software features

All but one of the above parameters can be determined relatively accurately before flight for the entire project. We know the technical parameters of the aircraft and the camera, the processing software background is also given, and the accuracy requirements and the final product to be made are included in the technical specification of the order. There is one thing that is typically not available or may not be available with sufficient accuracy for the area in question or just from an earlier date, and that is the topography model. The flight plan definitely requires some DTM from the area, which in most cases means an SRTM terrain model created as a result of satellite remote sensing. [5]

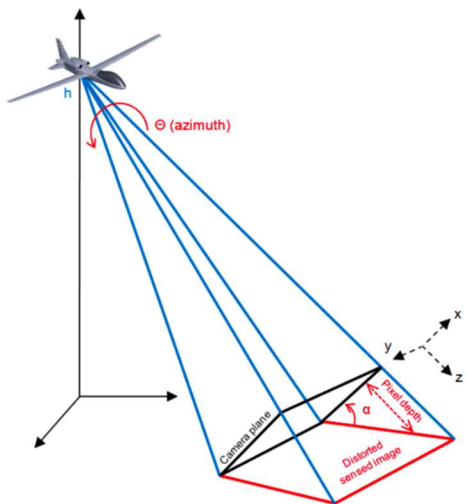
The well-known disadvantage of these types of topographical models is that their resolution is typically only around 20-30 meters or worse.

For the preparation of a flight plan, which can typically cover, hundreds, even thousands of square kilometers, such an accuracy of 20-30 meters may be sufficient, with the help of which in-line and between-line overlaps can be planned with good approximation.

However, as the hardware and software technologies used for aerial photography evolve (including camera compensation systems, higher resolution cameras, processing software backgrounds), and the accuracy and resolution of aerial photographs become better, there has been a demand from customers to improve the documentation of the following descriptors: field resolution within a given photograph, perspective tilt (1. Fig.), degree of exact overlap between images. They should be described with high accuracy

(up to 10-15 meters resolution for the entire area) and already in the design phase.

The team of Envirosense Hungary Ltd dealing with orthophoto processing and related developments has been commissioned to develop a software solution to these problems and documentation needs; the results of which are presented in this article.



1. Figure Perspective distortion and correction

II. DETAILED ALGORITHM DESCRIPTIONS

A. Generating overlap statistics for adjacent images

For flight planning software, the input parameter is usually a SRTM terrain model or an area-specific average terrain height. In addition, the boundary of the area to be surveyed, the desired overlap values, and the camera parameters (sensor size, pixel size, lens type) must be specified [11].

For the given sample an Ultracam Eagle M3 large format camera was used, with 120mm focal and 17004x26460 pixels sensor size (pixel sizes are 4.000 x 4.000 microns)

Using this data, the program calculates the coordinates of flight lines and shooting locations.

It is important to note that the set overlaps represent minimum overlap values for the software. Even at this design stage, the actual result may differ from image pair to image pair even due to terrain, as planning programs determine the flight altitude for each line, but in many cases as a uniform value for the whole block.

It is important for the customer to know the exact overlap percentage per image, taking into account the planned flight parameters, as well as the actual recording locations (GNSS) and aircraft tilt (IMU) based on the flight.

The algorithm we created was developed for the following specific layout conditions:

- The overlay on line must be greater than or equal to 72%, so that each point of the terrain is visible on at least 3 successive images of the same strip. A hole in the tri-stereoscopic cover will be considered a blocking anomaly.
- The overlay cross lines may in no case be less than 55%, so that every detail of the land is visible on at least 2 adjacent strips. A hole in the side stereoscopic cover will be considered a blocking anomaly.

- These draft flight plans will be delivered in shapefile format, accompanied by tables describing the recoveries (expressed in %). The table of recoveries (expressed in %) for each pair of photographs

Because geometric data is available, we chose QGIS to implement the task from the options offered by the customer for application development. [3]

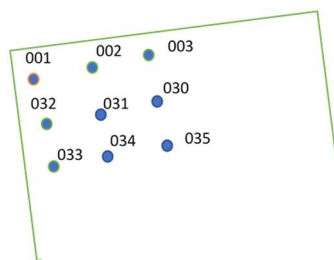
QGIS is a free, open source GIS software that allows users to edit, analyze, and map spatial data [1].

The program is suitable for handling raster and vector data in various formats and projections. Own applications can be developed with graphical programming on the interface, using Python or C++ programming language [1] [2].

The procedure we propose starts from the assumption that the geometry of the footprint file serving as input data, already contains the effects of the terrain. Otherwise, it would be necessary to project the footprint polygons onto real terrain for further steps.

The planned result would be a table consisting of three columns: the first column shows the image currently being examined, the second column contains its neighbors below each other, and the third column the percentage overlap of the two (2. Fig.).

Source Image	Paired Image	Overlap %
cap_00001	cap_00002	76.5
cap_00001	cap_0123	62.91
cap_00002	cap_00001	76.28
cap_00002	cap_00003	76.71
cap_00002	cap_0124	62.57
cap_00003	cap_00002	76.46
cap_00003	cap_00004	75.88
cap_00003	cap_0125	62.46
cap_00004	cap_00003	76.14
cap_00004	cap_00005	75.96
cap_00004	cap_0126	62.14
cap_00005	cap_00004	76.13
cap_00005	cap_00006	75.97
cap_00005	cap_0127	62.15
cap_00006	cap_00005	76.95
cap_00006	cap_00007	76.2
cap_00006	cap_0128	62.69
cap_00007	cap_00006	76.4
cap_00007	cap_00008	76.55
cap_00007	cap_0129	62.82
cap_00008	cap_00007	77.17
cap_00008	cap_00009	76.76
cap_00008	cap_0130	63.01
cap_00009	cap_00008	77.33
cap_00009	cap_00010	76.78
cap_00009	cap_0131	63.33
cap_00010	cap_00009	77.26
cap_00010	cap_00011	77.08
cap_00010	cap_0132	63.36
cap_00011	cap_00010	77.09
cap_00011	cap_00012	77.05
cap_00011	cap_0133	63.4
cap_00012	cap_00011	77.21
cap_00012	cap_00013	77.1
cap_00012	cap_0134	63.25



2. Figure The structure of the table

In terms of their location, we can talk about three cases:

- corner image with two neighbors, one in row and one in a neighboring row next to it
- border image, in which we can talk about three neighbors, two within the row and one on the side in the row next to it
- image inside a block, when it has two neighbors in a row, and two other ones from the strip next to it

Based on the above list and the previously described overlap minima that only the immediate neighbors of an image need to be considered, although the number of overlaps, including three-, four- and even five-times overlaps, is significantly higher than the above, so a method had to be found to eliminate them. [4]

It is common for flights to require a cross line perpendicular to the flight lines to improve aerial triangulation accuracy, but such cross lines no longer needed in the mosaicking phase of orthophoto making.

Therefore, for proper results, it is expected that these cross lines on the footprint map to be removed in advance.

#### 1) How the algorithm works:

As a first step, we need the size of the area in square meters defined by the field boundaries of each image. This can be defined with a simple basic GIS operation and stored as an attribute according to each polygon.

Because there are no identifiers for polygons in the footprint file to be used by default, we need to create them so that each area can be identified later. This is done in the second step.

With the following subroutine, an overlap operation is performed to map the intersection of each polygon. From now on, the result layer contains all the combinations of possible overlaps, associated IDs, and the area of the original polygons.

In order to obtain the percentage overlap values, we also need the area of each of the previously created intersections. We calculate these in a similar way as described in the first step.

Once both the original and the overlapping areas are known, their percentages can be calculated with a simple division operation, which is also stored as an attribute within the layer.

In the last step, we create the result table with an SQL query. To be able to filter out multiple overlaps, we examined the percentage of overlap that single-overlapping (direct) neighbors present. Based on these, we concluded that if we exclude elements smaller than 55% and greater than 95%, the resulting polygons 2-3 and 4, respectively, are obtained, which categories have been described above.

Elements around 100% should be excluded because overlapping polygons with themselves may result in elements with the same ID as the original or overlapping shape, resulting in elements greater than 95% overlap.

#### 2) Advantages and disadvantages of the algorithm

It is a prerequisite that footprints are created using a terrain model and available as input.

It is important to remove any crosslines before running the algorithm. Because, overlaps in the classical sense can only be interpreted in the case of parallel flight lines.

If the flight block were to be composed of sub-blocks, their processing should be done separately by the discussed program. This is because, in the case of sub-block flight, at least two frame overlaps must be provided under flight planning rules, so that in the case of joint processing at these locations, the number of overlaps would be twice as normal.

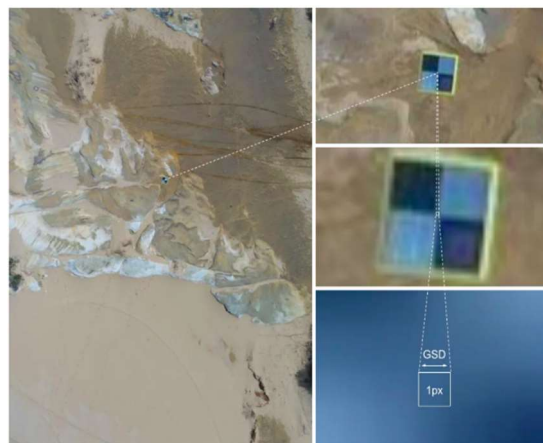
Before running, the path and file name of the table to be created must also be specified.

A disadvantage is that the removal of cross lines is not an automatic process. Also, since the identification generation is universal and automatic, its use requires attention especially in cases when working with actual post-flight data, since there will be image identifiers among the attributes.

The main advantage of our program is that it offers a general solution for determining the degree of overlap between adjacent images.

The tool can be used to process pre-flight, planned data; or using a realized post-flight map.

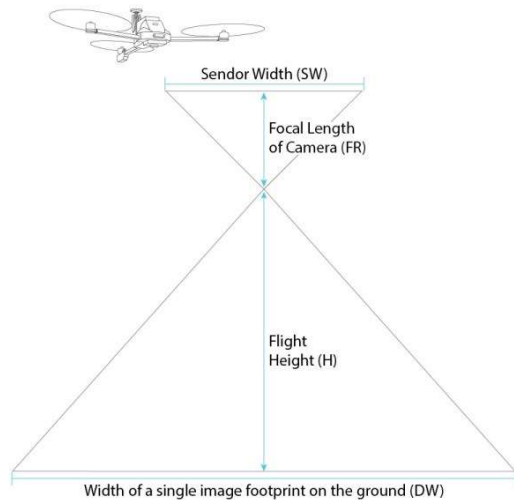
#### B. GSD calculation algorithm



3. Figure What do we mean by GSD?  
Size of a pixel on an aerial photo

In order to be able to meet the project order specifications for resolution, it is important to enter a parameter in the flight plan as to what resolution end product we need to make. Knowing this, the camera parameters and the terrain, the maximum flight altitude can be determined.

GSD (Ground Sample Distance) (3. Fig) is a measure of the pixel resolution of aerial photographs. Its calculation requires information on the focal length, the distance of the camera from the subject, and the resolution of the camera sensor. [8] (4. Fig)



4. Figure Components of GSD

Usually characterized by cm / pixel, it describes the distance that can be measured on the ground between the centers of two adjacent pixels. For example, a 12 cm / pix GSD covers a square with an area of 12 cm x 12 cm (144 cm<sup>2</sup>) on the ground.[9][10]

$$GSD = \text{pixel size} * \frac{H}{FR}$$

GSD values within images are not constant because they also depend on the distance from the center of the image and on the topography.

Even on a flat area within an image, it is easy to see that the maximum value of the resolution will be directly below the shooting location, and moving away from this, the value will continuously deteriorate, so the resolution will be lower. In addition to the location within the image, the topography can also have a significant effect on the GSD, as the terrain protrusions will be inherently closer to the camera than the deeper valleys, so the relative flight altitude can vary from point to point, bringing with it a change in resolution.

So, if we want to get a detail-rich orthophoto, it is advantageous to work with a small GSD. [7]

As we stated above, it can be seen that field resolution in aerial photography is a complex and variable value, which is why our customer needed to find a solution so that we can also map these changes on a map. One of the most interesting challenges in this was how to handle the excess information caused by overlapping images and how to select the boundaries of each image from which the resolution map can be composed.

The customer formulated the requirements as follows:

- *These flight plan projects will be delivered in shapefile format, accompanied by a map showing the planned resolutions (expressed in mm).*
- *“The useful part of an image is defined as the area for which the details of the terrain are*

*closer to the center of the image considered than to the center of the neighboring images”.*

Similar to the previous algorithm, we created the solution in QGIS and Python environments.

The layer containing the geometry of the shooting locations, with attribute data for the absolute flight altitude, must be provided as input data. This altitude value is interpreted to the focus point of the camera. As in the first application, the data for any cross lines must be removed beforehand.

The layer containing the footprints must be available to run the program, but this also without cross lines as we discussed the reasons before.

In order the change in resolution due to the topography appears in the final result, a data layer showing the topography of the area is also essential. It can be a STRM topography model or Lidar data.

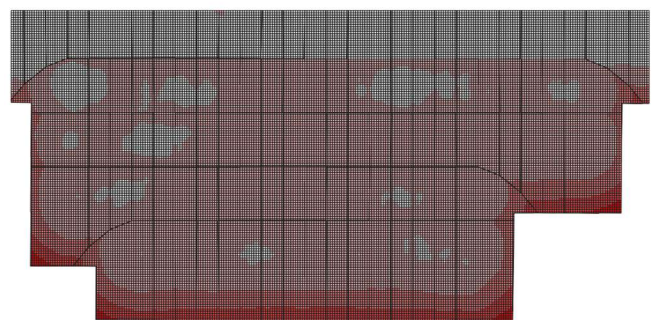
Using this data, we also obtain the resolution map in territorial unit that can also be specified as a parameter.

#### 1) How the algorithm works:

During development, the biggest difficulty was that during aerial photography, a given area appears in multiple photographs since they overlap, while the resulting map where ground resolution should be represented on a layer is without overlap and gap.

The value which has the smallest GSD value (smaller is better) in a given area is the one which have the closest distance to the camera, the closest to the centroid of any given footprint centroid. The areas which contain points that are closer to a given point than to any other are the Thiessen areas, their borders are the Thiessen polygons (also known as Voronoi polygons), and by its nature it is a polygon network without any overlap [13]. Technically the lines of the Thiessen polygons are oversimplified seam-lines. We used this Thiessen polygon calculation tool to simplify the dataset and get free of the overlays. (5. Fig.)

Each step of the algorithm, since its structure is significantly the same as the program developed for the third problem, will be described in detail in that chapter.



5. Figure GSD map White patches caused by DTM (white is smaller GSD, red is bigger GSD, smaller is better)

#### 2) Advantages and disadvantages of the algorithm:

The program created to solve the problem can be used to process the data of both planned and implemented flights, to create the field resolution map.

The sampling distance of the GSD must be adjusted to the resolution of the terrain model, since increasing the resolution

beyond this limit will only increase the running time, the accuracy of the map will not increase.

### C. Perspective tilt map of buildings

The presence of perspective distortions is a natural phenomenon in aerial photography end products. The only exceptions to this are the so-called true orthophotos. [8] This effect should be taken into account when producing traditional orthophotos. Our client's documentation obligation extends to this phenomenon as well, when applying and after the completion of the flight, they must show a map with the percentage of the apparent tilt of the buildings caused by the perspective mapping. [6]

According to the regulations:

- *These draft flight plans will be delivered in shapefile format, accompanied by a map showing the tiltings (in %). The map of the tilting (in %)*

It is easy to see that the amount of tilt increases concentrically away from the center of the given image, reaching its maximum at the edges of the frame.

Our developed algorithm expects similar input data as the one created by the GSD map, so it is necessary to specify a point file containing the shooting locations with altitude data, a footprint polygon file that takes into account the terrain, and an SRTM or Lidar terrain model available for the whole area.

The result is a map that can be used to thematically display tilt categories. These categories can be generated automatically in a GIS program or by the user. Typical category limits: 0-5-10-15-20%

#### 1) Operation of Tilt- and GSD calculation program

The first step here is to calculate the area of the footprint polygons in square meters.

Since these polygons do not yet have a unique identifier at the time of design, this must be created so that we can later establish a connection between the polygons and the shooting locations.

In order to determine the boundaries of the areas close to the center of each image, their centroids need to be calculated.

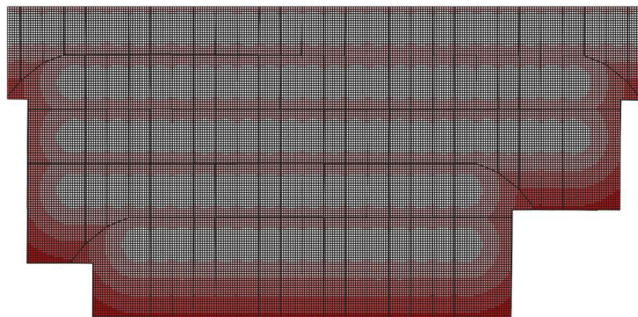
With the knowledge of the centroids, Thiessen polygons can be made, so from here we have the validity limits within each image.

In the next step, based on the identifiers created earlier, we connect the shooting coordinates with the polygons of the corresponding images in order to find the data of the two data levels within one layer.

An important step is to create a regular grid with terrain data, which will also determine the detail of the final tilt or resolution map.

Intersecting this and the previous derived Thiessen polygons yields a layer that also contains topographic data, flight altitude, and image center coordinates.

In the above result layer, all the data can already be found, on the basis of which the field resolution and the building tilt can be calculated by trigonometry. (6. Fig.)



6. Figure Perspective tilt map of buildings (white is smaller tilt, red is bigger tilt, smaller is better)

#### 2) Advantages and disadvantages of the algorithm:

As before, it is important that footprints are made using a terrain model.

Any crosslines should be removed before running, this step is not automatic.

It is recommended to process the subblocks separately. The program works without it, but anomalies should be expected in the areas affected by the overlap.

The image ID of the footprints and the ID of the shooting positions must match. Due to the automatic generation, it is advisable to pay attention to checking these.

If we are working with a large area and small sampling cells, we should expect increased system memory usage. To mitigate this problem, the application was created to automatically delete unnecessary attribute properties.

The advantage of the applications we create is that it provides a general solution for creating GSD and perspective tilt maps using such specific input data. It is also suitable for use with data showing the planned and realized status.

### III. CONCLUSIONS

Nowadays, the technological accuracy of aerial photography has reached the level that it can be realistically expected from the customers that already in the tender phase the plans are prepared in such depth and accuracy for the expected end product that certain technical characteristics are known with centimeter accuracy.

We have been commissioned to map such features, as the state customer already sets them as a requirement.

We had to find a GIS solution for three problems:

1. to determine the exact percentage of overlap with the images in the immediate vicinity of each image;
2. to show on a map the field resolution of the aerial photographs (GSD) to be taken for the whole flight area, taking into account the topography;
3. to make a map also on the basis of the topographical conditions of the extent to which we can expect perspective building tilts at any given point of the AOI.

Based on QGIS and Python, our three-person team has developed applications that offer solutions in such a way that they can be used in a universal way among others to be able to use for in-flight states compared to the planned versions.

Results will be verified in the coming weeks, when we can compare the planned data with the actual flights, and also the calculated results with the actual ones.

The development of our programs, like all other applications, is not over yet it is an iterative process, based on the first experiences of the customer, their further development is currently underway, and we have even been commissioned to prepare documentation solutions for Lidar data also.

#### IV. ACKNOWLEDGEMENT

The research was carried out at Envirosense Hungary Ltd. on behalf of a partner company in France.

We would like to thank the staff of the company for their help in the research and its publication.

#### V. REFERENCES

- [1] P. Longley, M. Goodchild, D. J. Maguire, and D. W. Rhind. *Geographic Information Systems and Science*. John Wiley & Sons, Hoboken, N.J, 3rd ed. edition, 2011. ISBN 0470721448. [p409, 410, 423]
- [2] J. Muenchow, P. Schratz, A. Brenning. RQGIS: Integrating R with QGIS for Statistical Geocomputing *The R Journal* Vol. 9/2, December 2017
- [3] Graser A, Olaya V. Processing: A Python Framework for the Seamless Integration of Geoprocessing Tools in QGIS. *ISPRS International Journal of Geo-Information*. 2015; 4(4):2219-2245. <https://doi.org/10.3390/ijgi4042219>
- [4] Katona, Janos ; Gulyas, Margit Horoszne Determination of factors modifying land value based on spatial data In: Drótos, Dániel; Vásárhelyi, József; Czap, László; Ivo, Petráš (szerk.) *Proceedings of the 19th International Carpathian Control Conference (ICCC 2018) Piscataway (NJ), Amerikai Egyesült Államok : IEEE, (2018) pp. 625-628.*
- [5] Alhusain, Othman ; Tóth, Zoltán ; Rakusz, Ádám ; Almási, László ; Farkas, Bertalan Vision-based System for Quality Control of Some Food Products *ISPRS JOURNAL OF PHOTOGRAMMETRY AND REMOTE SENSING XXXV pp. 477-482. , 6 p. (2004)*
- [6] Barsi, Árpád ; Fi, István ; Mélykúti, Gábor ; Lovas, Tamás ; Tóth, Zoltán Úthibák detektálása - Mobil felmérő rendszer fejlesztése a BME-n MÉLYÉPÍTŐ TŰKÖRKÉP: A SZAKMA LAPJA 2005 : 2 pp. 32-33. , 2 p. (2005) Matarka
- [7] Tóth, Zoltán ; Mélykúti, Gábor ; Barsi, Árpád Digitális videokamera kalibrációja *GEOMATIKAI KÖZLEMÉNYEK / PUBLICATIONS IN GEOMATICS* 8 pp. 297-302. , 6 p. (2005) *Folyóiratcikk/Szaccikk (Folyóiratcikk)/Tudományos*
- [8] Lucas Grégory; Halász László; Solymosi József. Exploring the capacities of airborne technology for the disaster assessment, *HADMÉRNÖK* 8 : 3 pp. 74-91. , 18 p. (2013)
- [9] Lucas Grégory, Considering time in orthophotography production: from a general workflow to a shortened workflow for a faster disaster response, *International Archives of Photogrammetry and Remote Sensing (2002-) XL3 : W3 pp. 249-255. , 7 p. (2015)*
- [10] Schickler, W., and A. Thorpe, 1998. Operational procedure for automatic true orthophoto generation, *International Archives of Photogrammetry and Remote Sensing*, 32(Part 4):527-532.
- [11] Enyedi, Péter ; Pap, Melinda ; Kovács, Zoltán ; Takács-Szilágyi, László ; Szabó, Szilárd Efficiency of local minima and GLM techniques in sinkhole extraction from a LiDAR-based terrain model *INTERNATIONAL JOURNAL OF DIGITAL EARTH* 12 : 9 pp. 1067-1082. , 16 p. (2019)
- [12] Ultracam-eagle M3 brochure [UC\\_Eagle\\_M3\\_en.pdf \(vexcel-imaging.com\)](https://www.vexcel-imaging.com/UC_Eagle_M3_en.pdf)
- [13] Okabe, Atsuyuki, Barry Boots, Kokichi Sugihara, and Sung Nok Chiu. 2000. *Spatial Tesselations: Concepts and Applications of Voronoi Diagrams*, 2nd edn. Chichester, UK: John Wiley & Sons.
- [Figure 1] [https://www.researchgate.net/figure/Schematic-of-the-perspective-distortion-and-correction-The-image-red-distorted\\_fig52\\_49460417/](https://www.researchgate.net/figure/Schematic-of-the-perspective-distortion-and-correction-The-image-red-distorted_fig52_49460417/)
- [Figure 3] <https://visionaerial.com/what-is-ground-sample-distance/>
- [Figure 4] <https://www.propelleraero.com/blog/ground-sample-distance-gsd-calculate-drone-data/>